

BENGKULU HARBOUR PROJECT

FINAL REPORT

VOL A

General Aspects

Feb '78

Dik Ludikhuize & Henk Jan Verhagen

Contents

General introduction	3
Acknowledgements	6
1. The history of the Bengkulu coast	7
2. Waves on the Bengkulu coast	12
3. Coastal morphology	29
4. Calculation of sediment transport	43
5. Economical considerations	58
References	68
Samenvatting	71

General introduction

The Indonesian government is stimulating development of areas outside Java to increase the food production of the country and to decrease the population density on Java. Also the Bengkulu district on the west coast of Sumatra has to be developed. Important for development is a good infrastructure, and in an archipelago like Indonesia sea-transport is cheap and easy. But harbours are necessary.

Nowadays Bengkulu has a small harbour with an average depth of 1 m, and of course this harbour is too shallow for normal shiphandling. Hence most of the merchantships are loaded and unloaded on the roadstead.

Further Bengkulu has two road connections with Palembang. These roads cross the Barisan mountainchain. They are in a poor condition. Improving these roads is difficult and expensive.

There is no railway traffic in the Bengkulu district. The nearest railway station is Lubuklinggau, just on the other side of the Bukit Barisan. To build a railroad through the Bukit Barisan is even more difficult than building a road, and plans to give Bengkulu a railway-connection are not realistic in the present circumstances.

Improving harbour facilities is necessary, because loading and unloading ships on the poor protected roadstead is not always possible, specially not in the January-March monsoon period.

Several possibilities are possible to improve the present situation

- I To improve the roadstead to assure protection against waves.
- II To improve the existing harbour in Bengkulu.
- III To build a new harbour at an other location, for example in the Pulau Bay.

Pulau Bay is a bay, about 20 km south of Bengkulu, protected by a sand spit from the sea, and with a depth of 10 m. The natural entrance of this bay is the mouth of the Air Teluk, which has silted up and is not navigable.



To make a good decision about what to do, it is necessary to know several things:

1. What are the needs of Bengkulu with respect to harbour facilities, now and in future?

A short investigation on this subject is discussed in chapter 5 of this volume. Short time needs (until 1985) in respect to the improvement of the existing harbour are discussed in vol.D. The needs after this year (in view of the lay out of the Pulau Bay harbour) will be studied in detail by Boss de Charante.

2. What is the wave climate along the coast of Bengkulu?

In this study (chapter 3) is tried to describe the wave-climate. Because not enough basic wave information is available the results have to be regarded with caution. A refraction analysis presented in vol C.

3. What is the morphological situation of the Bengkulu coast?

In this study the morphological system is discussed in chapter 4. Also the results of a sand transport computation are presented in that chapter.

The development of the computation-method is described in vol B.

4. What is the influence of artificial works on the morphological system?

This question has to be split into two sections:

- a, Improvement of the existing harbour.

This subject is discussed in detail in vol D.

- b. The new harbour facilities in the Pulau Bay.

This subject is not discussed in this report, a detailed investigation on this item is made in Indonesia.



Acknowledgements

We wish to thank everyone who did support us with this investigation. Very important for an investigation like this one is a good basis of data and informations. So we wish to thank specially ir. Burger, ir. v. Houweninge and ir. Van Oostrum of Nedeco, ir. Sumarko of the Bengkulu projectteam, mr. Govers of the Integrated Sea Transport planning, mr. Erkelens of LIPI/KITLV and mr. Kuiper of the ministry of the interior for all the information they have given.

The history of the Bengkulu coast

The oldest available information about the Bengkulu area was found in Valentijn (1726). In this book François Valentijn, a missionary, gave a description of South-East Asia, and also about Sumatra. In those days the English and the Dutch competed heavily in the far east. This competition continued until 1825 (treaty of London). Valentijn tells that *in 1686, 1687 and 1688 we got troubles with the English about Bangkoelo.* He complains that the English expelled the king of Bantam (who was a Dutch vazal), so that pepper wasn't sent anymore to the Dutch, but to the English.

The book of Valentijn also contains a map of Sumatra. Some details were drawn very clear. The town of Sillebar is not existing nowadays but is still mentioned on the topographical map of 1926. The Tanjung Kerbau cape is also indicated on the Valentijn-map, but on the wrong side of the Sillebar-river (This river is nowadays called Air Tanjungaur). It is possible that the river-mouth was indeed south of Tanjung Kerbau in the 17th century. The shape of Tanjung Kerbau will be discussed later.

On this map a town called Panarikan is indicated at a location NW of Sillebar at a cape. On this site one should expect Bengkulu. But Bengkulu is indicated more northward of this cape. The name Panarikan is not found on any other map.

Paulus (1917) mentioned however that in the beginning of the 18th century for reasons of public health the town of Bengkulu was moved six miles to the south. At the new site the English built the Fort Marlborough (between 1710 and 1714).

So one may expect that on the Valentijn-map still the old location is given, and Bengkulu-town was moved to the site of the old Panarikan-town, which name dissapeard in due course. And so Panarikan-river should be identical with the modern Bengkulu-river. The Bengkulu river of Valentijn has probably to be identified as the modern Air Itam.

At the beginning of the 19th century the English took over the government in the Dutch-Indies. From 1811 to 1816 Thomas Stamford Raffles became lieutenant-governor of Java and the other Dutch posessions. But after the Vienna congress the Dutch got back their colonies. The Bengkulu area however remained a point of discussion. In 1817 Raffles became lieutenant-governor of Bengkulu, and he tried to bind Sumatra and Malacca to the English empire. To support this imperialism he founded Singapore in 1819 (in those days Malacca was



Nieuwe kaart van het eiland
Nieuwe hoek van het eiland
Sumatra

Volkenyn 1726

a Dutch colony). At the treaty of London Sumatra was rendered to the Dutch government, but Malacca and Singapore stayed to the English.

Under his government Raffles ordered several detailed surveys of the Sumatran coast. These surveys were published by Gardner in 1829. From these data a map was drawn and published by Perthes (1837).

This map is the first trustworthy map of this area. Also several depths are indicated. The depth of the Pulau Bay was 6 to 7 fathom (ca. 11 m), which is about the same as nowadays. The shape of Tanjung Kerbau is nearly identical to the shape according to Valentijn. When this is conferred to modern maps one should conclude that in 1800 the sand spit was still not formed.

The next source of information is a chart surveyed by McDonald in 1856. On this chart a very detailed map of Pulau Bay is presented with many soundings. The depth is 6 fathoms (10 m). The depth in the area in front of the spit is 6 - 10 fathoms (10-14 m), which is also practically identical with the nowadays situation.

In 1860 F.G. Stek surveyed the area for a map in the "Algemene Atlas van Nederlandsch Indië". This map gives not much more information than the McDonald chart.

The Pulau Bay is both on the McDonald chart as on the Stek map nearly closed by a sand spit, which ends in the neighbourhood of Pasar Atjeh (This village has disappeared nowadays).

In 1904 a hydrographic chart is published. On this chart the McDonald data are used, so this chart adds no information to our knowledge.

After the construction of the harbour-môles of Bengkulu, the surveying vessel Van Gogh af the Dutch navy collected new data in 1908. On a chart published in 1908 the spit has grown somewhat since 1856.

Modern topographical surveying starts in this area in 1911. In this year the Bengkulu area was triangulated. On Tanjung Kerbau a third order triangulation pillar (T2049, Oedjung Telokpoengoer) was erected. In 1913 the surveyors found this pillar below the beach sand, the pillar was removed by the surf.

From this fact one might conclude that the coastline is not stationary. This is also mentioned by Zieck (1932): *Probably in connection with the monsoon, the sea has changing currents, so that the beach is alternating wide and small, and even sometimes disappears.*

In Knappert (1915) some information is given about the construction of the harbour of Bengkulu. The first plan was to build only the western

DE POELAU BAAI EN OMGEVING

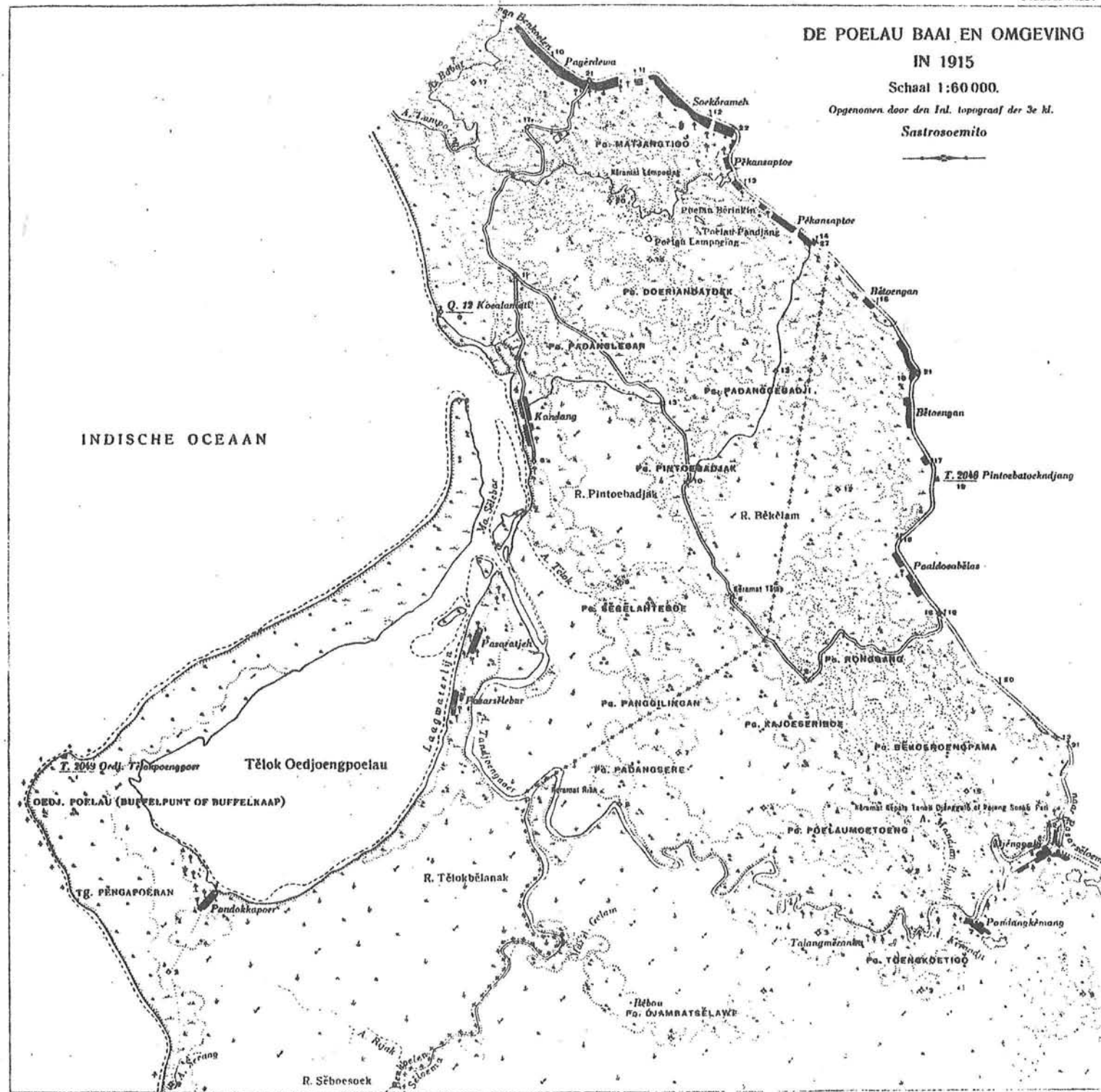
IN 1915

Schaal 1:60 000.

Opgenomen door den Ital. topograaf der 3e kl.

Sastrosoemito

INDISCHE OCEAAN



harbour môle. While building, heavy erosion was noticed east of the dam, near Fort Marlborough. Mr. Nobel, consultant of the port authorities advised to build also the eastern môle. This had a positive effect.

But problems were not solved, the harbour still silted up. So in December 1923 several proposals were made for improving. Chosen was a plan to dredge the harbour and to make an opening in the eastern harbour môle (Roos van Raadshoven 1924). This opening still exists, but the effect is very small.

Plans for the Pulau Bay are very old. The resident of Bengkulu had proposed to construct a harbour in this bay in 1896. As a result of this proposal the general consultant of port authorities in the Dutch Indies visited Pulau Bay in 1915 (Topod 1915). The plan was to construct a harbour for the export of coal from the Bukit Barisan; it should be the terminal of the railroad to Palembang (Paulus, 1919). The topographical service mentioned that a port construction in this bay probably would suffer from siltation problems (Topod 1915).

As mentioned the oldest available detailed chart is McDonald (1856). On this map a short sand spit is indicated. As can be seen of fig.

the spit grew relatively fast. Going back in history it is to expect that the spit started growing around 1800. This is confirmed by the maps of Perthes and Valentijn. They show an identical peninsula, without a clear sand spit, but only with a short hook.

A question is why the spit started growing in 1800. As indicated in the next chapter, the coast of Bengkulu is rising. Verstappen (1973) describes Bengkulu and Tanjung Kerbau as horsts. It is to expect that on the location of Tanjung Kerbau an island existed, which was connected in due course with the mainland. On this way sand transport was blocked for centuries. When sand started to pass again Tanjung Kerbau the genesis of the spit started. But the local depth was about 10 m. So it took the spit many years to rise above the water level.

2. Waves on the Bengkulu coast

Introcution

Knowledge of the wave climate along the coast is a basic need for coastal engineering. For a description of this wave-climate a lot of long term measurements in deep water are necessary. Unfortunately no long term measurements were made in the Bengkulu area. The Dwidelta corp. and the Yogyacarta University measured in a few short periods (9 days) wave heights and sometimes wave periods. These were no continuous measurements, but measurements once per hour, and with each measurement only ten waves were measured. Waves were only measured during daylight-time. Hence statistical operations with these data are impossible.

It is possible to predict waves with hindcasting procedures from detailed weather charts. Because the Indian Ocean south of the equator is not frequented by ships also meteorological data are scarce. More detailed information is available along the south coast of Java. So it is usefull to try to use these data for the Bengkulu area. These two areas are influenced by aproximately the same winds and storms.

Tides and currents

Because Bengkulu lies at the coast of an ocean no large tidal influences have to be expected. Indeed the tidal difference is only 60 cm (Admiralty tide table, 1976). More detailed date are presented in Koshiro (1974):

HHWL	1.25	m	+ chart datum
HWL	1.04	m	+ chart datum
MWL	0.70	m	+ chart datum
LWL	0.40	m	+ chart datum
LLWL	0.06	m	+ chart datum

No important ocean currents were measured (0.02 - 0.07 m/s, Dwidelta 1975). A slow drift occurs between the islands west of Sumatra and the Sumatran coast. This drift has a small influece on coastal morphology. The ocean drift has no influence on the waves.

The influence on morphology is discussed in the next chapter.

Wind systems near Bengkulu

In Indonesia winds are semi-annual, because of the monsson system. In January Australia is heated and therefore air flows towards this area. In July the central parts of China (Gobi) are heated and thus the air is flowing in the opposite direction. These winds are influenced by the rotation of the earth according to the law of Buijs-Ballot. The results

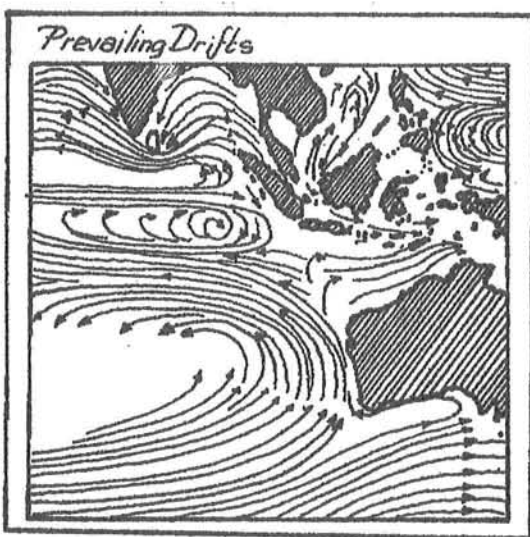


Fig. 2.1.

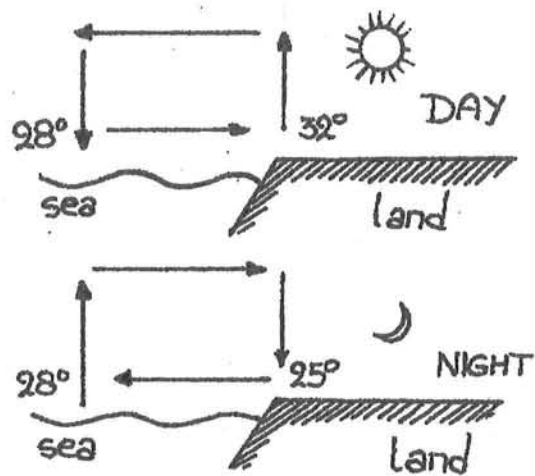


fig. 22 The daily monsoon system

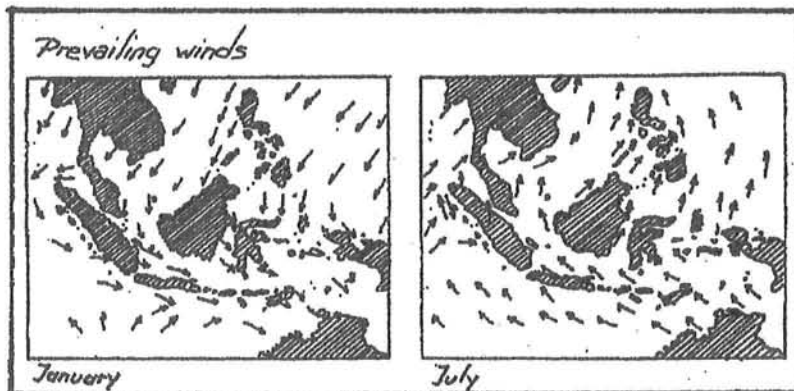
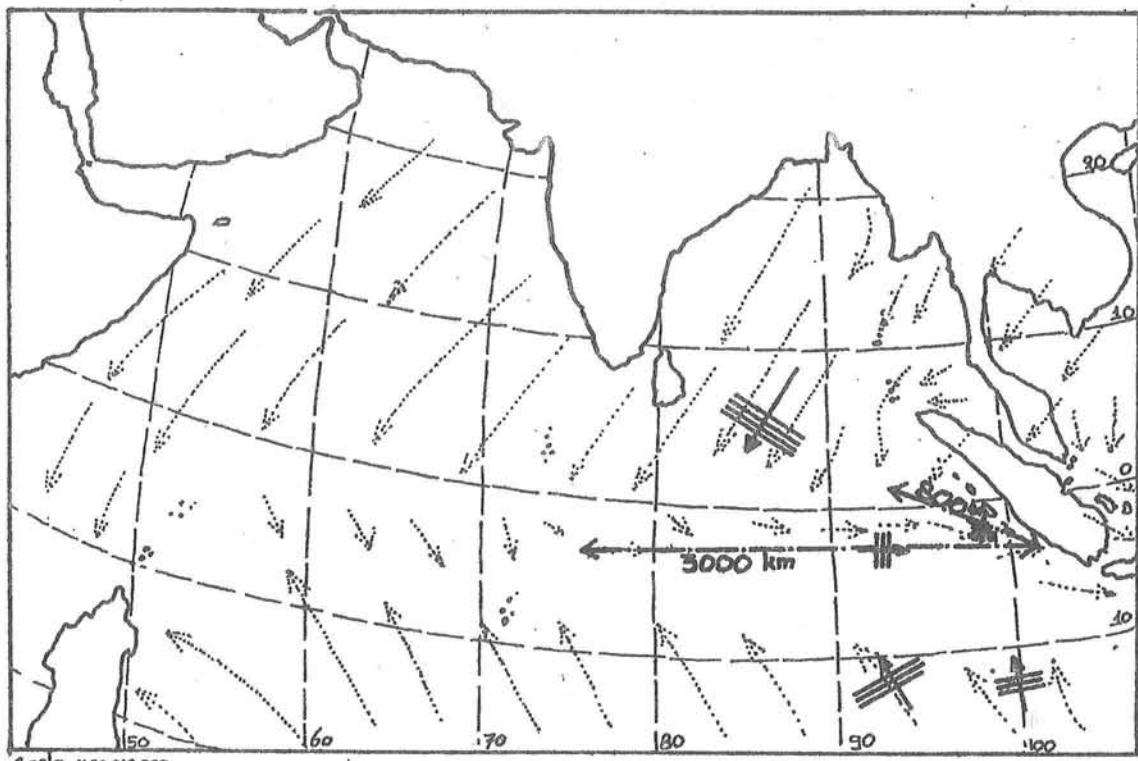


fig. 2.3

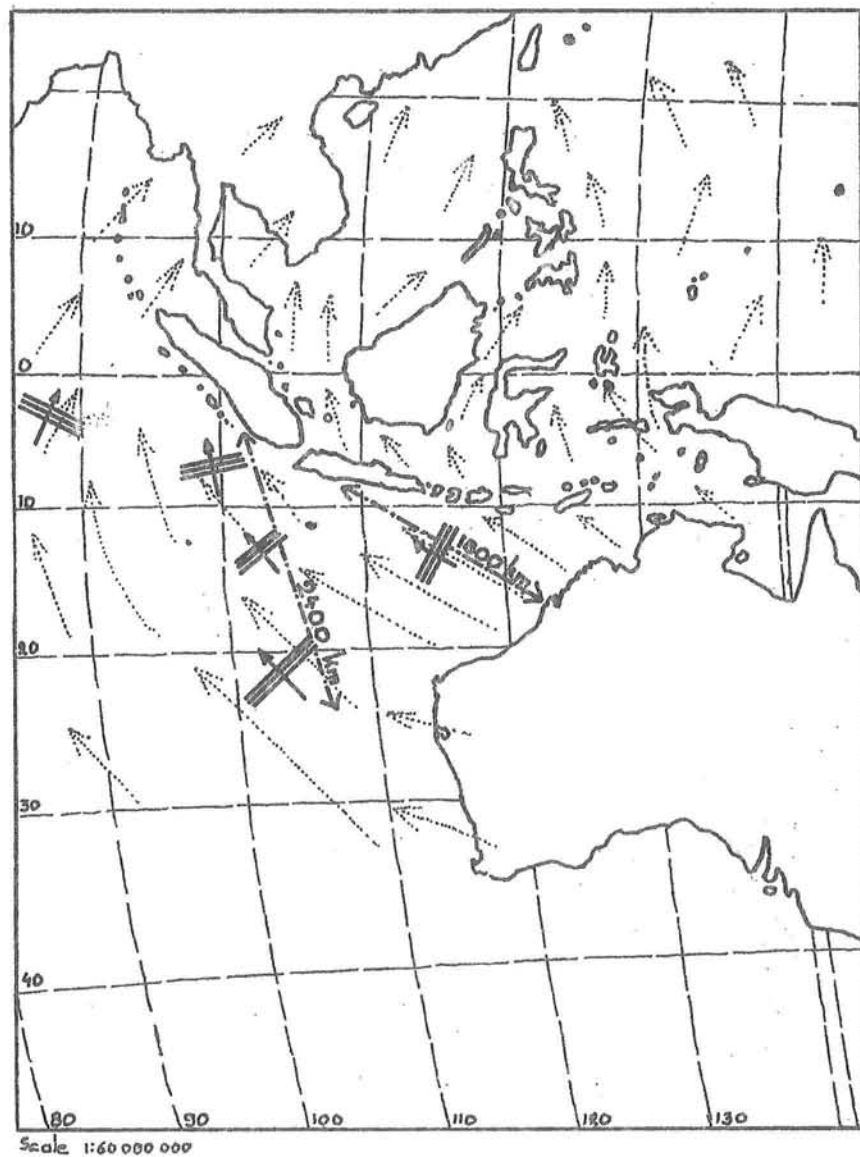
of this system are a SE wind in July and a NW wind in January along the western coast of Sumatra. Between these two periods the winds are changing (transition). This is in March/May and September/November. An other wind system is called "daily monsoon". During the day the land is warmer than the sea. At night the sea is warmer. Therefore by day the air flows from the sea to the land, and at night the air flows from land to sea. Local measurements show both the normal and the daily monsoon.

Wave types

As follows from the former paragraph two windsystems are present in this area. So we may expect also two types of wind waves; waves generated by the normal monsoon, and waves generated by the daily monsoon. Of course also swell is possible. This swell has to be generated in the storm areas at latitude 50° S. It will be shown that these swell waves are low (0.5 - 1.5 m) and very long (15 sec and more). The monsoon waves will vary from 1.5 to 5.0 m and have periods of 7 to 15 seconds.



Situation in January



Situation in July



The daily waves will be short (3 - 7 sec). The swell waves will come from a SW direction, specially in the period between May and September (winter on the southern hemisphere). The monsoon-waves will come from SE in June-August and from NW in December-February.

The daily waves will come from W and SW, and specially in the afternoon. In the next sections all wave types are described, which contribute to the wave-climate in the Bengkulu area. Before analysing and combining this information it is necessary to know for which purposes it will be used. The description of the wave climate is necessary for the calculation of:

- a breakwater. For this calculation significant wave heights of storms which are seldom exceeded (1 per 10-100 years) have to be known.
- wave heights in the harbour and on the roadstead. For this calculation wave heights have to be known which are exceeded a few times per year. During this time ships cannot be loaded or unloaded. The directions of the waves and their periods are important for this calculation. The direction is important because the entrance of the harbour and the protection of the roadstead have to be situated in such a way that the influence of waves is small. The period is important because with certain periods ship movements will increase. Specially the small vessels used for transportation of goods from the ships on the roadstead to the coast are hindered by the wind-waves. Waves with these periods should not often enter harbour and roadstead.
- the sand transport. For this calculation the wave heights (H_{rms} = Root mean square = $\sqrt{(\sum H^2)/n}$), the directions and the periods have to be known near the breakerzone.

The different wave types have to be combined just before the breakwater, in the harbour, on the roadstead and in the breakerzone.

The waves generated by the daily winds have little influence, because their heights are very small (ca. 40 cm). These waves may possibly be omitted from further calculation, unless their stirring-factor becomes important (sand transport). Also when considerable refraction or diffraction appears, these waves could become important, because they are less refracted, resp. diffracted than the longer waves of monsoon and swell. Also when the periods are near to the periods of resonance of ships it is not allowed to omit these waves.

Swell waves

Calculation of swell waves is nearly impossible when no detailed weather information is available about the whole ocean. But it can be assumed that swell at the south coast of Java is about the same as it is near Bengkulu (apart from nearshore effects, e.g. refraction). As can be seen on

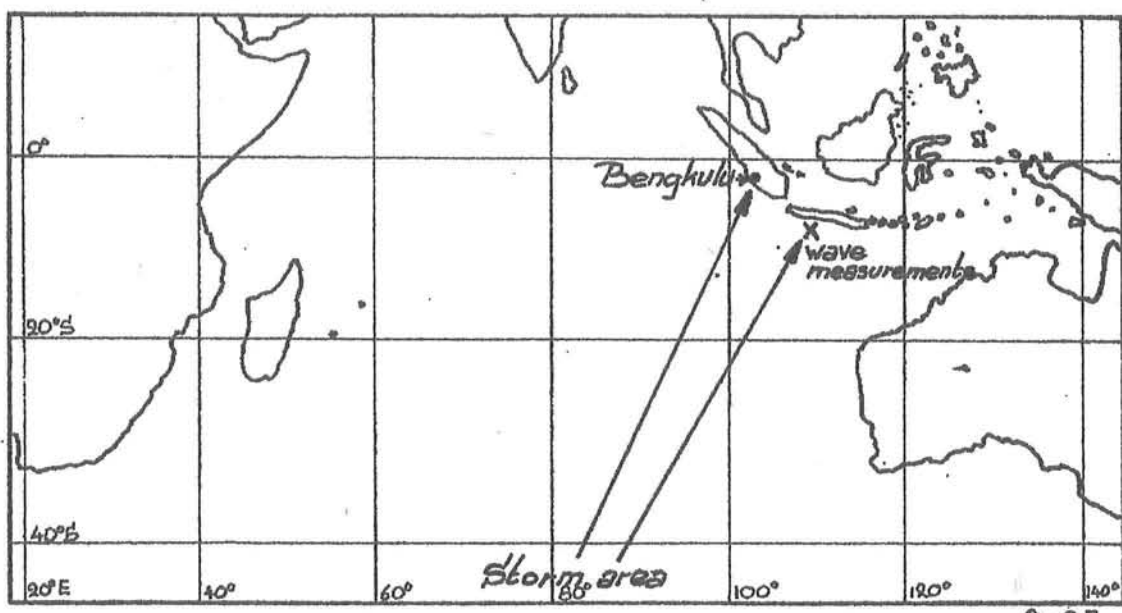


Fig. 2.5

the map of the Indian Ocean, the differences in direction and distance are nearly negligible.

From the southcoast of Java two types of wave measurements are available. A continuous measurement with a Wave-Rider (three months) and data of February, April, August and December. The latter data are obtained from ships by visual observation.

It is not clear how the last measurements were executed. It is not mentioned in the original report. The first idea is that these are observations of merchantmen, collected by the weather-bureaus. But merchantmen observations are collected in areas, and not in specific points. The given observations are from $8^{\circ}15'S/110^{\circ}30'E$ and from $7^{\circ}49'S/109^{\circ}10'E$.

These observations give very detailed information, e.g. waves of 15 sec and longer, with a height of 60 cm were measured. Therefore it is to suppose that these observations were made from survey-vessels. In tables frequencies of wave heights, wave periods and wave directions are given. Frequencies of wave heights are crosstabulated with directions and with periods. In the next two tables the annual average is given. This average is the mean value of the data from February, April, August and December. (see next page)

To determine the swell a crosstabulation of periods with directions is necessary. Unfortunately this table is missing, and it is not possible to calculate this table, because the original data are missing too. So it is necessary to analyse the available data very accurately.

direction	Significant wave height groups (m)								total %
	0.00 0.60	0.60 1.20	1.20 1.80	1.80 2.40	2.40 3.00	3.00 5.00	5.00 plus		
N	4.2	0.5	0.1	--	--	--	--	--	4.8
NE	5.7	0.9	0.2	--	--	--	--	--	6.8
E	13.2	3.7	2.3	1.4	1.0	0.8	0.3	22.7	
SE	9.8	2.7	1.6	1.0	0.7	0.5	0.2	16.5	
S	5.4	1.3	0.6	0.4	0.2	0.2	0.1	8.2	
SW	7.7	1.7	0.8	0.4	0.3	0.2	0.1	11.2	
W	12.9	2.7	1.4	0.7	0.5	0.3	0.1	18.6	
NW	8.4	2.0	0.6	0.2	--	--	--	11.2	
total %	67.3	15.5	7.6	4.1	2.7	2.0	0.8	100.0	

annual

table 2.1

Wave period	Significant wave height groups (m)							
	0.00 0.60	0.60 1.20	1.20 1.80	1.80 2.40	2.40 3.00	3.00 5.00	5.00 plus	
0 - 4 sec	57.3	34.9	20.3	10.5	5.3	2.3	0.0	
5 - 6 sec	26.0	35.5	31.9	22.0	14.4	8.0	4.0	
7 - 8 sec	10.7	17.2	27.1	34.3	31.6	23.9	16.9	
9 - 10 sec	4.0	7.5	11.5	18.7	27.7	35.2	36.3	
11 - 12 sec	1.2	2.9	5.2	8.1	11.7	16.5	24.0	
13 - 14 sec	0.5	1.4	2.8	4.2	5.6	7.0	8.4	
15 - 16 sec	0.2	0.4	0.8	1.4	2.1	3.9	5.4	
17 + sec	0.1	0.2	0.4	0.8	1.6	3.2	5.0	
total %	100	100	100	100	100	100	100	100

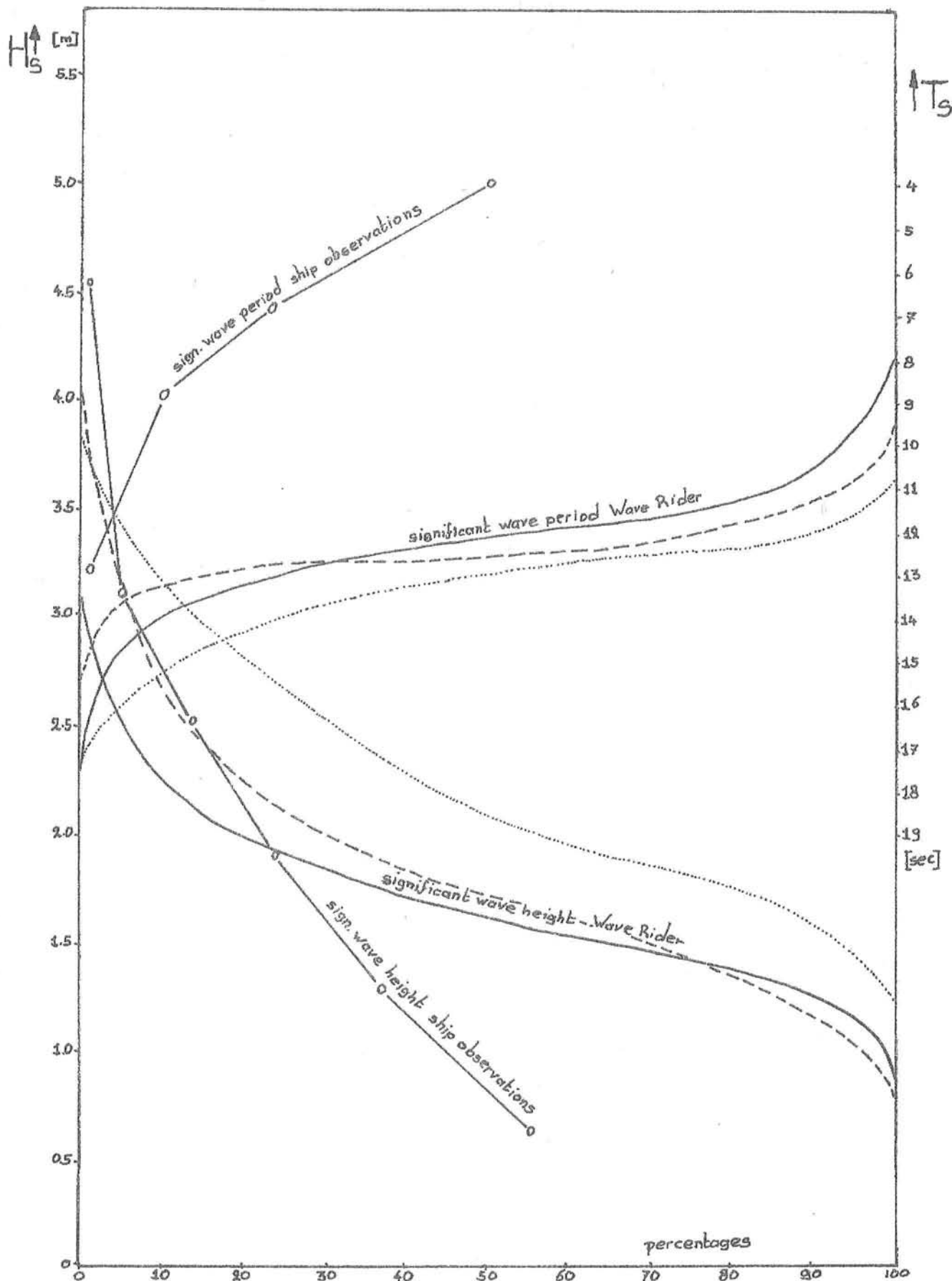
annual

table 2.2

Also at the south coast of Java three types of waves do exist (waves generated by local winds, by monsoon winds and by storm depressions). Only the swell from the storm depressions at 50° S is searched for. After some arithmetic it is possible to write table 2.2 in an other form (table 2.3).

Receipe for the conversion of table 2.2 into 2.3.

First multiply all numbers in colum 1 (0-0.6) with 0.673 (which is the percentage of waves with a wave-height less than 0.6 m, see table 2.1); the numbers in colum 2 with 0.155, the numbers in colum 3 with 0.076, etc. On this way a table is made with in the lowest row (total) the same numbers as in the lowest row of table 2.1. Now add all the values per row to get the percentage of waves in class 0-4 sec, in class 5-6 sec, etc. This percentage is called n_i . Then multiply the values of each row with $100/n_i$. The result is table 2.3.



Wave distribution south of Java

August — July..... September....

Fig. 3.5

Significant wave period	significant wave height group (m)								total %
	0.00 - 0.60	0.60 - 1.20	1.20 - 1.80	1.80 - 2.40	2.40 - 3.00	3.00 - 5.00	5.00 - plus		
0 - 4 sec	84	12	3	1	0	0	0	0	100
5 - 6 sec	65	20	9	3	2	1	0	0	100
7 - 8 sec	48	17	14	9	6	4	2	100	
9 - 10 sec	33	16	13	12	10	10	6	100	
11 - 12 sec	30	15	15	11	11	12	6	100	
13 - 14 sec	26	17	16	13	12	10	6	100	
15 - 16 sec	27	13	12	12	11	16	9	100	
17 + sec	22	10	10	11	14	20	13	100	

annual

table 2.3

Table 2.2 gives the distribution of T_s within the distinguishable wave-height groups. Table 2.3 gives the distribution of H_s within the distinguishable wave-period groups. From table 2.3 follows that the distribution of short waves differ from the distribution of long waves.

This can be seen better in a graphical impression of table 2.3 (fig. 2.7)

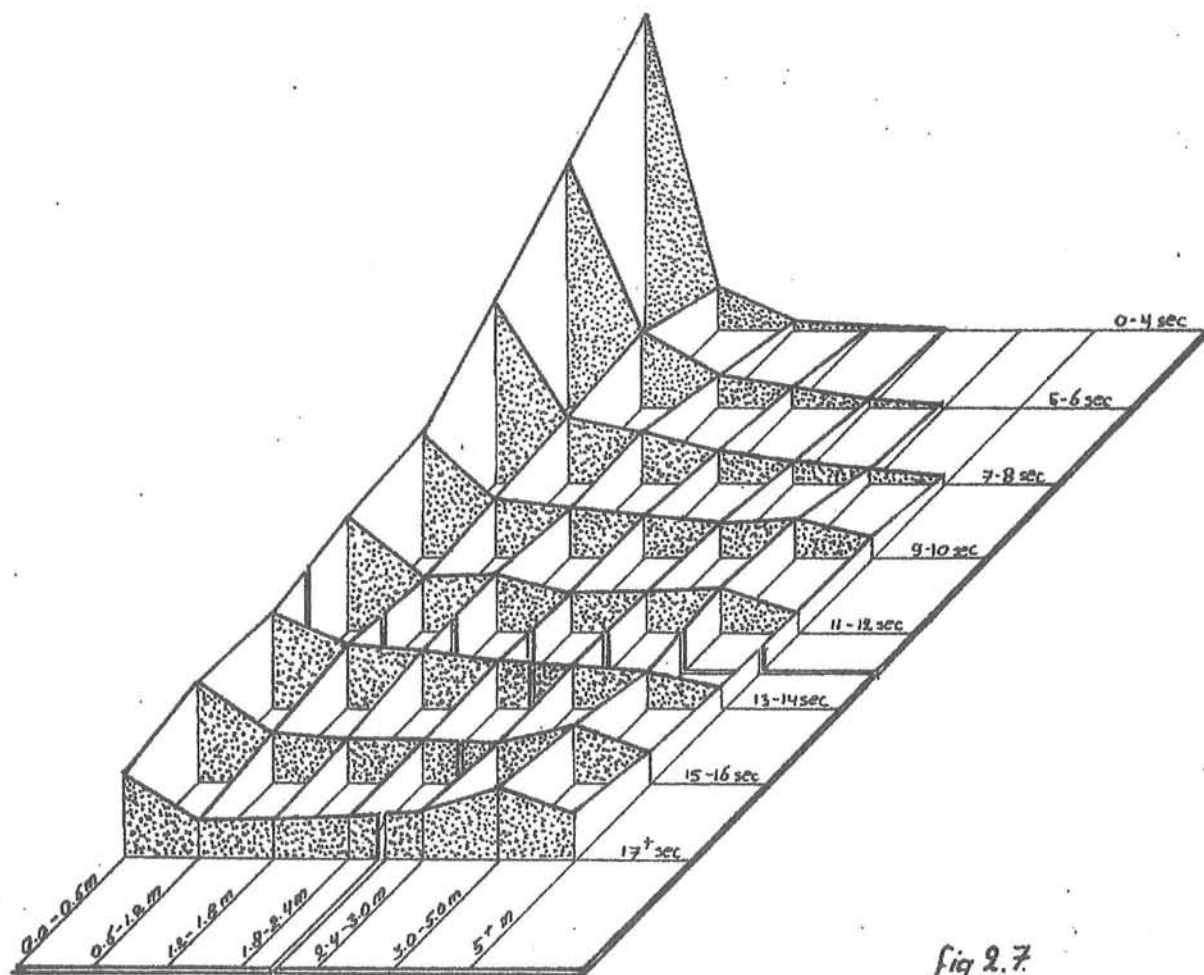


fig 2.7

In one wave-field the steepness of the waves will not vary very much, or, with other words, short waves are low and long waves are high. The short low waves are generated locally, and the long, high waves have had already a longer fetch.

In the Bengkulu area low, long waves can be distinguished. These waves have to be swell-waves. The three classes of waves are also indicated in fig. 2.7. The direction of the swell-waves has to be SW, because the area of origin is the zone at latitude 50° S.

It is not to expect that the high, long waves are swell waves too, because waves with heights between 1.2 and 2.4 m occur seldom. It is to be expected that the distribution of long waves is the sum of the distribution of swell waves (with a decreasing probability of occurrence when the wave height increases) and a distribution of monsoon waves (with an increasing proba-

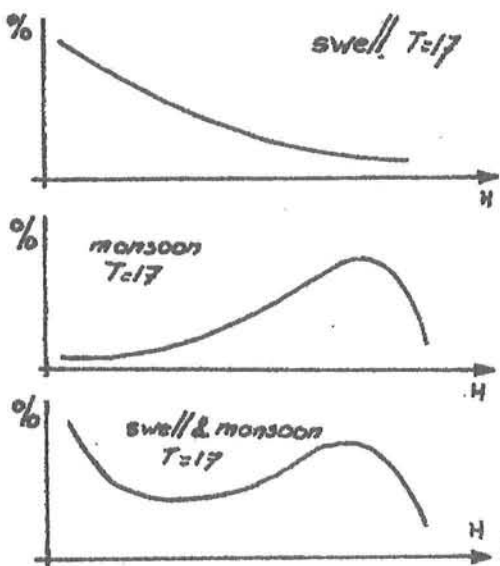


Fig. 2.8

bility of occurrence when the wave height increases until 5 m). This is indicated in adjacent figure.

Note: These figures are no spectra,
T is a constant!!

As already was indicated it is assumed that swell is generated only in the storm areas at 50° S. Of course storms occur also in other areas of the Indian Ocean, but these storms are probably of minor importance in comparision with

the 50° storms.

From the tables on the former pages the conclusion is that south of Java swell-waves with heights up to 1.80 m with periods of 13-17 seconds may occur.

From these data it is not possible to estimate the probability of occurrence of these waves.

When the results are compared with the data from the Wave-Rider measurements a different pattern of wave distribution becomes clear (fig. 2.6).

The difference between the two measurements is that on the ships much more small waves were measured, and in general the periods are too short. Possibly these differences are due to a systematic error in the wave measurements on the survey vessel. An other difference is that the Wave-Rider measurements are continuous measurements, observations from ships are only samples. Observation of long, low waves from a rather small vessel is extremely difficult.

The large number of small waves cannot be explained very well. Perhaps not enough large waves were measured because it was not possible to measure in bad weather.

The Wave-Rider measurements are very trustworthy, even the measurements of long, low waves.

As already mentioned Wave Rider data are only available for three months, July, August and September 1971. These three months have about the same climate. In August the mean wave height was less than it was in July and September. This can be explained as a period of relative good weather in the sea between Java and Australia in August 1971. July is known as the worst month in this region.

Wave periods in August are as long as they are in July, but longer than they are in September. In September spring starts in the southern hemisphere and the weather gets better. So less swell is coming from SW. Also transition starts and the influence of the monsoon winds decreases.

As already mentioned informations about how the ship obsevations were made are scarce. It is not known if these data are from one year or from a number of years. This may also be an explanation of the difference between the ship observations and the wave rider data.

The impression from these data is that the period of swell is 13 - 17 sec and the wave height is moderate (up to 1.8 m). This is the same conclusion as was made from the ship observations. The only difference is that long waves occur far more often than is indicated by the ship measurements.

In Bengkulu the same swell may be expected. Hence swell waves of 1 - 1.8 m and 13 - 17 sec from SW do occur, specially in July and August. In the other months swell with a shorter period and a lower wave height does occur, due to seasonal influences in the South Pole area.

In the storm area at 40 - 50 °S most storms have a western direction, as can be seen on the climatic map ok the KNMI (1952). Only in 2 - 8 % of the time wind with a force of 8 - 12 Beauford is blowing in the direction of Bengkulu. These winds are caused by storm depressions. These depressions are moving west. Hence in a certain area the wind blows only a short time (viz. only during the passage of the second half of the depression). We assume that this is only 10 hours in a normal situation.

For our computations we choose a wind speed of 45 knots, which follows also fromthe climatic map (KNMI 1952). Then according to Bretscheider (US Army 1973) wave height (H_s) is 5.7 m and the period is 10 seconds. After 5000 km these waves are changed into waves of only 0.7 m and 15 seconds.

Now we assume that on the ocean always somewhere such a wind is blowing, so that in "winter" at the Bengkulu coast all the time a swell with a H_s of 0.7 m and a period of 15 seconds arrives.

This is an average value. Sometimes there is a severe storm on the ocean. Then the resulting swell will be higher, but at other days there will be no swell at all. However, it is impossible to enter these differences into the computations.

It is clear that an exact determination of swell is not possible. But for calculations it is necessary to introduce a certain value. A good guess is the use of the following data:

in June July and August (winter in the southern hemisphere)	$H_{rms} = 0.5 \text{ m}$	$T = 15 \text{ sec}$
in March, April, May and September, October, November	$H_{rms} = 0.4 \text{ m}$	$T = 15 \text{ sec}$
in December, January, February	$H_{rms} = 0.3 \text{ m}$	$T = 15 \text{ sec}$

These swell waves originate from a wide area near the south pole, and can come to Bengkulu from different directions (165° - 225°). For calculations a significant swell direction of 200° is assumed, lacking a better value.

Monsoon waves

Monsoon waves are wind waves generated by a continuous wind. The speed of this wind is not extremely high, but it is a constant wind, blowing over a very long fetch.

From a detailed map of the Indonesian monsoon system (fig. 2.4) and from climatic maps (KNMI 1952) follows that in June - August a rather constant wind comes from SE. But in the December - February monsoon winds come from several directions between N and NW.

Because in the June - August period the wind situation is quite similar to the situation at the south coast of Java, the assumption can be made that the wave distribution is the same for both areas in this period.

In this period the monsoon waves propagate nearly parallel to the coastline. For the December - February period the situation is more complicated because comparison with the area south of Java is not allowed. The character of the monsoon winds near Bengkulu in December - February differ totally from those south of Java.

Only few wave measurements in open sea are available near Bengkulu. Some wave data can be found in the Oceanographic atlas of the world (US Navy 1975), but the number of observations is small (only 10 - 20 observations each month).

The impression is that most of the waves come from N, W and NW; wave heights vary from 1 to 3 m. It will be extremely difficult to estimate a reliable probability of occurrence.

Theoretically these observations include both monsoon waves and swell waves. But these observations are all visual observations from ships, and

Wave data from the Bengkulu region (US NAVY, 1976) (heights in m)

dir.	January					February					March							
	0	1	2	3	4	tot	0	1	2	3	4	tot	0	1	2	3	4	tot
N	05					05							17					17
NE						00							13					13
E							07						07					
SE	03					03												
S	13					13							07	25				32
SW	17	07				24							21					02
W	09	18				31							13					07
NW	05	01				07							23					03
CALM													07	13				20
tot	47	42				100							100	40	54	07		100

dir.	April					May					June							
	0	1	2	3	4	tot	0	1	2	3	4	tot	0	1	2	3	4	tot
N													13					13
NE	07																	
E																		
SE	29	21				50												
S		07				07												
SW																		
W	05					05												
NW	09					09												
Calm	14	07				21												30
tot	64	36				100							18	47	35			100

dir	July					August					September								
	0	1	2	3	4	tot	0	1	2	3	4	tot	0	1	2	3	4	tot	
N																			
NE																			
E																			
SE							08	10				18							
S							08	06				14							
SW							02					02							
W							19					19							
NW							10	15				25							
Calm								23				23							
tot						46	54					100				76	18	06	100

dir	October					November					December							
	0	1	2	3	4	tot	0	1	2	3	4	tot	0	1	2	3	4	tot
N								09				09						06
NE													02					02
E													06					06
SE		06				06		12	12			24		02				02
S	17	06				23		12	12			24						13
SW		01				01		01				01						02
W	10	31				41		22				22					06	12
NW		31				31		15				15		23	02	02		27
Calm								06				06		31				31
tot	17	22	61			100		76	24			100		15	69	08	08	100

long waves are mostly not recognised from ships. It is assumed in further calculations that these wave-data contain only information about the monsoon waves.

For calculation the year is devided into 5 seasons.

1 December January February	Monsoon-waves from NW
2 March April May	Transition, waves mostly from SE
3 June July August	Monsoon-waves from SE
4a September October November (50 %)	Transition, waves mostly from SE
4b September October November (50 %)	Transition, waves mostly from NW

Out of these data the following rms-values can be computed

December	1.1 m			
January	0.8 m	season 1	1.1 m	
February	1.3 m			
March	0.9 m			
April	0.6 m	Season 2	0.8 m	
May	?			
June	1.2 m			
July	?	Season 3	0.9 m	
August	0.7 m			
September	0.6 m			Season 4a 1.0 m
October	1.4 m	Season 4	1.1 m	
November	1.2 m			Season 4b 1.2 m

South of Java the following values were found:

Ship observations	February	0.8 m	Wave rider	July	1.5 m
	April	0.8 m		August	1.2 m
	July	1.4 m		September	1.3 m
	November	0.9 m		July-Sept	1.3 m

Ship observations south of Java are about 10 % lower than the wave rider data. Assuming that the wave-rider data are correct, it is reasonable to suggest that also the Bengkulu ship observations should be increased with 10 %. Further no wave data are available from July. It is to suppose that waves in July are even higher than waves in June.

Considering this, the following guess for the monsoon wave-height is made:

season	H _{rms}
1	1.2 m
2	1.0 m
3	1.3 m
4a	1.0 m
4b	1.2 m

Daily waves

Because of the daily monsoon system, in the afternoon a wind is blowing towards the coast. The fetch is not exactly known, but is expected to be about 20 km. The influence of micro climate phenomena is never considerable. The wind velocity is about 3 - 5 m/s in April (Dwidelta 1975). This wind will generate waves of 3 seconds and 0.4 m according to Brettschneider (US Army 1973). However, local observation indicated that higher waves do occur regularly. Because the daily monsoon is constant all over the year, it can be supposed that every afternoon these waves may occur.

The influence of the islands in front of the Sumatran coast

A part of the wave energy of the waves from the Indian Ocean is dissipated on the islands in front of the coast. In the Bengkulu area waves, not influenced by refraction, can reach the coast from a SW direction. Waves from a northern direction and a western direction loose a small part of their energy on the islands.

We shall neglect the diffraction of the waves from the just mentioned directions around the islands in front of the Bengkulu coast. The waves have still to travel about 200 - 300 km from the islands to the coast, therefore we assume that the wave energy is already redistributed.

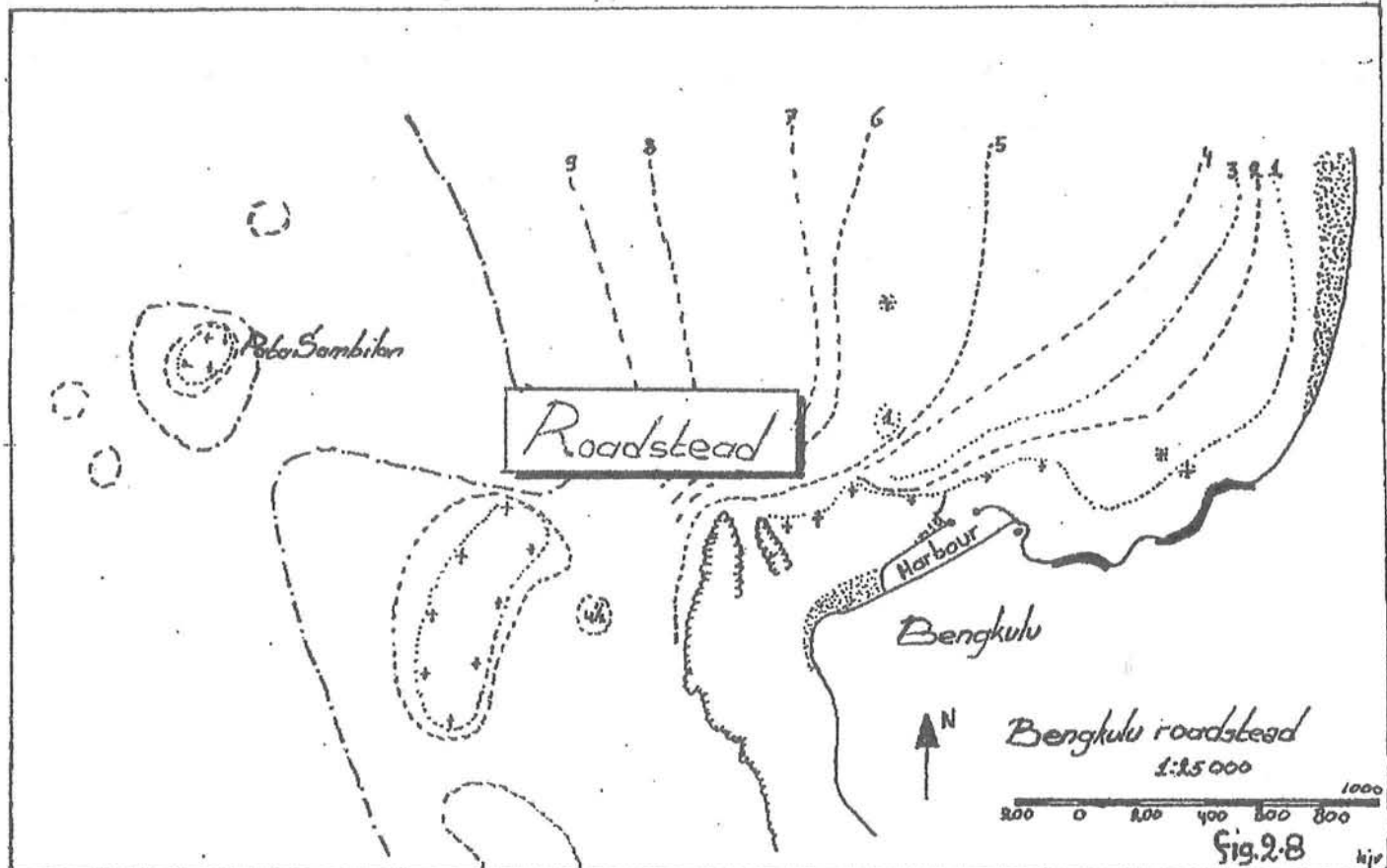
The only consequence might be that long waves enter the Bengkulu area from a direction which is slightly different from the directions which should be expected without refraction around these islands. The ocean waves which come from north-western directions have less influence in the Bengkulu area. There are two possibilities for these waves to reach the coast:

- The waves may travel through the gap between P. Pagai and P. Enggano. The influence of refraction on the shoals around these islands is negligible (see fig. 2.10).
- The waves can travel between the islands and the coast with wave orthogonals parallel to the coast. Most of these waves dissipate their energy on the coast after bent to the coast by refraction. Therefore few waves from this direction reach the Bengkulu coast.

Refraction and diffraction

As was already mentioned wave generating winds are blowing either from NW or SE, ie. parallel to the coastline.

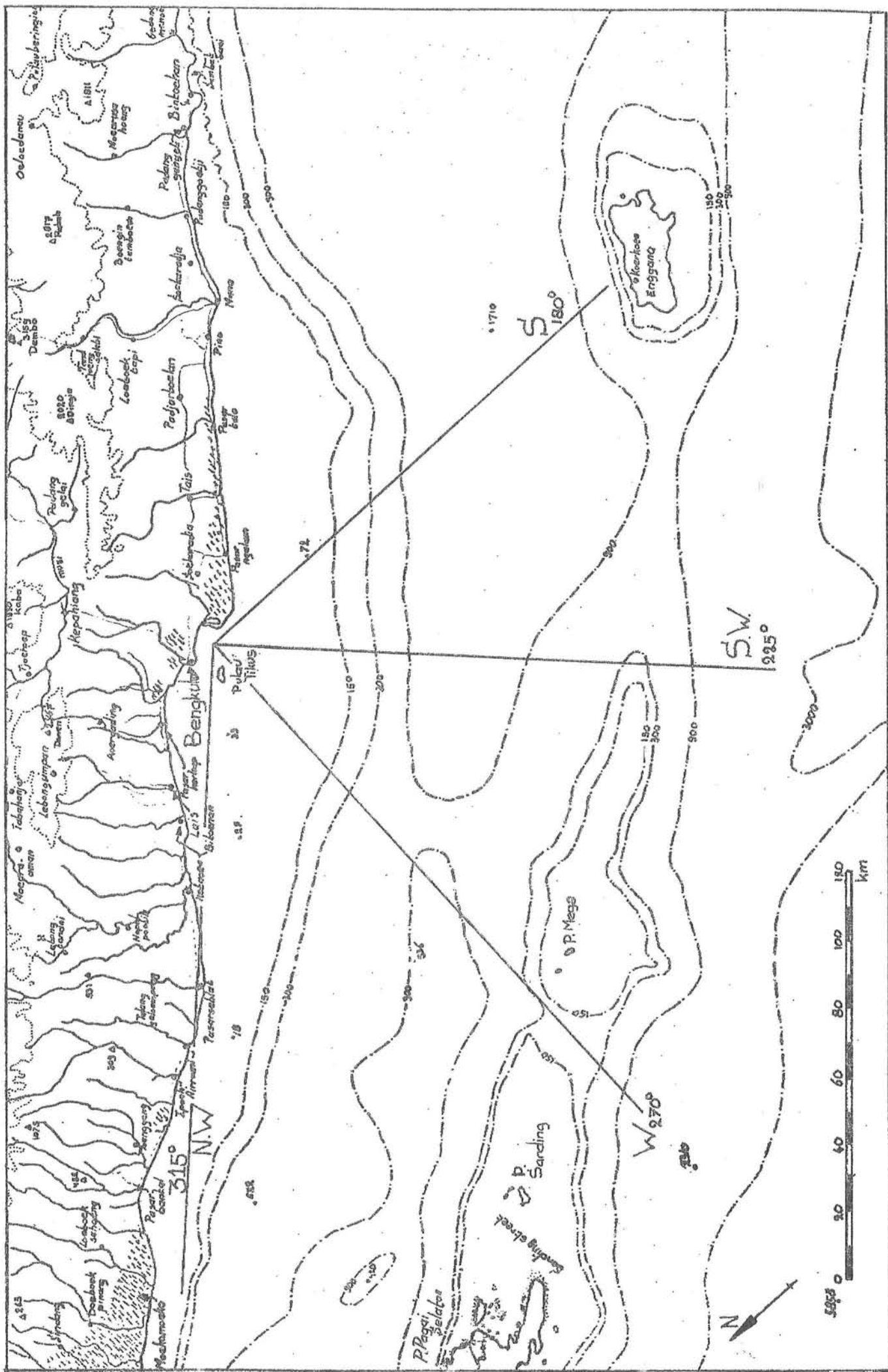
At sea wave orthogonals will also have about the same direction as the coastline. The period of the NW-monsoon is the worst season for the Bengkulu area. Information from literature and visitors agree that in this period loading and unloading of ships on the roadstead is extremely difficult. Waves coming from southern directions do not have any influ-

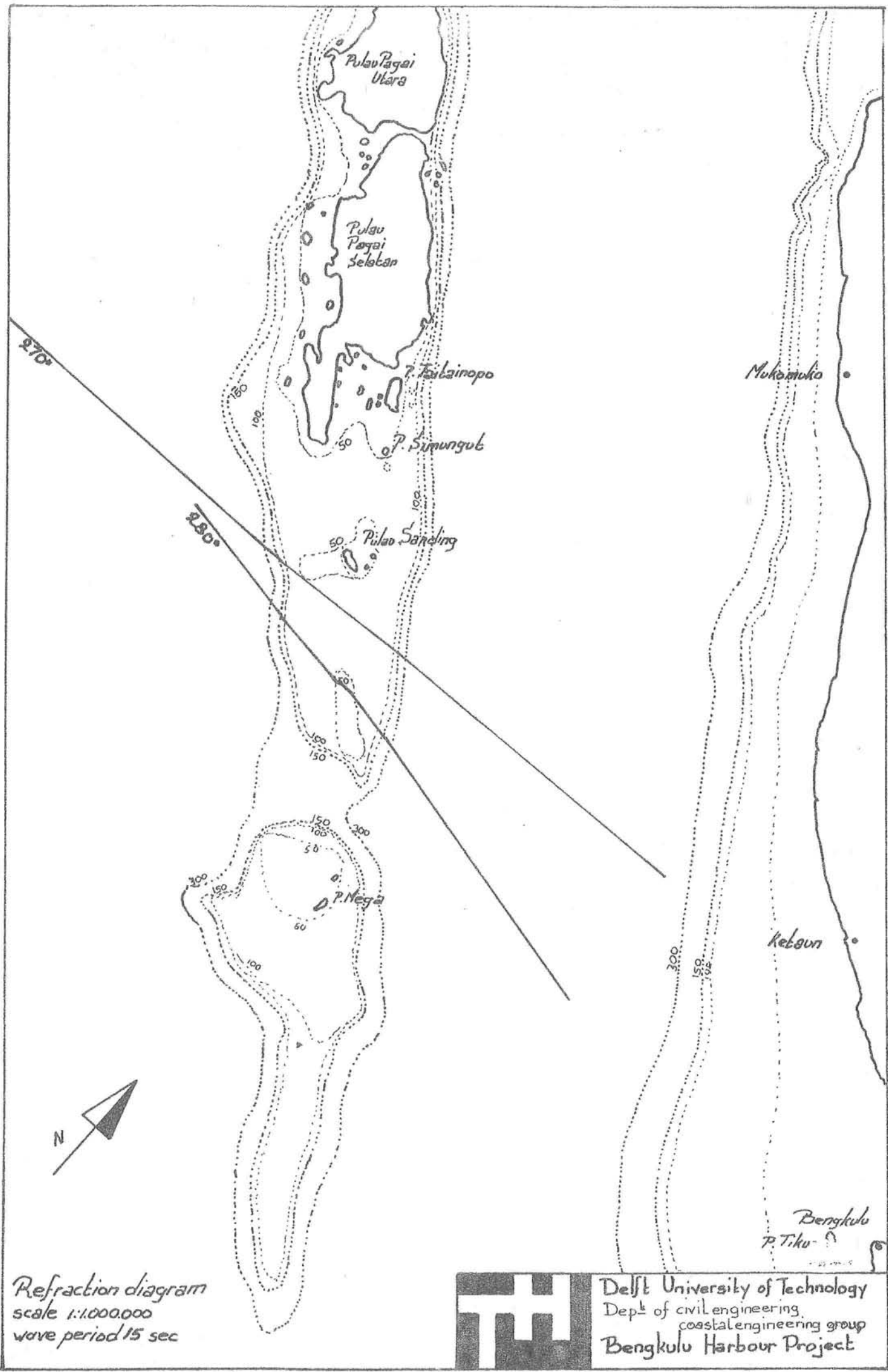


ence at all, because of the geographical position of the Bengkulu harbour. The roadstead of Bengkulu, just north of the harbour, is protected by some reefs west of Bengkulu (Pata Sambilan). Because of these reefs waves from west and south-west cannot reach Bengkulu harbour either. The Bengkulu roadstead has no protection against these waves. Both harbour and roadstead are not protected against waves from northern directions. The coastline north of Bengkulu until Pasar Seblat has a direction of 305° (for the locations of the mentioned towns and villages, see fig. 2.9). So waves may come from this or a more westward direction. Bathymetrics show that waves from 295° to 305° hardly will be refracted to the Bengkulu area. These waves will reach the coast either north of Laïs or south of Pasar Ngalam. Waves with directions between 285° and 295° have a maximum fetch of 200 km. From the south the limitation is 150° . Waves from a more eastward direction will have no influence in the Bengkulu area. The influence of the Enggano isle at 150 km, 170° - 109° , is expected to be small.

For several incoming waves of 7, 10 and 15 seconds refraction is calculated with a ray-refraction computer program. The results of these calculations are presented in vol D.

Diffraction around Tanjung Kerbau can be neglected, diffraction on the Bengkulu roadstead and near Bengkulu harbour is of minor importance. Therefore diffraction is neglected totally for the computation of wave-heights.





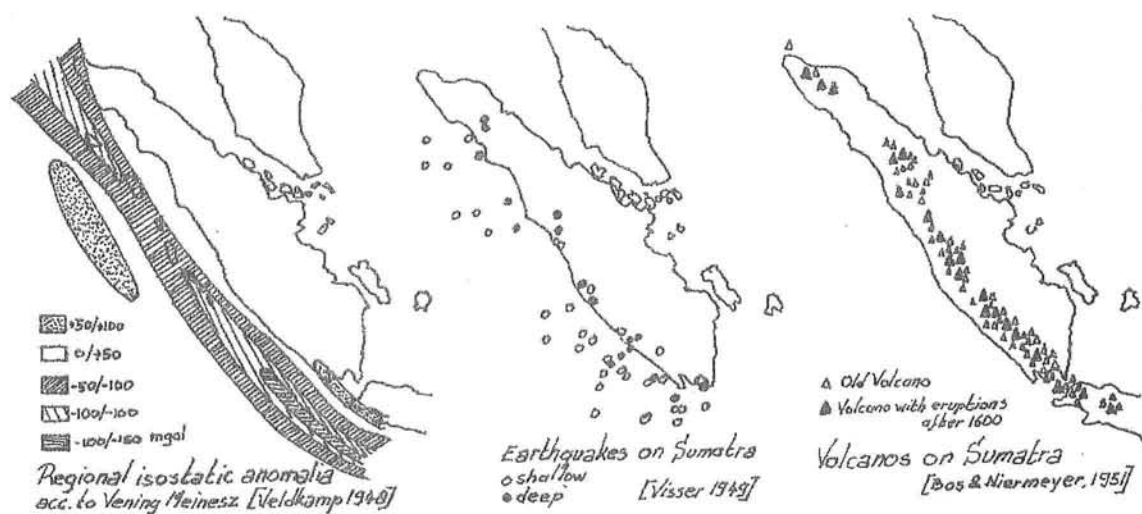
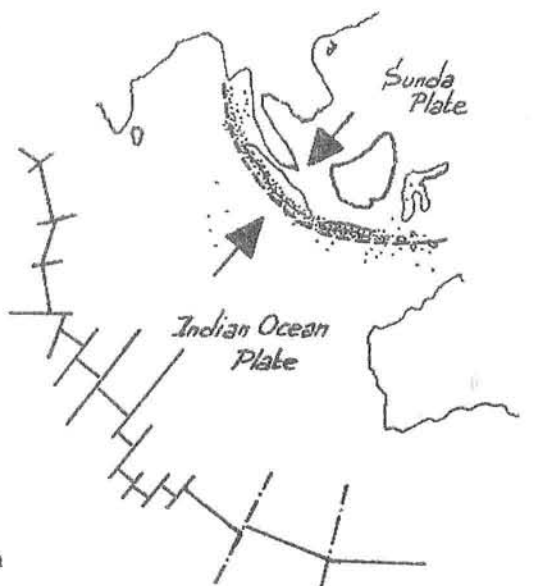
Delft University of Technology
 Dept. of civil engineering,
 coastal engineering group
 Bengkulu Harbour Project

3. Coastal Morphology

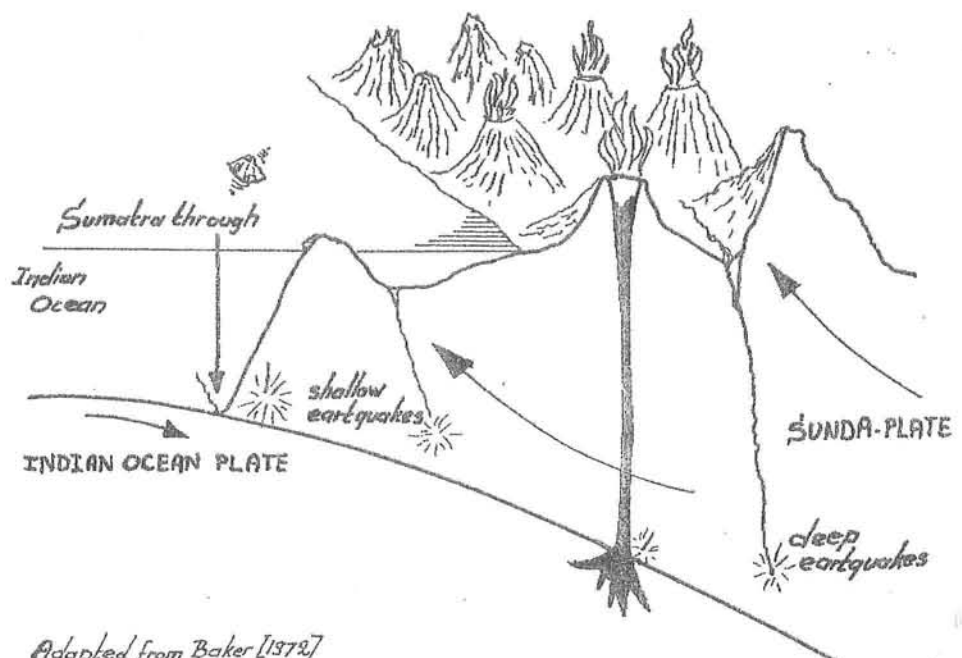
Some geological and geophysical considerations

On the west side of Sumatra a border between two geological plates is found. Geophysical research shows in this area an intense activity of earth-movements. Here the Indian Ocean Plate meets the Sunda Plate. Earthquakes show the edge where the Indian Ocean Plate is forced beneath the Sunda Plate. This system is also recognisable by gravimetry. Gravimetric research by Vening Meinesz showed negative anomalies on the west side of Sumatra.

Together with the locations of earthquakes (deep earthquakes on the eastern side of the fault and shallow quakes on the western side) and the location of the volcanos, they give a good impression of the tectonical system in West Sumatra.



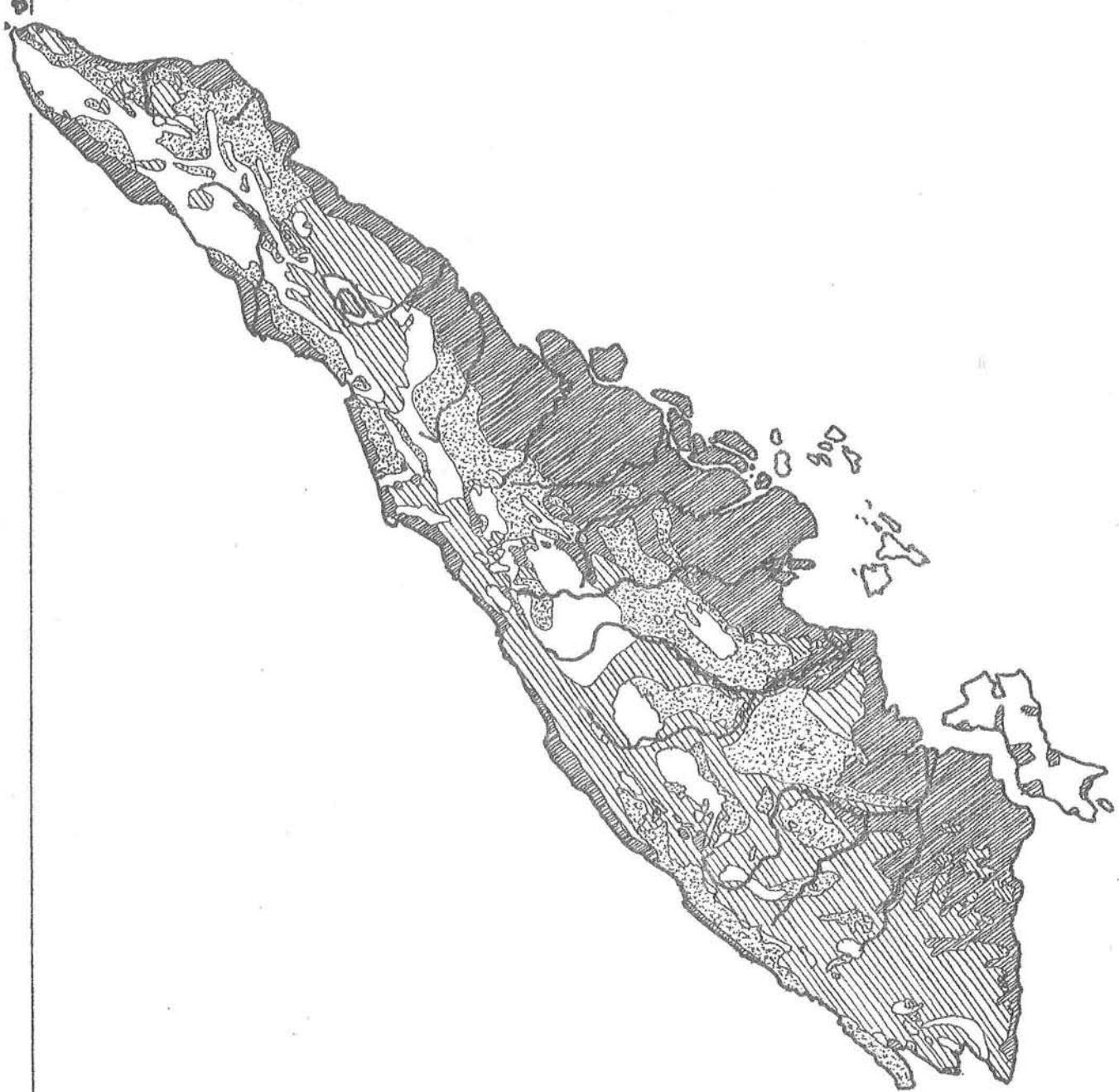
By this tectonical system the west-coast of Sumatra is moved upwards very slowly (slowly from a technical point of view, from a geological point of view it is quite fast). A negative beach propagation, i.e. the coastline moves seaward, is the result of this movement. On the coast a lot of coral reefs can be found several meters above m.s.l. Because the coast is rather steep this negative beach propagation has not caused a large extension of the land.



Adapted from Baker [1972]

On the geological map of Sumatra this area is found as a small quaternary strip along the coast. Near Bengkulu this strip starts south of Pulau Bay.

Observations of Erb (1905) show that the coast is still rising, with a (from a geological point of view) remarkable speed. Verstappen (1973) confirms this and suggests that Bengkulu and Tanjung Kerbau are lying on horsts which are somewhat higher than their surroundings.



█████ quaternary sediments

█████ quaternary and tertiary volcanic deposits

█████ tertiary sediments

█████ older formations

Sumatra
geological
scale 1:2,500,000

Fig 3.6

When indeed Tanjung Kerbau is a horst, it might have been an island in its first stage, like Pulau Tikus nowadays. If this is assumed so, a possibility for the formation of the coast is the following theory:

The separation-line between tertiary and quaternary sediments is regarded as the old coastline (see fig. 3.6). This is nearly a straight line (line I on fig. 3.7). Because of the tombolo effect a sediment-transport between the Kerbau island and the coast was impeded (II). This is assumed to have happened at the beginning of the quaternary. After this had resulted in the formation of a peninsula, the coast will accrete at the updrift side, and will erode at the downdrift side (as will be demonstrated later, resulting transport is directed northward). The result of this accretion is a long straight coastline and a triangular strip of quaternary sediment south of Tanjung Kerbau (III). This strip is also indicated on the geological map (fig. 3.6).

At the downdrift side of Tanjung Kerbau the coast will erode. But in this coast some fixed points exist, viz. Bengkulu cape and Ujung Tjoko. Due to these fixed points a broken coastline develops (because of erosion) (IV, fig. 3.7).

A few hundreds years ago, at the end of the 16th century, the coast south of Tanjung Kerbau reached an equilibrium and accreted no more. From this moment all sediment was transported around Tanjung Kerbau, and the spit started to develop. In those days the depth just behind Tanjung Kerbau was 15 - 20 m. On this submarine plateau the spit was formed.

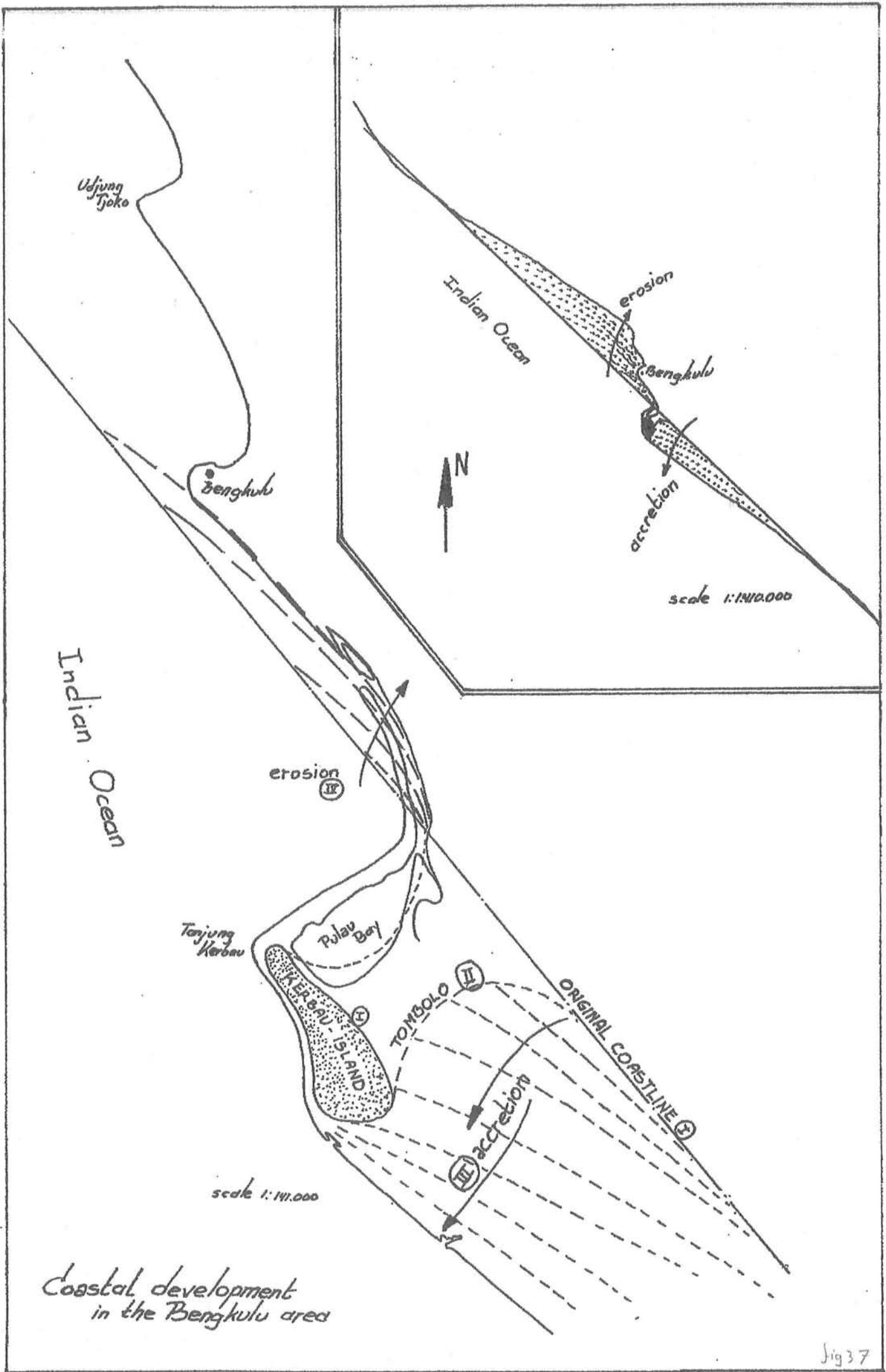
Dynamics of the Bengkulu coast

Morphology can be studied from the available charts, but also from aerial and satellite photographs. We had the opportunity to study a satellite-picture of this area, made by Landsat I in June 1973.

We had four prints, each from a different part of the electromagnetic spectrum. We had two infra-red photos, one from the green part of the spectrum and a photo from the yellow part of the spectrum.

The yellow print gives about the same impression as a panchromatic picture. On the green print submerged banks can be seen. On the infra-red ones the difference between land and water becomes clear. From this picture we have made a morphological map of the coast (fig. 3.9) and a detailed sketch of the mouth of the Air Teluk (fig. 3.13).

From the wave refraction analysis follows (see vol C) that monsoon waves enter the breakerline at the undisturbed coast, for example near Pasar Talo (see fig. 3.8) in June-August out of a southern direction; in the January-March monsoon these waves enter the breakerline out of a northern direction. So there will be a longshore current in a northern direction in the June-August period and a current in the opposite direction in the January-March period



Because of differences in wave height, angle of incidence and period of occurrence the northward current is somewhat stronger than the southward current. Therefore resulting transport will have a northern direction. Observations of visitors agree with this. The first description of the coast by Erb (1905) did already mention this current. Prof. Erb visited the south-western coast of Sumatra between Bengkulu and Belimbingo (near strait Sunda, south Sumatra). He observed a longshore current in northern direction. He found also a lot of pumice-stone. These stones came from the Krakatau eruption in 1883. It is only possible to find these stones there when a resulting transport in northern direction exists. Blocks (ca 3 m^3) are eroded from rocks at the coast, shattered by waves and transported north in pieces to the next beach where erosion of these stones continues. Also most of the river mouths were offset northward. Terpstra (1936) made a statistical analysis of these river offsets and confirmed the idea of a northward bound longshore current.

On general oceanographic maps (KNMI 1952) an ocean current is indicated in a southern direction, but this is a current outside the breakerzone.

On the satellite pictures the influence of both currents can be seen very well, specially along the undisturbed coast from Tanjung Kerbau to Manna.

The undersea banks are clearly influenced by currents (fig. 3.8)

The June August Monsoon period

In the June-August monsoon period a lot of sand is transported along the coast in a northern direction, due to the

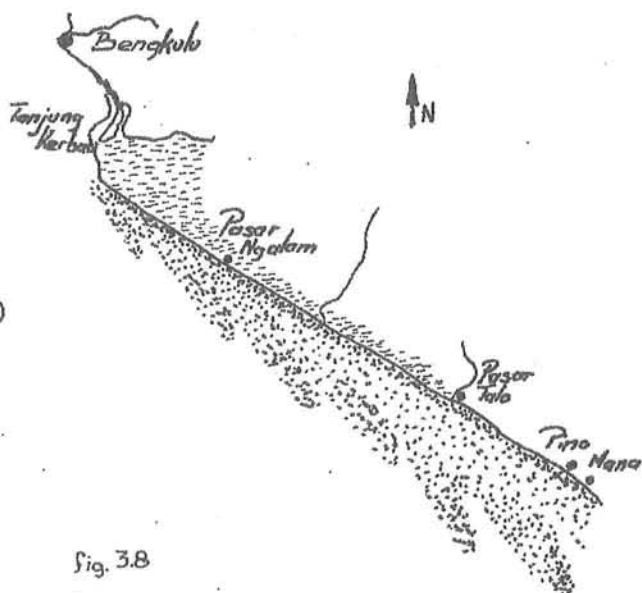
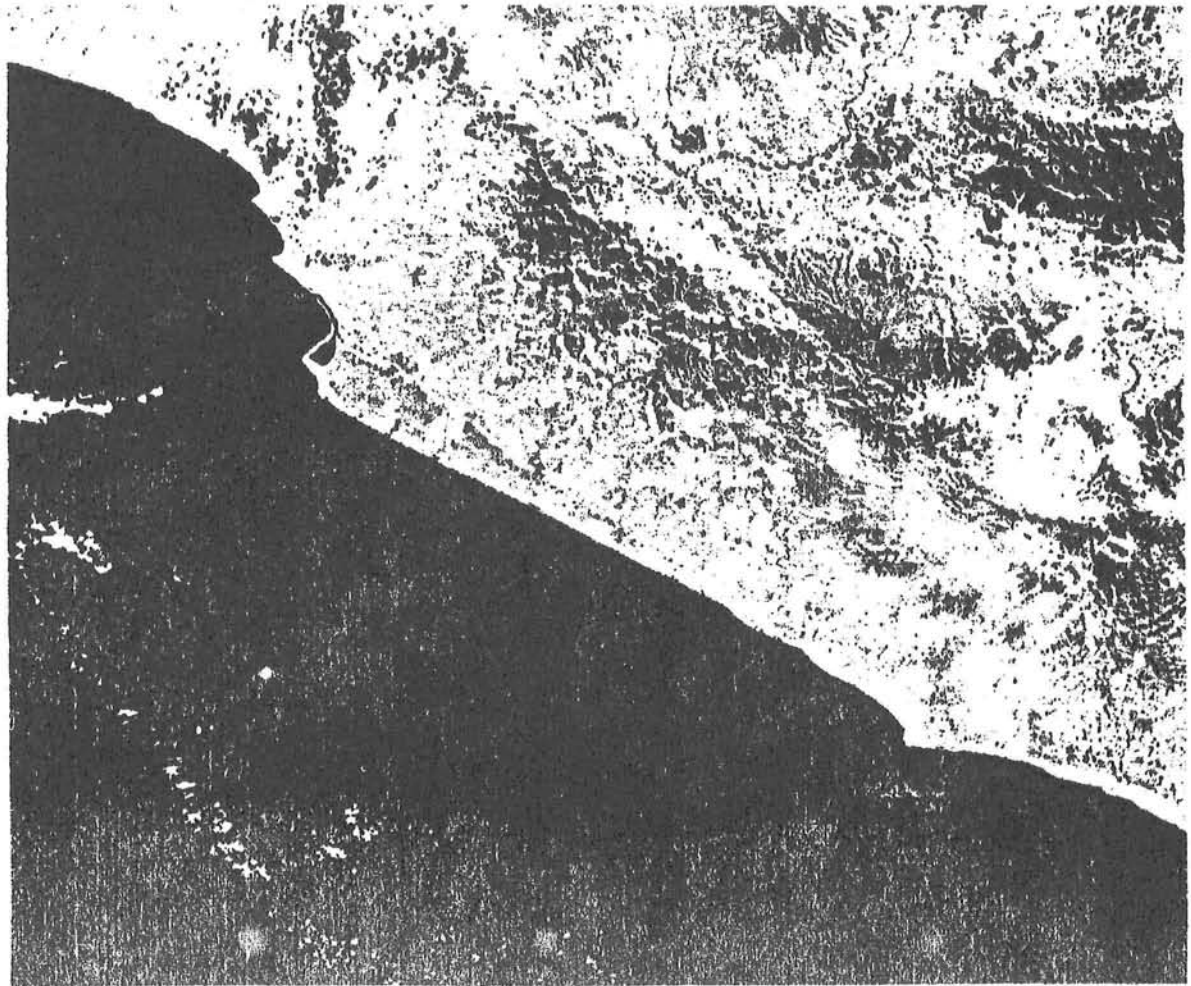
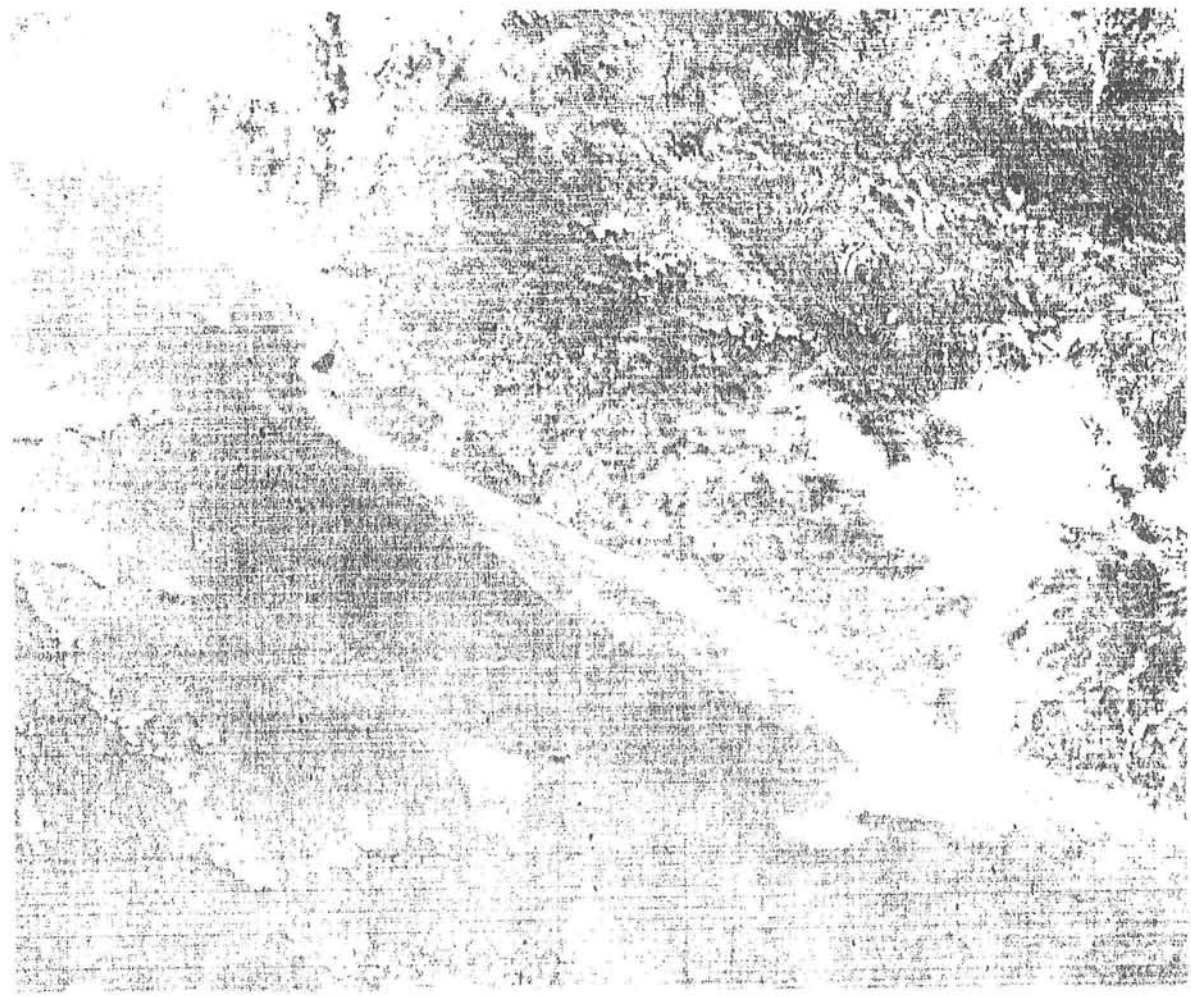


Fig. 3.8

just mentioned longshore current. Coming from the south the coast turns east at Tanjung Kerbau. Therefore the current stops and sand is dumped near a (see fig. 3.9; for convenience of the reader a 1:100000 print of this map is added to this report). This accretion area is visible on the satellite pictures, but can also be found on the charts.

In this period nearly no waves enter the breakerline along the Pulau Bay spit. Hence no wave induced longshore current will develop. Because of differences in wave-setup the local mean water level (MWL) along the coast will rise. This elevation of the MWL is a function of the wave height. Waves along the spit are lower than waves near f because of diffraction and

Landsat-picture E 1325-02491



spaced

infra-red

13 JUN 73
11000760

refraction. Therefore the MWL near f is higher than the MWL near e and d, and so a current will develop from f to e. It is to expect that this current will have a very low velocity, because of the long distance from f to e (a velocity less than 10 cm/sec). North of the mouth of the Air Teluk (from f to g) waves enter the breakerzone at an angle. Hence a current will be generated by the radiation stress.

Boths of these currents are able to transport sand. The sand is brought in suspension by the incoming waves and thereupon transported with the currents. Bottom and banks are therefore eroded near b, and most of this sand is transported in a northern direction to the Bengkulu cape (g, see fig. 3.10). There the situation is quite similar to the situation at Tanjung Kerbau, so sand will be dumped there. Because of the presence of reefs the situation is more complicated. Waves from a southern direction usually break on the reefs near h. The remaining waves will probably break on the coastal reef g (fig. 3.10).

Hence there are two breakerzones. Longshore currents will originate on the reef near g and directly along the coastline.

Because after Bengkulu cape nolonger a propulsing force exists, sand will settle at j.

January-March monsoon period

In the January March monsoon period wind waves come from western and north-western directions, swell is still coming from the south. Wind waves induce a radiation stress and so a longshore current along the Pulau Bay spit from Tanjung Kerbau to the mouth of the Air Teluk. Also a current starts in Bengkulu going to the same mouth.

This system of currents will erode the accretion near a (fig. 3.9) and transport the sand along the Pulau Bay spit. Near b the current stops and sand will be dumped there. This sand is transported to the Bengkulu cape in the other season.

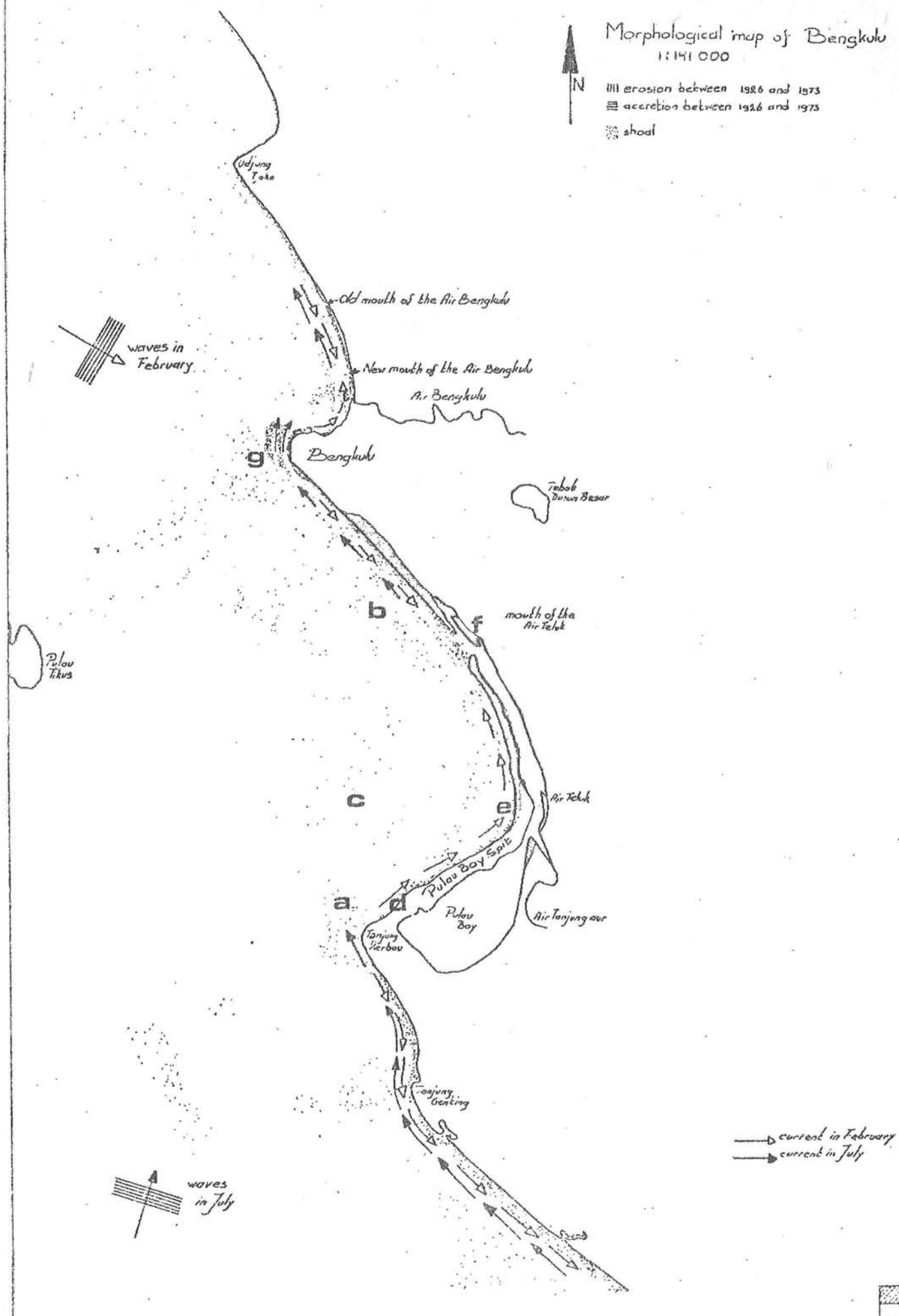
Along the Pulau Bay spit a shallow channel exists. This channel can be seen on the satelite pictures, but it is also possible to find it on the charts. The Dutch hydrographic chart indicates a rather flat bottom in this area with a depth of 16-18 m. But there are only few soundings and they are all taken from ships. The Dwidelta chart was made by soundings from a land base. Soundings started at the coast and sounding was continued until a depth of 20 m was reached. Then sounding was stopped. On the chart the impression is given that the whole area has a depth of 20 m. As can be seen from the satelite picture both charts are right and wrong. From the sounding data the conclusion can be made that this channel has a depth of 2 m below the surrounding bottom.

Near Bengkulu an identical current is generated as along the Pulau Bay. This longshore current erodes the accretion near j and transports the sediment along the harbour (fig. 3.10).

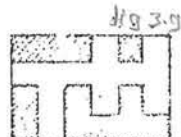
Morphological map of Bengkulu
1:141 000

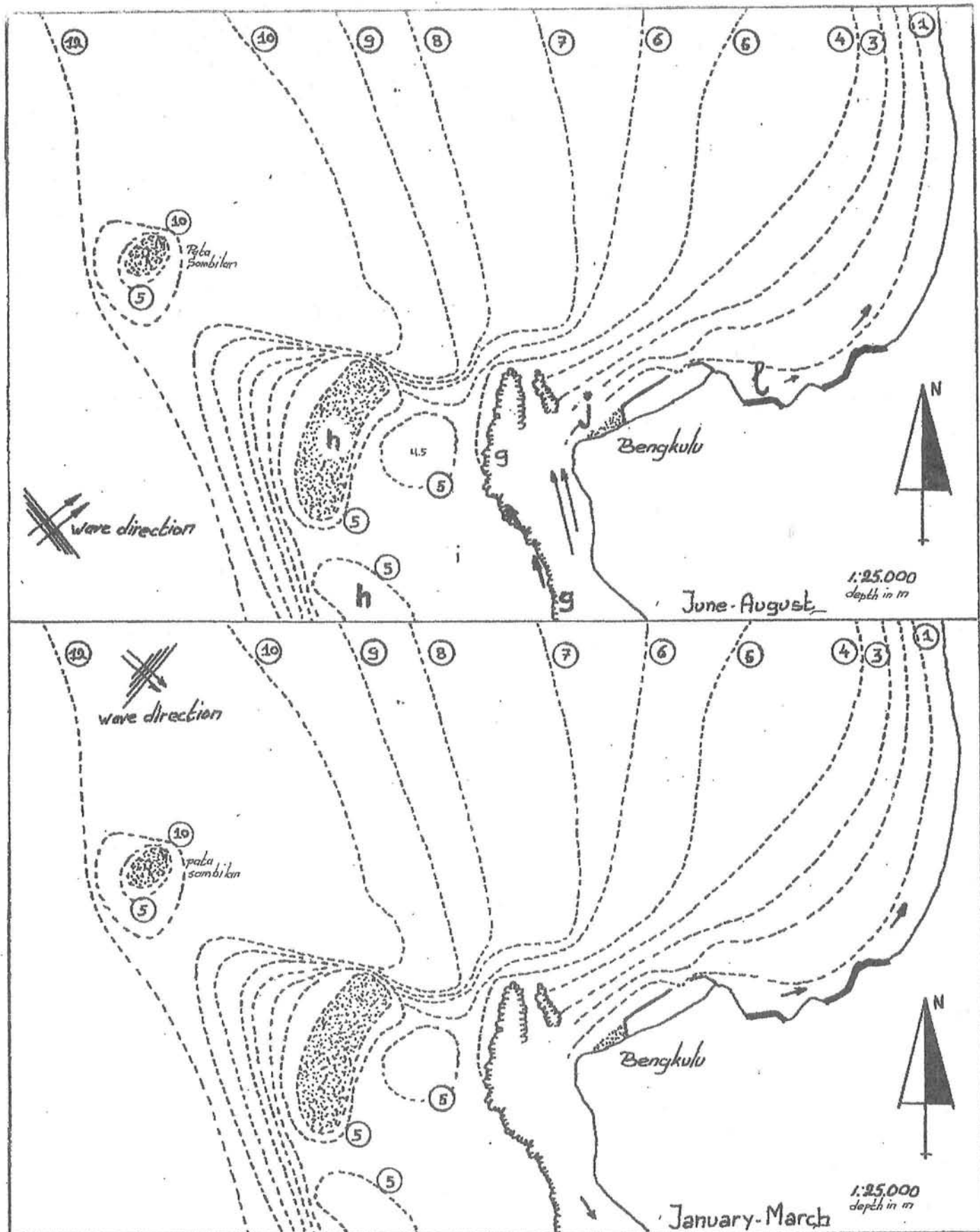


III erosion between 1926 and 1973
II accretion between 1926 and 1973
shoal



For convenience of the reader a 1:100 000 version of this map is added to this report





Currents near Bengkulu harbour

fig 2.10



Delft University of Technology
Dept¹ of civil engineering
coastal engineering group
Bengkulu harbour project

Just east of Bengkulu harbour there will be a wave induced current in eastern direction (near λ , fig. 3.10). This current exists also in the June-August monsoon period because waves from the south are refracted intensely by the reefs west of Bengkulu.

This indicated current will also erode the coast. Deposits from dredging activities in the harbour were removed by this current. This current also forms a spit in front of the mouth of the Air Bengkulu and this mouth will be offset in northern direction. (fig. 3.9).

The origin of the sand spit

Model investigations by Meistrell (1966) indicate that in the formation of spits three stages can be distinguished. First a submerged part is

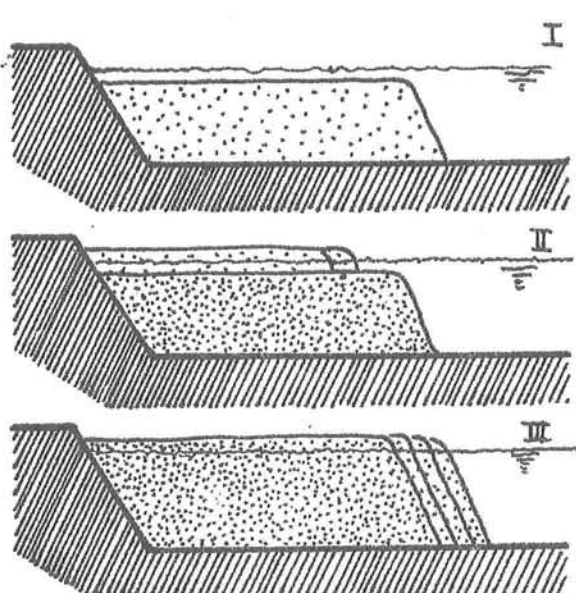


Fig. 3.11

formed. This submerged part will not rise above the water level directly. Evans (1942) stated that rising of the spit above the water level is only possible when the submerged part of the spit has a reasonable width. This wide, submerged part is called platform by Meistrell. In the second stage a dry spit is formed on this platform. In the third stage this dry spit can grow in length. These stages are also distinguishable at the Pulau Bay spit.

So it is to be expected that after the sediment could pass Tanjung Kerbau such a submerged platform was formed. After an unknown number of years this platform was wide enough for the formation of a dry spit. This happened around 1820.

From this moment the dry spit grew with a remarkable speed on the platform. About 30 years later the spit had covered the platform totally. When the spit had reached the coast, spit formation should have been finished after closing the Pulau Bay in normal situations. But the Air Tanjungaur debouches into the Pulau Bay and its discharge has to flow to the sea. Also a tidal prism of Pulau Bay (about $5\ 000\ 000\ m^3$) causes a small current (ca. $0.5\ m/s$). These currents were responsible for a gap between the spit and the coast. Hence the spit was bent north, and continued growing. A platform was no longer necessary because the spit grew in shallow water, just in front of the beach.

— Dwidelta, 1975
— Dwidelta, 1970
— Topographical map, 1926
— Naval Chart, 1918
— Naval Chart, 1856

scale 1:53.000

1975

1970

coastline of 1975 unknown
see also sketch from Landsat
picture (1973)



Growth of the Pulau Bay spit

1926

1918

1856

1910

Pulau Bay

Tanjung Kerbau

Air Teluk

Fig 3.12



The tidal current and river discharge eroded the old coast somewhat. From maps the total volume of the spit can be computed:

period I (until 1856)	accreted volume	$41.6 \times 10^6 \text{ m}^3$	(= $0.4 \times 10^6 \text{ m}^3/\text{year}$)
period II (until 1915)	accreted volume	$19.3 \times 10^6 \text{ m}^3$	(= $0.3 \times 10^6 \text{ m}^3/\text{year}$)
period III (until 1975)	accreted volume	$23.0 \times 10^6 \text{ m}^3$	(= $0.4 \times 10^6 \text{ m}^3/\text{year}$)

The first period is estimated to be 100 years, because both on the Valentijn (1726) as on the Raffles (1810) map no sand spit is recognised. But it is to expect that in the days of Raffles the submarine platform already was formed. Soundings on the Raffles-map are not detailed enough to recognize such a submerged platform.

The accretion in period III is $0.44 \times 10^6 \text{ m}^3/\text{year}$ (at the sea-side of the spit) and an erosion of $0.04 \times 10^6 \text{ m}^3/\text{year}$ (at the bay-side of the spit). Hence the feeding transport is at least $0.44 \times 10^6 \text{ m}^3/\text{year}$. It has to be noted that in the area north of the spit the coast also accreted somewhat in period III. On the satellite picture a changement of the coastline of about 350 m is visible. The length of this accretion is 5 km, the average depth is 10 m, So in period III $350 \times 5000 \times 10 = 17.5 \times 10^6 \text{ m}^3$ accreted north of the spit.

Because in the last 200 years hardly anywhere along the spit erosion occurred, and sand is transported along the coast to the edge of the spit without causing accretion, it is to be expected that this coast is in a situation of dynamical equilibrium (the spit grew only at its end).

In the Dwidelta report some erosion near d (fig. 3.9) was ascertained, but as can be seen on fig. 3.12 on this site the coast has grown since 1918. Hence it is to suppose that this erosion is only temporary.

Also the surveyors of the Topographical Service had problems with a moving coastline at this point (see chapt. 2). This phenomenon is caused by the fact that in one season sand is dumped near a and d, and that sand is transported along the spit in the other season.

A similar effect is also mentioned by Zieck (1932) as described in chapter 2.

Sand for growing of the spit from e to f (see fig. 3.9) is supplied by the February longshore current. But this current stops near f. In this area also sand is deposited from the southward current from g. In the July period this sand is carried away by an other current. But transport along the coast near f is low. So a large, but low sediment plateau will be build up here. Hence it is to expect that the mouth of the Air Teluk will stay at about the same site as nowadays, and therefore it is also to expect that the spit will not grow very much.

In 1918 the connection between Pulau Bay and the Indian Ocean was a short channel with nearly no hydraulical resistance. Because the spit grew, this channel got longer, hence the hydraulic resistance increased. This is the

reason why the influence of the tide is less nowadays than it was in 1918. So it is possible that in periods of low river discharge the mouth of the Air Teluk is nearly closed by a bar. This bar can be seen very well on the satellite picture (the sketch of this mouth is made from the satellite - picture).

Behind the bar and the spit a flooded marshy area can be seen. In this area water from the Air Teluk watershed is collected in time of low discharge. This water seeps through the spit to the ocean. In periods of large discharge the bar is carried away by the current. After the high run-off the bar is restored. Erb (1905) describes a similar system for several rivers in this area.

The bar is probably built up from the northern edge of the Pulau Bay spit and from the southern edge of a spit north of the rivermouth.

There is a possibility that the spit will break at an other site between e and f than at the present mouth. Such a break-through occurred also at other rivers in this region.

Recently the Air Bengkulu has made such a new mouth south of the original mouth.

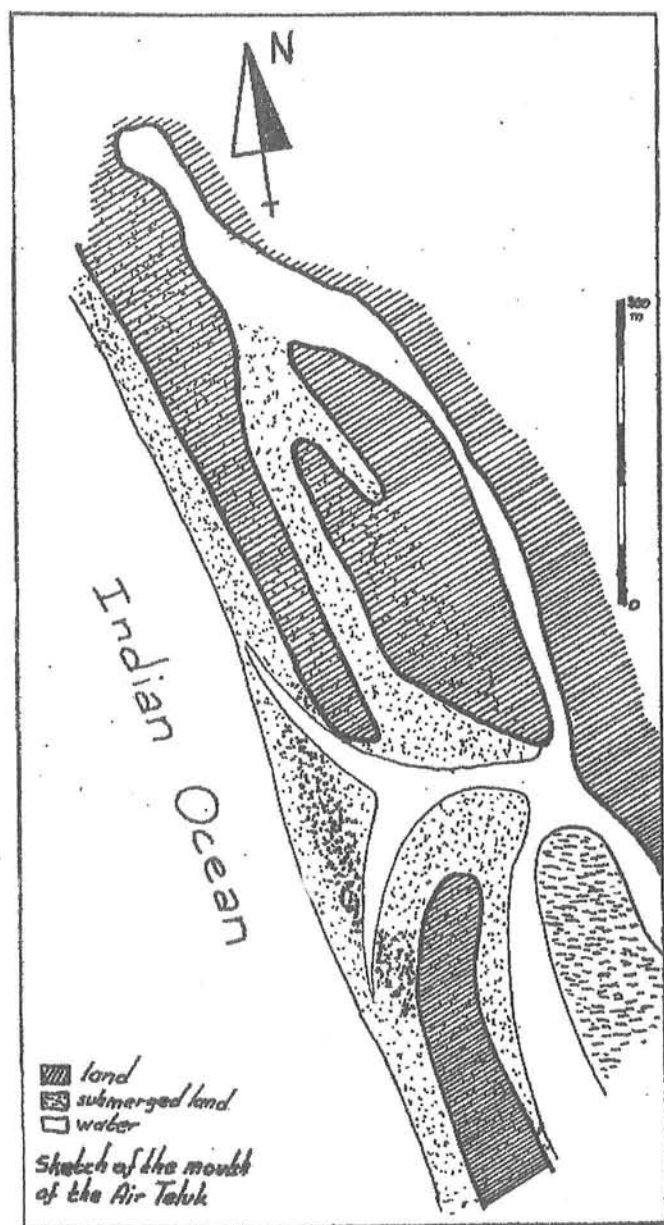


Fig. 3.13

4. Calculation of sediment transport

Introduction

Sediment transport along the coast is computed with the computer program, described in vol b.

The necessary input data are:

- a. Wave height (see chapter 2)
- b. Refraction (see vol d)
- c. Sediment distribution (see next section)

Calculation is carried out for nine cross-sections along the coast. The results of these computations are presented in fig. 4.2.

Sand of the Bengkulu beach

Six samples of beach material of the Bengkulu coast were received. These samples were sieved with the organic material (mostly lime from shells and coral). The exact percentage of organic material of sample nr. 3 was determined, viz. 11.9 % of the total weight was of an organic origin.

The density of the sample was 2.58, hence the density of the lime-particles has to be 2.14, assuming a sand density of 2.65.

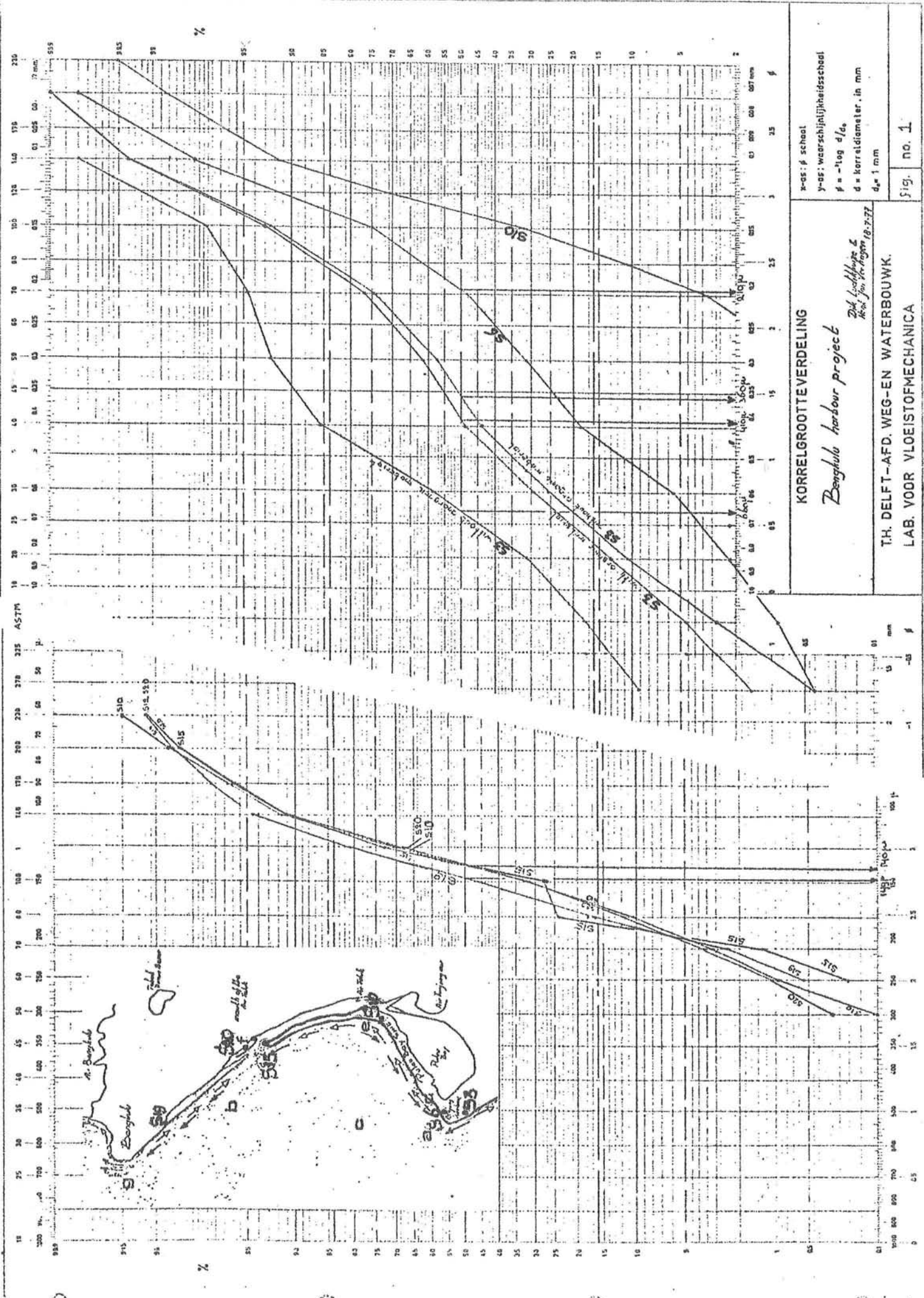
The distribution of both the organic and the anorganic part of sample S3 is given in fig. no. 1 (sample S3a is sample 3 after the organic material had been removed). The lime-percentage of the other samples is not determined exactly, but only one of these samples (S6) contains some organic material.

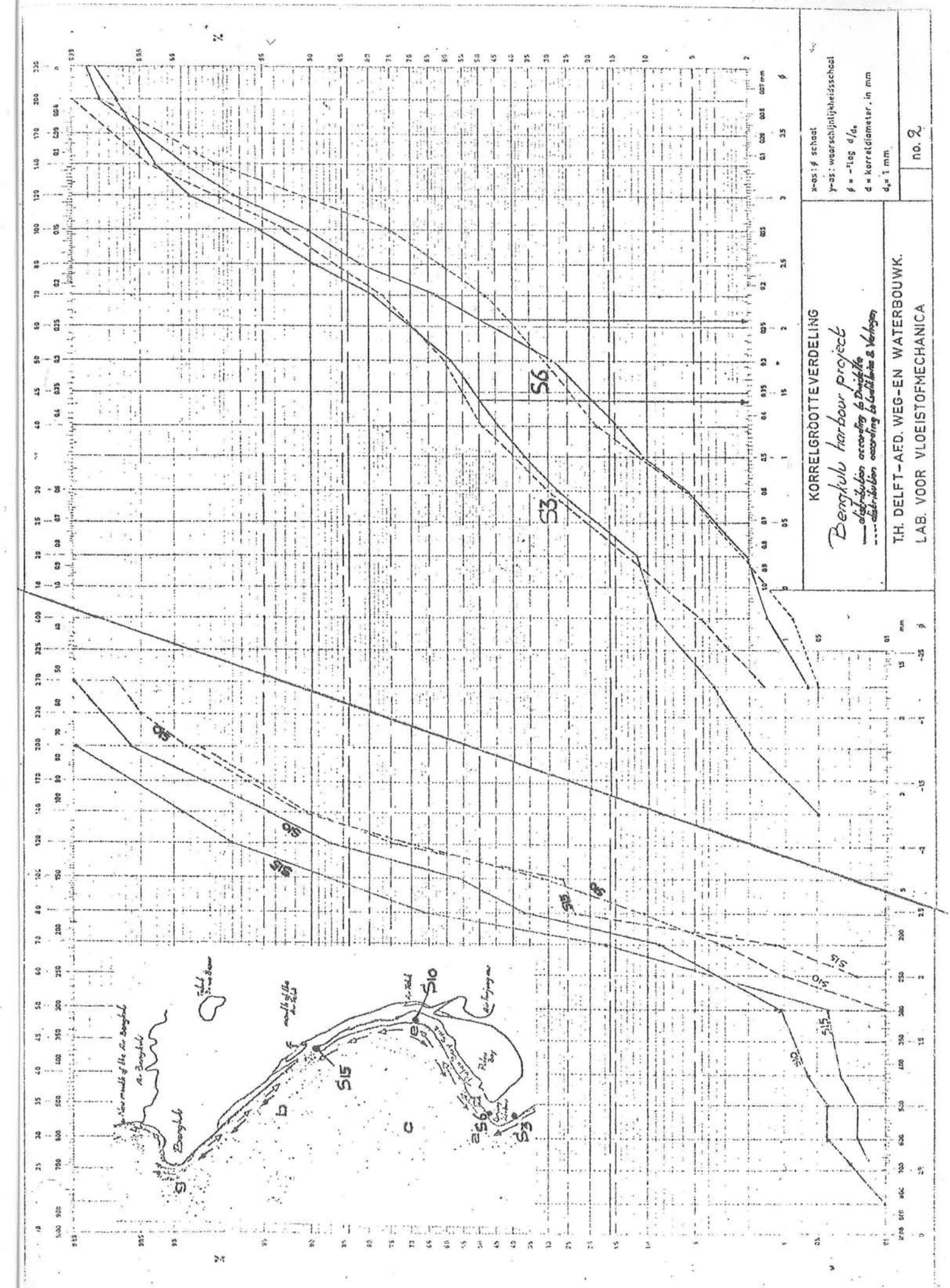
The grain size distribution of samples S10, S15, S19 and S20 is nearly the same, the sand near Tanjung Kerbau is much coarser due to the heavy breakers on this cape. Probably the finer fraction is transported around the cape as suspended load. The sand of sample S19 is also somewhat coarser than S20, S15 and S10. The wave height on this location might be somewhat higher than it is southward of this location.

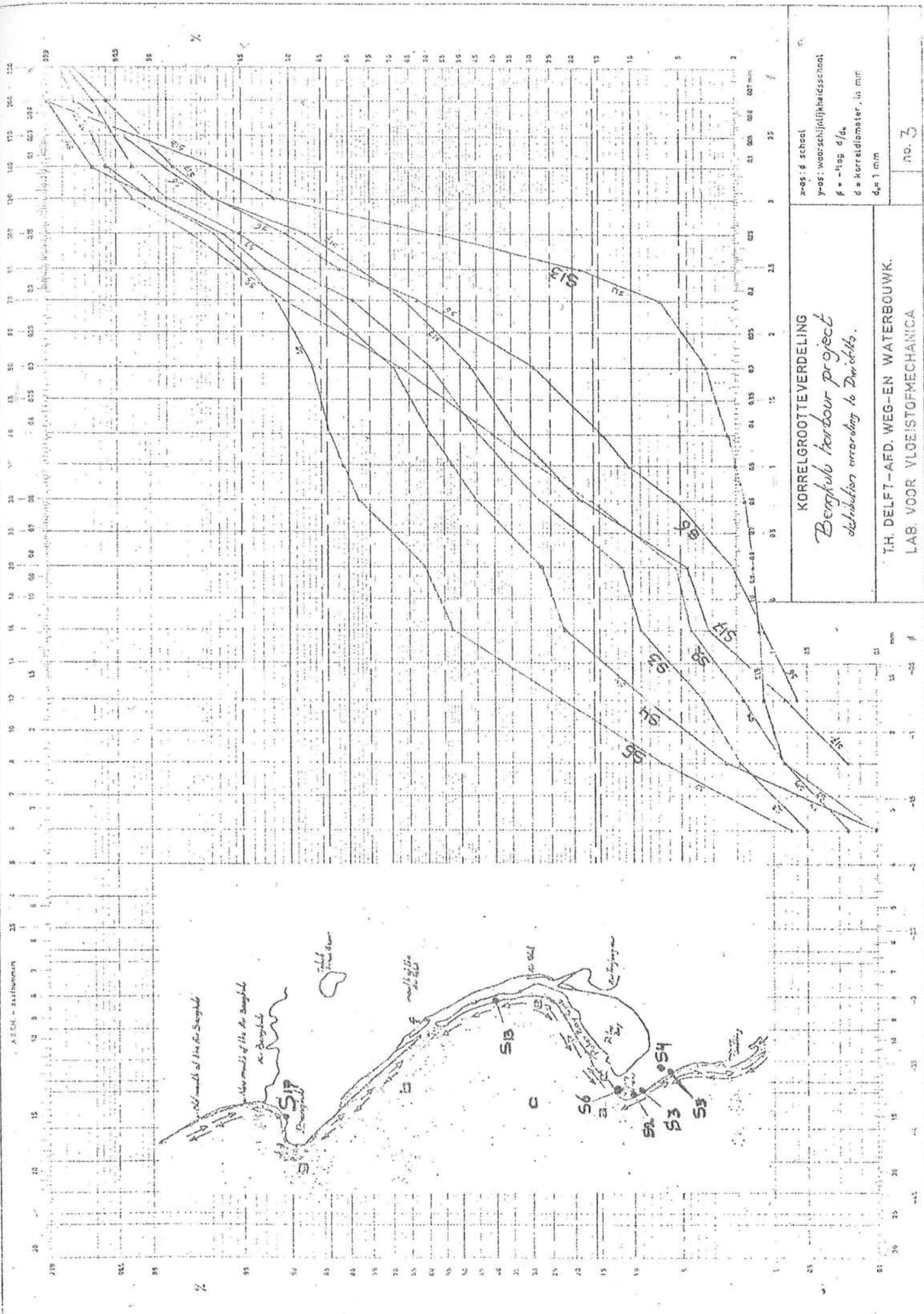
Summary of the distribution data

sample	d_{50}	d_{84}	d_{16}	σ
S3	410 μ	780 μ	190 μ	495 μ
S3 (anorgan)	360 μ	730 μ	184 μ	457 μ
S3 (organic)	660 μ	1210 μ	430 μ	820 μ
S6	210 μ	450 μ	132 μ	291 μ
S10	140 μ	160 μ	112 μ	136 μ
S15	140 μ	176 μ	112 μ	144 μ
S19	149 μ	170 μ	122 μ	146 μ
S20	140 μ	160 μ	112 μ	136 μ

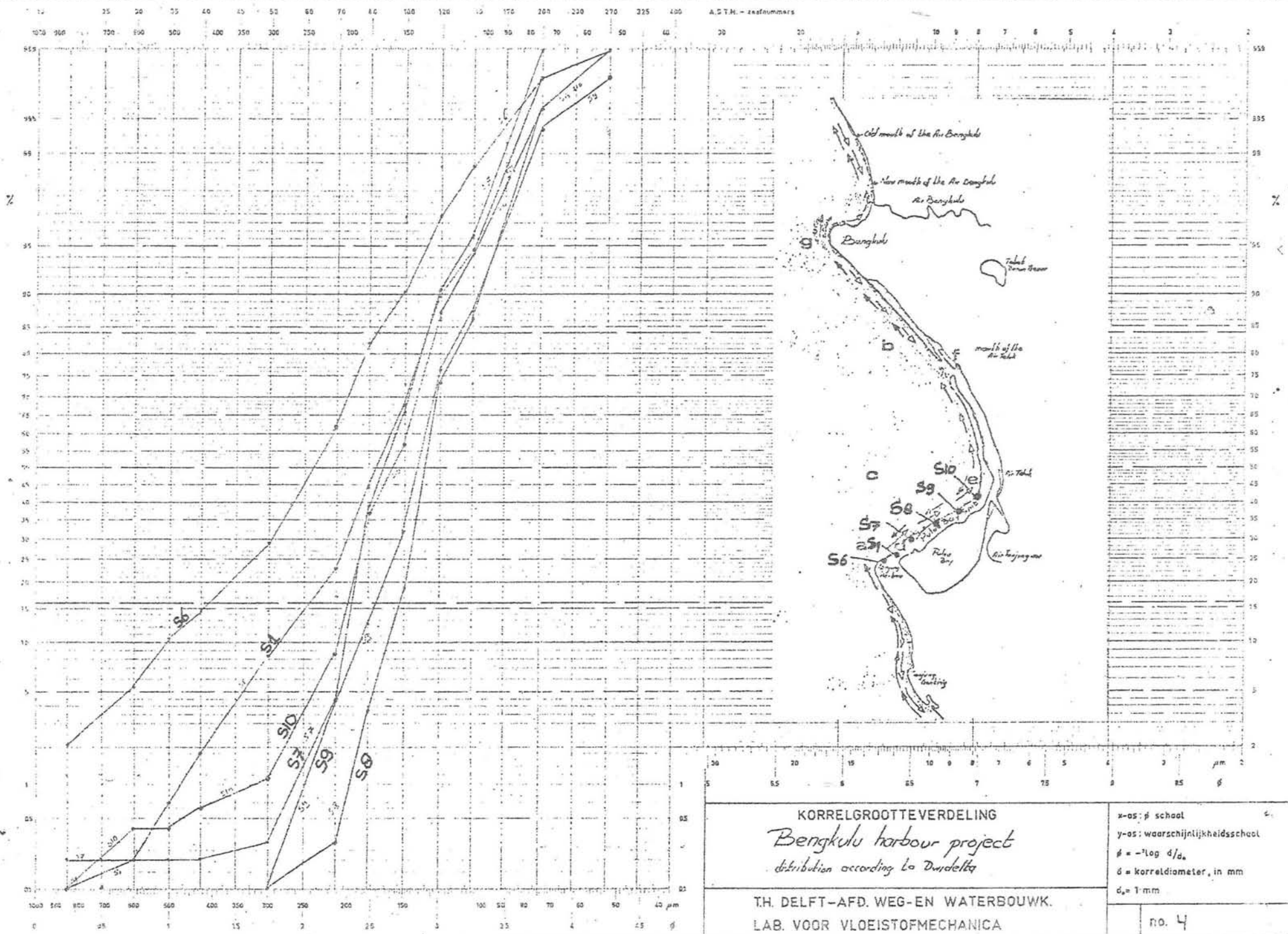
σ is the standard deviation of grain-sizes of the analysed sample. This value gives a measure of the uniformity of the grains.

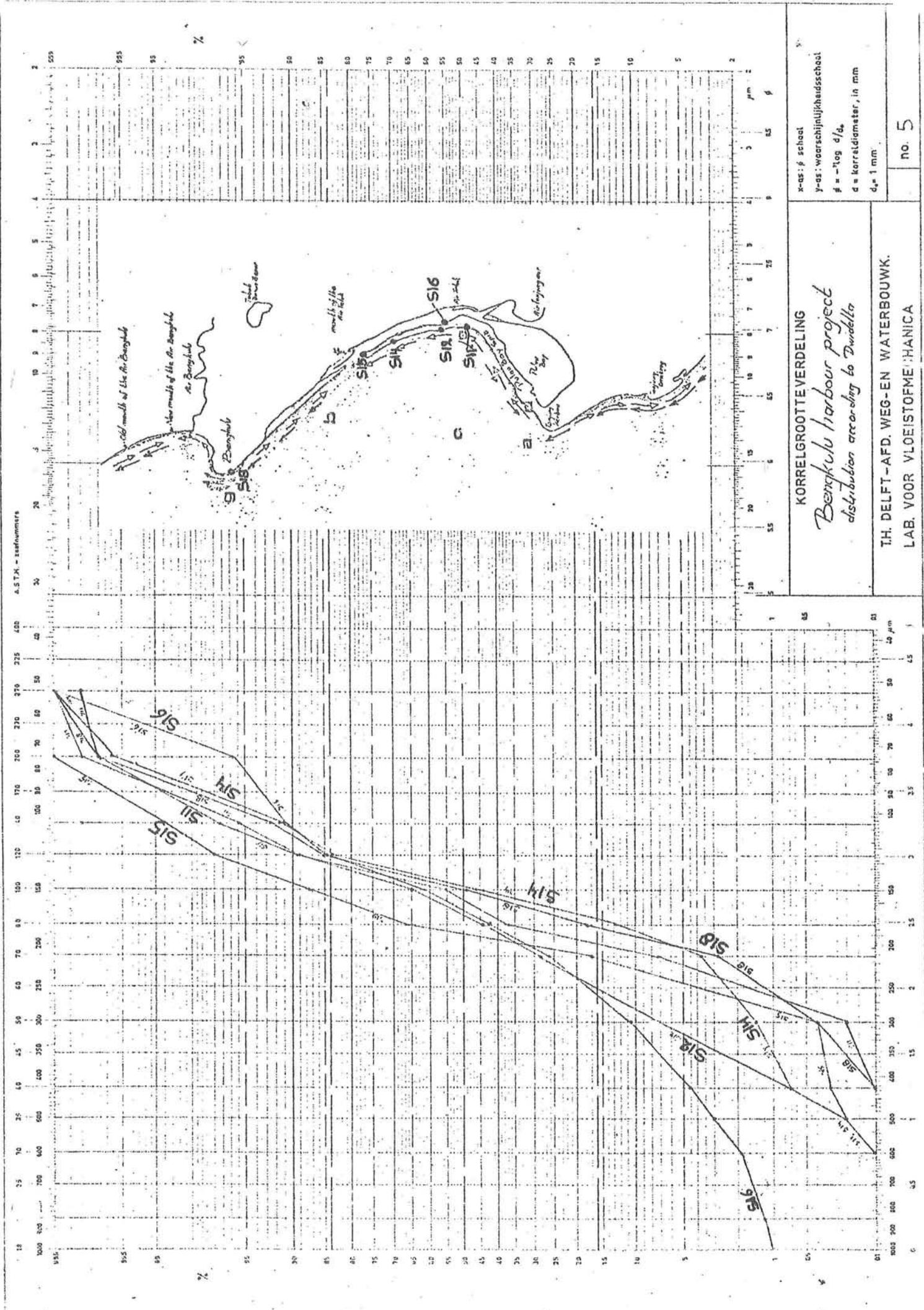






46





Comparision with other data

The Dwidelta corp did analyse also the other samples. These distributions are presented in diagram 2 - 5.

The Dwidelta analysis gives a result which is somewhat courser. This is probably caused by a manual sieving procedure and a percentage of moisture which was not zero.

Very clear is also (see fig. no. 3) that the data of sieve nr. 20 are incorrect. Too much sand passes through this sieve.

But in general the results are identical to the results obtained by sieving in Delft.

Grain sizes to be used in the sand transport formula

As can be seen from the summary of the distribution data for samples S10 - S20, one can calculate with a D_{50} of 150 μ . Samples S3 and S6 seem to be coarser, but one may expect that here also a fine fraction exists, but this fraction cannot settle because of breaker activity.

Hence in the following sand transport calcualtion a D_{50} of 150 μ is used and an D_{90} of 190 μ .

Input data

The required input (wave)data for the computer program are:

-breakerheight	
-period	of the first system of waves (monsoon-waves)
-angle of incidence	
-breakerheight	
-period	of the second system of waves (swell-waves)
-angle of incidence	

These data are determined in two steps. First the angle of incidence and the wave height are determined as close as possible to the breakerline (as far as it is allowed to use the computer program) see vol d. Then, starting with these data the breakerdepth and the waveheight and angle of incidence on the breakerline are computed, now assuming parallel depth contours.

In the next table the results of chapter 2 are summarized

seasons		T_{01}	T_{02}	H_{01}	H_{02}	ϕ_{02}	ϕ_{02}
Dec, Jan Feb;	season 1	10	15	1.2	0.3	285°	200°
Mar, Apr, May;	season 2	7	15	1.0	0.4	180°	200°
Jun, Jul, Aug;	season 3	10	15	1.3	0.5	180°	200°
Sep, Oct, Nov;	season 4a	7	15	1.0	0.4	180°	200°
Sep, Oct, Nov;	season 4b	7	15	1.2	0.4	285°	200°

T_{01} is the wave period (in sec), H_{01} the wave height (H_{rms} in m) and ϕ_{01} the direction on deep water of the monsoon waves. The suffix 02 indicates swell waves on deep water. With T_0 and ϕ_0 the refraction diagrams are calculated (vol d).

The first step

With these refraction diagrams the refraction coefficient ($K_r^{2\ddagger}$) and the angle of incidence (ϕ^\ddagger) is determined in front of the coast (at a depth h^\ddagger) for the different waves. The sign of ϕ^\ddagger indicates the direction of

the resulting transport due to these waves. A plus (+) sign means that the direction of the transport caused by these waves is northerly. See also adjacent figure.

For the locations of the cross-sections

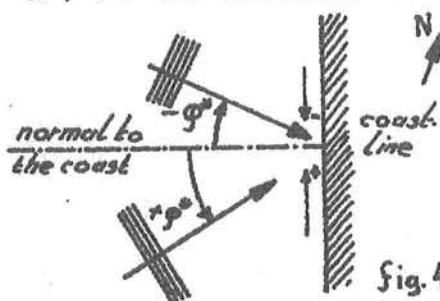


Fig. 4.1 see fig. 4.2. Depths in m.

Cross-section I direction of the coast 305°

line perpendicular to the coast 215° (seaward)

season	ϕ_1^\ddagger	ϕ_2^\ddagger	h_1^\ddagger	h_2^\ddagger	$K_r^{2\ddagger}$	$K_r^{2\ddagger}$
1	-70°	$+15^\circ$	deep	deep	1.0	1.0
2	$+35^\circ$	$+15^\circ$	deep	deep	1.0	1.0
3	$+35^\circ$	$+15^\circ$	deep	deep	1.0	1.0
4a	$+35^\circ$	$+15^\circ$	deep	deep	1.0	1.0
4b	-70°	$+15^\circ$	deep	deep	1.0	1.0

Cross-section II direction of the coast 320°

line perpendicular to the coast 230° (seaward)

season	ϕ_1^\ddagger	ϕ_2^\ddagger	h_1^\ddagger	h_2^\ddagger	$K_r^{2\ddagger}$	$K_r^{2\ddagger}$
1	-30°	$+15^\circ$	12	12	0.6	0.3
2	$+32^\circ$	$+15^\circ$	10	12	0.55	0.3
3	$+20^\circ$	$+15^\circ$	10	12	1.0	0.3
4a	$+32^\circ$	$+15^\circ$	10	12	0.55	0.3
4b	-40°	$+15^\circ$	10	12	0.7	0.3

Cross-section III direction of the coast 50°

line perpendicular to the coast 320° (seaward)

season	ϕ_1^\ddagger	ϕ_2^\ddagger	h_1^\ddagger	h_2^\ddagger	$K_r^{2\ddagger}$	$K_r^{2\ddagger}$
1	$+30^\circ$	-	10	-	0.5	-
2	-	-	-	-	-	-
3	-	-	-	-	-	-
4a	-	-	-	-	-	-
4b	$+32^\circ$	-	10	-	0.75	-

Cross-section IV direction of the coast 60°

line perpendicular to the coast 330°

season	ϕ_1^\ddagger	ϕ_2^\ddagger	h_1^\ddagger	h_2^\ddagger	$K_r^{2\ddagger}$	$K_r^{2\ddagger}$
1	$+30^\circ$	-	10	-	0.6	-
4b	$+40^\circ$	-	10	-	0.9	-

Cross-section V		direction of the coastline				355°
		line perpendicular to the coast				265°
season	ϕ_1^*	ϕ_2^*	h_1^*	h_2^*	$Kr_1^* 2$	$Kr_2^* 2$
1	+10°	-	5	-	0.75	-
Cross-section VI		direction of the coastline				330°
		line perpendicular to the coast				240°
season	ϕ_1^*	ϕ_2^*	h_1^*	h_{21}^*	$Kr_1^* 2$	$Kr_2^* 2$
1	-	+20°	-	10	-	0.4
2	+15°	+20°	5	10	0.25	0.4
3	+20°	+20°	10	10	0.5	0.4
4a	+15°	+20°	5	10	0.25	0.4
4b	-	+20°	-	10	-	0.4
Cross-section VII		direction of the coastline				315°
		line perpendicular to the coast				225°
season	ϕ_1^*	ϕ_2^*	h_1^*	h_2^*	$Kr_1^* 2$	$Kr_2^* 2$
1	-25°	0	5	5	0.5	0.6
2	+12°	0	5	5	0.35	0.6
3	+5°	0	5	5	1.0	0.6
4a	+12°	0	5	5	0.35	0.6
4b	-40°	0	10	5	1.0	0.6
Cross-section VIII		direction of the coastline				60°
		line perpendicular to the coast				330°
season	ϕ_1^*	ϕ_2^*	h_1^*	h_2^*	$Kr_1^* 2$	$Kr_2^* 2$
4b	+35°	-	5	-	1.0	-
Cross-section IX		direction of the coastline				350°
		line perpendicular to the coast				260°
season	ϕ_1^*	ϕ_2^*	h_1^*	h_2^*	$Kr_1^* 2$	$Kr_2^* 2$
1	+5°	-	5	-	0.98	-
4b	-25°	-	∞	-	1.0	-

With the above data the input-data for the computer program can be calculated, viz.

- h_{br} - breakerdepth
- γ - breakerindex
- ϕ_{br} - breakerangle
- r - ripple factor

The second step

For the calculation of h_{br} and ϕ_{br} is assumed that the depth contours are parallel to the coastline; this is a reasonable assumption.

To simplify the calculations, the input data are calculated back to deep water. A new angle of wave-approach (ϕ_0^*) is found, this angle does not have to match the original ϕ_0 of the waves. Therefore the refraction co-

efficient will differ from that which can be calculated with the angle ϕ_0^*
A new factor is introduced:

$$HH = H_0^* / H_0 = \sqrt{(kr^*{}^2 / Kr^2)} = Kr^* / Kr$$

Cross-section I beach slope $\alpha = 0.025$

season	ϕ_{01}	ϕ_{01}	HH ₁	HH ₂	RUN	h _{br1}	h _{br2}	γ_1	γ_2	ϕ_{br1}	ϕ_{br2}	T ₁	T ₂	r	time of the year
1	-70°	+15°	1.0	1.0	1	1.30	0.75	0.8	0.8	-12.5°	+1.75°	10	15	0.0175	25%
2	+35°	+15°	1.0	1.0	2	1.80	0.95	0.6	0.8	+12.5°	+1.95°	7	15	0.0175	25%
3	+35°	+15°	1.0	1.0	3	2.25	1.15	0.7	0.8	-9.7°	+2.15°	10	15	0.0175	25%
4a	+++identical with run 2++++														12½%
4b	-70°	+15°	1.0	1.0	4	1.30	0.95	0.7	0.8	-17.5°	+1.95°	7	15	0.0175	12½%

Cross-section II beach slope $\alpha = 0.025$

1	-51°	+35°	0.9	0.6	5	1.55	0.47	0.8	0.8	-11.5°	+3.1°	10	15	0.0175	25%
2	+43°	+35°	0.8	0.6	6	1.25	0.60	0.7	0.8	+12.5°	+3.5°	7	15	0.0175	25%
3	+35°	+35°	1.1	0.6	7	2.35	0.72	0.7	0.8	+10.0°	+3.75°	10	15	0.0175	25%
4a	+++identical with run 6++++														12½%
4b	-55°	+35°	1.0	0.6	8	1.75	0.60	0.6	0.8	-18.0°	+3.50°	7	15	0.0175	12½%

Cross-section III beach slope $\alpha = 0.01$

1	+57°	-	0.9	-	9	1.45	-	0.8	-	+11.5°	-	10	-	0.015	25%
4b	+43°	-	0.9	-	10	1.85	-	0.6	-	+15.5°	-	7	-	0.015	12½%

Cross-section IV beach slope $\alpha = 0.025$

1	+57°	-	1.0	-	11	1.55	-	0.8	-	+12.0°	-	10	-	0.015	25%
4b	+55°	-	1.1	-	12	1.95	-	0.6	-	+18.5°	-	7	-	0.015	12½%

Cross-section V beach slope $\alpha = 0.02$

1	+23°	-	0.9	-	13	2.00	-	0.7	-	+6.4°	-	10	-	0.015	25%
---	------	---	-----	---	----	------	---	-----	---	-------	---	----	---	-------	-----

Cross-section VI beach slope $\alpha = 0.03$

1	-	+51°	-	0.8	14	-	0.52	-	0.8	-	+4.35°	-	15	0.025	25%
2	+26°	+51°	0.5	0.8	15	0.85	0.65	0.8	0.8	+6.3°	+4.90°	7	15	0.0175	25%
3	+35°	+51°	0.8	0.8	16	1.60	0.80	0.8	0.8	+8.4°	+5.30°	10	15	0.0175	25%

4a +++identical with run 15++++

4b	-	+51°	-	0.8	17	-	0.65	-	0.8	-	+4.35°	-	15	0.025	12½%
----	---	------	---	-----	----	---	------	---	-----	---	--------	---	----	-------	------

Cross-section VII beach slope $\alpha = 0.025$

1	-77°	0	1.4	0.8	18	1.50	0.62	0.8	0.8	-13.5°	0	10	15	0.0175	25%
2	+21°	0	0.6	0.8	19	1.10	0.80	0.7	0.8	+6.3°	0	7	15	0.0175	25%
3	+11°	0	1.0	0.8	20	2.40	0.95	0.7	0.8	+3.5°	0	10	15	0.0175	25%

4a +++identical with run 19++++

4b	-55°	0	1.2	0.8	21	2.05	0.80	0.6	0.8	-19.0°	0	7	15	0.0175	12½%
----	------	---	-----	-----	----	------	------	-----	-----	--------	---	---	----	--------	------

Cross-section VIII beach slope $\alpha = 0.025$

4b	+74°	-	1.3	-	22	1.70	-	0.6	-	+20.5°	-	7	-	0.015	12½%
----	------	---	-----	---	----	------	---	-----	---	--------	---	---	---	-------	------

Cross-section IX beach slope $\alpha = 0.025$

1	+11°	-	1.0	-	23	2.25	-	0.7	-	+3.4°	-	10	-	0.015	25%
4b	-25°	-	1.0	-	24	2.15	-	0.6	-	-10.0°	-	7	-	0.015	12½%

Calculated sand transport capacities

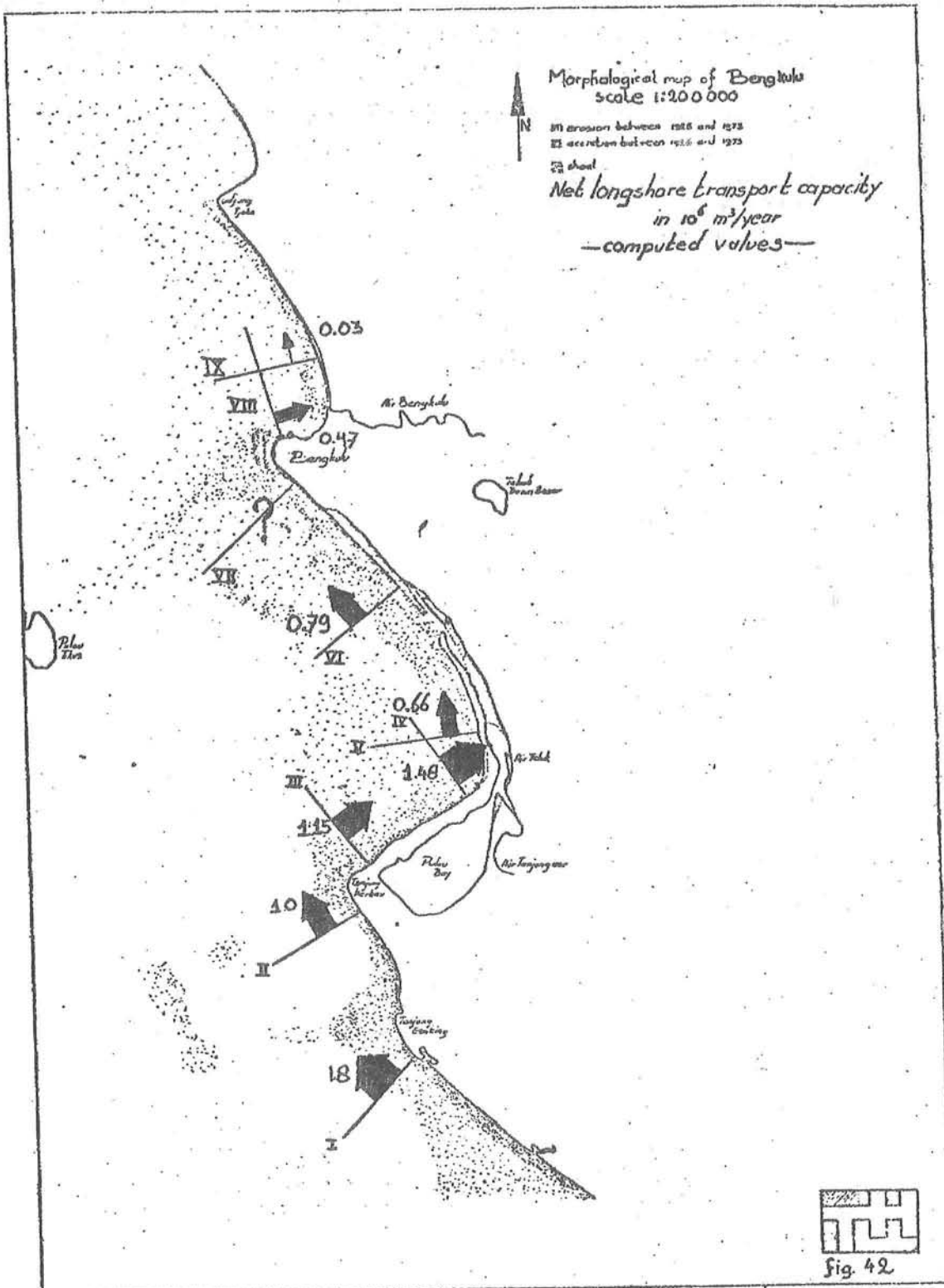
Cross-section I	season 1	$-0.45 \times 10^6 \text{ m}^3$
	season 2	$+0.67 \times 10^6 \text{ m}^3$
	season 3	$+1.46 \times 10^6 \text{ m}^3$
	season 4a	$+0.34 \times 10^6 \text{ m}^3$
	season 4b	$-0.22 \times 10^6 \text{ m}^3$
		$+1.80 \times 10^6 \text{ m}^3/\text{year}$
Cross-section II	season 1	$-0.71 \times 10^6 \text{ m}^3$
	season 2	$+0.32 \times 10^6 \text{ m}^3$
	season 3	$+1.64 \times 10^6 \text{ m}^3$
	season 4a	$+0.16 \times 10^6 \text{ m}^3$
	season 4b	$-0.40 \times 10^6 \text{ m}^3$
		$+1.00 \times 10^6 \text{ m}^3/\text{year}$
Cross-section III	season 1	$+0.67 \times 10^6 \text{ m}^3$
	season 4b	$+0.48 \times 10^6 \text{ m}^3$
		$+1.15 \times 10^6 \text{ m}^3/\text{year}$

The sand transport in season 2, 3 and 4a is neglected, because the waves causing this transport, are diffracted around Tanjung Kerbau and therefore small (so a small transport). Some calculations showed that the transport caused by these waves was about 25 % of the transport in season 1. This is within the accuracy of the whole calculation and hence it is neglected.

Cross-section IV	season 1	$+0.84 \times 10^6 \text{ m}^3$
	season 4b	$+0.64 \times 10^6 \text{ m}^3$
		$+1.48 \times 10^6 \text{ m}^3/\text{year}$
Cross-section V	season 1	$+0.66 \times 10^6 \text{ m}^3$
		$+0.66 \times 10^6 \text{ m}^3/\text{year}$
Cross-section VI	season 2	$+0.10 \times 10^6 \text{ m}^3$
	season 3	$+0.64 \times 10^6 \text{ m}^3$
	season 4a	$+0.05 \times 10^6 \text{ m}^3$
		$+0.79 \times 10^6 \text{ m}^3$
Cross-section VII	season 1	$-0.75 \times 10^6 \text{ m}^3$
	season 2	$+0.11 \times 10^6 \text{ m}^3$
	season 3	$+0.61 \times 10^6 \text{ m}^3$
	season 4a	$+0.06 \times 10^6 \text{ m}^3$
	season 4b	$-0.69 \times 10^6 \text{ m}^3$
		$-0.66 \times 10^6 \text{ m}^3/\text{year}$

Note: Due to uncertainties in refraction calculation this quantity is very doubtful

Cross-section VIII	season 4b	$+0.47 \times 10^6 \text{ m}^3$
		$+0.47 \times 10^6 \text{ m}^3/\text{year}$
Cross-section IX	season 1	$+0.49 \times 10^6 \text{ m}^3$
	season 4b	$-0.46 \times 10^6 \text{ m}^3$
		$+0.03 \times 10^6 \text{ m}^3/\text{year}$



The net longshore capacity data are presented in fig. 4.2. In cross-section VII a net transport capacity of $-0.66 \times 10^6 \text{ m}^3/\text{year}$ was found. This is not indicated in fig. 4.2, because this result is very dubious. As can be seen on the refraction diagrams the waves which enter to the coast from a southern direction are refracted very much by various reefs, so the values of h_{br} and ϕ_{br} are not reliable for the seasons 1 and 4b. From morphological observations we expect a small northward transport through this cross-section.

Morphological map of Bengkulu
scale 1:141 000

III erosion between 1926 and 1973

II accretion between 1926 and 1973

shoal

estimated sand transport
in $10^6 \text{ m}^3/\text{year}$

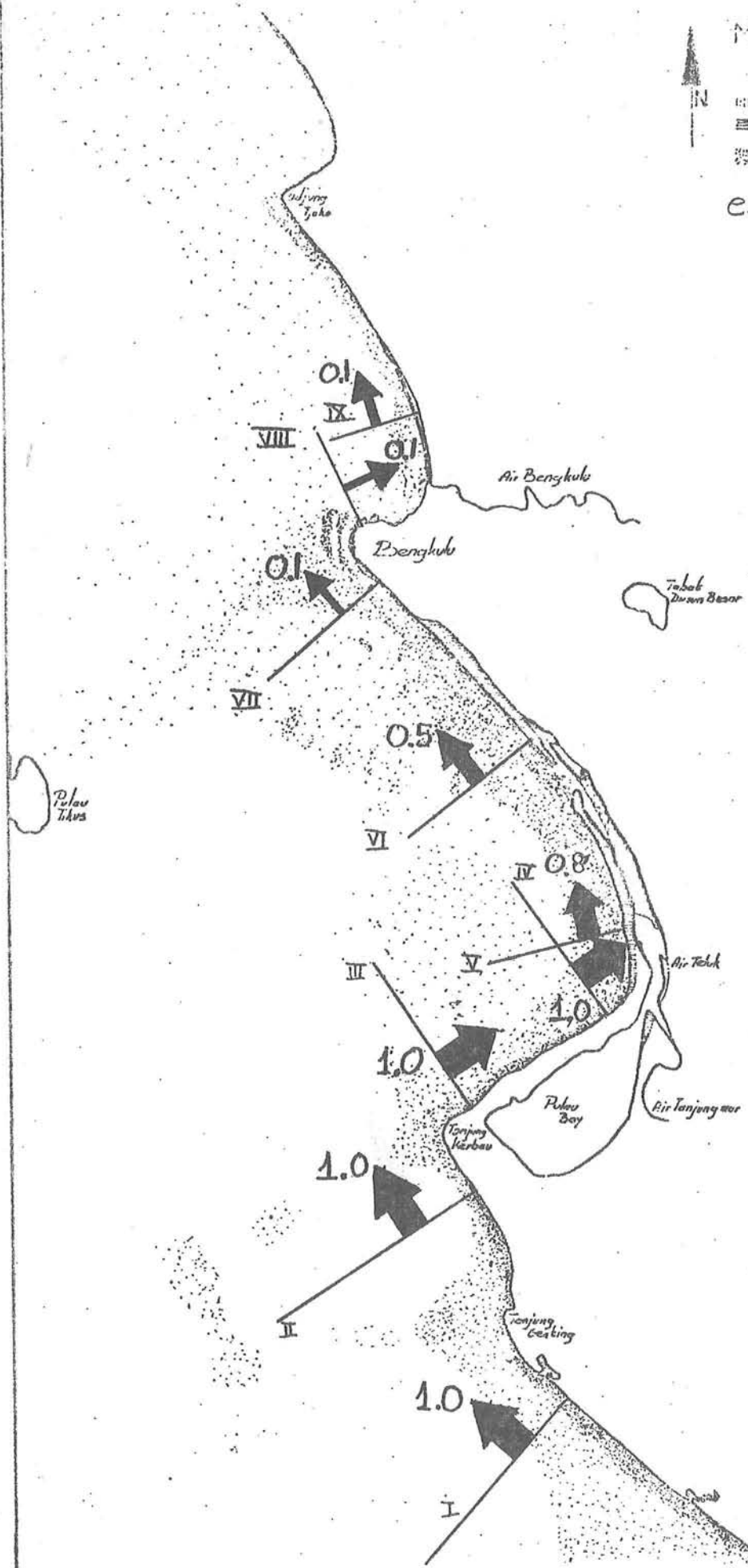
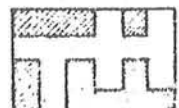


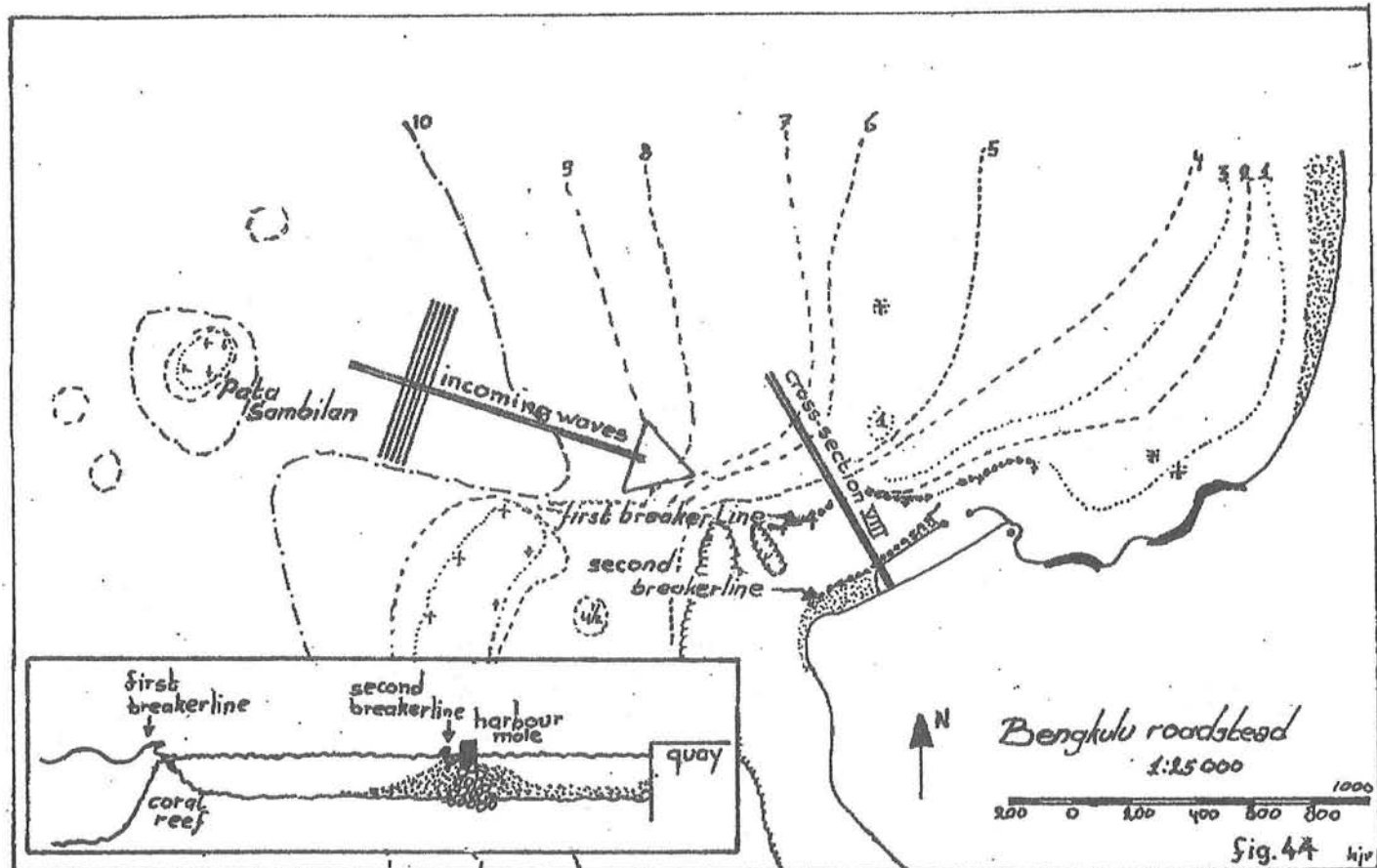
Fig 43



Because of the uncertainty in the input data, also the results have to be regarded with caution. Further one has to keep in mind that in reality not the sediment transport, but the sediment transport *capacity* is calculated. This is important in the vicinity of reefs.

Regarding the data of fig. 4.2 in comparision with the morphological description as given in chapter 3 our conclusion is (see fig. 4.3) that a resulting transport of about 1 million m³/year exists along the undisturbed coast south of Tanjung Kerbau and also along the Pulau Bay spit (The calculated values of 1.8 and 1.5 million are probably too high).

At e, between cross-section V and VI much sediment will accrete. This accretion is visible on the morphological map (see the 1:100 000 copy of fig. 3.9 added to this report), but also on aerial photographs made by prof. Bijker in the summer of 1977. From e to b the transport capacity is about 0.8 million m³/year, so 0.2 million m³/year has to accrete near e. This means that in the last 60 years 12 million m³ did accrete. From maps the volume of the accretion is not determined exactly, but estimated as $\frac{1}{2} \times 4000 \times 2000 \times 35 = 14$ million m³. So this fits rather well.



Between the cross-sections VI and VII the coastline is moved ca. 350 m in the direction of the sea over a distance of ca. 5000 m. The average depth is 10 m, so the accreted volume is $350 \times 5000 \times 10 = 17.5$ million m^3 .

This accretion also occurred in the last 60 years, together with an accretion of the spit (23 million m^3). So the total accretion in this period was 40 million m^3 or $0.67 m^3/year$.

We assumed a transport of 0.8 million $m^3/year$, so about 0.1 million $m^3/year$ will pass through cross-section VII as a resulting transport.

The transport capacity along the harbour is computed as 0.5 million $m^3/year$, but as can be seen from fig. 4.4 the incoming waves break on the coral reef in front of the harbour. On this reef is a large sand transport capacity, but this capacity is not saturated because there is not much sand available for transport.

After passing this reef the wave height is not very high (ca. 0.60 m). These small waves break on the second breakerline (at the beach) and originate there a transport capacity. There is plenty of sand, so the transport capacity will be utilised to its full extend.

This will be approx. 0.1 million $m^3/year$, coming from cross-section VI and going to the harbour.

This process is discussed in detail in vol. D.

5. Economical considerations

Introduction

In principle two possibilities exist for transportation of goods from and to Bengkulu.

1. By land (road and rail) to Palembang
2. By sea

Transport flows exist from Bengkulu to Jacarta, Palembang (both 36 %), Lubuklinggau (11%), Padang (8%), Surabaja (6%) and Semarang (3%).

For transports to Lubuklinggau sea transport is not interesting, but transports to the other towns may go over sea.

A decision has to be made which of these two possibilities has to be developed. For the development of sea transport improvement of the harbour facilities is necessary. For development of land transport it is necessary to improve the road from Bengkulu to Lubuklinggau, which is the nearest railway-station.

Due to financial problems it is not possible to do both. Because of the poor condition of the Bengkulu harbour the tendency is an increasing share of land transport.

From an economic point of view that solution has to be developed which is the cheapest in long terms. It is very difficult to calculate the cost-benefit rate of these two possibilities. As will be indicated harbour development is economically only attractive when the costs of improving harbour facilities does not exceed one milliard Rupiahs (Rp 1 000 000 000).

Of course also other considerations are important. Development of the Bengkulu district is easier when a good infrastructure with regional harbour facilities exists.

Perhaps harbour facilities may encourage more industrial activities. It is not possible to express all the benefits of harbour development in terms of money.

Hence the decision to invest one or two milliards of Rupiahs is a political decision, which has to be made by the Indonesian authorities. An important question is when this decision has to be made and whether it is possible to postpone some parts of the total decision to a later date.

In the next sections some date are investigated which can serve as a basis for these decisions.

Estimate of transport quantities

In order to estimate the amount of goods which will be transported through the harbour of Bengkulu, the Dwidelta corp. made an economical survey of the whole Bengkulu province (Dwidelta, 1975b). In this province most commodities are transported over land by truck and by train to and from Palembang (harbour on the east side of Sumatra). The harbours in the Bengkulu region play a less important role, properly speaking only the harbour of Bengkulu is important for the transportation over sea. The other harbours, Muko-muko, Ipuh, Bantal, Bintuhan and Manna are very small.

The commodities transported out of the Bengkulu region consist of spices, coffee, rattan, resin, rubber and other agricultural products; the incoming commodities consist of cement, corrugated iron sheet, sugar, salt, fish, rice, merchandise, kerosine, fertilizer and construction materials. Especially rubber and cement are transported over sea, so they are loaded and unloaded in the harbour of Bengkulu.

About 60 % (1973) of the economic activities in the Bengkulu province are in the agricultural, forestry and fishery sector, the importance of this sector is (economically) decreasing; other sectors are rapidly increasing (more than 5 % a year), such as industry, constructions, transport & communications, administration & defence. The growth of population in the Bengkulu province is estimated to be 2.3 % - 2.4 % for the next years until 1990; the total populations in 1973 was 555 400 inhabitants.

With these figures the Dwidelta corp. made an estimate of the production- and consumption figures. From the last figures the inflow (import) and outflow (export) of goods were calculated for the Bengkulu province and also (with some assumptions) for the Bengkulu harbour. When the mentioned figures (until 1974) concerning the amount of goods transported into and out of the Bengkulu region are compared with the estimated figures (of 1975) a discrepancy is shown. This discrepancy needs further investigations (e.g. an economical sub-project) and this is beyond the scope of this report.

Therefore an other estimate was made of the development of the transportation of goods in future, based upon the mentioned figures of inflow and outflow.

Outflow (in tons)

year	Bengkulu harbour	Ipuh, Bantal Muko-muko	Bintuhan Manna	Platform Scale Lubuk Tanjung	Platform Scale Pagar Alam
	I	II	III	IV	V
1970	9155	--	--	--	--
1971	9750	590	--	--	--
1972	8595	1845	700	--	--
1973	11225	1560	245	8550	--
1974	7830	2425	120	11600	19595

Outflow (totals) (in tons)

year	I	I+II	I - III	I - IV	I - V
1970	9155	--	--	--	--
1971	9750	10340	--	--	--
1972	8595	10435	11135	--	--
1973	11225	12785	13030	21585	--
1974	7830	10255	10375	21980	41575

Inflow (in tons)

year	Bengkulu harbour	Ipuh, Bantal Muko-muko	Bintuhan Manna	Platform Scale Lubuk Tanjung	Platform Scale Pagar Alam
	I	II	III	IV	V
1970	11890	--	--	--	--
1971	8130	95	--	--	--
1972	8650	345	90	--	--
1973	10320	390	--	13150	--
1974	9195	760	90	9575	17605

Inflow (totals) (in tons)

year	I	I + II	I - III	I - IV	I - V
1970	11890	--	--	--	--
1971	8130	8225	--	--	--
1972	8650	8995	9085	--	--
1973	10320	10715	ca 10800	ca 23950	--
1974	9195	9955	10045	20120	37725

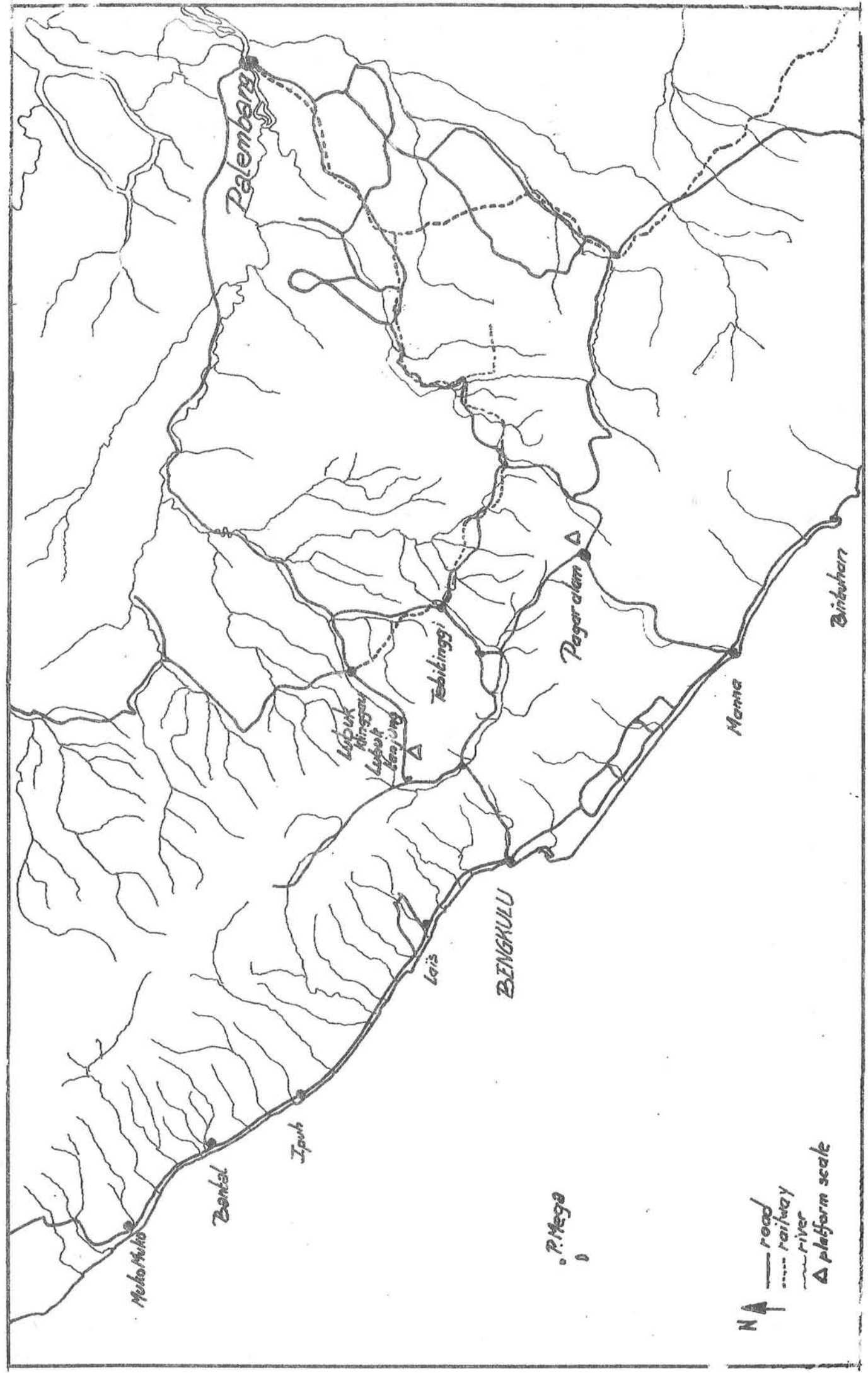
I - III sea transport

for locations see fig. 5.1

IV - V Land transport

Table 5.1
Transport quantities from and
to the Bengkulu region

Nedeco (1973) made a study of the transportation flows in Indonesia. One of the conclusions of this study was that the export (outflow) of traditional commodities (agricultural, forestry, fishery) is not growing very rapidly, only 0 % - 2 % a year. The import (inflow) is growing faster, about 4 % - 6 % a year. The mentioned figures for the Bengkulu province (inflow from and outflow to the other islands) point out to the same trend. Due to the poor condition of the Bengkulu har-



bour, its importance in total transportation is decreasing. Transportation over land (to Palembang) is rapidly increasing.

In order to obtain a good view of the development of future transports, an estimate is made of inflow and outflow of goods in the Bengkulu district and harbour. The following assumptions are made:

- I The export (outflow) will increase with 1 % a year until 1985, and then with 2 % a year.
- II a The import (inflow) will increase with 4 % a year until 1985, and then with 5 % a year.
 - b The import will increase with 4 % a year until 1985, and then with 3 % a year.
- III a The importance of the harbour will decrease with 1 % a year until 1980, and then with 0.5 % a year until 1985.
 - b The importance of the harbour will decrease with 1 % a year until 1980, and will stay the same until 1985 when the harbour is supposed to be improved.
- IV a The importance of the harbour will increase with 2 % a year from 1985 until 1990 and with 1 % a year from 1990 until 1995.
 - b The importance of the harbour will increase with 1 % a year after the harbour is improved (1985) for the next 10 years.
- V a The total inflow in 1974 was 37000 tons, the share of the harbour was 24 %.
 - b The total inflow in 1974 was 38000 tons, the share of the harbour was 25 %.
- VI a The total outflow in 1974 was 41000 tons, the share of the harbour was 18.5 %.
 - b The total outflow in 1974 was 42000 tons, the share of the harbour was 19.5 %.

With these given assumptions it is possible to calculate the inflow and outflow of the Bengkulu harbour in future. This calculation gives the minimum and maximum figures as indicated in table 5.2.

The minimum figures were calculated with the assumptions I, IIb, IIIa, IVb, and Va; the maximum figures were calculated with the assumptions I, IIa, IIIb, IVa and Vb.

Expected savings from the new harbour

This economical survey has the intention of being a survey of the amount of commodities that will be transported through the harbour (in future) and of the economical savings of the transportation costs, that are caused by the improvement of the harbour. The estimation of this last figure will be very rough, an error of more than 100 % is possible.

Outflow (in tons)

year	total outflow	share of the harbour in %.	share of the har- in tons.
1974	41000-42000	18.5 - 19.5 %	7585- 8190
1975	41410-42420	17.5 - 18.5 %	7245- 7850
1980	43520-44585	12.5 - 13.5 %	5440- 6020
1985	54740-46860	10.0 - 13.5 %	4575- 6325
1990	50500-51735	15.0 - 23.5 %	7575-12160
1995	55755-57120	20.0 - 28.5 %	11150-16280
2000	61560-63065	20.0 - 28.5 %	12310-17975

Inflow (in tons)

year	total outflow	share of the harbour in %.	share of the har- in tons
1974	37000-38000	24.0 - 25.0 %	8880- 9500
1975	38400-39520	23.0 - 24.0 %	8850- 9485
1980	46815-48080	18.0 - 19.0 %	8425- 9135
1985	54270-61365	15.5 - 19.0 %	8410-11660
1990	62915-78320	20.5 - 29.0 %	12895-22715
1995	72935-99960	25.5 - 34.0 %	18600-33985
2000	84550-127575	25.5 - 34.0 %	21560-43375

table 5.2 Future inflow and outflow
of the Bengkulu harbour

It only gives an indication of the amount of money (1 milliard or 10 milliard Rupiahs) which can be spent on this project. This financial limitation was calculated only with figures of the direct economic savings (i.e. not including the effects of stimulating economy by a better infrastructure). So the improvement of the infrastructure of the Bengkulu province was not taken into account. The improvement of this infra-structure could have influence upon the growth of industrial, agricultural or other activities.

As already indicated in the introduction of this chapter this may be a reason to invest more money into the harbour than the direct economical (transportation) profits.

The economical savings can be estimated from the figures of inflow and outflow of the Bengkulu harbour with the following assumptions:

- mean costs of transportation (freight costs, including handling and storage) are 10 - 15 Rp/kg (Dwidelta 1975b)
- savings because commodities are transported over sea instead of over land ca 10 % of the total transportation costs
- amount of goods over which no savings are calculated (some kind of a threshold value): inflow 11000 tons, outflow 6000 tons
- the savings are calculated after 1985, when the harbour is supposed to be improved.

	1985	1990	1995	2000
Inflow harbour (tons)	8440-11660	12895-22715	18600-33985	21560-43 575
Outflow harbour (tons)	4575- 6325	7575-12160	11150-16280	12310-17975
Inflow corrected (tons)	0- 660	1895-11715	9600-22985	10560-32375
Outflow corrected (tons)	0- 325	1575- 6160	5150-10280	6310-11975
Savings per year (million Rp.)	0- 1.5	3.5- 26.8	12.8- 49.9	16.9- 66.5

table 5.3 Expected savings

The total savings over 15 years are about 128 - 585 millions of Rupiahs. Taking into account only the direct economical savings and the costs of construction of the improvement can be paid off in 25 years without interest, the financial limitations of this project are aprx. one milliard Rupiahs (Rp 1 000 000 000). If interest is also taken into account the limitations are with 4 % ca 0.8 milliard Rupiahs and with 8 % ca 0.5 milliard Rupiahs.

In an other report (Dwidelta 1975) a financial survey is given of the costs of construction of a new harbour in Pulau Bay. In that survey the costs of improvement of the infrastructure are also given, specially the costs of new roads and road-improvements. The new roads and road-improvements are necessary for the transportation of stone from the Bukit Sunur quarry to the new harbour. The costs of nearly all of these roads were regarded as costs of improvement of the infra-structure and hence paid by other departments, not being the department of communications, or by the province itself. Therefore the direct direct economical savings are assumed to be spent entirely for the improvement of the harbour.

The conclusions to be drawn from this survey are that the traffic to and from Bengkulu harbour is too small to allow a large improvement, due to economical unattracitiveness.

Special developments

The assumptions made for the estimation of inflow and outflow are based on a "normal" economical growth. Special projects stimulating economical activities are not taken into account.

It came to our knowledge that the Indonesian government will start an agricultural project 50 - 100 km north of Bengkulu. This project may have a large influence on the economical development of the province, and thus on the devopment of the harbour.

This project is a transmigration project.

The Indonesian government tries to diminish overpopulation as well as food shortage on the densely populated islands of the country, in particular on Java.

People from these densely populated islands are enabled to settle in transmigration areas. After these areas have been brought under cultivation food production will start.

It is to expect that by means of modern agricultural methods¹⁾ these areas will have a large food surplus, which can be exported to islands with a food shortage.

So transmigration has two effects: less people on the densely populated islands, so less food shortage. And because the transmigrated people start food production in new agricultural areas total food production in Indonesia will increase.

The main problem of transmigration is that people are not interested in leaving their own islands and moving to other islands.

The area selected in the Bengkulu province is a jungle at this moment. In this area nearly no infra-structure exists. Due to this lack of infra-structure, roads, bridges, irrigation and drainage canals have to be constructed before agricultural activities can start. Also houses and other buildings have to be built.

It is obvious that this project will have an influence on the flow of goods. In the first stage of the project the import of construction materials and machines will be large.

Later the outflow of agricultural products will increase. This outflow will increase more than was expected in the former section. Also the inflow will increase more, due to the necessary commodities for the new agricultural areas (fertilizer, seeds).

It is quite uncertain how this project will develop. When it becomes a succes it will take about 5 - 10 years before this project has any

¹⁾ Modern agricultural methods are not identical with mechanisation !

influence on the economical activities of the Bengkulu province. As already mentioned the additional flow of goods as a result of this project was not taken into account in the estimation of the quantity of goods transported through the Bengkulu harbour.

Short term development

As indicated before the amount of goods transported by sea is decreasing and the importance of the rail and road connections are increasing.

Consequences are that transports from and to Bengkulu will be done by transport companies specialised in rail and road transport with branches in Palembang.

When a decision to build a new harbour would be made this year it would take 5 - 10 years before this new harbour will be operational. In the mean time nearly all transport will go by road and by rail via Palembang. Then it is very difficult for a new harbour to regain its place in the total transport flow. When land transportation has been established every company will have its connections in Palembang and although sea transport will be cheaper, many goods will be sent via Palembang.

Decision dates

When no decision at all is made sea transport will stop in a few years. Hence in a very short time the decision has to be made if sea transport should play a role in the future Bengkulu distribution system.

When this is decided in favour of sea transport the present situation at the Bengkulu roadstead has to be improved as soon as possible in such a way that sea transport keeps its part of total transportation from and to Bengkulu.

Two types of improvements are possible:

- Temporarily improvement of the Bengkulu roadstead and constructing a totally new harbour within 10 years.
- To improve the Bengkulu roadstead in such a way that this improvement is the basis for a new enlarged harbour.

In order to make a good decision about what to do it is necessary to investigate both possibilities.

The decision to improve the roadstead has to be made shortly. When this improvement is done in such a way that enlargement of the existing harbour and constructing a new harbour are both possible, the decision whether enlargement or constructing new can be made in a later stage when more and more detailed information about the development of the Bengkulu area is available.

References

This list of references includes also the references of vol B -D.

- Admiralty, 1971; Malacca strait and West Coast of Sumatra pilot, London.
- Admiralty, 1976; Admiralty tide table, London.
- Baker, P.E., 1972; Vulkanische eilanden, Natuur & Techniek, 40/383 - 393
- Battjes, J.A., 1972; Radiation stress in short crested waves, Journal of Marine Research, pp 56 - 64.
- Battjes, J.A., 1974; Computation of set-up, longshore currents, run-up and overtopping due to wind generated waves, thesis Delft.
- Bijker, E.W., 1967; Some considerations about scales for coastal models with movable beds, thesis Delft.
- Bijker, E.W., 1972; Topics in coastal engineering, lecture notes Delft University of Technology.
- Bos & Niermeyer, 1951; Atlas der gehele aarde, Groningen.
- Dwidelta 1973; Engineering Survey on the waters of the port of Bengkulu, Jakarta.
- Dwidelta 1975; Survey Pelabuhan Pulau Baai Bengkulu, Final Report. vol I - III, Jakarta.
- Dwidelta 1975 b; Economic study on land and sea transportation problems in Bengkulu area, Jakarta.
- ENSIE, 1952; encyclopedisch overzicht Sumatra, Amsterdam.
- Erb, J., 1905; Beiträge zur Geologie und Morphologie der Südl. Westküste von Sumatra, Zeitschrift des Geselsch. für Erdkunde, Berlin.
- Evans, H., 1942; The origin of spits, bars and related structures, Journal of Geology, vol 50, pp 846 - 865.
- Galvin, C.J., 1968; Breaker type classification on three laboratory beaches, Journal of Geophysical Research, vol 73, pp 3651 - 3659.
- Hydrografie 1904; Ministerie van Marine, Reede van Benkoelen.
- Hydrografie 1908; Ministerie van Marine, Reede van Benkoelen.
- Jonsson, I.G., 1966; Wave boundary layers and friction factors, 10th coastal engineering conference, Tokyo, vol I.
- Jonsson, Skovgaard & Jacobson 1974; Computation of longshore current 14th coastal engineering conference, Copenhagen, vol II.
- Kinsman, B., 1965; Wind Waves, Englewood cliffs N.J.
- Knappert, L., 1915; Memorie van overgave van de gouverneur van Benkoelen.

- KNMI, 1952; Indische Oceaan, Oceanografische en Meteorologische gegevens, publicatie 135, De Bilt.
- Koshiro, R., 1974; The study report of Bengkulu part master-plan Japanese maritime advisory team.
- Longuet-Higgins, M.S., 1970; Longshore currents, generated by obliquely incident sea-waves, Journal of geophysical research pp 6778 - 6801.
- Longuet-Higgins & Steward 1973; A note on wave set-up, Journal of Marine Research, pp 4 - 10.
- McDonald 1857; Kaart van de reede van Bengkoelen en de Poeloe-Baai, Nederlandsche Marine, Komm. tot verd der Ind.zeek.
- Meistrell F.J., 1966; The spit-platform concept, Laboratory observation of spit development, University of Alberta, Edmonton.
- Nedeco 1973; Aspects of port development planning, The Hague.
- Nedeco 1976; Pulau Bay Port, a proposal for a complementary investigation, The Hague.
- Paulus, I 1917-1935; Encyclopedie van Nederlandsch-Indië 's-Gravenhage
- Perthes J., 1837; Karte von der Insél Sumatra, Gotha.
- Popp & Booij 1977; Ray Refraction Program, Delft University of Technology
- Roos van Raadshoven 1924; Memorie van overgave van de gouverneur van Benkoelen.
- Skovgaard, Jonsson & Bertelsen 1975; Computation of wave-heights due to refraction and friction, proc ASCE, WW1, may '75.
- Stek F.G., 1860; Kaart Bengkulen middendeel, in Algemene Atlas van Nederlandsch-Indië, P. Baron Melville van Cambée & WF Versteeg.
- Swart, D.H. 1974; Offshore sediment transport and equilibrium beach profiles, thesis Delft.
- Terpstra, H. 1936; De richting van het materiaaltransport langs de westkust van Sumatra, De Ingenieur in Ned.Indië vol IV, pp 179 - 180.
- Topod 1913; Jaarverslag van den Topografischen Dienst in Nederlandsch- Indië, Batavia.
- Topod 1915; Jaarverslag van den Topografischen Dienst in Nederlandsch-Indië, Batavia.
- Topod 1926; Topographische kaart, blad XL VIII, Weltevreden
- T.O.W. 1976; Computation of longshore transport, Delft Hydraulics Laboratory, R 968-I.
- v. Tuyt J., 1931; De westkust van Sumatra ten zuiden van Kroë de mijningenieur, pp. 89 - 91.

- Umbgrove, J.H.F., 1931; De koraalriffen van Emmahaven, Leidse geologische mededelingen, pp. 9 -24.
- U.S. Army, 1973: Corps of Engineers, Shore Protection Manual, CERC, Fort Belvoir.
- U.S. Navy, 1976; Marine climatic atlas of the world, vol III Indian Ocean.
- Valentijn, F., 1726; Keurlijke Beschryving van Choromandel....., 't Nederlandsch Comptoir op 't Eiland Sumatra...., deel V, Dordrecht/Amsterdam.
- Veldkamp, J., 1948; Zwaartekracht, ENSIE vol V, Amsterdam.
- Verstappen, H.T., 1973; A geomorphological reconnaissance of Sumatra and adjacent islands, Groningen.
- Visser, S.W., 1949; Seismologie, Gorinchem.
- Yogyacarta University, 1975; Modelonderzoek Pulaubaai.
- Zieck, W.J.R., 1932; Memorie van overgave van de gouverneur van Benkoelen.

Samenvatting

In verband met de ontwikkeling van de buitengebieden moeten de havenfaciliteiten in Bengkulu (West-Sumatra) verbeterd worden. (de huidige prauwhaven is ca. 2 voet diep). De Indonesische overheid heeft daarbij haar keus laten vallen op de ontwikkeling van een haven in de Pulau Baai, ca. 20 km ten zuiden van Bengkulu.

Om een indruk te krijgen in de behoefte van deze streek is een beknopt vervoerseconomisch vooronderzoek gedaan.

Als hoofdonderzoek is het golfklimaat en de kustmorphologie van deze streek onderzocht. Bij het vaststellen van het golfklimaat moet, wegens gebrek aan gegevens, gebruik gemaakt worden van golfgegevens elders in Indonesië. Bij de bestudering van de kustmorphologie bleek een halfjaarlijks ritme te bestaan in het sedimenttransport, veroorzaakt door de moesson. Verder bleek het zandtransport aangedreven te worden door een tweetal gelijktijdig optredende golfsystemen.

Om het zandtransport ten gevolge van een dergelijk stelsel golven uit te rekenen is een berekeningsmethode opgezet, gebaseerd op de theorie van Bijker-Frijlink. Deze berekeningsmethode is verwerkt in een computerprogramma.

Met behulp van dit computer-programma, het vastgestelde golfklimaat en een uitgebreide refractieberekening is het zandtransport langs de kust bepaald. Om op korte termijn de havenfaciliteiten te kunnen verbeteren, is een ontwerp gemaakt om de bestaande haven tijdelijk uit te diepen en toegankelijk te maken voor kleine schepen, dit als een overgangsfase totdat de nieuwe Pulau Baai haven gereed is.

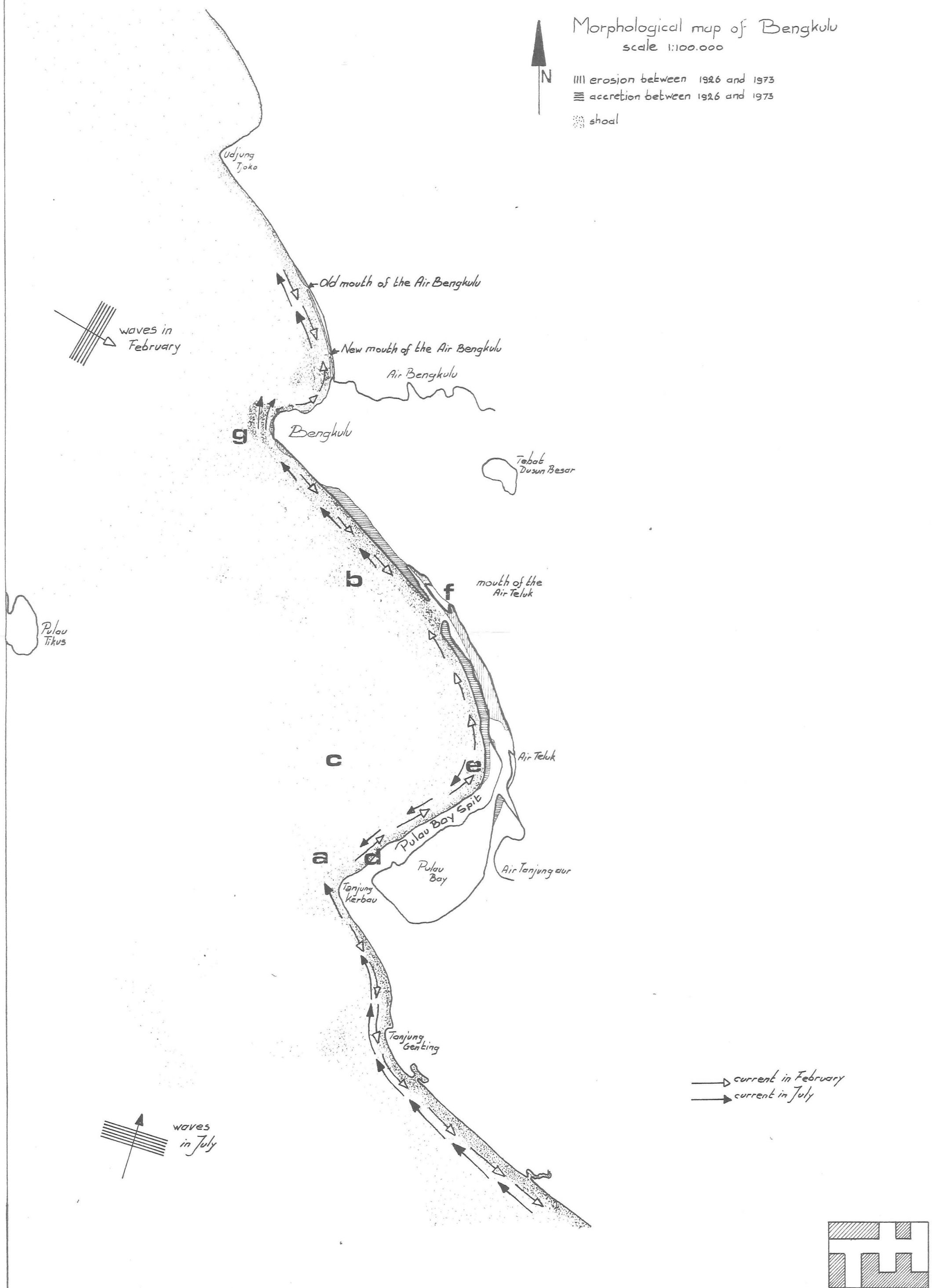
Morphological map of Bengkulu
scale 1:100.000



||| erosion between 1926 and 1973

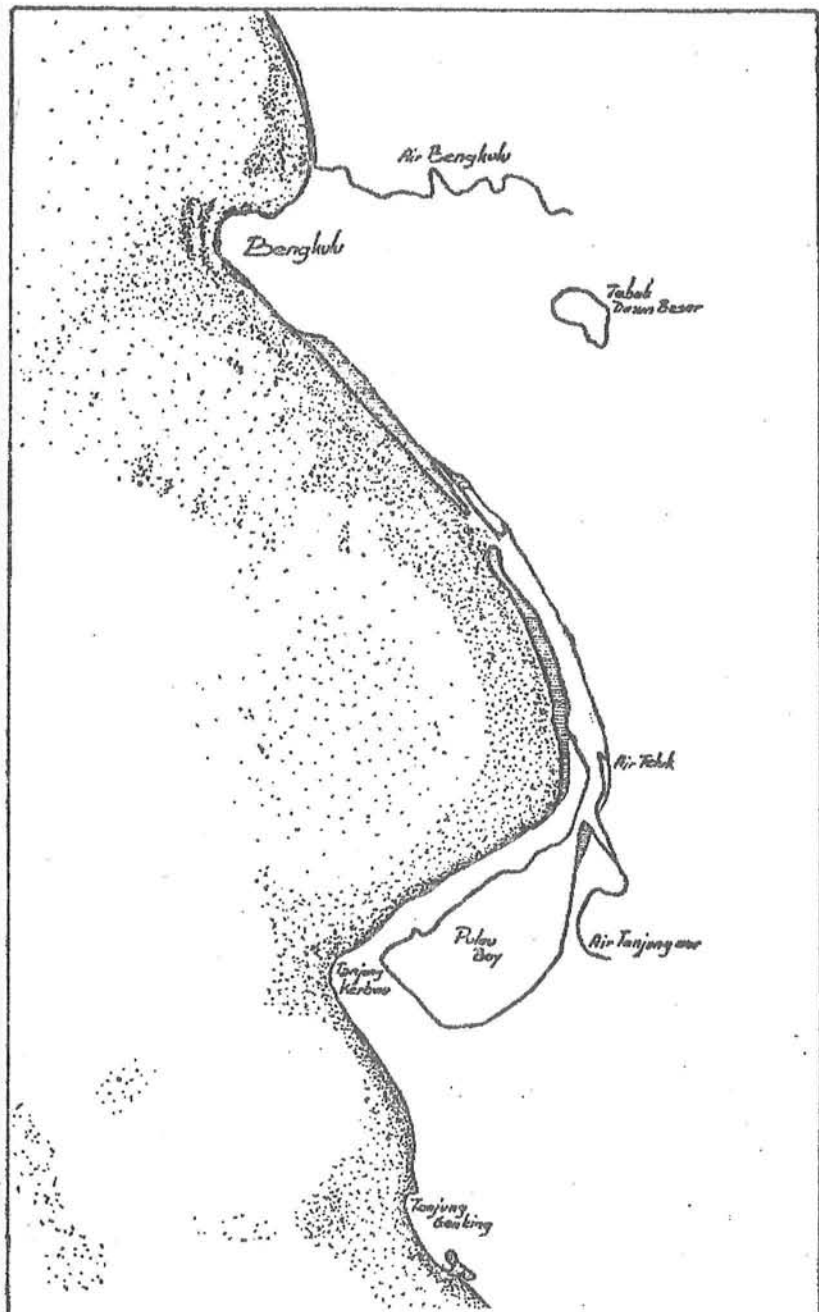
≡ accretion between 1926 and 1973

◎ shoal





**Delft University of Technology
Dept of Civil Engineering
Coastal Engineering Group**



**BENGKULU
HARBOUR
PROJECT**

FINAL REPORT VOL B

The influence of cross-swell on longshore sediment transport

Feb '78

Dik Ludikhuize & Henk Jan Verhagen

Contents

1. Introduction	2
2. Some characteristics of cross-swell	4
3. Derivation of a sand transport formula	5
4. A numerical approach	12
5. Some numerical aspects	19
6. Determination of the input data	23
7. A calculation by hand	25
8. Analysis of the accuracy of the sand transport calculations	32

Appendix: a listing and an output of the computer program

1. Introduction

In the Bengkulu area in most time waves come from two or three directions at the same time, which accomplishes sand transport calculations. The effect of waves on sand-transport is non-linear, and therefore a simple addition of sand-transport due to the separate wave systems is not allowed.

A simulation model for sand transport due to several wave systems was not found in literature, so an existing computation method had to be adapted to allow computation of sand transport caused by waves from several directions. In this study the wave system is described by two monochromatic waves, with different wave-height, period and angle of incidence. The effects of the stochastic character of waves are neglected. Wave-height, wave-period as well as angle of incidence should have been described in a probabilistic way with a directional energy spectrum.

This is not done because directional spectra from the Bengkulu coast are not known. Even the monochromatic data: wave-height, period and direction are highly unreliable. Also such a spectral approach is far beyond the scope of this study.

The derivations in this report are fitted for such a spectral approach but computations will cost very much work. The main problem will be the book-keeping of a large amount of data in the computer program. Some preliminary computations for a special case, in which the calculation method with spectra was based on Battjes (1974), indicate some small differences in the total transport, but large differences in the distribution of this transport.

Longshore velocity and sediment transport are calculated according to the formulae of Bijker and Frijlink (Bijker 1967, Bijker 1972). This is done because it is possible to adapt these formulae for a situation in which the waves come from several directions, which is not possible with the CERC-formula (US Army 1973).

The White-Ackers formula is not chosen because we were not very familiar with the physical backgrounds of this formula, and also because a first calculation with this formula resulted in a transport-quantity which was much too large. We were somewhat surprised by this result, because according to TOW (1976) this formula fits very well to measurements. A more detailed inspection of the data presented in TOW (1976) showed however that all measurements were

measurements in hydraulic models and no prototype measurements. Perhaps different coefficients have to be chosen for a good description of the prototype.

The Bijker-Frijlink formulae are well fitted for a derivation with two waves. No problems occur with the formulae themselves, but with several approximations and solutions. The simplification according to Bakker (Bijker 1972) as well as the results of the numerical computations given by Bijker (1967) are not applicable. For the calculation of the sediment-transport with these adapted Bijker-Frijlink formulae, a computer program had to be developed.

As already mentioned the two wave-systems are described by means of different crossing waves. Such a system is called cross-swell. When the crossing waves enter the breaker-line from opposite directions, the resulting velocity will be very low, because the propulsing forces also work in opposite directions. Bottom shear stress will increase, as well as the stirring factor.

An other effect is also important. When only one wave is broken and the other still isn't, this non-broken wave will not contribute to the propulsing force, but will increase both shear-stress and stirring factor.

In this study only the influence of the waves on sand transport is taken into account, and not the influence of the waves on each other.

Both waves are considered to be linear (first order) even when they have been broken. The interaction of both waves in the breakerzone is discussed in a separate report.

2. Some characteristics of cross-swell

It is assumed that in cross-swell both waves do not influence each other, so one may suppose that the maximum wave height is the sum of the original wave heights ($H_T = H_1 + H_2$).

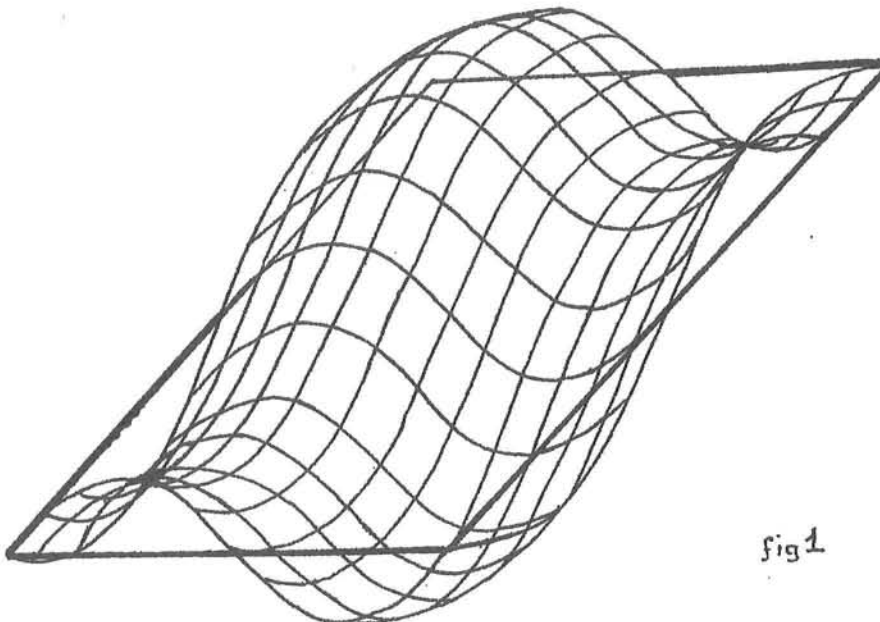


fig 1

But this maximum will occur only at one point, and not along a line, like in normal waves. At a certain time the surface can be described by $\eta = a_1 \sin k_1 x + a_2 \sin k_2 y$ (η is the deviation from the SWL, a is the amplitude of the original wave, k is the wave number $k = \frac{2\pi}{L}$). This is visualised in fig. 1.

For computations in which the energy is important, it is not allowed to use $V = \frac{1}{8} \rho g H_T^2$, but $V = \frac{1}{8} \rho g (H_1^2 + H_2^2)$. This is shown in annex I.

On the surface no crest-lines can be distinguished, only crest-points.

Problems

When the periods of the two incoming waves are identical (exactly identical), calculation is very difficult, because of devision by zero. In nature this will not occur, because the waves are not monochromatic, and they do not have the same period. In such cases phase-lagging becomes also important. In normal cases the phase-lag between the two incoming waves can be neglected.

Some ideas about these special cases are presented in annex II.

3. Derivation of a sand transport formula

The calculation of sand transport in a cross-swell situation asks for a formula in which the different parameters can be distinguished. Therefore the CERC-formula is not fit for these kind of calculations. A formula which includes more specific parameters is the Bijker-formula. The derivation of this formula, given by Bijker (1967), is only valid for waves from one direction. Hence it is necessary to extend the Bijker-formula to a two wave situation.

In the following derivation is assumed that both waves are monochromatic, and break independently on the same line as they should break

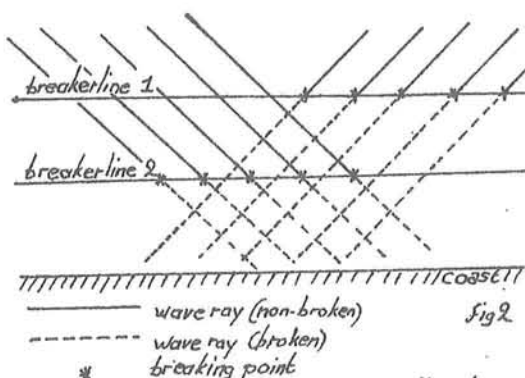


Fig 2

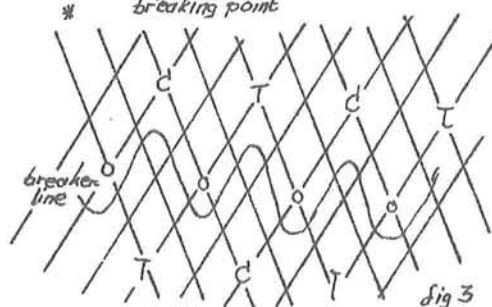


Fig 3

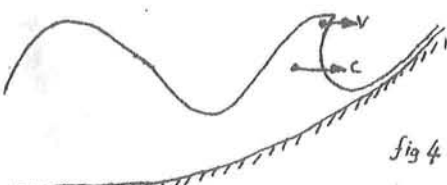


Fig 4

in a one wave situation. Hence two breakerlines will appear, as indicated in adjacent figure. Thus: both waves do not influence each other. When as breaking-criterion is chosen a quotient $\frac{H}{h}$, it is also possible to defend that the combined wave will break when the total H is larger than γh . This results in a curved breakerline. The curves in this line will move constantly, so no real breakerline can be distinguished, but only a breakerzone.

In this report is chosen for the two-line model, because the breaking criterion $\frac{H}{h}$ is not necessarily the real reason for breaking. A wave breaks because the velocity at the top is much larger than the velocity

of the wave (and normally the velocity at the top is a function of H). So it is supposed that the velocity-difference only causes breaking for the waves with the same direction as these breaking-inducing velocities. This aspect will be discussed in a separate report.

Longshore transport will be calculated in several steps. First the propulsive force is calculated (F_r). Then the shear stress due to both the incoming waves is calculated (τ). This shear stress is a

function of the longshore velocity ($\tau = \tau(v)$). By equating $F_r = \tau$ it is possible to determine the longshore velocity. The next step is a determination of the stirring-factor, due to the two waves. This stirring factor and the longshore velocity are entered in the transport formula to find the bottom-transport. The last step is the determination of the suspended load with the method of Einstein.

The propulsing force

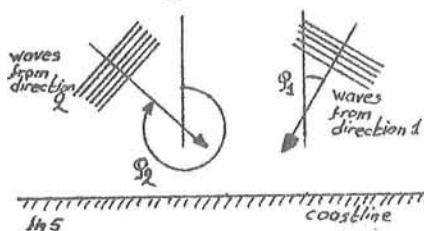
To compute sand transport it is necessary to compute first the longshore velocity. In this case two force components determine the magnitude of the resulting velocity, viz. the wave-forces due to the radiation stress, and the friction forces on the bottom.

It is supposed that the current is not accelerated (a few notes on acceleration can be found in annex VIII), and the wave heights are constant along the coast. So only the radiation stress S_{xy} is important and S_{yy} and S_{xx} may be neglected.

In shallow water S_{xy} is described by:

$$S_{xy} = E_1 \sin\phi_1 \cos\phi_1 + E_2 \sin\phi_2 \cos\phi_2$$

in which E_1 is the energy of the waves from direction 1 ($= \frac{1}{8} \rho g H_1^2$)



and E_2 is the energy of waves from direction 2 ($= \frac{1}{8} \rho g H_2^2$). For a detailed derivation of this formula see annex III.

$$\cos\phi = \cos\phi_{br} \quad \text{and} \quad \sin\phi = \sqrt{h/h_{br}} \sin\phi_{br}$$

Hence:

$$S_{xy} = E_1 \sqrt{h_1/h_{br}} \sin\phi_{br} \cos\phi_{br} + E_2 \sqrt{h_2/h_{br}} \sin\phi_{br} \cos\phi_{br}$$

After both waves are broken one can assume a linear relationship between waterdepth and waveheight $H=Ah$. So we get:

$$S_{xy} = \frac{1}{8} \rho g A_1^2 h^2 \sqrt{h/h_{br}} \sin\phi_{br} \cos\phi_{br} +$$

$$\frac{1}{8} \rho g A_2^2 h^2 \sqrt{h/h_{br}} \sin\phi_{br} \cos\phi_{br}$$

A_1 is not necessarily equal to A_2 , because A depends on the type of breaking.

A variable Φ is introduced:

$$\Phi = \frac{A_1^2}{\sqrt{h_{br}}} \sin\phi_{br} \cos\phi_{br} + \frac{A_2^2}{\sqrt{h_{br}}} \sin\phi_{br} \cos\phi_{br}$$

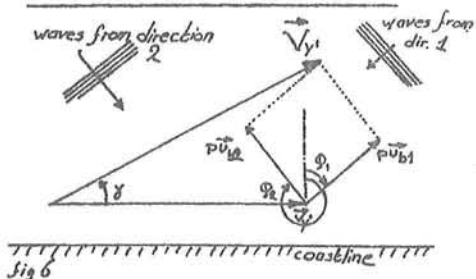
so:

$$S_{xy} = \frac{1}{8} \rho g h^{5/2} \Phi$$

To get the propulsive force per unit of area one has to differentiate S_{xy} with respect to x :

$$\frac{\partial S_{xy}}{\partial x} = F_r = \frac{5}{16} \rho g h^{3/2} \operatorname{tga} \Phi$$

The bottom shear stress



The longshore velocity $\vec{V}_{y'}$ is at a certain moment:

$$\vec{V}_{y'} = \vec{v}_{y'} + p \vec{u}_{b1} + p \vec{u}_{b2}.$$

The magnitude of this velocity is:

$$v_{y'} = \sqrt{v_{y'}^2 + p^2(u_{b1}^2 + u_{b2}^2) + 2v_{y'}p(u_{b1}\sin\phi_1 + u_{b2}\sin\phi_2)} + \frac{2v_{y'}p(u_{b1}\sin\phi_1 + u_{b2}\sin\phi_2)}{2p^2u_{b1}u_{b2}\cos(\phi_1 - \phi_2)}.$$

The angle γ between the resultant instantaneous bed shear and the main current is in this case defined by:

$$\cos\gamma = \frac{v_{y'} + p(u_{b1}\sin\phi_1 + u_{b2}\sin\phi_2)}{v_{y'}}$$

The component on the resultant bed shear in the direction of the main current is given by:

$$\begin{aligned} \tau'(t) &= [v_{y'} + p(u_{b1}\sin\phi_1 + u_{b2}\sin\phi_2)] \frac{\rho \ell^2}{y^2} \sqrt{v_{y'}^2 + p^2(u_{b1}^2 + u_{b2}^2)} + \\ &\quad \frac{2v_{y'}p(u_{b1}\sin\phi_1 + u_{b2}\sin\phi_2) + 2p^2u_{b1}u_{b2}\cos(\phi_1 - \phi_2)}{2v_{y'}p(u_{b1}\sin\phi_1 + u_{b2}\sin\phi_2) + 2p^2u_{b1}u_{b2}\cos(\phi_1 - \phi_2)} \\ &= \frac{v_*^2}{\kappa^2} \{ 1 + \frac{p\kappa}{v_*} (u_{b1}\sin\phi_1 + u_{b2}\sin\phi_2) \} \frac{\rho \ell^2}{y^2} \sqrt{1 + \frac{p^2\kappa^2}{v_*^2} (u_{b1}^2 + u_{b2}^2)} + \\ &\quad \frac{2\frac{p\kappa}{v_*}(u_{b1}\sin\phi_1 + u_{b2}\sin\phi_2) + 2\frac{\kappa^2}{v_*^2}u_{b1}u_{b2}\cos(\phi_1 - \phi_2)}{2\frac{p\kappa}{v_*}(u_{b1}\sin\phi_1 + u_{b2}\sin\phi_2) + 2\frac{\kappa^2}{v_*^2}u_{b1}u_{b2}\cos(\phi_1 - \phi_2)} \\ &= \frac{v_*^2}{\kappa^2} \{ 1 + \frac{\xi}{v} (u_{b1}\sin\phi_1 + u_{b2}\sin\phi_2) \} \frac{\rho \ell^2}{y^2} \sqrt{1 + \frac{\xi^2}{v^2} (u_{b1}^2 + u_{b2}^2)} + \\ &\quad \frac{2\frac{\xi}{v}(u_{b1}\sin\phi_1 + u_{b2}\sin\phi_2) + 2\frac{\xi^2}{v^2}u_{b1}u_{b2}\cos(\phi_1 - \phi_2)}{2\frac{\xi}{v}(u_{b1}\sin\phi_1 + u_{b2}\sin\phi_2) + 2\frac{\xi^2}{v^2}u_{b1}u_{b2}\cos(\phi_1 - \phi_2)} \\ &= \rho v_*^2 \{ 1 + \frac{\xi}{v} (u_{b1}\sin\phi_1 + u_{b2}\sin\phi_2) \} \sqrt{1 + \frac{2\xi}{v} (u_{b1}\sin\phi_1 + u_{b2}\sin\phi_2)} + \\ &\quad \frac{\xi^2}{v^2} (u_{b1}^2 + 2u_{b1}u_{b2}\cos(\phi_1 - \phi_2) + u_{b2}^2) \end{aligned}$$

in which $\ell = \kappa y'$ and $\xi = p\kappa c/\sqrt{g}$

Suppose $\cos(\phi_1 - \phi_2) \approx 1$ (A1)

$$\frac{\tau'(t)}{\tau} = \{1 + \frac{\xi}{v}(u_{b1}\sin\phi_1 + u_{b2}\sin\phi_2)\} \sqrt{1 + 2\frac{\xi}{v}(u_{b1}\sin\phi_1 + u_{b2}\sin\phi_2) + \frac{\xi^2}{v^2}(u_{b1} + u_{b2})^2}$$

According to Bakker $\frac{\xi}{v}(u_{b1}\sin\phi_1 + u_{b2}\sin\phi_2)$ is small in respect to $\frac{\xi^2}{v^2}(u_{b1} + u_{b2})^2$. Hence: (A2)

$$\frac{\tau'(t)}{\tau} = \{1 + \frac{\xi}{v}(u_{b1}\sin\phi_1 + u_{b2}\sin\phi_2)\} \sqrt{1 + \frac{\xi^2}{v^2}(u_{b1} + u_{b2})^2}$$

and with assuming $\frac{\xi}{v}(u_{b1} + u_{b2}) \gg v$ follows (A3)

$$\begin{aligned} \frac{\tau'(t)}{\tau} &= \{1 + \frac{\xi}{v}(u_{b1}\sin\phi_1 + u_{b2}\sin\phi_2)\} \frac{\xi}{v} |u_{b1} + u_{b2}| \\ \tau' &= \frac{\rho vg}{C^2} \{1 + \frac{\xi}{v}(u_{b1}\sin\phi_1 + u_{b2}\sin\phi_2)\} \frac{\xi}{v} |u_{b1} + u_{b2}| \\ &= \frac{\rho vg}{C^2} \xi \{|u_{b1} + u_{b2}| + \frac{\xi}{v}(u_{b1}\sin\phi_1 + u_{b2}\sin\phi_2)|u_{b1} + u_{b2}|\} \end{aligned}$$

$$u_{b1} = \hat{u}_{b1} \sin\omega_1 t \quad \text{and} \quad u_{b2} = \hat{u}_{b2} \sin\omega_2 t$$

Note: It is assumed that $\hat{u}_{b1} = \hat{u}_{b2}$, because after breaking both waves have the same height when $A_1 = A_2$. (A4)

$$\begin{aligned} \tau' &= \frac{\rho vg}{C^2} \xi \{| \hat{u}_b \sin\omega_1 t + \hat{u}_b \sin\omega_2 t | + \frac{\xi}{v} (\hat{u}_b \sin\omega_1 t \sin\phi_1 + \\ &\quad \hat{u}_b \sin\omega_2 t \sin\phi_2) | \hat{u}_b \sin\omega_1 t + \hat{u}_b \sin\omega_2 t | \} \\ &= \frac{\rho vg}{C^2} \xi \hat{u}_b \{ | \sin\omega_1 t + \sin\omega_2 t | + \xi \frac{\hat{u}_b}{v} (\sin\omega_1 t \sin\phi_1 + \\ &\quad \sin\omega_2 t \sin\phi_2) | \sin\omega_1 t + \sin\omega_2 t | \} \end{aligned}$$

A time average over a long interval T is:

$$\begin{aligned} \bar{\tau}' &= \frac{\rho vg}{C^2} \xi \hat{u}_b \{ \frac{1}{T} \int_0^T | \sin\omega_1 t + \sin\omega_2 t | dt + \xi \frac{\hat{u}_b}{v} \frac{1}{T} \int_0^T (\sin\omega_1 t \sin\phi_1 + \\ &\quad \sin\omega_2 t \sin\phi_2) | \sin\omega_1 t + \sin\omega_2 t | dt \} \\ &= \frac{\rho vg}{C^2} \xi \hat{u}_b \{ F(\omega_1, \omega_2) + \xi \frac{\hat{u}_b}{v} F'(\omega_1, \omega_2, \phi_1, \phi_2) \} \end{aligned}$$

The functions F and F' were computed numerically
(see table on the next page)

period		$T_1 = 7 \text{ sec}$	$T_1 = 7 \text{ sec}$	$T_1 = 10 \text{ sec}$
		$T_2 = 10 \text{ sec}$	$T_2 = 15 \text{ sec}$	$T_2 = 15 \text{ sec}$
F		0.856	0.863	0.916
ϕ_1	ϕ_2	F'	F'	F'
5°	350°	0.001	0.001	0.001
5°	345°	0.000	0.002	0.000
10°	345°	0.002	0.001	0.002
10°	340°	0.001	0.002	0.002
10°	335°	0.001	0.002	0.001
15°	340°	0.003	0.001	0.004
15°	335°	0.002	0.002	0.003
20°	335°	0.004	0.001	0.005

$$F = \frac{1}{T} \int_0^T |\sin \omega_1 t + \sin \omega_2 t| dt$$

$$F' = \frac{1}{T} \int_0^T (\sin \omega_1 t \sin \phi_1 + \sin \omega_2 t \sin \phi_2) |\sin \omega_1 t + \sin \omega_2 t| dt$$

In shallow water after breaking:

$$\bar{u}_b = \frac{H}{2} \sqrt{g/h} \quad \text{or} \quad \frac{Ah}{2} \sqrt{g/h} = \frac{A\sqrt{gh^3}}{2}$$

Hence

$$\begin{aligned} \tau' &= \frac{A\rho\xi\sqrt{g^3h}}{2C^2} v \{ F + \frac{A\xi\sqrt{gh}}{2v} F' \} \\ &= \frac{A\rho\xi\sqrt{g^3h}}{2C^2} Fv + \frac{A\xi^2g^2\rho h}{4C^2} F' \end{aligned}$$

When a permanent situation is assumed, i.e. the longshore current is not accelerated, then $F = \bar{v}$, or:

$$\begin{aligned} \frac{5}{16}\rho g A^2 h^{3/2} \operatorname{tg} \alpha \Phi &= \frac{\rho\sqrt{g^3h}A}{2C^2} F\xi v + \frac{\rho g^2 A^2 h \xi^2}{4C^2} F' \\ \frac{5}{16}\rho g A^2 h^{3/2} \operatorname{tg} \alpha \Phi - \frac{\rho g A^2 h \xi^2}{4C^2} F' &= \frac{\rho\sqrt{g^3h}A}{2C^2} \xi F v \\ v &= \frac{5\rho g A^2 h^{3/2} \operatorname{tg} \alpha \Phi 2C^2}{16\rho\sqrt{g^3h}A\xi F} - \frac{\rho g A^2 h \xi^2 F' 2C^2}{4C^2 \rho\sqrt{g^3h}A\xi F} \\ v &= \frac{5AC^2 h \operatorname{tg} \alpha \Phi}{8\xi F \sqrt{g}} - \frac{\sqrt{(gh)A\xi} F'}{2F} \end{aligned}$$

On this way a semi-analytical solution is found for v , but several assumptions were made (A1 to A4). In a totally numerical approach these assumptions are not necessary, as will be explained in the next chapter.

The stirring-factor

Because of waves the shear stress increases. The increase of this shear stress will be larger than the increase by only one wave. The increase can be described according to Bijker by a stirring-factor

$$\frac{\tau_R}{\tau_C} = \frac{pk \overline{V^2}}{pk \frac{y}{V^2}}$$

As indicated on page 7

$$\frac{v^2}{y} = \frac{v^2}{y} + p(u_{b1}^2 + u_{b2}^2) + 2v_y p(u_{b1} \sin\phi_1 + u_{b2} \sin\phi_2) + 2p^2 u_{b1} u_{b2} \cos(\phi_1 - \phi_2)$$

$$u_{b1} = \hat{u}_{b1} \sin\omega_1 t \quad u_{b2} = \hat{u}_{b2} \sin\omega_2 t$$

$$\frac{v^2}{y} = \frac{1}{kT} \int_0^{kT} \left(\frac{v^2}{y} + p^2 \hat{u}_{b1}^2 \sin^2\omega_1 t + p^2 \hat{u}_{b2}^2 \sin^2\omega_2 t + 2v_y p \hat{u}_{b1} \sin\omega_1 t \sin\phi_1 + 2v_y p \hat{u}_{b2} \sin\omega_2 t \sin\phi_2 + 2p^2 \hat{u}_{b1} \hat{u}_{b2} \sin\omega_1 t \sin\omega_2 t \cos(\phi_1 - \phi_2) \right) dt$$

kT is a period after which $\omega_1 t$ and $\omega_2 t$ are in phase again.

$$\begin{aligned} \frac{\tau_r}{\tau_c} &= \frac{1}{kT} \int_0^{kT} \left(1 + \frac{p^2 \hat{u}_{b1}^2}{v^2} \sin^2\omega_1 t \right) dt + \int_0^{kT} \frac{p^2 \hat{u}_{b2}^2}{v^2} \sin^2\omega_2 t dt + \\ &\quad \int_0^{kT} \frac{2 \hat{u}_{b1}}{v y} \sin\omega_1 t \sin\phi_1 dt + \int_0^{kT} \frac{2 \hat{u}_{b2}}{v y} \sin\omega_2 t \sin\phi_2 dt + \\ &\quad \int_0^{kT} \frac{p \hat{u}_{b1} \hat{u}_{b2}}{v^2} \{ \cos(\omega_1 t - \omega_2 t) - \cos(\omega_1 t + \omega_2 t) \} \cos(\phi_1 - \phi_2) dt \\ &\quad \bullet \frac{1}{kT} \int_0^{kT} \left(1 + \frac{p^2 \hat{u}_{b1}^2}{v^2} \sin^2\omega_1 t \right) dt = 1 + \frac{1}{kT} \left[\frac{p^2 \hat{u}_{b1}^2}{v^2} \left(\frac{1}{2} t - \frac{1}{4\omega_1} \sin 2\omega_1 t \right) \right]_0^{kT} = \\ &\quad 1 + \frac{1}{kT} \frac{p^2 \hat{u}_{b1}^2}{v^2} \frac{1}{2} kT = 1 + \frac{1}{2} \frac{p^2 \hat{u}_{b1}^2}{v^2} \\ &\quad \bullet \frac{1}{kT} \int_0^{kT} \frac{2 \hat{u}_{b1}}{v y} \sin\omega_1 t \sin\phi_1 dt = \frac{1}{kT} \frac{2 \hat{u}_{b1}}{v y} \left[\left(-\frac{1}{\omega_1} \cos\omega_1 t \right) \sin\phi_1 \right]_0^{kT} = \\ &\quad \frac{1}{kT} \frac{2 \hat{u}_{b1}}{v y} \sin\phi_1 \left(-\frac{1}{\omega_1} + \frac{1}{\omega_1} \right) = 0 \\ &\quad \bullet \frac{1}{kT} \int_0^{kT} \frac{p^2 \hat{u}_{b1} \hat{u}_{b2}}{v^2} \{ \cos(\omega_1 t - \omega_2 t) - \cos(\omega_1 t + \omega_2 t) \} \cos(\phi_1 - \phi_2) dt = \\ &\quad \frac{p^2 \hat{u}_{b1} \hat{u}_{b2} \cos(\phi_1 - \phi_2)}{kT v^2} \int_0^{kT} (\cos(\omega_1 - \omega_2)t - \cos(\omega_1 + \omega_2)t) dt \\ &\quad \frac{p^2 \hat{u}_{b1} \hat{u}_{b2} \cos(\phi_1 - \phi_2)}{kT v^2} \left[\frac{\sin(\omega_1 - \omega_2)t}{\omega_1 - \omega_2} - \frac{\sin(\omega_1 + \omega_2)t}{\omega_1 + \omega_2} \right]_0^{kT} \end{aligned}$$

$$kT = a \frac{2\pi}{\omega_1} = b \frac{2\pi}{\omega_2} \quad (a \text{ and } b \text{ are integers})$$

$$\omega_1 - \omega_2 = \frac{2\pi}{kT}(a-b) \rightarrow \sin(\omega_1 - \omega_2)kT = \sin 2\pi(a-b) = \sin 2\pi = 0$$

$$\rightarrow \cos(\omega_1 - \omega_2)kT = 1$$

$$\omega_1 + \omega_2 = \frac{2\pi}{kT}(a+b) \rightarrow \sin(\omega_1 + \omega_2)kT = \sin 2\pi(a+b) = \sin 2\pi = 0$$

$$\rightarrow \cos(\omega_1 + \omega_2)kT = 1$$

$$\frac{p^2 \hat{u}_{b1} \hat{u}_{b2} \cos(\phi_1 - \phi_2)}{kT v_y} (0 - 0 + 0 - 0) = 0$$

so

$$\begin{aligned}\frac{\tau_r}{\tau_c} &= 1 + \frac{1}{2} \frac{p^2 \hat{u}_{b1}^2}{v^2 y} + \frac{1}{2} \frac{p^2 \hat{u}_{b2}^2}{v^2 y} \\ &= 1 + \frac{1}{2} \left(\xi \frac{\hat{u}_{b1}}{v} \right)^2 + \frac{1}{2} \left(\xi \frac{\hat{u}_{b2}}{v} \right)^2\end{aligned}$$

Hence, the Bijker formula for waves from two directions is:

$$S_b = 5 D \frac{v \sqrt{g}}{C} \exp \left[\frac{-0.27 \Delta D C^2}{\mu v^2 \{1 + \frac{1}{2} \left(\xi \frac{\hat{u}_{b1}}{v} \right)^2 + \frac{1}{2} \left(\xi \frac{\hat{u}_{b2}}{v} \right)^2\}} \right]$$

in which

$$v = \frac{5C^2 h \tan \alpha}{8 \xi F \sqrt{g}} \quad \Phi = \frac{A \xi F' \sqrt{gh}}{2F}$$

Note: The velocity formula is only valid when the two waves are broken.

4. A numerical approach

Because sand transport calculations with a lot of variables cost much time, and because some parts of these calculations can only be solved by numerical computations, a computer-program was made to simplify these calculations.

A problem with computer programmes is always that the influence of several variables is not quite clear. Also the computer gives answers in very accurate numbers, but this accuracy is not realistic. A large error because of the uncertainty in the input data may be expected.

The input data are the constants ρ (water density), g (gravity constant), κ (Von Karman constant), D (D_{50} particle size), D_{90} (D_{90} particle size), Δ ($(\rho_{\text{particle}} - \rho_{\text{water}})/\rho_{\text{water}}$), R (ΔR , ripple height), HBR (breaker depth), ALFA (beach slope), A (quotient of broken wave-height and waterdepth), FI (angle of incidence), T (period), KGV (smallest common value of both periods).

The values R , HBR, and KGV have to be calculated first. R is calculated apart because both waves give different ripple-heights. This problem is discussed in detail in chapter 7. HBR is not calculated because this value is influenced heavily by local refraction. Refraction is calculated with other methods. This is discussed in vol C. KGV is not calculated because it is very easy to do it by hand and very difficult for a computer (for "normal" wave periods).

Fig. 7 represents a flow diagram of the program. First the available input-data are read and printed back. Some constants are calculated (w , ω_1 , ω_2 , $L_{\text{br}2}$, ϕ_o).

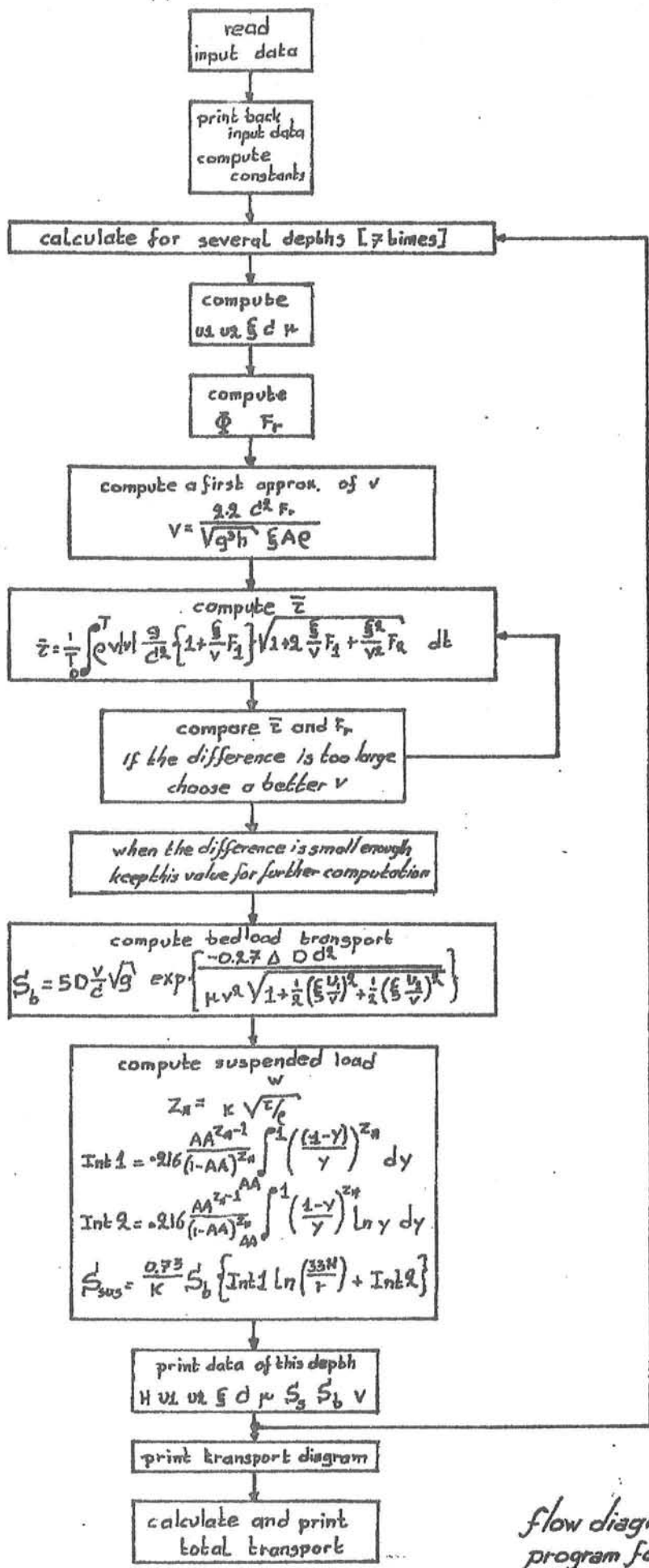
w is the fall-velocity of a sand particle in water, which is computed with the empirical formula

$$w_s = \exp \{-0.1941(\ln D)^2 - 1.961 \ln D - 6.2988\} \quad (\text{TOW 1976})$$

This empirical formula is used instead of the formula $w = g\Delta^2/18v$, because this second formula is only valid for spheres, and assumes a laminar flow around these spheres. Normal sea sand often falls with such a speed that the flow around the particle is changing from laminar to turbulent. The given TOW formula is valid for a water temperature of 20 °C, which is realistic for the Bengkulu coast.

ω_1 and ω_2 are the wave frequencies. When one of the waves does not exist, its period is given a high value, so the frequency gets a small value (0.0000001). This value is not zero because otherwise divisions by zero will occur, which will stop the numerical process.

$L_{\text{br}2}$ is the wavelength of the second wave on the second breakerline.



flow diagram computer
program for transport
calculations fig 7

This value is necessary to compute the shoaling and refraction coefficients for the second wave between the two breakerlines. First the wavelength is approximated with the formula of Eckert, and this value is improved by a three step iteration.

```
LB:=2*G*PI/W2/W2*SQRT(TANH(HBR2*H2*W2/G));
'FOR'P:=1'STEP'1'UNTIL'3'DO''BEGIN'
L2:=2*G*PI/W2/W2*TANH(2*PI*HBR2/LB);
LB:=(2*L2+LB)/3;'END';
```

Afterwards the value of LB is multiplied with a factor to simplify the calculation of the shoaling-coefficient. This will be discussed later in this paragraph.

After the calculation of these constants sand transport is calculated for several depths, well distributed over the breakerzone.

First the depth itself is calculated. (NOTE: in the program the capital H always means depth, in this text is used the small h for depth and the capital H for wave height. In the program the wave-height is not computed explicitly). Also the wave numbers and the bottom velocities are calculated (k_1 , k_2 , u_1 , u_2). For calculation of the wave numbers it is necessary to calculate the wavelength, which is done with the same procedure as described above.

Note: L_1 and L_2 are dummy variables, L_1 is both the wavelength of the first and the second wave. Also the coefficients C, ξ and μ and the propulsing force F are calculated.

For the calculation of k_2 and u_2 a difference has to be made between the broken and the unbroken wave. For calculation of these variables it is necessary to know the waveheight, which is calculated implicitly. For a broken wave the waveheight is $H = Ah$, but for an unbroken wave no such simple relation exists.

The actual unbroken waveheight is

$$H = H_{br} \times K_s^x \times K_r^x$$

K_s^x is a reversed function of the shoaling coefficient and K_r^x is a reversed function of the refraction coefficient.

$$K_s^x = \frac{\sqrt{1 + \frac{4\pi h_{br2}/LB}{\sinh(2 h_{br2}/LB)} \sqrt{\frac{L}{2}} \tanh(2 h_{br2}/LB)}}}{\sqrt{1 + \frac{2kh}{\sinh(kh)}} \sqrt{\frac{1}{k} \tanh(kh)}}$$

Note: Parallel depth contours are assumed

$$H = H_{br} \sqrt{(n_b c_b)/(nc)} \quad nc = \frac{1}{2} (1 + \frac{2kh}{\sinh kh}) \sqrt{\frac{g}{k} \tanh kh}$$

$$\approx (1 + \frac{2kh}{\sinh kh}) \sqrt{\frac{\tanh kh}{k}}$$

$$K_r^x = \sqrt{\cos\phi_{br}/\cos\phi}$$

$$\text{Note: } H/H_b = \sqrt{b_r/b} = \sqrt{\cos\phi_{br}/\cos\phi}$$

$\cos\phi$ is not known, but can be calculated with:

$$\begin{aligned} \sin\phi_{br}/\sin\phi &= c_{br}/c = \sqrt{\frac{1}{k_{br}} \tanh(k_{br} h_{br}) / \frac{1}{k} \tanh(kh)} \\ &= \sqrt{L_b \tanh(k_{br} h_{br}) / L \tanh(kh)} \end{aligned}$$

Note: in the program $L_b \tanh(k_{br} h_{br})$ is called FI0, ϕ is called FIH

Between the breakerlines the propulsing force is caused by the broken wave only, so Φ is calculated with ϕ_1 and h_{br1} only.

```

FI0:=LB*TANH(2*PI/LB*HBR2);
LB:=HBR2*SQRT((1+4*PI/LB*HBR2/SINH(2*PI/LB*HBR2))* 
    SQRT(LB/ 2*PI*TANH(2*PI/LB*HBR2)));
FIH:=ARCSIN(SQRT(L1/FI0*TANH(K2*H)*SIN(FI2)));
U2:=NHW2*LB/2/SINH(K2*H)/SQRT((1+2*K2*H/SINH(K2*H))* 
    SQRT(TANH(K2*H)/K2))*SQRT(COS(FI2)/COS(FIH));
FI:=SIN(FI1)*COS(FI1)/SQRT(HBR1);

```

When both waves are broken the situation is relatively simple. Shoaling coefficients are not important and refraction is hidden in the propulsion force.

```

U1:=NHW1/2/SINH(K1*H);
U2:=NHW2/2/SINH(K2*H);
FI:=SIN(FI1)*COS(FI1)/SQRT(HBR1)+SIN(FI2)*COS(FI2)/SQRT
    (HBR2);

```

In the derivation on page 7 a constant $\xi = p\kappa C/g^{1/2}$ was introduced. p is the ratio of the bottom velocity (according to wave formula) and the real velocity at a distance $r/33$ (width of the viscous sublayer). According to Bijker (1967) p has a theoretical value of 0.39. In experiments a value of 0.45 was obtained.

Investigations of Jonsson (1966) indicate that p is not a constant, but a variable, dependent from the amplitude at the bottom. According to Jonsson (after some rearranging) $p = f_w^{1/2}/2\kappa^2$ in which f_w can be approximated by $\ln f_w = -5.977 + 5.213 (\frac{a_o}{r})^{-0.194}$.

a_o is the amplitude at the bottom, r is the Nikurads roughness which is supposed to be equal to two or three times the ripple-height.

Jonsson used in his derivation the value of a_o , because he started his derivation with the formula

$$\tau_{max} = f_w^{1/2} \rho u_{max}^2$$

instead of

$$\tau = f \frac{1}{2} \rho |u| \quad (\text{at any time.})$$

He noticed that τ_{\max} and u_{\max} are not acting simultaneously. To determine f he used the first formula instead of the second, because in the first it is possible to express f_w as a function on some known variables. Thereafter he proved that for a rough turbulent case $f_w \approx f$. Jonsson did not prove that the maximum deviation at the bottom (amplitude) is indeed the parameter governing the phenomenon. He only proved that the amplitude describes (for a one-wave situation) the phenomenon. Perhaps the mean deviation, or the root-mean-square deviation is the real parameter.

For a one-wave situation these parameters differ only a multiplicator, which might be built into the formula. These multiplicators have different values in a two-wave situation.

Because the real parameter is not known, in this report is assumed that the amplitude describes the phenomenon in a two-wave situation too. In annex IV is shown that this might be a good guess.

However a problem is that in case of two waves with different periods no real amplitude can be computed. There is a maximum amplitude

$(a_{\max} = \sqrt{(u_1/\omega_1)^2 + (u_2/\omega_2)^2 + 2u_1u_2/\omega_1\omega_2 \cos(\phi_1 - \phi_2)})$ which occurs seldom, and also a minimum amplitude, which occurs seldom too:

$$a_{\min} = \sqrt{(u_1/\omega_1)^2 + (u_2/\omega_2)^2 - 2u_1u_2/\omega_1\omega_2 \cos(\phi_1 - \phi_2)}$$

In our computations we use the mean of these amplitudes.

Notes: Several calculations have indicated that the influence of variations in this is very small.

In the computer program a procedure is incorporated to calculate this amplitude in case of two identical waves. This procedure is used only in special cases (see annexes).

In the program the amplitude is called EPS.

Then it is possible to calculate ξ , μ and F_r

$$KSI := C * SQRT(EXP(-5.977 + 5.213A((EPS/R)^(1/12) * (-.194)))) / 2/G;$$

$$MU := (C/7.82/LN(12MH/D90))^(1/5);$$

$$FR := 5/16 * ROMG * SQRT(HMHMH) * ALFA * FI;$$

F_r is the propulsing force due to the radiation stresses S_{xy} . The influence of a varying waveheight along the coast is neglected.

Also a permanent situation is supposed (no longshore acceleration).

This propulsing force is compared with the dissipating force ($\bar{\tau}$) and from this comparison v can be computed.

Note: In chapter 3 angles are measured clockwise. In the computer-program these angles have to be measured counterclockwise. This is because a minus sign is omitted in the equation $\bar{\tau} = F_r$. In reality this equation should be read as $\bar{\tau} + F_r = 0$.

The component of the resultant instantaneous bed shear in the direction of the main current is:

$$\tau = \rho v_x^2 \left\{ 1 + \frac{\xi}{v} (u_{b1} \sin \phi_1 + u_{b2} \sin \phi_2) \right\} \sqrt{1 + 2 \frac{\xi}{v} (u_{b1} \sin \phi_1 + u_{b2} \sin \phi_2) + \frac{\xi^2}{v^2} (u_{b1}^2 + 2u_{b1}u_{b2} \cos(\phi_1 - \phi_2) + u_{b2}^2)}$$

in which $u_{b1} = \hat{u}_{b1} \sin \omega_1 t$ and $u_{b2} = \hat{u}_{b2} \sin \omega_2 t$

Now two functions can be defined:

$$F_1(\omega_1, \omega_2, \hat{u}_{b1}, \hat{u}_{b2}, \phi_1, \phi_2, t) = \hat{u}_{b1} \sin \omega_1 t \sin \phi_1 + \hat{u}_{b2} \sin \omega_2 t \sin \phi_2$$

$$F_2(\omega_1, \omega_2, \hat{u}_{b1}, \hat{u}_{b2}, \phi_1, \phi_2, t) = u_{b1}^2 + 2u_{b1}u_{b2} \cos(\phi_1 - \phi_2) + u_{b2}^2$$

Hence, substituting $\frac{v^2}{x}$ as $v^2 g/C^2$ becomes:

$$\tau = \rho v^2 g/C^2 \left\{ 1 + \frac{\xi}{v} F_1 \right\} \sqrt{1 + 2 \frac{\xi}{v} F_1 + \frac{\xi^2}{v^2} F_2}$$

Because τ has the same direction as v , it is necessary to write v as $v|v|$.

A time average over a long period is $\bar{\tau} = \frac{1}{T} \int_0^T \tau d\tau$.

When a permanent situation is assumed, i.e. the longshore current is not accelerated, then:

$$\bar{\tau} = F_r$$

$$F_r = \frac{5}{16} \rho g h^{3/2} \operatorname{tg} \alpha \Phi$$

So in the equation $\bar{\tau} = F_r$ only v is unknown. Unfortunately it is not possible to solve this equation analytical. Hence a numerical approach is chosen.

An approximation of v is according to chapter 3

$$v = \frac{5 A C^2 h \operatorname{tg} \alpha \Phi}{8 \xi F_r \sqrt{g}}$$

F has a value of about 0.9, hence this can be written as

$$v = 2.2 C^2 F_r / \xi \rho A \sqrt{g h}$$

This approximation serves as a starting value for the numerical process.

To allow an investigation of phase-lags (see Annex) it is necessary to introduce a phase difference. For this purpose u_2 is written as $u_2 = \hat{u}_2 \sin(\omega t + \text{phase})$. This is done in the functions F_1 and F_2 . The numerical aspects of the procedure to calculate v will be discussed in the next chapter.

After the longshore velocity has been computed, it is possible to compute the bedload transport with the modified Bijker formula, as derived in chapter 3.

Because this formula needs no special numerical attention, the computer can calculate bedload-transport directly.

```

S:=5*D*V/C*SQRT(G)*EXP(-.27*DELTA*D*CAC/(MU*V*V*(1+(KSI*U1/
V)*(KSI*U1/V)/2+(KSI*U2/V)*(KSI*U2/V)/2)));
OUTSTRING(1,'('SEDIMENT TRANSPORT (BEDLOAD) ')');
FLO(1,4,3,S);
OUTSTRING(1,'(' M3/M YEAR')');
LINE(1,1);

```

Suspended load is computed according to the method of Einstein as described in Bijker (1972). Suspended load is

$$S_{\text{sus}} = \frac{0.73}{\kappa} S_b \left\{ \text{Int1} \ln \left(\frac{33h}{r} \right) + \text{Int2} \right\} \quad x)$$

in which

$$\text{Int1} = 0.216 \frac{AA^{z_x-1}}{(1-AA)^{z_x}} \int_{AA}^1 \left\{ \frac{1-y}{y} \right\}^{z_x} dy$$

$$\text{Int2} = 0.216 \frac{AA^{z_x-1}}{(1-AA)^{z_x}} \int_{AA}^1 \left\{ \frac{1-y}{y} \right\}^{z_x} \ln y dy$$

$$AA = r/h$$

$$z_x = w_s/\kappa v_x = w_s/\sqrt{\tau/\rho}$$

w_s is the fall-velocity of sand particles, τ is the bottom shear stress, caused by current and waves. The integrals are computed numerically with a procedure, described in the next chapter.

Finally a graphical presentation of the important data is made and the total transport is calculated. The way in which this is done is also described in the next chapter.

A complete listing of the program is given at the end of this report.

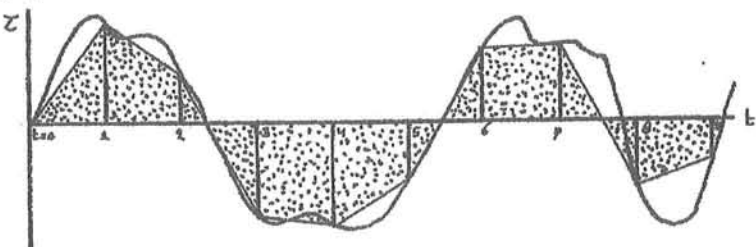
x) The formula in Bijker (1972) is $S_s = 1.83 S_b$ (....). This formula is not derived properly, but is said to be the result of "some mathematics". Carrying out these mathematics (see annex V) leads to $S_s = \frac{0.73}{\kappa} S_b$ (....). For a value of $\kappa = 0.4$ this is identical with 1.83. But in the formula presented in this report $\kappa = 0.384$, reasons to keep κ in the formula of S_s .

5. Some numerical aspects

In this chapter some numerical procedures are discussed. Only the mathematical tools are discussed to transform analytical equations to numerical algorithms.

The calculation of $\bar{\tau}$ and v

As indicated on page 17 in the computer program the time average $\bar{\tau} = \frac{1}{T} \int_0^T \tau d\tau$ has to be computed numerically.



T is a long period after which the function repeats itself (recurrence interval). This is the smallest common product (KGV) of T_1 and T_2 . The KGV of 10 and 15 seconds is 30, for 7 and 10 seconds it is 70. It is very time consuming to calculate this KGV-value with a computer, and for normal wave periods it is very simple to calculate this value by hand. Hence this period has to be entered as input data on the same card as T_1 and T_2 .

The integral is computed in 53 steps *), with the trapezium-rule, i.e. the surface of the dotted area is computed instead of the real surface. For oscillating functions this is quite accurate. (The time-average of the function $F_1 (= \hat{u}_{b1} \sin \omega_1 t \sin \phi_1 + \hat{u}_{b2} \sin \omega_2 t \sin \phi_2)$, see page 17) was also calculated with this procedure. The answer was of the order 10^{-17} , which is quite near to the exact answer 0)

For numerical reasons, four variables are used, TAU, TAUOLD, TAUMEAN and SUMTAU.

$$\text{TAUMEAN} = \frac{1}{\text{STEPS}} \sum_{t=1}^{\text{STEPS}} \frac{\text{TAU} - \text{TAUOLD}}{2}$$

$$\begin{aligned} \text{TAUOLD} &= \text{TAU}_{t-1} \\ \text{TAU} &= \text{TAU}_t \end{aligned}$$

Note: In the program also the variable PHASE is introduced. Normally $\text{PHASE} = 0$; this variable is only used in special cases, see Annex II.

*) The number 53 is chosen because with this number coincidences of step-period and wave-period will only occur with periods of 53 seconds, which is a rare wave.

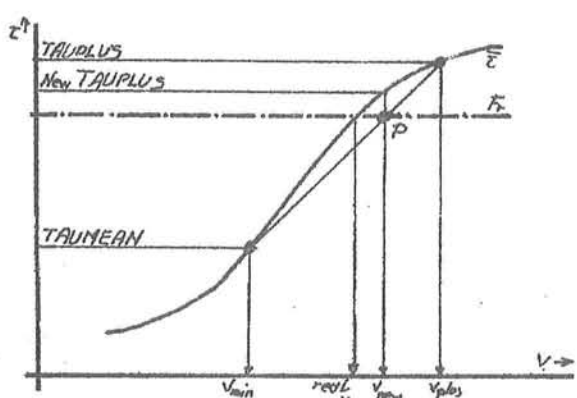
```

TAUOLD:=TAUMFAN+SUMTAU*EPS;
*FOR*T:=0*STEP*EPS*STEPS*UNTIL*RGV<10**10*10**10*
F1:=U1*SIN(W1*T)*SIN(F11)+U2*SIN((2*T+PHASE)*SIN(F12));
F2:=U1*U1*SIN(W1*T)*SIN(W1*T)+U1*U2*SIN(W1*T)*SIN((2*T+PHASE)*
COS(F11-F12)*2+U2*U2*SIN((2*T+PHASE)*SIN((2*T+PHASE));
TAU:=R0*V #G/C/C*(1+S1*F1/V)*SIN(1+2*KST*#1/V+KST*KST*F2/V/V)*ABS(V);
TAUMFAN:=(TAU+TAUOLD)/2;
TAUOLD:=TAU;
SUMTAU:=SUMTAU+TAUMFAN;
*END*;
TAUMFAN:=SUMTAU/STEPS;

```

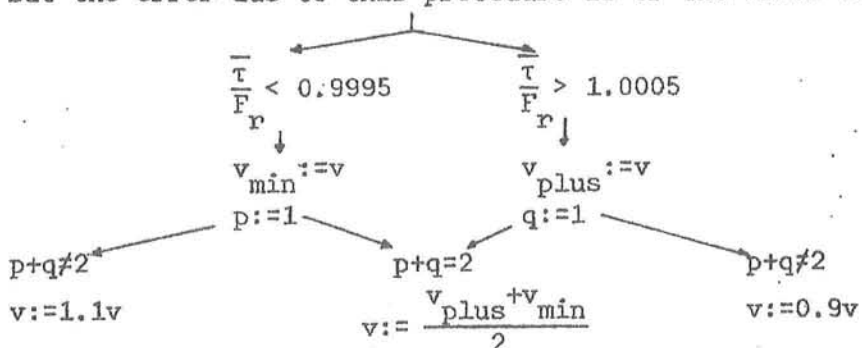
The velocity is given implicit as $\bar{\tau}(v) = \frac{1}{T} \int_0^T \tau(v) dt = F_r$. After the integral is solved with the trapezium rule, as described on the former page, the equation has still to be solved. This is done with a regula-falsi procedure.

First the approximate value of v is computed. This value is entered in the formula and $\bar{\tau}$ is computed. The value of $\bar{\tau}$ is compared with F_r . When $\bar{\tau}$ is too large, v is decreased until a value of $\bar{\tau}$ is found, which is smaller than F_r . On the other hand when the first value of $\bar{\tau}$ is smaller than F_r , v is increased until a value of $\bar{\tau}$ is found which is larger than F_r . In this way two values of $\bar{\tau}$ are known (with corresponding values of v), of which one is larger than the searched



$\bar{\tau}$ (this value is called TAUPLUS), and one is smaller than $\bar{\tau}$ (TAUMIN). Then the point is calculated where the connection-line from TAUMIN to TAUPLUS crosses the F_r line (point P), and a new value of v is found. Then is checked if the $\bar{\tau}$ corresponding to this new value of v does not

differ more than 0.0005 from F_r . If this is true the process is stopped, else a new step is carried out. As can be seen from the figure the accuracy is low when $\frac{d\bar{\tau}}{dv}$ is nearly zero. No exact error-calculation was made, but the error due to this procedure is or the order 0.02 %.



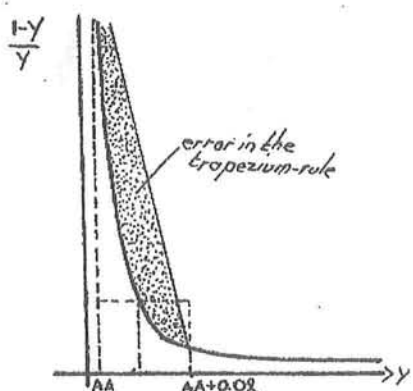
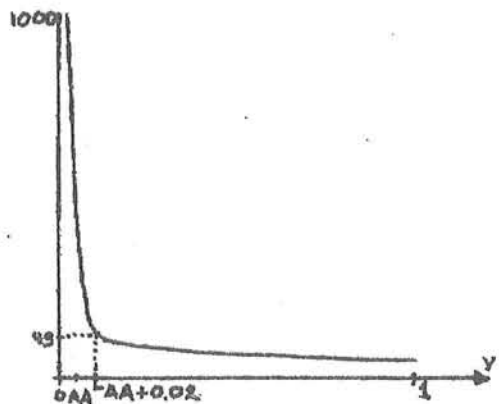
```

*IF *TAUMEFAN/FN<.9995 THEN *PREGIN*
VMIN:=V;
P:=J;
*IF *P+Q=2 THEN *PREGIN*
V:=(VMIN+VPLUS)/2;
*GOTO *THREE*END*;
V:=1.1*V;
*GOTO *THREE*END*;
*IF *TAUMEFAN/FN>1.0005 THEN *PREGIN*
VPLUS:=V;
Q:=J;
*IF *P+Q=2 THEN *PREGIN*
V:=(VMIN+VPLUS)/2;
*GOTO *THREE*END*;
V:=0.9*V;
*GOTO *THREE*END*;
LINE(1,1)*

```

Computation of suspended load

The integrals Int1 and Int2 have to be solved numerically. For Int1 an analytical solution is only possible when z_x is an integer. Integration of these integrals causes some troubles, because of the steepness near $y = 0$. As an example the function $\text{Int}0 = \int_{0.001}^1 \frac{1-y}{y} dy$ is sketched in adjacent figure. Integration-steps of $\frac{1-AA}{53} \approx 0.02$ are rather coarse, specially near AA. (In the sketched case $0.001 \int_{AA}^{AA+0.02} \frac{1-y}{y} dy \approx 0.02 \int_{AA}^1 \frac{1-y}{y} dy$)



The trapezium-rule gives a very large error hence the area is computed using the value in the middle between AA and AA + 0.02. This decreases the error; specially in the steep area, but gives not a result which is accurate enough.

So integration is devided into two parts. First the interval between AA and 1 is devided in 53 steps, and then the first step is devided again in another 53 steps. On this way the result is quite reliable.

For numerical treatment the integral Int0 is rewritten as:

$$\text{Int}0 = \text{eps} \times \sum_{T=1}^{50} \frac{1 - (AA + (T - \frac{1}{2}) \times \text{eps})}{AA + (T - \frac{1}{2}) \times \text{eps}}$$

in which eps is the width of a step; $\text{eps} = \frac{1-\text{AA}}{\text{STEPS}}$ (or $\text{eps} = \frac{1-\text{AA}}{\text{STEPS}^2}$ for the first interval).

The accuracy of this calculation depends on the amount of steps. To investigate the number of steps Int1 and Int2 were calculated with various numbers of steps, viz. STEPS = 50, 100, 200 and 300. The results of these analysis are presented in Annex VI. A calculation with steps = 50 seems to be accurate enough in this case.

In the program an axiliary variable M is used to simplify the computations.

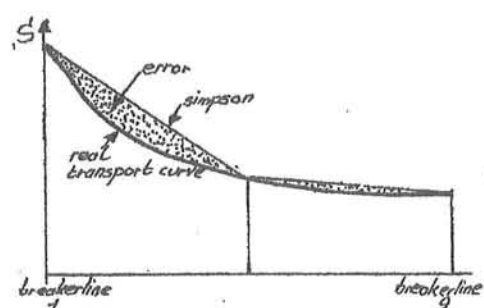
```

TALIMEAN:=R0*V*V*G/C/C*(1+(KSI*U1/V)*(KSI*U1/V)/2
+ (KSI*U2/V)*(KSI*U2/V)/2);
ZX:=W/KAPPA/SQRT(TALIMEAN/R0);
AA:=R/H;
INT1:=INT2:=0;
EPS:=(1-AA)/STEPS;
*FOR*T:=1/STEPS+STEP*1/STEPS+UNTIL*1      *DO*!*BEGIN*
M:=((1-AA-(T-.5)/STEPS)*EPS)/(AA+(T-.5)/STEPS)**ZX;
INT1:=INT1+M;
INT2:=INT2+M*LN(AA+(T-.5)/STEPS));
*END*;
INT1:=INT1/STEPS;
INT2:=INT2/STEPS;
*FOR*T:=2/STEP*1+UNTIL*STEPS+DO*!*BEGIN*
M:=((1-AA-(T-.5)*EPS)/(AA+(T-.5)*EPS))**ZX;
INT1:=INT1+M;
INT2:=INT2+M*LN(AA+(T-.5)*EPS));
*END*;
M:=.216*(AA**(ZX-))/((1-AA)**ZX);
INT1:=INT1*EPS*M;
INT2:=INT2*EPS*M;
SUS:=0.73*S*(INT1*LN(33*H/R)+INT2)/KAPPA;
OUTSTRING(1,*(ISPD)RENT TRANSPORT (SUSPENDED));
FLO(1+4.3*SUS);
OUTSTRING(1,*(IN3/M SEC OR));
FIX(1,7.0*SUS*31536000);
OUTSTRING(1,*(IN3/M YEAR));

```

Computation of the total transport

When the sand transport on each of the seven depths is known, the total transport is calculated. Within the two breakerlines three points, so



total transport is computed with the simpson rule. Because the concave shape of the real transport curve is nearly always the same the real transport is 5 % less as the transport calculated with simpson. Hence in the program the calculated transport between the breakerlines is multiplied with 0.95. Transport between the coast and breakerline 2 is calculated with a five-points polynome, correction is not necessary.

with 0.95. Transport between the coast and breakerline 2 is calculated with a five-points polynome, correction is not necessary.

6. Determination of the input data

As an example the following two-wave system is calculated:

1. Monsoon waves $H_{01} = 1.30 \text{ m}$ (r.m.s.-wave height)
 $T_1 = 10 \text{ sec}$ $\phi_{01} = 35^\circ$ $\phi_{br1} = 10^\circ$
 $K_{r1} = 0.91 \approx \sqrt{\frac{\cos\phi_{02}}{\cos\phi_{br1}}}$

2. Swell waves $H_{02} = 0.50 \text{ m}$ (r.m.s.-wave height)
 $T_2 = 15 \text{ sec}$ $\phi_{02} = 10^\circ$ $\phi_{br2} = 2^\circ$
 $K_{r2} = 0.99$

Notes: ϕ is the angle between wave-orthogonals and a line perpendicular to the coast.

The root-mean-square waveheight $H_{rms} = \sqrt{(H_i^2/n)}$ is a measure for the energy of the waves.

The given waveheights (deep water waveheights) and directions of the wave orthogonals are estimated. So it has to be investigated what are the effects of changes in these data.

Estimation of breakerheight and breakerdepth

The breakerheight and breakerdepth are in particular influenced by the wavelengths (periods) and the beach slope. The ratio between breakerheight and -depth is the breaking index γ . This index can be found (estimated) when two parameters are known, viz.:

$$\frac{H_0}{L_0 \alpha^2} \quad \text{and} \quad \frac{H_{br}}{g \alpha T^2}$$

in which: H_0 (m) r.m.s. wave height on deep water

L_0 (m) wavelength on deep water

α (-) tangent of the beach slope

H_{br} (m) r.m.s. breakerheight

g (m/s^2) acceleration of gravity

T (sec) wave period.

The only coefficient which is not exactly known is H_{br} , because it depends on the shoaling factor K_s and the refraction factor K_r . These two factors depend on the breakerdepth, which is not known. Because the breakerheight cannot be calculated directly, the calculation becomes an iteration process:

-estimate breakerheight H_{br}

-calculate breakerindex γ

-calculate breakerdepth $h_{br} = H_{br}/\gamma$

-calculate the shoaling and refraction factor K_s and K_r

-calculate the breakerheight, and check this figure with the estimated breakerheight.

monsoon: $H_{01} = 1.30 \text{ m}$; $L_{01} = \frac{g}{2\pi} T^2 = 156 \text{ m}$; $\alpha = 1/50$; $\phi_{01} = 35^\circ$

$$H_{br1} = H_{01} K_{s1} K_{r1};$$

$$\phi_{br1} = \arcsin \left(\frac{c_{br1}}{c_{01}} \sin \phi_{01} \right). \quad K_s = \sqrt{\frac{1}{2} \frac{1}{n_1} \frac{1}{c_1/c_{01}}}$$

estimation: $H_{br1} \approx 1.50$

$$\frac{H_{01}}{L_{01} \alpha^2} = \frac{1.30}{156(1/50)^2} = 20.83$$

When this factor is larger than 4.8 the breakertype is spilling (Galvin 1968, Swart 1974).

$$\frac{H_{br1}}{g \alpha T_1^2} = \frac{1.50}{9.8 (1/50) 10^2} = 0.77$$

When this factor is larger than 0.068 the breakertype is spilling.

This indicates that the breakertype is spilling; the breakerindex γ is about 0.6. The breakerdepth will be $1.50/0.6 = 2.50 \text{ m}$. The breaker height and depth can now be checked by means of Table C1 of the Shore Protection Manual (volC) (US Army, 1973).

$$h_{br1} \approx 2.50 \text{ m} \rightarrow h/L_0 = 2.50/156 = 0.0160 \rightarrow$$

$$K_{s1} = 1.288; \phi_{br} = \arcsin (0.3117 \sin 35^\circ) = 10.3^\circ$$

$$K_{r1} = 0.9125.$$

$$H_{br1} = 1.30 \times 0.9125 \times 1.288 = 1.53 \text{ m (102%)}$$

The breakerheight was assumed to be 1.50 m.

$$\text{So breakerheight } H_{br1} = 1.50 \text{ m} \quad \gamma = 0.6$$

$$\text{breakerdepth } h_{br1} = 2.50 \text{ m}$$

$$\text{breakerangle } \phi_{br1} = 10.3^\circ$$

swell: $H_{02} = 0.50 \text{ m}$; $T_2 = 15 \text{ sec}$; $L_{02} = 351 \text{ m}$; $\alpha = 1/50$; $\phi_{02} = 10^\circ$

estimation $H_{br2} = 0.92 \text{ m}$

$$\frac{H_{02}}{L_{02} \alpha^2} = 3.56 < 4.8 \rightarrow \text{plunging}$$

$$\frac{H_{br2}}{g \alpha T_2^2} = 0.021 < 0.068 \rightarrow \text{Plunging}$$

The breakertype will be plunging, $\gamma = 0.8$

The breakerdepth is $h_{br2} = 0.92/0.8 = 1.15 \text{ m}$.

$$h_{br2} = 1.15 \rightarrow h/L_0 = 0.00328$$

$$K_{s2} = 1.876; \phi_{br2} = \arcsin (0.1431 \sin 10^\circ) = 1.4^\circ$$

$$K_{r2} = 0.9925$$

$$H_{br2} = 0.50 \times 1.876 \times 0.9925 = 0.93 \text{ m (101%)}$$

The breakerheight was assumed to be 0.92 m

$$\text{So breakerheight } H_{br2} = 0.92 \text{ m}$$

$$\text{breakerdepth } h_{br2} = 1.15 \text{ m}$$

$$\text{breakerangle } \phi_{br2} = 1.4^\circ$$

7. A calculation by hand

The breakerheight and -depth of the two wave-types are now known. The sand transport can be calculated by means of the following formulae:

$$v = \frac{5 A C^2 \alpha h}{8 \sqrt{g} \xi F} \left\{ \frac{\sin \phi_{br1} \cos \phi_{br1}}{\sqrt{h_{br1}}} + \frac{\sin \phi_{br2} \cos \phi_{br2}}{\sqrt{h_{br2}}} \right\} - \frac{A F' \xi \sqrt{g} h}{2F}$$

$$S_b = 5 D \frac{v}{C} \sqrt{g} \exp \left\{ \frac{-0.27 \Delta D C^2}{\mu v^2 \left\{ 1 + \frac{1}{2} \left(\frac{u_{01}}{v} \right)^2 + \frac{1}{2} \left(\frac{u_{02}}{v} \right)^2 \right\}} \right\}$$

In which:

A the ratio between the breakerheight and -depth (H/h) in the breakerzone. This figure is assumed to be constant.

C Chézy-friction-coefficient for a "bottom"-roughness r ; r is 2 or 3 times the ripple-height Δr .

α tangent of the beach slope

h waterdepth

g acceleration of gravity (9.8 m/s²)

ξ multiplication factor for the orbital velocity at the bottom: $\frac{pkC}{\sqrt{g}}$,
in which $p = p_{Jonsson} = \sqrt{(f_w/2\kappa^2)}$; $f_w = \exp \left\{ -5.98 + 5.21 (a_o/r)^{-0.19} \right\}$
 κ is the Von Karman constant $\kappa = 0.384$; a_o is the amplitude of the displacement of a waterparticle at the bottom

u_o amplitude of the orbital (horizontal) velocity at the bottom

F function of T_1 and T_2

F' function of T_1 and T_2

h_{br} breakerdepth

ϕ_{br} breakerangle, angle between wave orthogonals (at breaking) and a line perpendicular to the coast

μ ripple factor $\mu = \left(\frac{C}{C_{90}} \right)^{1.5}$; $C_{90} = 18 \log \frac{12h}{D_{90}}$

Δ relative density of sand and water: $\frac{\rho_s - \rho_w}{\rho_w}$

D grain size, in this formula D_{50}

v water velocity in the breakerzone (longshore velocity)

S_b bedload transport

Notes: In this formula is assumed that the breakertype (represented by A) of both waves is the same.

The functions F and F' are calculated with the assumptions that

$u_{01} = u_{02}$ (bottom-velocities). This is not true, specially not between the two breakerlines.

Because the calculation is very complicated the sand transport is calculated in some special points. The total sand transport is calculated by means of a mean sand transport between two points:

$$S_{btot} = \frac{S_{b1} + S_{b2}}{2} (X_2 - X_1)$$

The only factor which is not known is the ripple height. A method to calculate ripple-heights is presented in TOW (1976). This method is based on laboratory and field measurements.

Calculation of the ripple-height

$$Q = \frac{H}{h} \left(\frac{L}{k} \right)^2 \quad P = Q/13.6 \quad \text{for} \quad Q > 34.8$$

$$P = 1 + Q/22.3 \quad \text{for} \quad Q < 34.8$$

$$A_o = \frac{1}{\sqrt{\pi P}} \left(1 - \frac{1}{8P} - \frac{1}{128P^2} \right) \quad \beta = \frac{1}{90} \arccos (A_o)^{\frac{1}{2}P}$$

Q , P , A_o and β are constants.

H is the wave height (significant wave height or height of the broken wave); h is the water depth and L is the wave length.

$t_{crest} = \beta \times T$ is the time during which the orbital velocity has the same direction as the wave celerity; T is the wave period.

$u_{ov} = \frac{2\pi}{T} \frac{H(1-A_o)}{\sinh k(h+H(1-A_o))}$ is the maximum orbital velocity at the bed according to a wave theory proposed by Van Hijum.

$\hat{a}_o = u_{ov} \times t_{crest}$, orbital amplitude at the bottom

$\Delta r = A_r \times \hat{a}_o \left(\hat{a}_o / \sqrt{L \times D_{50}} \right)^{-1.56}$ D_{50} is the grainsize.

A_r is a constant dependent on L , D_{50} , w and Re . (w is the fall-velocity, Re is the Reynolds number).

The calculation of Δr is valid when $u_{ov}/v_{\infty} > 10$.

A_r can be determined with the following equation:

$$A_r = C_p Re_o^{0.31} (L/D_{50})^{0.05} Re_{\infty}^{-0.5}$$

$$C_p = 1.475 \exp (0.645 - 9.2 \times 10^{-4} \sqrt{L/D_{50}} - (0.009Re + 0.2))$$

$$\exp(-0.008Re)$$

$$Re = \frac{w D_{50}}{v}$$

$$\log (1/w) = 0.447 (\log D_{50})^2 + 1.961 \log D_{50} + 2.736$$

$$v = 1.792 \times 10^{-6} \exp (-0.042 T^{0.87}) \quad \text{for } 0 < T < 30 {}^\circ C$$

$$Re_o = \frac{w (D_{50} - D_0)}{v} \quad D_0 = 50 \times 10^{-6} \text{ m}$$

$$Re_{\infty} = \frac{w (D_{50}^v + D_{\infty})}{v} \quad D_{\infty} = 500 \times 10^{-6} \text{ m}$$

for $D_{50} = 150 \times 10^{-6}$ and $T = 25^\circ\text{C}$

$$v = 8.98 \times 10^{-7}$$

$$w = 1.685 \times 10^{-2}$$

$$Re_o = 1.88; Re_\infty = 12.20; Re = 2.81;$$

$$C_p = 1.457 \exp (0.645 - 9.2 \times 10^{-4} \times \sqrt{(L/d_{50})} - 0.220)$$

The calculation of the "real" Δr with two wave-types is very complicated because the \hat{a}_o and L cannot be calculated. So for each wave-type a Δr is calculated, for different waterdepths. It is important to know whether Δr is dependent on depth.

Because this calculation is rather cumbersome, it is automatized by a separate computer program. This program is not included in the sand transport program because of the difficulty just mentioned.

waterdepth $h = 2.5 \text{ m}$

Monsoon-wave $H = 1.5 \text{ m}$ (broken wave); $T = 10 \text{ sec}$; $h/L_o = 0.0160$, so

according to the shore protection manual $L = 48.7 \text{ m}$

$$Q = 227.7; P = 16.74; A_o = 0.1369; \beta = 0.2173; t_{\text{crest}} = 2.17 \text{ s};$$

$$u_{ov} = 1.60 \text{ m/s}; \hat{a}_o = 1.60 \times 2.17 = 3.47 \text{ m};$$

$$L/D_{50} = 3.25 \times 10^5; A_r = 0.553.$$

$$\Delta r = 3.47 \times 0.553 \times \left(\frac{3.47}{(48.7 \times 150 \times 10^{-6})} \right)^{-1.56} = 0.0059 \text{ m}$$

Swell-wave $H = 1.09 \text{ m}$ (significant wave); $T = 15 \text{ sec}$ $L = 73.7 \text{ m}$

$$\hat{a}_o = 3.65; A_r = 0.494.$$

$$\Delta r = 0.0071 \text{ m}$$

waterdepth $h = 1.0 \text{ m}$

Monsoon-wave $H = 0.6 \text{ m}$ (broken wave); $T = 10 \text{ sec}$; $L = 31.1 \text{ m}$;

$$\hat{a}_o = 1.65 \text{ m}; A_r = 0.609$$

$$\Delta r = 0.0070 \text{ m}$$

Swell-wave $H = 0.8 \text{ m}$ (broken wave); $T = 15 \text{ sec}$; $L = 46.9 \text{ m}$;

$$\hat{a}_o = 1.94 \text{ m}; A_r = 0.558.$$

$$\Delta r = 0.0081 \text{ m}$$

The above calculations show that Δr does not vary much in the breaker-zone. Therefore the roughness r can be assumed to be constant in the breakerzone. (An other reason is that a good multiplication factor to calculate r out of Δr is not at hand)

$$r = 2 \text{ or } 3 \text{ times } \Delta r$$

So: assume $r = 0.02 \text{ m}$.

In the computer program (see listing on page 28) the nomenclature is almost equal to the nomenclature, used in the above calculation, only A_o is called AX. Note: In the program H = wave-height.

```

*BEGIN*
*REAL*D,DMAX,DZERO,TEMP,NU,W,REYNZERO,REYNMAX,REYNOLDS,A,H,L,Z,T,Q,P,G,
  AX,B,BETA,AMAX,AR,DELTAR,BX;
*REAL**PROCEDURE*ARCCOS(F);*REAL*F;
ARCCOS:=ARCTAN(SQRT(1/(1-F*F)-1));
*REAL**PROCEDURE*SINH(F);*REAL*F;
SINH:=(EXP(F)-EXP(-F))/2;
*REAL**PROCEDURE*TANH(F);*REAL*F;
TANH:=(EXP(F)-EXP(-F))/(EXP(F)+EXP(-F));
OUTSTRING(1,*("CALCULATION OF THE RIPPLE-MEIGHT")*)$LINE(1,2);
READ(0,D);READ(0,TEMP);
G:=10;
DMAX:=.0005;DZERO:=.00005;
NU:=.000001792*EXP(-.042*(TEMP**.87));
W:=EXP(-.1941*(LN(D))+(LN(D))-1.961*LN(D)-6.2998);
REYNZERO:=W*(D-DZERO)/NU;
REYNMAX:=W*(DMAX+D)/NU;
REYNOLDS:=W*D/NU;
A:=.645-(.009*REYNOLDS+.2)*EXP(-.008*REYNOLDS);
B:=1/SQRT(REYNMAX);
CONTINUE;
READ(0,H);*IF*H>1000*THEN*GOTO*FINISH;
  READ(0,Z);READ(0,T);
L:=G*T*T/2/PI*SQRT(TANH(4*PI*PI/T/T/G));
*FOR*P:=1*STEP*1*UNTIL*3*DO*REGIN;
AX:=G*T*T/2/PI*TANH(2*PI*Z/L);
L:=(2*AX+L)/3;END*;
Q:=H*L*L/Z/Z/Z;
*IF*Q>34.8*THEN*P:=0/13.6*ELSE*P:=1+0/22.3;
AX:=1/SQRT(PI*P)*(1-1/8/P+1/128/P/P);
BX:=AX**(1/P/2);
BETA:=ARCCOS(BX)*2/PI;
AMAX:=2*PI/T*H*(1-AX)/SINH(2*PI/L*(Z+H*(1-AX)))*BETA*T;
AR:=1.475*EXP(A-.00092*SQRT(L/D))*H*(REYNZERO**(.31*((L/D)**.05)));
DELTAR:=AR*AMAX*((AMAX/SQRT(D*L))**(-1.56));
OUTSTRING(1,*("TEMP      D      H      L      DEPTH      T      DELTA R")*)$LINE(1,1);
FIX(1,2,0,TEMP)$FLO(1,3,2,0)$FIX(1,2,2,H)$FIX(1,3,6,L)$FIX(1,2,2,Z);
FIX(1,2,0,T)$FLO(1,3,2,DELTAR);
LINE(1,1);
OUTSTRING(1,*("*****")*)$LINE(1,4);
*GOTO*CONTINUE;
FINISH:PAGE();
*END*

```

CALCULATION ON THE RIPPLE-HEIGHT

TEMP	D	H	L	DEPTH	T	DELTA R	by hand
+25	$.150^{\circ}-03$	+1.50	+50	+2.50	+10	$.597^{\circ}-02$	$.59 \cdot 10^{-2}$
+25	$.150^{\circ}-03$	+1.10	+76	+2.50	+15	$.716^{\circ}-02$	$.71 \cdot 10^{-2}$
+25	$.150^{\circ}-03$.60	+31	+1.00	+10	$.703^{\circ}-02$	$.70 \cdot 10^{-2}$
+25	$.150^{\circ}-03$.80	+47	+1.00	+15	$.807^{\circ}-02$	$.81 \cdot 10^{-2}$
+25	$.150^{\circ}-03$.66	+16	+1.10	+5	$.526^{\circ}-02$	

Differences with the hand-calculation are due to the determination of the wave-length. In the hand-calculation L is determined with the tables in the shore protection manual, in the program L is computed with the formula of Eckert, followed by a three step optimizing algorithm, as described on page 14.

Sand transport calculations

The calculation of the velocity of the longshore current and the bed-load transport are executed in the following way:

for $h_{br2} < h < h_{br1}$

$$v = 2.372 \times 10^{-3} \frac{c_r h}{p} - 2.515 \times 10^{-4} p c_r \sqrt{h}$$

$$A = 0.6, \phi_{br1} = 10.3^\circ; h_{br1} = 2.5 \text{ m}; = 0.384; F = 0.916; F' = 0.002.$$

for $0 < h < h_{br2}$

$$v = 2.858 \times 10^{-3} \frac{c_r h}{p} - 2.515 \times 10^{-4} p c_r \sqrt{h}$$

$$\phi_{br2} = 1.4^\circ; h_{br2} = 1.15 \text{ m}$$

$$c_r = 18 \log(12h/r); p = \sqrt(f_w/2k^2); f_w = \exp(-5.98 + 5.21(a_o/r)^{-0.19})$$

$$r = 0.02 \text{ m}$$

$$S_b = 74042 \frac{v}{c_r} \exp\left(-\frac{6.48 \times 10^{-5} \times c_r^2}{\mu v^2 (1+\frac{1}{2}(\frac{\xi u_{01}}{v})^2 + \frac{1}{2}(\frac{\xi u_{02}}{v})^2)}\right)$$

$$D_{50} = 150 \times 10^{-6}; \Delta = 1.6; g = 9.8.$$

$$\mu = (c_r/c_{D90})^{1.5}; \xi = pkc_r/\sqrt{g}; u_o = \frac{\pi H}{T \sinh(2\pi h/L)}; a_o = \frac{u_o^T}{2\pi}$$

Velocity and sand transport is calculated for the following waterdepths:

$$h_i = 1.15 + i \frac{2.50 - 1.15}{8} \quad (i=1,2,\dots,8); h_j = 0 + j \frac{1.14}{4} \quad (j=1,\dots,4)$$

Suspended load

Sand transport does not only take place on the bottom, sand will be transported also suspended in the water. This transport is called suspended-load-transport and depends on (acc. to Einstein *)

-bottom transport S_b

-fall velocity of the suspended material w_s

-waterdepth

-the roughness of the bottom r .

$$S_s = \frac{0.73}{\kappa} S_b (\text{Int1} \ln(33h/r) + \text{Int2}) = B S_b$$

$$S_{tot} = S_s + S_b = S_b (B + 1) \text{ m}^3/\text{m/year}$$

* The original publication is not studied, but only the reference in Bijker (1972). To investigate what is meant by "some mathematics" the complete derivation is made in annex V.

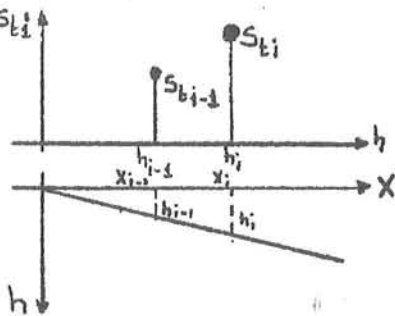
$$\text{Int1 and Int2 depend on } Z_{\frac{w}{kv}} = \frac{w_s}{kv} ; \quad v_{\frac{w}{kv}} = \sqrt{\left(\frac{\tau_r}{\tau_c}\right) \frac{v_g^2}{C}} ;$$

$$A = r/h; \quad w=0.01685; \quad k= 0.384; \quad r = 0.02 \text{ m}$$

Int1 and Int2 can be read in a figure in Bijker (1972).

h (m)	H_2	a_o	C	v	S_b	$B+1$	S_{tot}
2.500	0.77	2.33	57.2	1.27	1531	87.1	13.33
3.331	0.79	2.28	56.6	1.17	1418	78.2	11.09
2.163	0.80	2.23	56.0	1.07	1306	75.6	9.87
1.994	0.81	2.25	55.4	0.97	1192	68.6	8.18
1.825	0.83	2.34	54.7	0.89	1103	62.5	6.89
1.656	0.85	2.49	54.0	0.80	998	52.9	5.28
1.488	0.88	2.75	52.8	0.70	889	45.2	4.02
1.319	0.90	2.92	52.2	0.64	819	42.4	3.47
1.150	0.93	3.23	51.1	0.55	721	38.9	2.80
1.150	0.93	3.23	51.1	0.67	882	39.5	3.48
0.863	0.69	2.62	48.9	0.46	612	26.4	1.61
0.575	0.46	1.77	45.7	0.26	359	16.5	0.59
0.288	0.23	1.61	40.3	0.11	143	6.9	0.01

In adjacent table S_{tot} is in $10^4 \text{ m}^3/\text{m/year}$.



Total transport is calculated as follows:

Transport between h_i and h_{i-1} is:

$$\frac{S_{ti} + S_{ti-1}}{2} (x_i - x_{i-1}) ; \quad x_i - x_{i-1} = (h_i - h_{i-1}) \frac{1}{\alpha}$$

Total transport in the breakerzone:

$$S_t \sum_{i=1}^n \frac{S_{ti} - S_{ti-1}}{2} (h_i - h_{i-1}) \frac{1}{\alpha}$$

For $h_{br2} < h < h_{br1}$

$$S_{t1} \text{ (for } n_1 = 8) = 4.798 \times 10^6 \text{ m}^3/\text{year} \text{ (100 %)}$$

$$S_{t1} \text{ (for } n_1 = 4) = 4.868 \times 10^6 \text{ m}^3/\text{year} \text{ (101.5 %)}$$

$$S_{t1} \text{ (for } n_1 = 2) = 5.047 \times 10^6 \text{ m}^3/\text{year} \text{ (105.2 %)}$$

For $0 < h < h_{br2}$

$$S_{t2} \text{ (for } n_2 = 4) = 0.568 \times 10^6 \text{ m}^3/\text{year} \text{ (100 %)}$$

$$S_{t2} \text{ (for } n_2 = 2) = 0.670 \times 10^6 \text{ m}^3/\text{year} \text{ (118 %)}$$

The transport in the whole breakerzone is $5.366 \times 10^6 \text{ m}^3/\text{year}$.

In the computer program S_t is approximated with $n_1 = 3$ and $n_2 = 4$, this transport becomes $5.526 \times 10^6 \text{ m}^3/\text{year}$. This transport is a bit too high and therefore better approximated by $0.95 \times 5.526 \times 10^6 = 5.278 \times 10^6$.

The factor 0.95 is chosen because S_{t1} ($n_1=8$) is also an approximation of the transport, the real transport will be about 1 % less.

The total sand transport calculated with two incoming waves can not be checked with the CERC-formula, therefore total sand transport is calculated with the computer for both waves alone.

$$H_0 = 1.30; h_{br} = 2.50; k_r = 0.9 \quad \phi_{br} = 10^\circ \quad T = 10 \text{ sec}$$

$$S_{tot} (\text{comp}) \quad 4.56 \times 10^6 \text{ m}^3/\text{year}$$

$$S_{tot} (\text{CERC}) \quad 2.84 \times 10^6 \text{ m}^3/\text{year}$$

$$H_0 = 0.50. \quad h_{br} = 1.10; k_r = 0.95; \phi_{br} = 2^\circ \quad T = 15 \text{ sec}$$

$$S_{tot} (\text{comp}) \quad 1.46 \times 10^6 \text{ m}^3/\text{year}$$

$$S_{tot} (\text{CERC}) \quad 1.39 \times 10^6 \text{ m}^3/\text{year}$$

From the above figures the conclusion can be drawn that the difference in sand transport between CERC and computerprogram depends on the wave period. Therefore sand transport is also calculated for a wave with a period of 5 sec.

$$H_0 = 0.58; h_{br} = 1.10; k_r = 0.998 \quad \phi_{br} = 2^\circ \quad T = 5 \text{ sec} \quad r = 0.015$$

$$S_{tot} (\text{comp}) \quad 0.924 \times 10^5 \text{ m}^3/\text{year}$$

$$S_{tot} (\text{CERC}) \quad 0.691 \times 10^5 \text{ m}^3/\text{year}$$

$$\text{So: } T = 5 \text{ sec} \quad S_{\text{comp}}/S_{\text{CERC}} = 1.34$$

$$T = 10 \text{ sec} \quad S_{\text{comp}}/S_{\text{CERC}} = 1.61$$

$$T = 15 \text{ sec} \quad S_{\text{comp}}/S_{\text{CERC}} = 1.05$$

Note: In these formula the H_{rms} is used; in the CERC-formula a factor 0.024 is used.

8. Analysis of the accuracy of the sand transport calculations

Only the calculation of sand transport is not enough. All relative errors in the input data have to be taken into account for the determination of a relative error in the sand transport. This relative error in the sand transport will not be a standard of the accuracy of the used formula. The deviation of the real value can only be determined by sand transport measurements along the coast.

The intention of this chapter is the determination of the accuracy of the input data for the sand transport calculation, in order to obtain a more or less accurate figure for the sand transport (relative error of $\pm 50\%$).

The input data are (for the computer-program):

κ	Von Karman constant
ρ	density of seawater (kg/m^3)
Δ	relative desity of sediment ($\rho_s - \rho / \rho$)
g	acceleration of gravity (m^2/sec)
D_{90}, D_{50}	grain sizes (m)
α	tangent of the beach slope
γ_1, γ_2	breaker indexes of the two wave system
ϕ_{br}	breaker-angle
T	period (sec)
h_{br}	breakerdepth (m)
r	bottom roughness (m)

The relative errors of (the constants) κ , ρ , g and Δ are small in comparison with the other relative errors, so these errors are neglected. The variable D_{90} appears only in the factor μ in the exp-function of the sand-transport formula. The influence of an error in D_{90} is therefore very small and can be neglected too.

For the remaining variables an analysis (by means of the computer) is made of the influences of their relative errors on the total sand transport.

In this report only the results are presented. In annex VII a more detailed consideration is given.

beach conditions

The computer calculation for the influences of D_{50} , r and α are made with the data of the first period (Dec-Feb) in the first cross-section. The results of these calculations were:

bottom roughness r :	0.015 . 0.020 . 0.025	m
calc. total transport :	2.03 . 1.61 . 1.34	million m^3/year

When $r = 0.020$ is regarded as the 100 % value, there follows:

- an increase of ca. 25 % in the bottom roughness results in a decrease of 15 % in sand transport
- a decrease of ca. 25 % in the bottom roughness results in an increase of 25 % in sand transport.

grain-size D_{50}	:	130	150	170	μm
calc. total transport:		1.75	1.61	1.46	million m^3/year

When $D_{50} = 150 \mu\text{m}$ is regarded as the 100 % value there follows:

- an increase of ca. 13 % of the grain-size results in a decrease of ca 9 % of the sand transport
- a decrease of ca. 13 % of the grain-size results in an increase of ca 9 % of the sand transport

beach slope α	:	1:33	1:40	1:50	
calc. total transport:		2.04	2.01	1.98	million m^3/year

When $\alpha = 0.025$ (1:40) is regarded as the 100 % value there follows

- an increase of ca. 20 % of the beach slope results in an increase of ca. 1.5 % of the transport
- a decrease of ca 20 % of the beach slope results in a decrease of ca 1.5 % of the sand transport.

Conclusions:

- a- The beach slope α is not important when only the total sand-transport has to be known. When the distribution of the sand transport over the breakerzone has to be known the beach slope becomes very important. The variation of the total transport because of a variation in the beach slope α is negligible.
- b- Because of variations of the grain-size (D_{50}) along the coast a variation of about 10 % of the total sand transport is expected.
- c- The bottom-roughness (r) cannot be calculated. So a large error in this factor is possible. Therefore a variation of about 20 - 25% of the total transport is expected.
- d- The total variation of the sand transport because of D_{50} and r is about 25 - 30 %.

In the last part of this chapter the influence of errors in the wave parameters (wave-data) are analysed. These parameters are

H_0 - deepwater wave-heights (H_{rms})
 ϕ_0 - deepwater angle of wave incidence
 T - period of the waves

The sand transport depends on a two-wave system. This system is very complex, yet is tried to calculate the influences of errors in both wave-types. A more detailed description of the applied method is given in Annex VII.

Calculation of the influence of an error in the period of one of the wave-types gives the following result:

- an increase of the period (T) with 20 % results in an increase of the total transport of ca. 7 %
- a decrease of the period with 20 % results in a decrease of the total transport of ca. 5 %

The variation of the total transport caused by errors in the periods of the two wave-types is valued at 10 %.

Calculation of the influence of an error in the deepwater waveheight of one of the two waves is very complicated. It appears that the variation of the total transport is not "constant" at different deepwater waveheights. A good approximation is:

- an increase of the deepwater waveheight with 25 % results in an increase of the total transport with ca 90 %.
- a decrease of the deepwater waveheight with 25 % results in a decrease of the total transport with 45 %.

Because no detailed measurements of the deepwater waveheight are available, it is almost impossible to give a certain variance for this parameter.

For the calculation of the variation of the total sand transport only an error in the estimation of the refraction coefficient is taken into account. The variation of the total sand transport, because of this error is valued at 40 %.

The arguments, as mentioned above, are used for the calculation of the variation of the total sand transport due to errors in the deepwater waveangle. A good approximation of this variation is:

- a variation of the angle of incidence with 15 % results in a variation of the total sand transport of ca. 50 %.

For the calculation of the variation of the total sand transport only an error in the estimation of the breakerangle is taken into account. The variation of the total transport, because of this error is valued at 35 %.

Conclusions:

- The variation of the total sand transport, due to errors in the wave-approach, wave-height or wave period (wave-parameters) is about 50 %.
- As already mentioned the variation of the transport due to errors in D_{50} and r (coastal parameters) is valued at 25 %.

It is not allowed to combine these errors, because the second error is constant along the coast, due to the fact that D_{50} is constant along the coast.

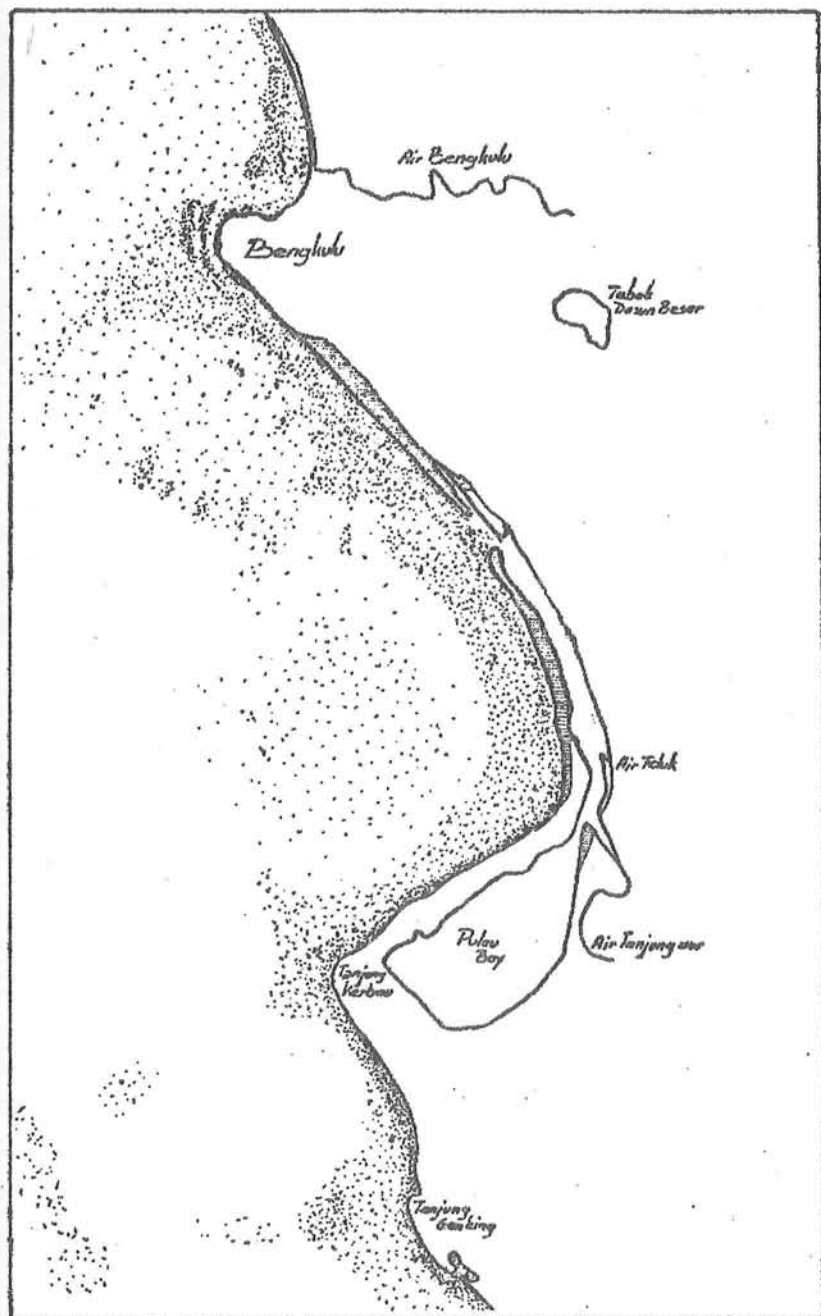
Remark So reliable wave data are vital for a good prediction of sediment transport. Hence it is advised to start wave observations (on deep water, during at least one year) immedeately.

References

- Battjes, J.A. (1972); Radiation stesses in short crested waves;
Journ. of Marine Res. pp 56-64
- Battjes, J.A. (1974); Computation of set-up, longshore currents, run-up
and overtopping due to wind generated waves, diss. Delft
- Bijker, E.W. (1967); Some considerations about scales for coastal models
with movable bed, diss. Delft
- Bijker, E.W. (1972); Topics in coastal engineering, lecture notes Delft
University of Technology
- Jonsson, I.G. (1966); Wave boundary layers and friction factors, 10th
coastal engineering conference, Tokyo, vol I.
- Jonsson, Skovgaard & Jacobson (1974); Computation of longshore current,
14th coastal engineering conference, Copenhagen, vol II.
- Kinsman, B. (1965) Wind Waves, prentince hall
- TOW (1976); Computation of longshore transport, Delft Hydraulic Labo-
ratorium, R968-I
- Skovgaard, Jonsson & Bertelsen (1975); Computation of wave-heights due
to refraction and friction, proc. ASCE, WW1, may '75
- US Army (1973); Shore protection manual, Coastal Engineering Research
Center



**Delft University of Technology
Dept of Civil Engineering
Coastal Engineering Group**



**BENGKULU
HARBOUR
PROJECT**

Final report

Annexes to vol B

Feb '78

Dik Ludikhuize & Henk Jan Verhagen

Contents

- Annex I Calculation of the energy of cross-swell
- Annex II Some ideas about cross-swell
- Annex III Radiation stress caused by cross-swell
- Annex IV The friction factor f_w and the amplitude
- Annex V Formula of Einstein for the calculation of suspended load
- Annex VI The accuracy of the computer procedure to solve the Einstein-integrals
- Annex VII Determination of the accuracy of the calculated sand transport
- Annex VIII Acceleration of a longshore current.

Calculation of the energy of cross-swell

The potential energy in a small area $dxdy$ is the product of the mass above (or below) S.W.L. and the distance from the mass-center to S.W.L.
This mass is $\rho g \eta dxdy$
The distance is $\frac{1}{2}L^2$
So $dE_p = \rho g \eta dxdy \cdot \frac{1}{2}L^2 = \frac{1}{2}\eta^2 \rho g dxdy$

Hence [for perpendicular waves]

$$\begin{aligned} E_p &= \int_0^{L_1} \int_0^{L_2} \frac{1}{2} \eta^2 \rho g dxdy \\ &= \frac{1}{2} \rho g \int_0^{L_1} \int_0^{L_2} \eta^2 dxdy \end{aligned}$$

L is the wave-length.

$$\eta = a_1 \sin k_1 x + a_2 \sin k_2 y \quad k = \frac{2\pi}{L}$$

$$\eta^2 = a_1^2 \sin^2 k_1 x + a_2^2 \sin^2 k_2 y + 2a_1 a_2 \sin k_1 x \sin k_2 y$$

$$\begin{aligned} \int_0^{L_1} \int_0^{L_2} \eta^2 dxdy &= \int_0^{L_1} \int_0^{L_2} (a_1^2 \sin^2 k_1 x + a_2^2 \sin^2 k_2 y + 2a_1 a_2 \sin k_1 x \sin k_2 y) dxdy \\ &= a_1^2 \int_0^{L_1} \int_0^{L_2} \sin^2 k_1 x dxdy + a_2^2 \int_0^{L_1} \int_0^{L_2} \sin^2 k_2 y dxdy + 2a_1 a_2 \int_0^{L_1} \int_0^{L_2} \sin k_1 x \sin k_2 y dxdy \\ &= a_1^2 \int_0^{L_1} \left[x - \frac{1}{2}k_1 \sin 2k_1 x \right] dy + a_2^2 \int_0^{L_2} \left[y - \frac{1}{2}k_2 \sin 2k_2 y \right] dx + 0 \\ &= \frac{1}{2}a_1^2 L_1 \left[y \right]_0^{L_2} + \frac{1}{2}a_2^2 L_2 \left[x \right]_0^{L_1} \\ &= \frac{1}{2}a_1^2 L_1 L_2 (a_1^2 + a_2^2) \end{aligned}$$

$$\begin{aligned} \text{So } E_p &= \frac{1}{2} \rho g L_1 L_2 (a_1^2 + a_2^2) \\ &= \frac{1}{4} \rho g L_1 L_2 \left(\frac{1}{4} H_1^2 + \frac{1}{4} H_2^2 \right) \\ &= \frac{1}{16} \rho g L_1 L_2 (H_1^2 + H_2^2) \end{aligned}$$

The potential energy per unit surface is:

$$V_p = E_p / L_1 L_2 = \frac{1}{16} \rho g (H_1^2 + H_2^2)$$

And because the potential energy per unit surface is equal to the kinetic energy, the total energy becomes:

$$V_t = \frac{1}{8} \rho g (H_1^2 + H_2^2) = \frac{1}{8} \rho g H_1^2 + \frac{1}{8} \rho g H_2^2 = V_1 + V_2$$

and not $\frac{1}{8} \rho g H_t^2$

Note: When the waves are not perpendicular an identical derivation leads to the same result.

η = deviation from S.W.L.

E = energy of a wave

V = energy of a wave per unit surface

L = wave length

a = amplitude

H = wave height

ρ = density of water

g = acceleration of gravity

k = wave number [$2\pi/L$]

Some ideas about cross-swell

1. Introduction

In chapter 3 of vol B an adoption of the Bijker-Frijlink formula is given. This derivation is not valid for cases in which the two waves have identical periods, because in the numerical process sometimes divisions by $T_1 - T_2$ are made. And division by zero is not possible. Because in nature two identical periods do not occur, this causes no problems.

An other point of interest is phase-lagging. In the derivation of vol B we assumed that phase differences are not important over a long time. This is true in cases in which the periods differ, but not in case of identical periods, and perhaps not in cases like $T_1 = \frac{1}{2}T_2$.

In this annex we will try to get an idea of cross-swell in case of identical waves, and of the importance of phase-lagging. Because it is far beyond the scope of our study to investigate the real behaviour of cross-swell in model experiments or in nature, we have to assume many things.

First is tried to give a mathematical description of the velocity near the bottom in case of cross-swell in general. In chapter 3 of this annex this is done for a special case, viz. with two identical periods. As will be shown, phase-lagging becomes important in such cases. Some problems with continuity of sand and water will appear. In chapter 4 the results of a numerical example are given, to show the effect of this phase-lagging. In chapter 5 is indicated why in normal cases these difficulties will not occur.

It has to be noticed that the ideas presented in this annex are only ideas. They are the results of mathematics based on reasonable assumptions, but are not based on real scientific research. To be sure of the behaviour of cross-swell, years of investigations are necessary.

2. The bottom-velocity

Normally the velocity on the bottom is given as a function of the waveheight. This is only possible in a one-dimensional case. When two dimensions are involved, like in case of cross-swell, this is impossible, because the waveheight is a scalar-function, and the velocity is a vector-function. We assume that both the incoming waves do not influence each other, hence

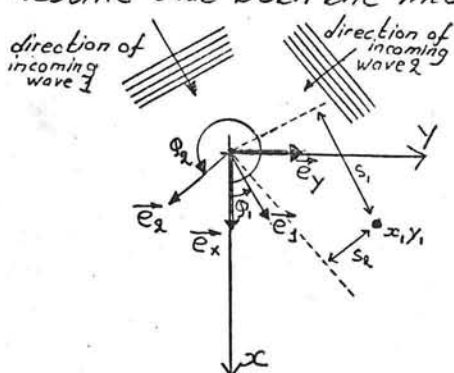


fig. 1

/ / / / / / / / / / / / coastline / / / /

$$\text{one may add the two original velocity-vectors}$$

$$\vec{U}_b(x, y, t) = \vec{U}_{b1}(x, y, t) + \vec{U}_{b2}(x, y, t) \quad *)$$

or:

$$\vec{U}_b = \frac{H_1 \omega_1}{2 \sinh(kh)} \sin(\omega_1 t - k_1 s_1) \vec{e}_1 + \frac{H_2 \omega_2}{2 \sinh(kh)} \sin(\omega_2 t - k_2 s_2) \vec{e}_2 \quad (1)$$

[s_1 and s_2 are distance-parameters in the directions of \vec{e}_1 and \vec{e}_2].

To interpret this equation, it has to be rewritten in normal cartesian coordinates.

s is the distance to a line perpendicular to the direction \vec{e}_i and going through the origin.

*) $\vec{U}_b(x, y, t)$ means that the vector \vec{U}_b is a function of x, y and t . \vec{e}_1 is the vector of unity in the direction of the first wave, \vec{e}_x is the vector of unity in the x direction

The equation of this line is $y = -\frac{1}{tg \varphi} x$, or $x + tg \varphi, y=0$. The distance from a point x, y to this line is:

$$s_1 = \frac{|x_1 + y_1 tg \varphi|}{\sqrt{1 + tg^2 \varphi}}$$

Now equation (4) can be rewritten as:

$$\vec{v}_b = \frac{H_1 \omega_1}{2 \sinh(k_1 h)} \sin\left(\omega_1 t - k_1 \frac{|x_1 + y_1 tg \varphi_1|}{\sqrt{1 + tg^2 \varphi_1}}\right) \vec{e}_1 + \frac{H_2 \omega_2}{2 \sinh(k_2 h)} \sin\left(\omega_2 t - k_2 \frac{|x_1 + y_1 tg \varphi_2|}{\sqrt{1 + tg^2 \varphi_2}}\right) \vec{e}_2$$

or

$$\vec{v}_b = \left[\frac{H_1 \omega_1}{2 \sinh(k_1 h)} \sin\left(\omega_1 t - k_1 \frac{|x_1 + y_1 tg \varphi_1|}{\sqrt{1 + tg^2 \varphi_1}}\right) \cos \varphi_1 + \frac{H_2 \omega_2}{2 \sinh(k_2 h)} \sin\left(\omega_2 t - k_2 \frac{|x_1 + y_1 tg \varphi_2|}{\sqrt{1 + tg^2 \varphi_2}}\right) \cos \varphi_2 \right] \vec{e}_x$$

$$+ \left[\frac{H_1 \omega_1}{2 \sinh(k_1 h)} \sin\left(\omega_1 t - k_1 \frac{|x_1 + y_1 tg \varphi_1|}{\sqrt{1 + tg^2 \varphi_1}}\right) \sin \varphi_1 + \frac{H_2 \omega_2}{2 \sinh(k_2 h)} \sin\left(\omega_2 t - k_2 \frac{|x_1 + y_1 tg \varphi_2|}{\sqrt{1 + tg^2 \varphi_2}}\right) \sin \varphi_2 \right] \vec{e}_y$$

From this formula can be concluded that the bottom-velocity is harmonic with frequencies ω_1 and ω_2 at any point (x_1, y_1) . Assumed is that in the origin both waves are in phase. To achieve this one has to choose the origin on the right way.

The distance between two wave crests can be measured in the direction of propagation (L_p) or transverse to this direction (L_s). This second distance is called L_s because in this direction the wave system resembles somewhat a standing wave.

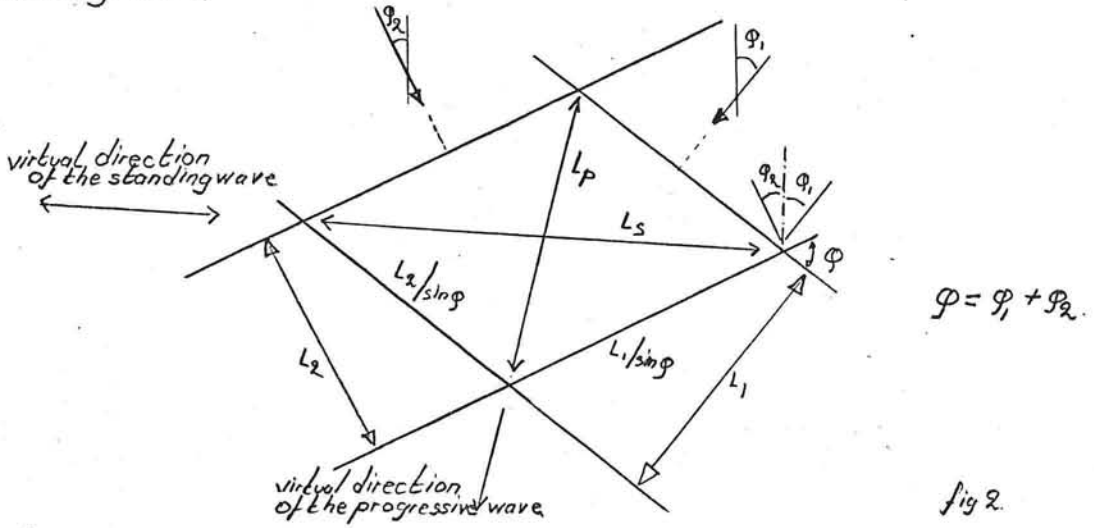


fig 2.

The distance L_p is

$$L_p^2 = \left(\frac{L_2}{\sin \varphi}\right)^2 + \left(\frac{L_1}{\sin \varphi}\right)^2 - \frac{2 L_1 L_2}{\sin^2 \varphi} \cos \varphi$$

$$= \frac{1}{\sin^2 \varphi} (L_1^2 + L_2^2 - 2 L_1 L_2 \cos \varphi)$$

The distance L_s is

$$L_s^2 = \left(\frac{L_2}{\sin \varphi}\right)^2 + \left(\frac{L_1}{\sin \varphi}\right)^2 + \frac{2 L_1 L_2}{\sin^2 \varphi} \cos \varphi$$

$$= \frac{1}{\sin^2 \varphi} (L_1^2 + L_2^2 + 2 L_1 L_2 \cos \varphi)$$

When the incoming waves are perpendicular $\varphi = 90^\circ$, then $L_p^2 = L_1^2 + L_2^2$; $L_s^2 = L_1^2 + L_2^2$

Note: L_p and L_s are called virtual wave length, because the direction of wave propagation does not necessarily match to the direction of L_p and L_s . They match only when $L_1 = L_2$. This will be discussed in the next chapter

3. A special case

As already indicated when $T_1 = T_2$ phase-differences become important. In this chapter some ideas are developed what might happen in such a special case.

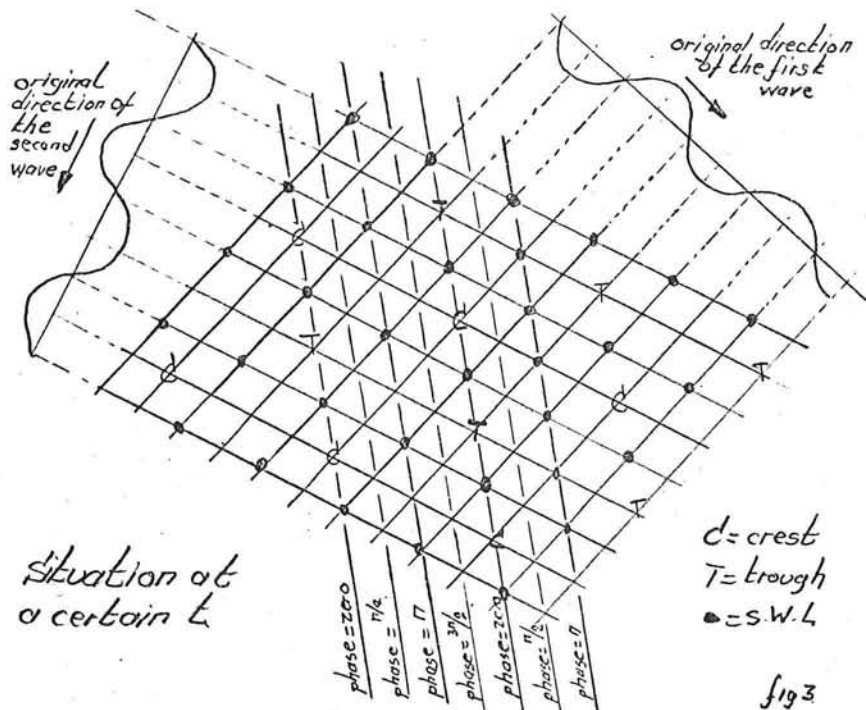


fig. 3

Because the celerity of both waves is the same, the resulting celerity has the same direction as the connection line of crests and troughs. This line is called the "phase=zero"-line. This name will be explained later.

Note: When either the celerity or the length is not identical, the resulting celerity is not necessarily directed to the phase-lines. For a discussion of this more general case, see the next chapter.

Along the "phase=zero"-line a propagating wave with a length $L_p = \frac{L_1}{\sin \varphi} \sqrt{V_c(1+\cos \varphi)}$ and a period T can be distinguished. The wave height is of course $H_p = H_1 + H_2$. On a line in the middle between two "phase=zero"-lines, a wave propagates with the same L_p and T but with a wave-height $H = |H_1 - H_2|$. This line is called "phase=π"-line.

The formula of the bottom-velocity, as derived on page II-2 can now be simplified because $\omega_1 = \omega_2$

$$kh = k_1 h$$

$$\cos \varphi_1 = \cos \varphi_2$$

$$\sin \varphi_1 = -\sin \varphi_2$$

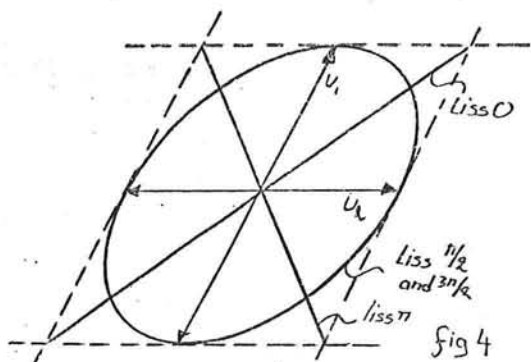
$$\tan \varphi_1 = -\tan \varphi_2$$

So

$$\vec{v}_b = \left[H_1 \sin(\omega t - k \frac{|x+y \tan \varphi_1|}{\sqrt{1+ \tan^2 \varphi_1}}) + H_2 \sin(\omega t - k \frac{|x-y \tan \varphi_1|}{\sqrt{1+ \tan^2 \varphi_1}}) \right] \frac{\omega \cos \varphi}{a \sinh(kh)} \vec{e}_x \\ + \left[H_1 \sin(\omega t - k \frac{|x+y \tan \varphi_1|}{\sqrt{1+ \tan^2 \varphi_1}}) - H_2 \sin(\omega t - k \frac{|x-y \tan \varphi_1|}{\sqrt{1+ \tan^2 \varphi_1}}) \right] \frac{\omega \sin \varphi}{a \sinh(kh)} \vec{e}_y$$

When this formula is worked out in its components, it becomes clear that \vec{v}_{bx} is both dependent on t and y [and on x of course]. When H_1 and H_2 are equal \vec{v}_{by} is zero on several phase-lines, for any value of x and t .

The bottom-velocity can be rendered in a Lissajoux-figure. In this figure are drawn the two bottom-velocities v_x and v_y (see fig. 4 on the next page). When both the velocities have the same phase (i.e. the phase-difference is zero) the resulting velocity is always a straight line [Liss. 0]. When the phase-difference is π , it is also a straight line [Liss. π]. For a difference of $\frac{\pi}{2}$ and



In the Lissajoux-figure is an ellipse. It has to be noticed that only on the phase=zero and on the phase=pi-lines the bottom-velocity is sometimes zero. On the other lines the bottom-velocity is never zero. This fact may have an influence on sand-transport.

This is illustrated in the table below. The numerical example is calculated from $\hat{u}_1 = 2 \frac{\text{m}}{\text{s}}$, $\hat{u}_2 = 1 \frac{\text{m}}{\text{s}}$ and $\varphi = 30^\circ$.

phase diff	max. velocity	example	min. velocity	example	mean velocity	example
0	$\sqrt{\hat{u}_1^2 + \hat{u}_2^2 + 2\hat{u}_1\hat{u}_2 \cos\varphi}$	2.9	0	0	$\frac{2}{\pi}\sqrt{\hat{u}_1^2 + \hat{u}_2^2 + 2\hat{u}_1\hat{u}_2 \cos\varphi}$	1.85
$\pi/2$	\hat{u}_1	2	\hat{u}_2	1	$(\hat{u}_1 + \hat{u}_2)/2$	1.5
π	$\sqrt{\hat{u}_1^2 + \hat{u}_2^2 - 2\hat{u}_1\hat{u}_2 \cos\varphi}$	1.1	0	0	$\frac{2}{\pi}\sqrt{\hat{u}_1^2 + \hat{u}_2^2 - 2\hat{u}_1\hat{u}_2 \cos\varphi}$	0.71
$3\pi/2$	\hat{u}_1	2	\hat{u}_2	1	$(\hat{u}_1 + \hat{u}_2)/2$	1.5

Sand can be transported by a fluid with a rather low velocity when it is in suspension. But to become suspended it has to be stirred up. For this stirring a large velocity [in any direction] is necessary. Or, more explicitly, a large bottom shear stress. When a velocity is sinusoidal, only during a part of the time this shear-stress is large enough to cause stirring. This situation occurs normally with waves from one direction. But in case of cross-swell waves may come from several directions, and the shear-stress-time diagrams have only this shape on the lines phase=zero and phase=pi.

Between these lines the velocity is never zero, e.g. on the lines phase= $\pi/2$ and phase= $3\pi/2$ [see the Lissajoux-diagram, fig 4]. Hence sediment is stirred up during a much longer time, than it is stirred up along the lines phase=zero and phase=pi. Also sand will not deposit very much on the areas between these lines, because the time to settle is shorter. Because of the (small) longshore current this suspended sediment is transported along the coast. Regarding this transport and the varying stirring, it is to expect that on the lines phase= $\pi/2$ and phase= $3\pi/2$ more sand is transported than on the lines phase=zero and phase=pi.

So one could expect a larger depth on the lines phase= $\pi/2$ and phase= $3\pi/2$. This in spite of the fact that the maximum velocity is larger on the line phase=zero than on the other lines.

Of course this can only be true in the initial stage; after a short period sand transport becomes equal on all the lines, but then the influence of differences in stirring-period is expressed in terms of local depth differences. On this way ripples may occur with a "wavelength" of $\frac{l_s}{2} \operatorname{cosec}(\varphi_i - \varphi_e)$, or

$$l_R = \frac{l_s \operatorname{cosec}(\varphi_i - \varphi_e)}{2 \sin \varphi} \sqrt{2(1 + \cos \varphi)}$$

For $l_s = 50 \text{ m}$, $\varphi = 30^\circ$ and $(\varphi_i - \varphi_e) = 0^\circ$, l_R becomes 90 m.

The above considerations are rather speculative. As far as we know, no model investigations were done on this field, so it is not possible to say anything about the quantitative effects of the enlarged stirring period. Hence in the numerical examples given in chapter 4 the influence of this phenomenon is neglected.

The wave-height along the coast will vary also, with intervals of about L_s meters. On the lines phase=zero, wave height is $H_1 = |H_1 + H_2|$, on the lines phase=π, wave-height is $H_2 = |H_1 - H_2|$. [Note: When $H_1 = H_2$, on the lines phase=π, wave-height is zero!!].

The first impression that due to this height-difference, set-up will vary also is not correct. Wave set-up is only described by the Bowen-formula $H = A(d + \bar{z})$ [Battjes 1974] in case of one wave direction ($d = \text{original water depth}$, $\bar{z} = \text{set-up}$).

According to Battjes, set-up is described by

$$\frac{dS_{xx}}{dx} + \rho g h \frac{d\bar{z}}{dx} = 0$$

S_{xx} is the radiation-stress component in the x -direction.

In case of cross-swell S_{xx} is not $\frac{1}{8} \rho g (H_1 + H_2)^2$, but

$$S_{xx} = (1 + \frac{1}{2} \cos 2\varphi_1) E_1 + (1 + \frac{1}{2} \cos 2\varphi_2) E_2$$

[see Annex III]

which results in

$$S_{xx} = \frac{3}{16} \rho g A_1^2 (h_1^2 - \frac{h_1^3}{h_{br1}} \sin^2 \varphi_{br1}) + \frac{3}{16} \rho g A_2^2 (h_2^2 - \frac{h_2^3}{h_{br2}} \sin^2 \varphi_{br2})$$

in which:

$$h = d + \bar{z}$$

h_{br} = breaker-depth

A = ratio between waveheight and water depth

φ_{br} = breaker-angle.

Because $\frac{dS_{xx}}{dy} = 0$, set-up is constant along the coast, assuming that h_{br1} and h_{br2} are independent from y [see chapter 3, vol B].

A problem

In most cases a longshore current will be generated. This current is slowed down by friction. When a large bottom velocity (due to waves) exists, friction is also large, and will prevent a large longshore velocity. As can be seen in the table on the former page, the mean (wave) velocity has its maximum on the lines phase=zero, and its minimum on the lines phase=π.

So the longshore velocity should have its maximum on the lines phase=π, and its minimum on the lines phase=zero.

But this can't be true, because large differences in longshore velocity are only possible when the depth-differences between the lines phase=zero and phase=π are considerable [$v_h = v_{h_1}$, eq. of continuity].

These differences in depth are small. So the conclusion is that in case of cross-swell with two identical wave-periods, the velocity formula is not describing the process very well, and that one has to average over all phases.

It is not clear how this should be done. To investigate this detailed velocity-measurements in cross-swell situations are necessary.

4. A numerical example

To illustrate the effect of some of the items mentioned in the former chapter in the computer program the possibility is made to calculate sand transport in case of two identical wave periods. Then also the phase-difference has to be entered.

As an example a case is calculated in which both waves are equal. One wave enters the breakerline perpendicular, for the other wave the angle of incidence is 10°.

Some other data: $k = 0.38$ $\Delta = 1.60$ $h_{br1} = h_{br2} = 2.50 \text{ m}$

$D_{g0} = 190 \mu$ $R = 0.02 \text{ m}$ $b_y \propto = 0.02$

$D_{g0} = 150 \mu$ $A = 0.6$ $T_1 = T_2 = 10 \text{ sec}$

The results of these computations are:

phase	$v_{\text{breakerline}}$	v_{mean}	total sediment transport
0	0.983 m/s	0.450 m/s	3 765 748 m³/year
$\pi/3$	1.041 m/s	0.478 m/s	4 101 122 m³/year
$2\pi/3$	1.253 m/s	0.583 m/s	7 149 672 m³/year
π	1.693 m/s	0.866 m/s	13 866 496 m³/year
$4\pi/3$	1.262 m/s	0.589 m/s	7 166 999 m³/year
$5\pi/3$	1.047 m/s	0.481 m/s	4 379 702 m³/year

$$\frac{s_T}{S_0} = 3.8$$

Note: When the perpendicular wave is disregarded, and transport is calculated for the 10° wave only, the results are:

$$v_{br} = 1.369 \text{ m/s} \quad v_{\text{mean}} = 0.655 \text{ m/s} \quad S_{\text{tot}} = 4 561 101 \text{ m³/year}$$

From these data it is clear that in case of two waves with identical wavelengths it is not allowed to overgo the fact that phase-lagging exists.

Also for cases when two waves have different heights, a large difference is calculated. E.g. when the perpendicular wave keeps a breaker depth of 2.5 m, but the oblique wave decreases until a breaker depth of 1.1 m, $S_0 = 311 134 \text{ m³/year}$ and $S_T = 1 399 881 \text{ m³/year}$ ($\frac{S_T}{S_0} = 4.6$).

As already indicated in the former chapter, these large differences in velocity and sand transport are impossible consequent on continuity. So one has to conclude that in case of cross-swell with identical wave periods this program cannot be used. A correct answer might be an average over all the phase-differences, but without further research it is impossible to be sure about this.

When the two waves have different periods, the effect of phase-lagging is negligible. This is discussed in the next chapter. As an example the 'standard case' was calculated with six phase lags ($T_1/T_2 = 1/15$, hence an influence can possibly be seen on phase = $2\pi/3$ and $4\pi/3$). The results are presented in the following table:

phase	$v_{\text{outerbreakerline}}$	$v_{\text{innerbreakerline}}$	Total sediment transport
0	2.034 m/s	1.039 m/s	9 222 892 m³/year
$\pi/3$	2.033 m/s	1.035 m/s	9 199 548 m³/year
$2\pi/3$	2.033 m/s	1.035 m/s	9 199 548 m³/year
π	2.034 m/s	1.039 m/s	9 222 892 m³/year
$4\pi/3$	2.034 m/s	1.037 m/s	9 218 879 m³/year
$5\pi/3$	2.034 m/s	1.037 m/s	9 218 879 m³/year

$$\begin{aligned} T_1 &= 10 \text{ sec} & T_2 &= 15 \text{ sec} \\ h_{br1} &= 2.5 \text{ m} & h_{br2} &= 1.1 \text{ m} \\ \varphi_1 &= 20^\circ & \varphi_2 &= 5^\circ \end{aligned}$$

Indeed, the differences are negligible.

5. The influence of cross-swell in general

In most cases the two incoming waves will not have the same period. Then the direction of the celerity does not match with the connection-line of the crests. Before dealing with the most general case, a situation will be discussed in which the water depth is small. Then the celerity is independent from the wave period, but only from the actual depth, which is the same for both waves [$c = \sqrt{gh}$].

So a crest-point will propagate along an other line than along the connection-lines between the crests (the phase-lines). See fig. 7. The consequence is that along a coast phase-lines do exist, but that they are not staying at the same place. The velocity of these lines is indicated in fig 7 with an arrow, marked v_{phase} . Consequently special effects, as described in the former chapters, will not occur. So phase-lagging will have not any influence on the mean

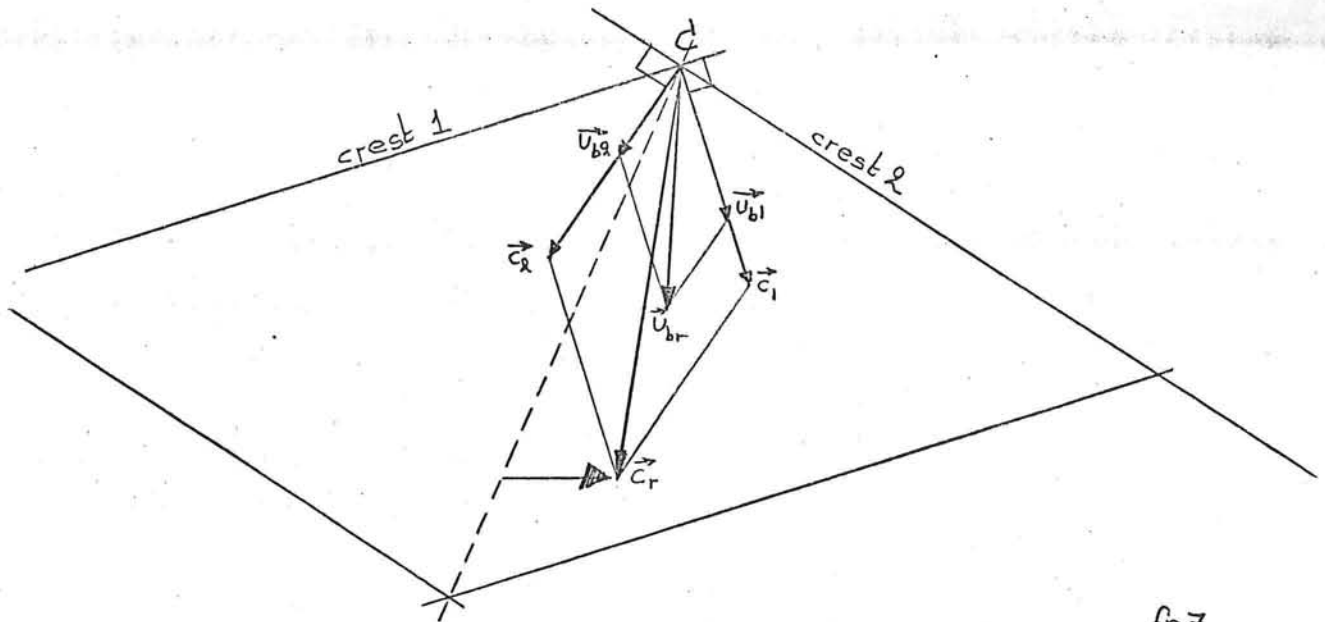


fig 7

sand transport along the coast [Of course it will have an influence on short time phenomena].

In other words: When at a cross-section A two waves enter the breakerline with a phase-lag φ and when through that cross-section a mean sand transport S exists, then the mean sand transport through any other cross-section is also S .

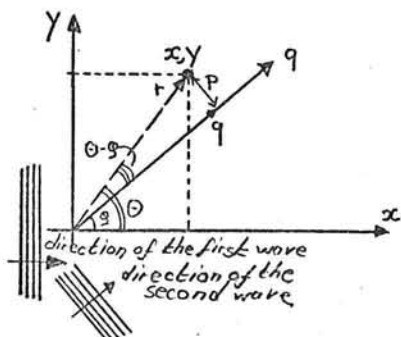
An other case is when at a certain day two waves enter the breakerline at cross-section A with a phase-lag φ , and at an other day the same waves enter the breakerline with another phase-lag, then the two sediment-transports are not necessarily identical.

Radiation-stress caused by cross-swell

The formulae for radiation-stress were derived (by Longuet-Higgins and Stewart) for a one-wave system. It is not known whether the radiation-stress of a two-wave system can be found by addition, or that other relations have to be derived. The intention of this annex is to investigate the radiation-stress in a cross-swell situation.

In the following discussions the following conventions will be used:

- the origin of the coordinates will be placed at the still water level, the x -axis will have the direction of wave propagation of one of the waves. The positive z -axis extends upwards from the still water level [SWL]
- the water density, ρ , is constant.
- the two waves do not influence each other.



wave 1: direction of propagation : x -axis
wave 2: direction of propagation : q -axis

$$[1] \quad \eta(x, y, t) = \eta_1 + \eta_2$$

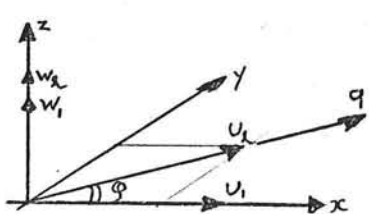
$$[2] \quad \eta_1 = a_1 \cos(k_1 x - \omega_1 t)$$

$$[3] \quad \eta_2 = a_2 \cos(k_2 q - \omega_2 t + ph) \quad q = f(x, y)$$

$$r = \sqrt{x^2 + y^2}; \quad q = r \cos(\theta - \phi); \quad \theta = \arctan\left(\frac{y}{x}\right)$$

$$[4] \quad \eta = \sqrt{x^2 + y^2} * \cos\{\arctan\left(\frac{y}{x}\right) - \phi\}$$

$$[5] \quad \eta = a_1 \cos(k_1 x - \omega_1 t) + a_2 \left(k_2 \left[\sqrt{x^2 + y^2} * \cos\{\arctan\left(\frac{y}{x}\right) - \phi\} \right] - \omega_2 t + ph \right)$$



$$[6] \quad \vec{u}_1 = \frac{a_1 \omega_1}{\sinh(k_1 h)} \cosh k_1(z+h) \cos(k_1 x - \omega_1 t) \hat{e}_x$$

$$[7] \quad \vec{w}_1 = \frac{a_1 \omega_1}{\sinh(k_1 h)} \sinh k_1(z+h) \sin(k_1 x - \omega_1 t) \hat{e}_z$$

$$[8] \quad \vec{u}_2 = \frac{a_2 \omega_2}{\sinh(k_2 h)} \cosh k_2(z+h) \cos(k_2 q - \omega_2 t + ph) \hat{e}_q$$

$$[9] \quad \vec{w}_2 = \frac{a_2 \omega_2}{\sinh(k_2 h)} \sinh k_2(z+h) \sin(k_2 q - \omega_2 t + ph) \hat{e}_z$$

in which η = wave profile

a = amplitude of the original waves [maximum deviation of the surface]

$k = 2\pi/L$, wave number

$\omega = 2\pi/T$, frequency

t = time

x, y, z , position in the three dimensional cartesian frame of reference

h = water depth

u = instantaneous horizontal velocity of a particle

w = instantaneous vertical velocity of a particle

$\hat{e}_q = \cos\phi \hat{e}_x + \sin\phi \hat{e}_y$, vector of unity in q -direction.

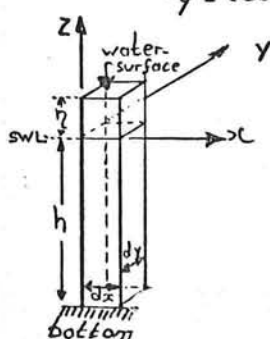
The total flux of horizontal momentum in the direction of the x -axis:

$$[10] \quad P_x = \int_{-h}^h \int_0^h (p + \rho u^2) dz dy \quad u = u(x, y, t)$$

The radiation-stress will be:

$$[11] \quad S'_{xx} = (\overline{P_x} - P_0) dy$$

Unlike in the one-wave system, the horizontal velocity in the x -direction will vary. Therefore dy is introduced, because of this the velocity (u) is only a function of x and t .



S_{xx} is separated into three parts:

$$[12] \quad S_{xx} = S_{xx}^{(1)} + S_{xx}^{(2)} + S_{xx}^{(3)}$$

$$[13] \quad S_{xx}^{(1)} = \left\{ h \int_0^b \overline{\rho u^2 dz} \right\} dy$$

$$[14] \quad S_{xx}^{(2)} = \left\{ -h \int_0^b (\bar{p} - P_0) dz \right\} dy$$

$$[15] \quad S_{xx}^{(3)} = \left\{ \int_0^b p dz \right\} dy$$

$\int_a^b \overline{f(x) dx}$ denotes the time average
of the integral $\int_a^b f(x) dx$

Equation [13] is split again:

$$[16] \quad S_{xx}^{(1)} = \left\{ -h \int_0^b \overline{\rho u^2 dz} + \int_0^b \overline{\rho u^2 dz} \right\} dy$$

ρ is a function of the amplitude a too, so the last term will yield only a term of third order. Since only first and second order terms are considered this last term is neglected.

$$[17] \quad S_{xx}^{(1)} = \left\{ -h \int_0^b \overline{\rho u^2 dz} \right\} dy$$

Both limits of the integral are constants, so $S_{xx}^{(1)}$ becomes

$$[18] \quad S_{xx}^{(1)} = \left\{ -h \int_0^b \overline{\rho u^2} dz \right\} dy$$

For eq. [14] the same technique can be used:

$$[19] \quad S_{xx}^{(2)} = \left\{ -h \int_0^b (\bar{p} - P_0) dz \right\} dy = \left\{ -h \int_0^b (\bar{p} - \bar{p}_0) dz \right\} dy$$

P_0 is excluded from the time average, because it is supposed to be a constant.

$$[20] \quad S_{xx}^{(2)} = \left\{ -h \int_0^b (\bar{p} - P_0) dz \right\} dy$$

The mean flux of vertical momentum across a horizontal plane must be equal to the water above that plane. The average waterlevel is $z=0$, therefore:

$$[21] \quad \bar{p} + \rho w^2 = -\rho g z = P_0$$

$$[22] \quad \bar{p} - P_0 = -\rho w^2$$

Substitution into [20] yields:

$$[23] \quad S_{xx}^{(2)} = \left\{ -h \int_0^b -\rho w^2 dz \right\} dy$$

Adding $S_{xx}^{(1)}$ and $S_{xx}^{(2)}$ yields, using [18] and [23].

$$[24] \quad S_{xx}^{(1)} + S_{xx}^{(2)} = \left\{ -h \int_0^b (\overline{\rho u^2} - \rho w^2) dz \right\} dy$$

The third term of S_{xx} was (eq 15)

$$S_{xx}^{(3)} = \left\{ \int_0^b \overline{\rho^2 p dz} \right\} dy$$

Assumed is that p is nearly equal to the hydrostatic pressure measured from the instantaneous surface η .

$$[25] \quad p = \rho g (\eta - z); \text{ so } S_{xx}^{(3)} \text{ becomes}$$

$$[26] \quad S_{xx}^{(3)} = \left\{ \int_0^b \overline{\rho g (\eta - z) dz} \right\} dy = \left\{ \rho g \left(\int_0^b \overline{\eta^2 dz} - \int_0^b \overline{z^2 dz} \right) \right\} dy$$

$$[27] \quad S_{xx}^{(3)} = \left\{ \frac{1}{2} \rho g \overline{\eta^2} \right\} dy$$

The instantaneous watersurface is (eq. 5)

$$\eta = a_1 \cos A_1 + a_2 \cos A_2 \quad \text{in which } A_i = k_i x - \omega_i t$$

$$A_i = k_i \left[\sqrt{x^2 + y^2} \cos \arctg \left(\frac{y}{x} \right) - \varphi_i \right] x - \omega_i t + \varphi_h$$

$$\overline{\eta^2} = \overline{(a_1 \cos A_1 + a_2 \cos A_2)^2} = \overline{a_1^2 \cos^2 A_1 + a_2^2 \cos^2 A_2 + 2a_1 a_2 \cos A_1 \cos A_2} = a_1^2 \overline{\cos^2 A_1} + a_2^2 \overline{\cos^2 A_2} + 2a_1 a_2 \overline{\cos A_1 \cos A_2}$$

$$\text{Note } \overline{\cos^2 q} = \frac{1}{\pi} \int_0^{\pi} \cos^2 q dq = \frac{1}{2}$$

$$\overline{\cos q_1 \cos q_2} = 0$$

$$\overline{\eta^2} = \frac{1}{2} a_1^2 + \frac{1}{2} a_2^2 + 0$$

*) for a proof of these statements, see page III-7

$$[28] S_{xx}^{(3)} = \int_{-h}^h \rho g \left(\frac{1}{2} \omega_1^2 + \frac{1}{2} \omega_2^2 \right) dy = \int_{-h}^h \rho g (\omega_1^2 + \omega_2^2) dy$$

From the above equations it becomes clear that $S_{xx}^{(3)}$ is independent from y , so
[29] $S_{xx}^{(3)} = \frac{1}{2} \rho g (\omega_1^2 + \omega_2^2)$

Calculation will be continued with the other parts of S_{xx} . (eq 24)

$$S_{xx}^{(1)} + S_{xx}^{(2)} = \int_{-h}^h \int_0^h \rho (\bar{U}^2 - \bar{W}^2) dz dy$$

In which $U = \bar{U} = U + \vec{e}_x = U_x \vec{e}_x + U_z \vec{e}_z$
using equation [6] and [8] yields:

$$[30] U = \frac{\omega_1 \omega_2}{\sinh(k_1 h)} \cosh k_1(z+h) \cos(k_1 x - \omega_1 t) \vec{e}_x + \frac{\omega_1 \omega_2 \cos \varphi}{\sinh(k_1 h)} \cosh k_2(z+h) \cos(k_2 y - \omega_2 t) \vec{e}_x$$

using equation [7] and [9] yields:

$$[31] W = \bar{W} = \frac{\omega_1 \omega_2}{\sinh(k_1 h)} \sinh k_1(z+h) \sin(k_1 x - \omega_1 t) \vec{e}_z + \frac{\omega_1 \omega_2}{\sinh(k_1 h)} \sinh k_2(z+h) \sin(k_2 y - \omega_2 t) \vec{e}_z$$

Equation [24] can be written in the following way:

$$S_{xx}^{(1)} + S_{xx}^{(2)} = \int_{-h}^h \int_0^h \rho (\bar{U}^2 - \bar{W}^2) dz dy = \\ = \left\{ \rho \int_{-h}^h \int_0^h \left[(U_x^2 + 2U_x U_z + U_z^2) - (W_z^2 + 2W_z W_x + W_x^2) \right] dz dy \right\}$$

$$[32] = \rho \int_0^h \left\{ \int_{-h}^h \left[(U_x^2 + 2U_x U_z + U_z^2) - (W_z^2 + 2W_z W_x + W_x^2) \right] dz \right\} dy$$

It can be proved that $2U_x U_z = 0$ and $2W_z W_x = 0$ [see page III-7]; so eq [32] becomes:

$$[33] S_{xx}^{(1)} + S_{xx}^{(2)} = \rho \int_0^h \left\{ \int_{-h}^h \int_0^h \bar{U}^2 dz + \int_{-h}^h \int_0^h \bar{W}^2 dz - \int_{-h}^h \int_0^h \bar{U}_z^2 dz - \int_{-h}^h \int_0^h \bar{W}_x^2 dz \right\}$$

Using equations [6], [7], [8] and [9] yields:

$$S_{xx}^{(1)} + S_{xx}^{(2)} = \rho \int_0^h \left\{ \frac{\omega_1^2 \omega_2^2}{\sinh^2(k_1 h)} \frac{\cosh^2 k_1(z+h) dz}{\cos^2(k_1 x - \omega_1 t)} - \int_{-h}^h \int_0^h \cosh^2 k_1(z+h) dz \right. \\ \left. + \frac{\omega_1^2 \cos^2 \omega_2}{\sinh^2(k_2 h)} \frac{\cosh^2 k_2(z+h) dz}{\cos^2(k_2 y - \omega_2 t)} - \int_{-h}^h \int_0^h \cosh^2 k_2(z+h) dz \right. \\ \left. - \frac{\omega_1^2 \omega_2^2}{\sinh^2(k_1 h)} \frac{\sinh^2(k_1 x - \omega_1 t)}{\sin^2(k_1 x - \omega_1 t)} - \int_{-h}^h \int_0^h \sinh^2 k_1(z+h) dz \right. \\ \left. - \frac{\omega_1^2 \omega_2^2}{\sinh^2(k_2 h)} \frac{\sinh^2(k_2 y - \omega_2 t)}{\sin^2(k_2 y - \omega_2 t)} - \int_{-h}^h \int_0^h \sinh^2 k_2(z+h) dz \right\}$$

The time average of $\cos^2 q$ and $\sin^2 q$ is $\frac{1}{2}$; the integral $\int_{-h}^h \int_0^h \cosh^2 k_i(z+h) dz$ yields:

$$\begin{aligned} & \frac{1}{k_i} \int_{k_i 0}^{k_i h} \cosh^2 q dq \quad q = k_i(z+h) \\ &= \frac{1}{k_i} \int_{k_i 0}^{k_i h} \left(\frac{\cosh 2q}{2} + \frac{1}{2} \right) dq \\ &= \frac{1}{k_i} \int_{k_i 0}^{k_i h} \left[\frac{\sinh 2q}{4} + \frac{1}{2} q \right]_0^{k_i h} = \frac{\sinh 2k_i h}{4k_i} + \frac{1}{2} h. \end{aligned}$$

$$So: [34] \int_{-h}^h \int_0^h \cosh^2 k_2(z+h) dz = \frac{\sinh 2k_2 h}{4k_2} + \frac{1}{2} h$$

Also can be proved that:

$$[35] \int_{-h}^h \int_0^h \sinh^2 k_1(z+h) dz = \frac{\sinh 2k_1 h}{4k_1} - \frac{1}{2} h$$

$$[36] \int_{-h}^h \int_0^h \sinh^2 k_2(z+h) dz = \frac{\sinh 2k_2 h}{4k_2} - \frac{1}{2} h.$$

So, using [34] to [37], 33 yields:

$$[38] S_{xx}^{(1)} + S_{xx}^{(2)} = \rho \int_0^h \left\{ \frac{\omega_1^2 \omega_2^2}{\sinh^2(k_1 h)} \cdot \frac{1}{2} \left[\frac{\sinh 2k_1 h}{4k_1} + \frac{1}{2} h \right] \right. \\ \left. + \frac{\omega_1^2 \cos^2 \omega_2}{\sinh^2(k_2 h)} \cdot \frac{1}{2} \left[\frac{\sinh 2k_2 h}{4k_2} + \frac{1}{2} h \right] \right. \\ \left. - \frac{\omega_1^2 \omega_2^2}{\sinh^2(k_1 h)} \cdot \frac{1}{2} \left[\frac{\sinh 2k_1 h}{4k_1} - \frac{1}{2} h \right] \right. \\ \left. - \frac{\omega_1^2 \omega_2^2}{\sinh^2(k_2 h)} \cdot \frac{1}{2} \left[\frac{\sinh 2k_2 h}{4k_2} - \frac{1}{2} h \right] \right\}$$

From the above equation it becomes clear that $S_{xx}^{(1)} + S_{xx}^{(2)}$ is independent from y , so dy can be omitted

For a one-wave system the following equation is valid:

$$[39] \quad \omega^2 = gk \tanh(kh)$$

Is this equation also valid for a two-wave system?

$$[37] \quad \eta = a_1 \cos(k_1 x - \omega_1 t) + a_2 \cos(k_2 q - \omega_2 t + ph)$$

Suppose: the velocity potential $\tilde{\Phi}(x, y, z, t)$ is:

$$[40] \quad \tilde{\Phi}(x, y, z, t) = \tilde{\Phi}_1(x, y, z, t) + \tilde{\Phi}_2(x, y, z, t) = g = f(x, y)$$

$$= \frac{\omega_1 a_1}{k_1} \frac{\cosh k_1 (h+z)}{\sinh k_1 h} \sin(k_1 x - \omega_1 t) + \frac{\omega_2 a_2}{k_2} \frac{\cosh k_2 (h+z)}{\sinh k_2 h} \sin(k_2 q - \omega_2 t + ph)$$

This equation of $\tilde{\Phi}(x, y, z, t)$ has to meet the following conditions:

$$[41] \quad \frac{\partial^2 \tilde{\Phi}}{\partial z^2} + \frac{\partial^2 \tilde{\Phi}}{\partial y^2} + \frac{\partial^2 \tilde{\Phi}}{\partial x^2} = 0 \quad (\text{Laplace equation})$$

$$[42] \quad \frac{\partial \tilde{\Phi}}{\partial z} = \frac{\partial \tilde{\Phi}}{\partial x} \quad \text{on } z=0$$

$$[43] \quad \frac{\partial \tilde{\Phi}}{\partial z} = 0 \quad \text{on } z=-h$$

$$[44] \quad \frac{\partial \tilde{\Phi}}{\partial t} = a_1 \omega_1 \sin(k_1 x - \omega_1 t) + a_2 \omega_2 \sin(k_2 q - \omega_2 t + ph)$$

$$\frac{\partial \tilde{\Phi}}{\partial z} = \frac{\omega_1 a_1}{k_1} k_1 \frac{\sinh k_1 (h+z)}{\sinh k_1 h} \sin(k_1 x - \omega_1 t) + \frac{\omega_2 a_2}{k_2} k_2 \frac{\sinh k_2 (h+z)}{\sinh k_2 h} \sin(k_2 q - \omega_2 t + ph)$$

$$[45] \quad \left(\frac{\partial \tilde{\Phi}}{\partial z} \right)_{z=0} = a_1 \omega_1 \sin(k_1 x - \omega_1 t) + a_2 \omega_2 \sin(k_2 q - \omega_2 t + ph)$$

With [44] and [45] the condition of [42] is proved.

$$[46] \quad \left(\frac{\partial \tilde{\Phi}}{\partial z} \right)_{z=-h} = \frac{\omega_1 a_1}{k_1} k_1 \frac{\sinh 0}{\sinh k_1 h} \sin(k_1 x - \omega_1 t) + \frac{\omega_2 a_2}{k_2} k_2 \frac{\sinh 0}{\sinh k_2 h} \sin(k_2 q - \omega_2 t + ph) = 0 + 0 = 0$$

With [46] the condition of [43] is proved.

$$[47] \quad \frac{\partial^2 \tilde{\Phi}}{\partial z^2} = \frac{\partial}{\partial z} \left(\frac{\partial \tilde{\Phi}}{\partial z} \right) = \frac{\omega_1 a_1}{k_1} k_1^2 \frac{\cosh k_1 (h+z)}{\sinh k_1 h} \sin(k_1 x - \omega_1 t) + \frac{\omega_2 a_2}{k_2} k_2^2 \frac{\cosh k_2 (h+z)}{\sinh k_2 h} \sin(k_2 q - \omega_2 t + ph)$$

$$[48] \quad \frac{\partial^2 \tilde{\Phi}}{\partial x^2} = \frac{\partial}{\partial x} \left(\frac{\partial \tilde{\Phi}}{\partial x} \right) = \frac{\partial}{\partial x} \left\{ \frac{\omega_1 a_1}{k_1} \frac{\cosh k_1 (h+z)}{\sinh k_1 h} k_1 \cos(k_1 x - \omega_1 t) + \frac{\omega_2 a_2}{k_2} \frac{\cosh k_2 (h+z)}{\sinh k_2 h} k_2 \cos(k_2 q - \omega_2 t + ph) \right\}$$

$$= \frac{\omega_1 a_1}{k_1} \frac{\cosh k_1 (h+z)}{\sinh k_1 h} (-k_1^2) \sin(k_1 x - \omega_1 t) + \frac{\omega_2 a_2}{k_2} \frac{\cosh k_2 (h+z)}{\sinh k_2 h} (-k_2^2) \sin(k_2 q - \omega_2 t + ph) \left(\frac{\partial^2 \tilde{\Phi}}{\partial x^2} \right)$$

$$+ \frac{\omega_1 a_1}{k_1} \frac{\cosh k_1 (h+z)}{\sinh k_1 h} k_1 \cos(k_1 x - \omega_1 t + ph) \left(\frac{\partial^2 \tilde{\Phi}}{\partial x^2} \right)$$

$$[49] \quad \frac{\partial^2 \tilde{\Phi}}{\partial y^2} = 0 + \frac{\omega_2 a_2}{k_2} \frac{\cosh k_2 (h+z)}{\sinh k_2 h} (-k_2^2) \sin(k_2 q - \omega_2 t + ph) \left(\frac{\partial^2 \tilde{\Phi}}{\partial y^2} \right)^2$$

$$+ \frac{\omega_2 a_2}{k_2} \frac{\cosh k_2 (h+z)}{\sinh k_2 h} k_2 \cos(k_2 q - \omega_2 t + ph) \left(\frac{\partial^2 \tilde{\Phi}}{\partial y^2} \right)$$

For the first wave can be proved that $\left(\frac{\partial^2 \tilde{\Phi}}{\partial z^2} + \frac{\partial^2 \tilde{\Phi}}{\partial x^2} + \frac{\partial^2 \tilde{\Phi}}{\partial y^2} \right)_1 = 0$ with [47], [48] and [49]. Therefore [41] exists only out of terms of the second wave. So directly can be proved (by axis-transformation)

$$\left(\frac{\partial^2 \tilde{\Phi}}{\partial z^2} + \frac{\partial^2 \tilde{\Phi}}{\partial x^2} + \frac{\partial^2 \tilde{\Phi}}{\partial y^2} \right)_2 = 0.$$

By means of eq. [40] can be proved $\left(\frac{\partial \tilde{\Phi}}{\partial z} + \frac{p}{C} + g z = 0 \right)$ for $z=0$ and $p=0$ that

$$\omega_1^2 = gk_1 \tanh k_1 h$$

$$\omega_2^2 = gk_2 \tanh k_2 h$$

Equation [38] can be rewritten with equation [47] to:

$$[50] \quad S_{xx}^{(1)} + S_{yy}^{(1)} = \frac{eg a_1^2 k_1}{\sinh 2k_1 h} \left[\frac{\sinh 2k_1 h + i h}{4k_1} \right] + \frac{eg a_2^2 k_2}{\sinh 2k_2 h} \left[\frac{1 - \sin^2 \varphi}{4k_2} \right] \left[\frac{\sinh 2k_2 h + i h}{4k_2} \right]$$

$$- \frac{eg a_1^2 k_1}{\sinh 2k_1 h} \left[\frac{\sinh 2k_1 h - i h}{4k_1} \right] - \frac{eg a_2^2 k_2}{\sinh 2k_2 h} \left[\frac{\sinh 2k_2 h - i h}{4k_2} \right]$$

$$= \frac{eg a_1^2 k_1 h}{\sinh 2k_1 h} + \frac{eg a_2^2 k_2 h}{\sinh 2k_2 h} - eg a_1^2 \sin^2 \varphi \left[\frac{1}{4} + \frac{k_1 h}{2 \sinh 2k_1 h} \right]$$

S_{xx} becomes using eq [29], [42] and [50]:

$$[51] \quad S'_{xx} = \frac{1}{4} eg (a_1^2 + a_2^2) + \frac{1}{2} eg \frac{e^{-2k_1 h}}{\sinh 2k_1 h} + \frac{1}{2} eg \frac{e^{-2k_2 h}}{\sinh 2k_2 h} - \frac{1}{2} eg a_1^2 \left[\frac{1}{2} + \frac{k_1 h}{\sinh 2k_1 h} \right] / \sin^2 \varphi$$

Using the energy-density of the waves: $E_1 = \frac{1}{2} \rho g q_1^2$ and $E_2 = \frac{1}{2} \rho g q_2^2$, [51] becomes:

$$[52] \quad S_{xx} = E_1 \left(\frac{\epsilon k_1 h}{\sinh 2k_1 h} + \frac{1}{i} \right) + E_2 \left(\frac{\epsilon k_2 h}{\sinh 2k_2 h} + \frac{1}{i} \right) - E_2 \left[\frac{1}{i} + \frac{k_1 h}{\sinh 2k_1 h} \right] \sin^2 \varphi.$$

When S_{yy} has to be determined, it is necessary to examine the flow of momentum in the YZ-plane:

$$[53] \quad S_{yy} = \left\{ -h \int_{-h}^0 (p + \rho v^2) dz - h \int_{-h}^0 P_0 dz \right\} dx$$

Like S_{xx} , S_{yy} is split into:

$$[54] \quad S_{yy} = S_{yy}^{(1)} + S_{yy}^{(2)} + S_{yy}^{(3)}$$

$$[55] \quad S_{yy}^{(1)} = \left\{ -h \int_{-h}^0 e v^2 dz \right\} dx$$

$$[56] \quad S_{yy}^{(2)} = \left\{ -h \int_{-h}^0 (p - P_0) dz \right\} dx$$

$$[57] \quad S_{yy}^{(3)} = \int_0^h p dz = S_{xx} = \frac{1}{4} \rho g (q_1^2 + q_2^2) \quad [\text{cf. eq. [25] to [29]}]$$

Equation [55] can be rewritten as:

$$[58] \quad S_{yy} = \left\{ -h \int_{-h}^0 \rho v^2 dz + \int_0^h \rho v^2 dz \right\} dx$$

The second term is neglected, like in eq. [16] and [17].

$$[59] \quad S_{yy} = \left\{ -h \int_{-h}^0 \rho v^2 dz \right\} dx$$

$$[60] \quad S_{yy} = \left\{ -h \int_{-h}^0 \rho w^2 dz \right\} dx \quad (\text{cf. eq. [21] to [23]})$$

$$[61] \quad S_{yy}^{(1)} + S_{yy}^{(2)} = \left\{ -h \int_{-h}^0 (\rho v^2 - \rho w^2) dz \right\} dx$$

In the same way as $S_{xx}^{(1)} + S_{xx}^{(2)}$ this can be rewritten:

$$[62] \quad v = v \vec{e}_y = \vec{v}_{zy} = \frac{q_2 \omega_2 \sinh}{\sinh 2k_2 h} \cosh k_2(z+h) \cos(k_2 y - \omega_2 t + ph) \vec{e}_y$$

$$[63] \quad w = w \vec{e}_z = w_1 + w_2$$

Equation [61] yields, using [62] and [63]:

$$[64] \quad S_{yy}^{(1)} + S_{yy}^{(2)} = \rho dx \left\{ \frac{\alpha_2^2 \omega_2^2 \sin^2 \varphi}{\sinh^2 k_2 h} \int_{-h}^0 \cosh^2 k_2(z+h) dz \overline{\cos^2(k_2 y - \omega_2 t + ph)} \right. \\ \left. - \frac{\alpha_2^2 \omega_2^2}{\sinh^2 k_2 h} \overline{\sin^2(k_2 x - \omega_2 t)} \int_{-h}^0 \sinh^2 k_2(z+h) dz \right. \\ \left. + \frac{\alpha_2^2 \omega_2^2}{\sinh^2 k_2 h} \overline{\sin^2(k_2 y - \omega_2 t + ph)} \int_{-h}^0 k_2(z+h) dz \right\}$$

Using eq. [34] to [37], equation [64] yields:

$$[65] \quad S_{yy}^{(1)} + S_{yy}^{(2)} = \rho dx \left\{ \frac{\alpha_2^2 \omega_2^2 \sin^2 \varphi}{\sinh^2 k_2 h} \left[\frac{\sinh 2k_2 h}{4k_2} + \frac{1}{i} h \right] \right. \\ \left. - \frac{\alpha_2^2 \omega_2^2}{\sinh^2 k_2 h} \left[\frac{1}{i} \frac{\sinh 2k_2 h}{4k_2} - \frac{1}{i} h \right] - \frac{\alpha_2^2 \omega_2^2}{\sinh^2 k_2 h} \left[\frac{1}{i} \frac{\sinh 2k_2 h}{4k_2} - \frac{1}{i} h \right] \right\}$$

From this equation it becomes clear that $S_{yy}^{(1)} + S_{yy}^{(2)}$ is independent from x , so dx can be omitted. The total radiation-stress in the Y-direction becomes, using eq. [54], [59], [57] and [65]:

$$S_{yy} = E_2 \frac{2k_2}{\sinh 2k_2 h} \left[\frac{\sinh 2k_2 h}{4k_2} + \frac{1}{i} h \right] (1 - \cos^2 \varphi) - E_2 \frac{2k_1}{\sinh 2k_1 h} \left[\frac{\sinh 2k_1 h}{4k_1} - \frac{1}{i} h \right]$$

$$- E_2 \frac{2k_1}{\sinh 2k_1 h} \left[\frac{\sinh 2k_1 h}{4k_1} - \frac{1}{i} h \right] + \frac{1}{i} (E_1 + E_2)$$

$$[66] \quad S_{yy} = E_1 \frac{k_1 h}{\sinh 2k_1 h} + E_2 \left(\frac{2k_1 h}{\sinh 2k_1 h} + \frac{1}{i} \right) - E_2 \left(\frac{k_1 h}{\sinh 2k_1 h} + \frac{1}{i} \right) \cos^2 \varphi.$$

Shear stresses

One has to investigate the possibility of the transfer of x-momentum across the plane $y=\text{constant}$. Since this momentum-transfer manifests itself as a shear stress, the pressure at the point does not contribute. This results in a more simple equation than [11] or [53], viz.:

$$[67] \quad S_{xy} = \int_{-h}^h \rho u v dz$$

This equation can be split:

$$[68] \quad S_{xy} = \int_{-h}^0 \rho u v dz + \int_h^0 \rho u v dz \\ = \int_{-h}^0 \rho u v dz + 0$$

(because $\int_h^0 \rho u v dz$ is of the third order)

in which [69] $u = u_x + u_{zx}$ and [62] $v = u_{zy}$. So [68] yields:

$$[69] \quad S_{xy} = \int_{-h}^0 \rho (u_x u_{zy} + u_{zx} u_{zy}) dz = \\ = \int_{-h}^0 \rho (\bar{u}_x \bar{u}_{zy} + \bar{u}_{zx} \bar{u}_{zy}) dz$$

It can be proved that $\bar{u}_x \bar{u}_{zy} = 0$, because it is assumed that $\omega_1 + \omega_2$ [$u_i = f(t) \cos q_i z$; $u_{iy} = f(ty) \cos q_i z$ and $\cos q_i x \cos q_i z = 0$].
Eq [69] becomes, using [81]:

$$[70] \quad S_{xy} = \rho \int_{-h}^0 \frac{\omega_1^2 \omega_2^2}{\sinh^2 k_1 h} \cosh^2 k_1 (z+h) \overline{\cos^2(k_1 q - \omega_1 t + ph)} \sin \varphi \cos \varphi dz \\ = \frac{\rho \omega_1^2 \omega_2^2}{\sinh^2 k_1 h} \overline{\cos^2(k_1 q - \omega_1 t + ph)} \sin \varphi \cos \varphi \int_{-h}^0 \cosh^2 k_1 (z+h) dz$$

Using [34], [35] and [59], equation [70] yields:

$$[71] \quad S_{xy} = \frac{\rho \omega_1^2 \omega_2^2 k_1}{\sinh^2 k_1 h} \sin \varphi \cos \varphi \left[\frac{\sinh 2k_1 h}{4k_1} + \frac{1}{2} \right] \\ = E_1 \left[\frac{k_1 h}{\sinh 2k_1 h} + \frac{1}{2} \right] \sin \varphi \cos \varphi \quad (E_1 = \frac{1}{2} \rho g \omega_1^2)$$

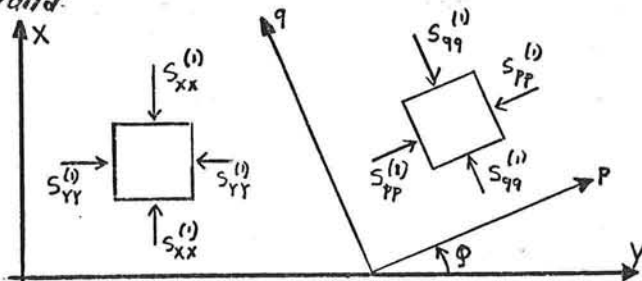
Now all radiation-stresses are known. The results have to be interpreted, because it is important to know whether radiation stresses of two different waves may be added. Summarising the results of the above derivation gives:

$$[52] \quad S_{xx} = E_1 \left(\frac{2k_1 h}{\sinh 2k_1 h} + \frac{1}{2} \right) + E_2 \left(\frac{2k_1 h}{\sinh 2k_1 h} + \frac{1}{2} \right) - E_2 \left(\frac{k_1 h}{\sinh 2k_1 h} + \frac{1}{2} \right) \sin^2 \varphi$$

$$[66] \quad S_{yy} = E_1 \left(\frac{k_1 h}{\sinh 2k_1 h} \right) + E_2 \left(\frac{k_1 h}{\sinh 2k_1 h} + \frac{1}{2} \right) - E_2 \left(\frac{k_1 h}{\sinh 2k_1 h} + \frac{1}{2} \right) \cos^2 \varphi$$

$$[71] \quad S_{xy} = E_2 \left(\frac{k_1 h}{\sinh 2k_1 h} + \frac{1}{2} \right) \sin \varphi \cos \varphi$$

When it is supposed that radiation stresses may be added, the following formulae are valid:



$$S_{xx}^{(1)} = E_1 \left(\frac{2k_1 h}{\sinh 2k_1 h} + \frac{1}{2} \right)$$

$$S_{yy}^{(1)} = E_1 \left(\frac{k_1 h}{\sinh 2k_1 h} \right)$$

$$S_{xy}^{(1)} = E_2 \left(\frac{2k_1 h}{\sinh 2k_1 h} + \frac{1}{2} \right)$$

$$S_{yy}^{(2)} = E_2 \left(\frac{k_1 h}{\sinh 2k_1 h} + \frac{1}{2} \right)$$

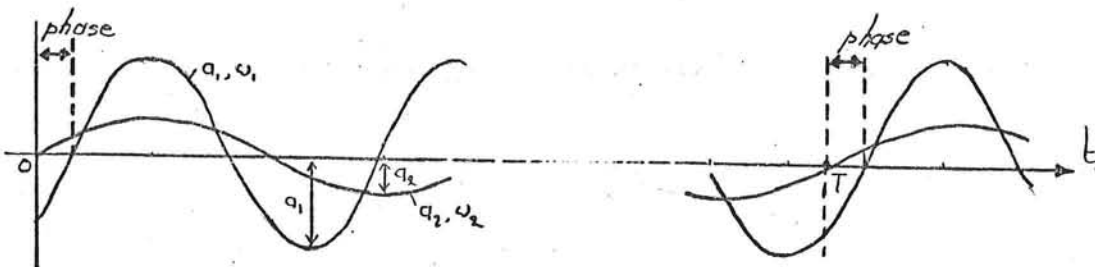
When the radiation stresses in the xy-frame of reference are determined the formulae [52], [66] and [71] are found.

So it is proved that radiation stresses can be added under the following assumptions

- the two incoming waves do not influence each other
- the periods of these two waves are not identical. In that case difficulties will arise with the determination of the time averages

Time average of a quadratic goniometric function

$$\begin{aligned} \{q_1 \cos \omega_1 t + q_2 \cos(\omega_2 t + ph)\}^2 &= \frac{1}{T_0} \int_0^T \{q_1 \cos \omega_1 t + q_2 \cos(\omega_2 t + ph)\}^2 dt \\ &= \frac{1}{T_0} \int_0^T \{q_1^2 \cos^2 \omega_1 t + 2q_1 q_2 \cos \omega_1 t \cos \omega_2 t \cos(\omega_2 t + ph) + q_2^2 \cos^2(\omega_2 t + ph)\} dt \\ &= \frac{1}{T_0} \int_0^T q_1^2 \cos^2 \omega_1 t dt + \frac{1}{T_0} \int_0^T 2q_1 q_2 \cos \omega_1 t \cos(\omega_2 t + ph) dt + \frac{1}{T_0} \int_0^T q_2^2 \cos^2(\omega_2 t + ph) dt \end{aligned} \quad \text{III-6}$$



$$\begin{aligned} T &= k_1 T_1 & \omega_1 &= 2\pi/T_1 \\ T &= k_2 T_2 & \omega_2 &= 2\pi/T_2 \end{aligned}$$

$k_1, k_2 \in \mathbb{N}$

$$\frac{1}{T_0} \int_{T_0}^T q_1^2 \cos^2 \omega_1 t dt = \frac{1}{k_1 T_1} \cdot k_1 \int_{T_0}^{T_1} q_1^2 \cos^2 \omega_1 t dt = \frac{k_1}{k_1 T_1} \cdot \frac{1}{2} q_1^2 T_1 = \frac{1}{2} q_1^2$$

$$\frac{1}{T_0} \int_{T_0}^T q_2^2 \cos^2 \omega_2 t dt = \frac{1}{k_2 T_2} \cdot k_2 \int_{T_0}^{T_2} q_2^2 \cos^2 \omega_2 t dt = \frac{k_2}{k_2 T_2} \cdot \frac{1}{2} q_2^2 T_2 = \frac{1}{2} q_2^2$$

$$\frac{1}{T_0} \int_{T_0}^T 2q_1 q_2 \cos \omega_1 t \cos (\omega_2 t + ph) dt = \frac{\alpha_1 \alpha_2}{T_0} \int_{T_0}^T \{ \cos 2(\omega_1 t + \omega_2 t + ph) + \cos 2(\omega_1 t - \omega_2 t - ph) \} dt$$

[Note: $\cos \alpha + \cos \beta = 2 \cos \frac{\alpha+\beta}{2} \cos \frac{\alpha-\beta}{2}$

$$= \frac{\alpha_1 \alpha_2}{T} \int_0^T \{ 2(\omega_1 + \omega_2) t + 2ph \} dt + \frac{\alpha_1 \alpha_2}{T} \int_0^T \{ 2(\omega_1 - \omega_2) t - 2ph \} dt$$

$$\omega_1 + \omega_2 = \frac{2\pi}{T_1} + \frac{2\pi}{T_2} = 2\pi \left(\frac{1}{T_1} + \frac{1}{T_2} \right) = 2\pi \left(\frac{k_1}{k_1 T_1} + \frac{k_2}{k_2 T_2} \right) = 2\pi \left(\frac{k_1}{T_1} + \frac{k_2}{T_2} \right) = \frac{2\pi}{T} (k_1 + k_2) = \frac{2\pi}{T_3} \quad T_3 = \frac{T}{k_1 + k_2}$$

$$\omega_1 - \omega_2 = \frac{2\pi}{T_1} - \frac{2\pi}{T_2} = 2\pi \left(\frac{k_1}{T_1} - \frac{k_2}{T_2} \right) = \frac{2\pi}{T} (k_1 - k_2) = \frac{2\pi}{T_4} \quad T_4 = \frac{T}{|k_1 - k_2|}$$

[Note: $\omega_1 \neq \omega_2$]

$$\frac{\alpha_1 \alpha_2}{T} \int_0^T \{ 2(\omega_1 + \omega_2) t + 2ph \} dt + \frac{\alpha_1 \alpha_2}{T} \int_0^T \{ 2(\omega_1 - \omega_2) t - 2ph \} dt$$

$$= \frac{\alpha_1 \alpha_2}{(k_1 + k_2) T_3} \int_0^{T_3} \cos (2\omega_3 + 2ph) dt + \frac{\alpha_1 \alpha_2}{|k_1 - k_2| T_4} \int_0^{T_4} \cos (2\omega_4 t - 2ph) dt$$

$$= \frac{\alpha_1 \alpha_2}{T_3} \cdot 0 + \frac{\alpha_1 \alpha_2}{T_4} \cdot 0$$

$$\therefore \overline{\{ q_1 \cos \omega_1 t + q_2 \cos (\omega_2 t + ph) \}}^2 = \frac{1}{2} q_1^2 + \frac{1}{2} q_2^2 = \frac{1}{2} (q_1^2 + q_2^2)$$

The friction factor f_w and the amplitude

As already indicated in vol B (p 15) the Jonsson formula is used to calculate f_w . In this formula f_w is a function of the amplitude. The choice to use the amplitude of an other wave-parameter seems to be rather arbitrarily. In case of one wave it does not matter very much, but in case of two waves it becomes more important. To show that the amplitude is not such a bad choice in this case either, the following considerations are made.

First a situation with waves with identical periods is considered.

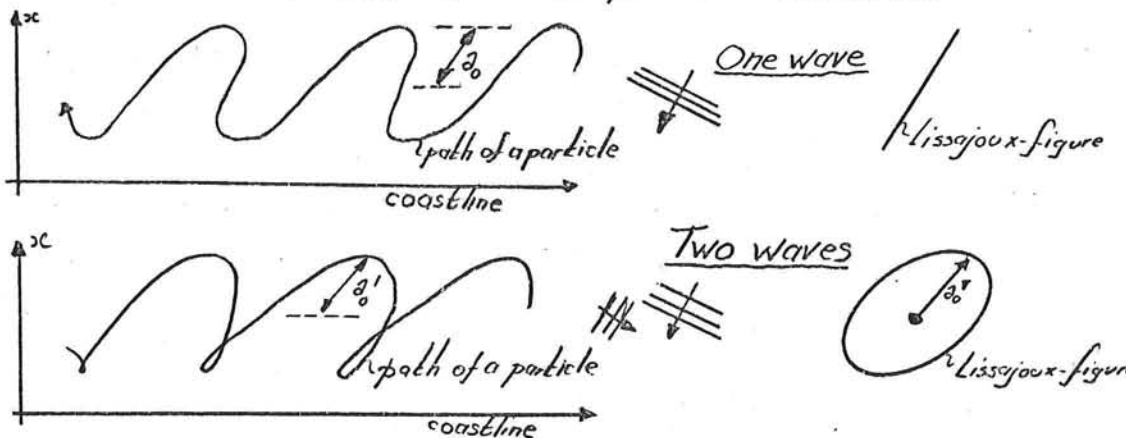


fig.1

In the above figure the Lissajoux-figures and the paths of the particles are sketched. In the two-waves case the amplitude \bar{a}_0 is the amplitude of the Lissajoux-figure of both waves. In such cases it seems to be allowed to use the Lissajoux-amplitude. The Lissajoux-figures of two identical waves are given in fig. 2 [page III-2]. The waves have only a phase difference. It is clear that this phase-difference has a large influence on the value of \bar{a}_0 . Efforts to find an analytical solution of the amplitude as a function of the phase-diff failed, so a numerical algorithm is made to find this maximum, which is called EPS.

'BEGIN'

```
'REAL' DT, AX, AY, AOLDER, AOLD, ANEW, BX, BY, B;
'INTEGER' K;
DT:=KGV/STEPS;
BY:=U2*COS(F11-F12); BX:=U2*SIN(F11-F12);
AX:=AOLDER:=0;
AY:=AOLD:=U1*SIN(F11-F12)/W1;
K:=0;
LOOP: K:=K+1
AY:=(U1*COS(W1*K*DT)+BY*COS(W2*K*DT+PHASE))/W1;
AX:=BX*(COS(W2*K*DT+PHASE))/W1;
ANEW:=SQRT(AY*AY+AX*AX);
'IF' AOLD=ANEW 'THEN' B:=0 'ELSE'
B:=(AOLDER-AOLD)/(AOLD-ANEW);
'IF' B<=0 'THEN' "BEGIN"
'IF' AOLD >= ANEW 'THEN' "BEGIN"
'IF' AOLDER < AOLD 'THEN' "BEGIN"
'IF' K>2 'THEN' "BEGIN"
EPS:=AOLD;
'GOTO' TWO;
'END'; 'END'; 'END'; 'END';
AOLDER:=AOLD; AOLD:=ANEW;
'GOTO' LOOP;
TWO:'END'
```

When the waves are not monochromatic the situation differs. When stochastic waves come from one direction, the path of a particle is indicated below.

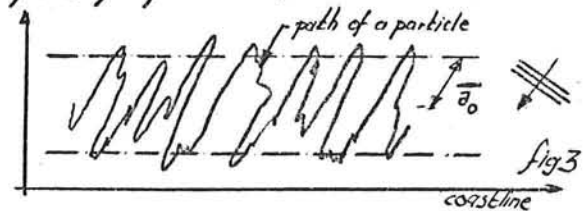


fig.2

For computations an average maximum amplitude (\bar{a}_0) is used. When two monochromatic waves enter the breaker-zone, each with a different period, the path of a particle is quite similar to the path in fig. 3.

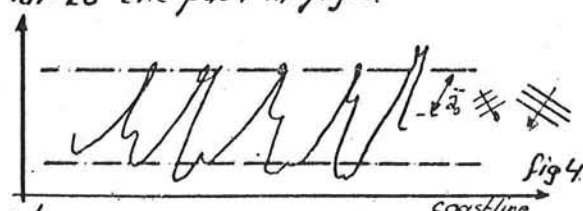


fig.3

The belonging Lissajoux-figure is sketched in figs. In these case one should take

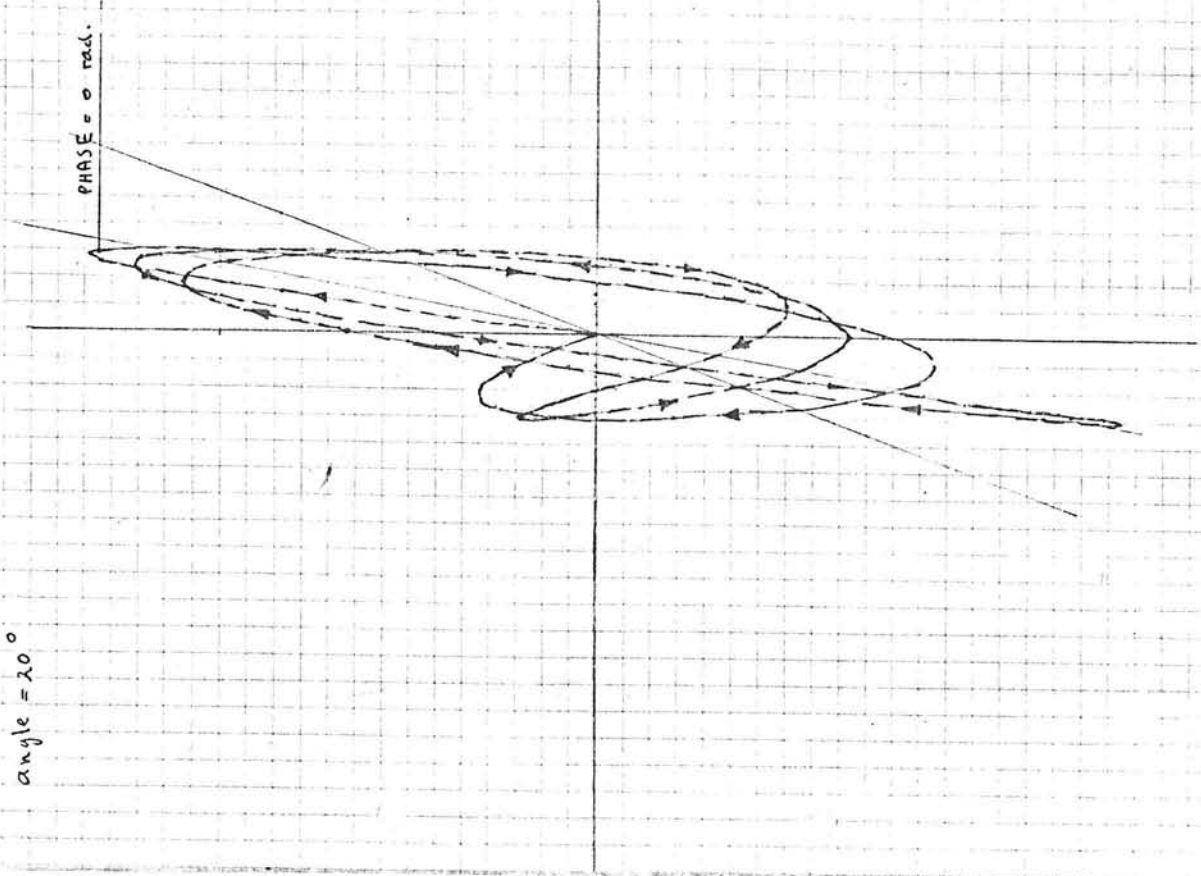
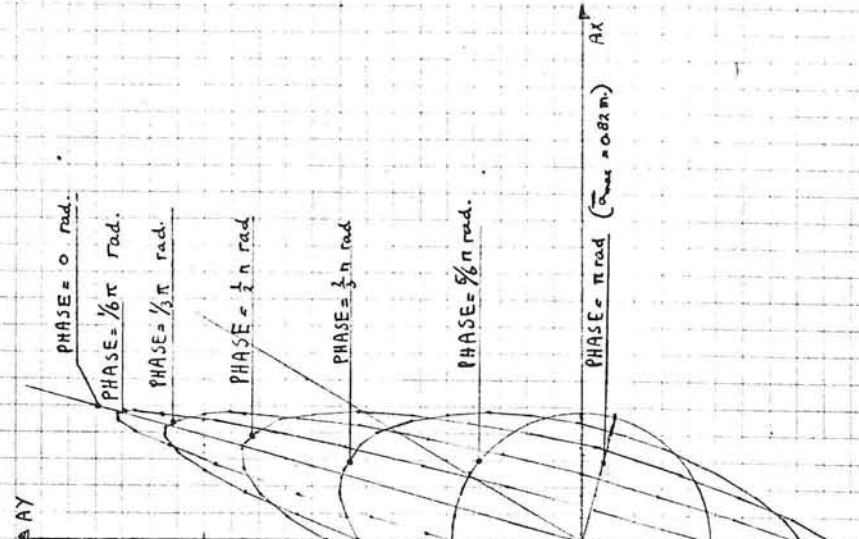
$$\frac{A_{bottom}}{T_1} = \frac{A_{bottom}}{\lambda} = 10 \text{ sec.}$$

$$Q_r = \frac{1}{2\pi} \text{ rad.}$$

$$A_{bottom} = 1.40 \text{ m.}, A_{bottom} z = 0.75 \text{ m.}$$

$$\text{Period } 1 \approx 10 \text{ sec. ; Period } 2 \approx 1500 \text{ sec.}$$

$$\text{angle} = 20^\circ$$



$$AX = \int_0^T \cos \omega_1 t * \sin \omega_2 t dt = \sin \omega_2 \left[\frac{1}{\omega_1} * \sin \omega_1 t \right]_0^T =$$

$$= \sin \left(\frac{1}{6}\pi \right) * \frac{10}{2\pi} * \sin \omega_1 T = \frac{5}{2\pi} \sin \left(\frac{2\pi T}{10} \right)$$

$$AY = \frac{10}{2\pi} \cdot \sin \left(\frac{2\pi T}{10} + \phi \right) + \frac{5\sqrt{3}}{2\pi} \sin \left(\frac{2\pi T}{10} \right)$$

$$A = \sqrt{AX^2 + AY^2}$$

fig 2

fig 5

also the average of the "amplitudes." But this average cannot be calculated exactly, therefore it is assumed to be equal to the mean of the maximum-amplitude and the minimum amplitude.

$$\text{The maximum amplitude is } \bar{a}_{\max} = \sqrt{\left(\frac{u_1}{\omega_1}\right)^2 + \left(\frac{u_2}{\omega_2}\right)^2 + 2 \frac{u_1 u_2}{\omega_1 \omega_2} \cos(\varphi_2 - \varphi_1)}$$

$$\text{The minimum amplitude is } \bar{a}_{\min} = \sqrt{\left(\frac{u_1}{\omega_1}\right)^2 + \left(\frac{u_2}{\omega_2}\right)^2 - 2 \frac{u_1 u_2}{\omega_1 \omega_2} \cos(\varphi_2 - \varphi_1)}$$

To test if this approximation is correct, the real mean amplitude is computed in several cases

periods	10/15	10/17	10/10
$\frac{\bar{a}_{\max} + \bar{a}_{\min}}{2}$	2.39	2.62	1.95
real mean amplitude	2.43	2.66	3.08
for phase = 0	2.43	2.70	2.97
$\frac{\pi}{6}$	2.43	2.67	2.66
$\frac{2\pi}{6}$	2.43	2.64	2.17
$\frac{3\pi}{6}$	2.43	2.62	1.54
$\frac{4\pi}{6}$	2.20	2.50	0.80

It is clear that the approximation is acceptable when the periods differ. For equal periods this approximation is not acceptable.

Fortunately in those cases the average amplitude can be calculated with the algorithm presented on page IV-1.

Formula of Einstein for the calculation of suspended load

$$\begin{aligned}
 S'_S &= \int_{z=a}^{z=h} c(z) \cdot v(z) dz \\
 c(z) &= c_0 \left\{ \frac{(1-\frac{z}{h})(\frac{z}{h})}{\frac{z}{h}(1-\frac{z}{h})} \right\}^{z_*} & c_0 = \frac{S_b}{6.35 \cdot V_* \cdot Q} & Q = t \\
 & & z_* = \frac{V_*}{K \cdot V_x} & \\
 v(z) &= \frac{V_*}{K} \ln \frac{33z}{r} & v_* = \sqrt{\frac{z_*}{\rho}} & \\
 S'_S &= \int_a^h c_0 \frac{V_*}{K} \left\{ \frac{(1-\frac{z}{h})(\frac{z}{h})}{\frac{z}{h}(1-\frac{z}{h})} \right\}^{z_*} \ln \left(\frac{33z}{r} \right) dz \\
 y &= \frac{z}{h} \Rightarrow z = h \cdot y \quad dz = h dy \quad ; \quad A = \frac{q}{h} = \frac{r}{l_h} \\
 S'_S &= \int_A^1 \frac{c_0 V_*}{K} \frac{A^{z_*}}{(1-A)^{z_*}} \left(\frac{1-y}{y} \right)^{z_*} \ln \left(\frac{33h \cdot y}{r} \right) h dy \\
 &= \frac{c_0 V_*}{K} \frac{\left(\frac{1}{h}\right)^{z_*} \cdot h}{(1-A)^{z_*}} \int_A^1 \left(\frac{1-y}{y} \right)^{z_*} \left\{ \ln \frac{33h}{r} + \ln y \right\} dy \\
 &= \frac{c_0 V_* r}{K} \int_A^1 \frac{A^{z_*-1}}{(1-A)^{z_*}} \int_A^1 \left(\frac{1-y}{y} \right)^{z_*} \left\{ \ln \frac{33h}{r} + \ln y \right\} dy \\
 &= \frac{S_b V_* r}{6.35 V_* r K} \int_A^1 \frac{A^{z_*-1}}{(1-A)^{z_*}} \int_A^1 \left(\frac{1-y}{y} \right)^{z_*} \ln \frac{33h}{r} + \frac{A^{z_*-1}}{(1-A)^{z_*}} \int_A^1 \left(\frac{1-y}{y} \right)^{z_*} \ln y dy \Big] \\
 Int 1 &= 0.216 \frac{A^{z_*-1}}{(1-A)^{z_*}} \int_A^1 \left(\frac{1-y}{y} \right)^{z_*} dy \\
 Int 2 &= 0.216 \frac{A^{z_*-1}}{(1-A)^{z_*}} \int_A^1 \left(\frac{1-y}{y} \right)^{z_*} \ln y dy \\
 S_S &= \frac{S_b}{6.35 K} \cdot \frac{1}{0.216} \left\{ Int 1 \ln \left(\frac{33h}{r} \right) + Int 2 \right\} \\
 &= \frac{0.729}{K} S_b \left\{ Int 1 \cdot \ln \left(\frac{33h}{r} \right) + Int 2 \right\}
 \end{aligned}$$

Hence in Bijker [1972] in this formula the value of $K=0.4$ is already entered in the formula as the constant 1.03 [$= 0.729/0.4$].

The accuracy of the computer procedure to solve the Einstein integrals

For the calculation of the accuracy is assumed that $\text{Int1}[300]$ and $\text{Int2}[300]$ are the real values of Int1 and Int2 . [Note: $\text{Int1}[300]$ means an iteration with 300 steps to calculate Int1 . This is not completely true, because $\text{Int1}[400]$ and $\text{Int2}[400]$ would give a more exact value. But this assumption is justified by the fact that the errors in Int1 and Int2 become smaller when the amount of steps increases. When the amount of steps becomes two times larger, the errors in Int1 and Int2 become two times smaller. Therefore it is probably justified to assume that the maximum error in $\text{Int1}[300]$ is not larger than.

$$1.5 \left(\frac{0.06}{8} \right) + 1.5 \left(\frac{0.06}{4} \right) + \dots = 1.5 * 0.06 \sum_{i=1}^n \frac{1}{2^i}$$

for $n \rightarrow \infty$ max. error is $0.5 * 0.06 * 0.5 = 0.045\%$
The maximum error in $\text{Int2}[300]$ is 0.06%.

Therefore it is justified to assume that the error in $\text{Int1}[50]$ is about 0.35% and in $\text{Int2}[50]$ about 0.40%. These errors are small in comparison with other errors made in the calculation of the sand transport. So 50 steps in the calculation of Int1 and Int2 is enough to get an accurate value of the suspended-load-transport. Another conclusion is that the determination of Int1 and Int2 with the diagrams presented in Bijker [1972] is not accurate. It is difficult to read the diagrams properly, and it is therefore highly recommended to calculate Int1 and Int2 . The error made in the determination of Int1 and Int2 with the diagrams varies from 1 to 10%.

Note: For $z_* \in \mathbb{N}$ an analytical solution of Int1 exists.

$$z_* = 0 \quad \text{Int1} = 0.216 \frac{A^{-1}}{(1-A)} A \int_0^1 \left(\frac{1-y}{y} \right)^0 dy = \frac{0.216}{A} (1-A)$$

(For Int2 no analytical solution is found)

$$z_* = 1 \quad \text{Int1} = 0.216 \frac{A^0}{(1-A)} \int_0^1 \left(\frac{1-y}{y} \right)^1 dy = \frac{0.216}{A} (A - 1 - \ln A)$$

$z_* = 0$	$A = 10^{-3}$	$\Rightarrow \text{Int1} = 215.784$	$[\text{Int1}[300] = 1.0000 * \text{Int1}, \text{error} < 0.01\%]$
	$A = 10^{-2}$	$\Rightarrow \text{Int1} = 21.384$	$[\text{Int1}[300] = 1.0000 * \text{Int1}, \text{error} < 0.01\%]$
$z_* = 1$	$A = 10^{-3}$	$\Rightarrow \text{Int1} = 1.277569$	$[\text{Int1}[300] = 0.9962 * \text{Int1}, \text{error} \approx 0.38\%]$
	$A = 10^{-2}$	$\Rightarrow \text{Int1} = 0.788764$	$[\text{Int1}[300] = 0.9993 * \text{Int1}, \text{error} \approx 0.07\%]$

Int1 , errors in %

	max.error $\text{Int1}[50]$	mean error $\text{Int1}[50]$	max.error $\text{Int1}[100]$	mean error $\text{Int1}[100]$	max.error $\text{Int1}[200]$	mean error $\text{Int1}[200]$	max.error $\text{Int1}[10]$	mean error $\text{Int1}[10]$
$A = 10^{-3}$	0.29	0.16	0.14	0.07	0.06	0.03	7.0	4.2
$A = 10^{-2}$	0.72	0.27	0.45	0.15	0.14	0.04	3.9	1.6

Int2	max error $\text{Int2}[50]$	mean error $\text{Int2}[50]$	max error $\text{Int2}[100]$	mean error $\text{Int2}[100]$	max error $\text{Int2}[200]$	mean error $\text{Int2}[200]$	max error $\text{Int2}[10]$	mean error $\text{Int2}[10]$
$A = 10^{-3}$	0.35	0.24	0.24	0.11	0.08	0.04	7.3	4.2
$A = 10^{-2}$	0.82	0.44	0.58	0.25	0.19	0.07	6.2	2.8

$\text{Int1}[0]$ is the determined value from the diagram in Bijker [1972]. Each percentage is the result of 8 calculations of Int1 or Int2 with different values of z_* .

errors in %	max error $B[50]$	mean error $B[50]$	max error $B[100]$	mean error $B[100]$	max error $B[200]$	mean error $B[200]$	max error $B[10]$	mean error $B[10]$
$A = 10^{-3}$	0.31	0.16	0.17	0.07	0.06	0.03	7.8	4.4
$A = 10^{-2}$	0.64	0.21	0.36	0.10	0.10	0.05	6.8	3.1

$$B = \text{Int1}\left(\ln \frac{33}{A}\right) + \text{Int2}$$

Determination of the accuracy of the calculated sand transport

In all cross-sections (a total of nine) the heights and directions of the waves are determined. The method for the calculation of the breakerdepths, breakerangles and breaker-indexes is presented in vol A. Some difficulties will arise when the (relative) error in all these data has to be taken into account.

No specific problems will arise with the calculation of the relative error in the total sand transport caused by inaccuracies of the coastal parameters (α , A , D_{50} etc). However problems will arise with the calculation of the relative error in the total transport caused by errors in the determination of the wave-parameters (wave-height, period and direction).

Input data for the calculation of the total sand transport:

$h_{br,1}, h_{br,2}$	breakerdepths	wave parameters
T_1, T_2	periods	
$\varphi_{br,1}, \varphi_{br,2}$	breakerangles	
δ_1, δ_2	breaker indexes	
α	tangent of the beach slope	
r	bottom roughness	coastal parameters
g	gravity	
ρ	density of seawater	
Δ	relative density of beach material	
D_{50}, D_{go}	grain sizes of beach material	
k	Von Karman constant	

The relative errors in α , ρ , g and Δ are small in comparison with the other relative errors (and the error in the formula), so these relative errors are neglected. The parameter D_{go} appears only in the factor in the exp-function ($\mu = C/18 \log \frac{D_{go}}{D_{50}}$), see vol B. Hence the influence of an error in D_{go} is very small, and can be neglected too.

For all calculations the following parameters are assumed to be constants:

$g = 9.8 [m/s^2]$ $\rho = 1023 [kg/m^3]$ $\alpha = 1.6$ $\alpha_c = 0.384$ $D_{go} = 190 * 10^{-6} [m]$.
All calculations are executed with the data of the first cross-section. The following deep-water data are assumed to be valid

$$H_{br,1} = 1.20 \text{ m } T_1 = 10 \text{ sec } \varphi_{br,1} = -70^\circ \quad H_{br,2} = 0.30 \text{ m } T_2 = 15 \text{ sec } \varphi_{br,2} = +15^\circ$$

Calculation of the influence of the bottom-roughness (r)

Assuming the beach slope $\alpha = 0.025$, the breakerdepths, angles and indexes can be calculated. $r = 0.02 \text{ m}$ is assumed to be the standard case:

$$\begin{aligned} h_{br,1} &= 1.30 \text{ m } \gamma = 0.8 \quad \varphi_{br,1} = -12.5^\circ \quad T_1 = 10 \text{ sec} \\ h_{br,2} &= 0.75 \text{ m } \gamma = 0.8 \quad \varphi_{br,2} = +1.7^\circ \quad T_2 = 15 \text{ sec} \end{aligned}$$

The above parameters are kept constant, while the bottom-roughness r is varied. The mean value of the bottom roughness is about 0.02 m (see the calculation method presented in vol B). The bottom roughness is varied from 0.015 until 0.025 .

In the table on the next page the variables which are changing when the bottom roughness changes, are given:

C = Chery-factor.

$KSI = \xi = p \cdot k \cdot C / \sqrt{g}$

$MU = C/18 \log \frac{D_{go}}{D_{50}}$

$S_t^* = \text{total transport at depth } h = \dots [m^3/\text{year}]$

v = longshore current velocity

S_f = bottom transport

B = multiplication factor for the calculation of suspended load

$S_s = S_f * B$

changing variables (% with regard to SI)														
	C	%	KSI	%	MU	%	V	%	S _b	%	B	%	S _t *	%
$h=1.3$ SI $r=0.015$ $r=0.025$	52	100	1.67	100	0.45	100	-1.555	100	-2.070	100	52.3	100	-1.08×10^6	100
	54	104	1.65	99	0.48	107	-1.655	106	-2.114	109	65.3	125	-1.38×10^5	128
	50	96	1.69	101	0.43	96	-1.477	95	-2.032	98	43.9	84	-0.89×10^5	82
$h=0.75$ SI $r=0.015$ $r=0.025$	48	100	1.49	100	0.43	100	-0.814	100	-1.134	100	25.7	100	-2.91×10^4	100
	50	104	1.48	99	0.46	107	-0.878	108	-1.168	103	31.2	121	-3.64×10^4	125
	46	96	1.51	101	0.40	93	-0.764	94	-1.06	98	21.9	85	-2.42×10^4	83
$h=0.75$ ST $r=0.015$ $r=0.025$	48	100	1.49	100	0.43	100	-0.692	100	-0.958	100	24.8	100	-2.38×10^4	100
	50	104	1.48	99	0.46	107	-0.749	108	-0.989	103	30.0	121	-2.97×10^4	125
	46	96	1.51	101	0.40	93	-0.647	93	-0.931	97	21.3	86	-1.98×10^4	83

In the above table the changing variables are examined at three depths, viz the two breaker-depths of the different wave systems. At the second breakerline the variables are calculated at both sides of the breakerline so at one side without and at the other side with influence of the second wave.

The variation of the total transport due to variation of the bottom-roughness is:

$$\begin{aligned} S_t &: 1.612 \times 10^6 \text{ m}^3/\text{year} & 100\% \\ r=0.015 &: 2.027 \times 10^6 \text{ m}^3/\text{year} & 126\% \\ r=0.025 &: 1.343 \times 10^6 \text{ m}^3/\text{year} & 83\% \end{aligned}$$

From the above table it becomes clear that the variation in sand transport does not depend on the depth (The variation with depth is very small and therefore neglected). When the total sand transport of the standard case is assumed to be the mean value, a relation can be given between S_t/\bar{S}_m and r/r_m .

and r/r_m . \bar{S}_m = total transport of the standard case, r_m = bottom roughness of the standard case. This relation might be non-linear, but an approximation with a linear relation will not deviate much (1 or 2%) from a non-linear relation. So the relation between r/r_m and S_t/\bar{S}_m is assumed to be linear.

$$\begin{aligned} \text{relations for } r/r_m < 1 & \quad \frac{S_t}{\bar{S}_m} = \{(\frac{r}{r_m}) - 1\} * (-1.02) + 1 \\ \text{for } r/r_m \geq 1 & \quad \frac{S_t}{\bar{S}_m} = \{(\frac{r}{r_m}) - 1\} * (-0.68) + 1 \\ \text{non-linear relation: } \frac{S_t}{\bar{S}_m} & \approx (\frac{r}{r_m})^{-0.86} \end{aligned}$$

It is not allowed to extrapolate this figure. So it can only be used when $0.75 \leq r_m \leq 1.25$.

Calculation of the influence of the grain-size D_{50}

For the calculation of the influence of the grain-size D_{50} the standard-case (SI) is used with varying grain-sizes, viz $130 \times 10^{-6} \text{ m}$, $150 \times 10^{-6} \text{ m}$, $170 \times 10^{-6} \text{ m}$

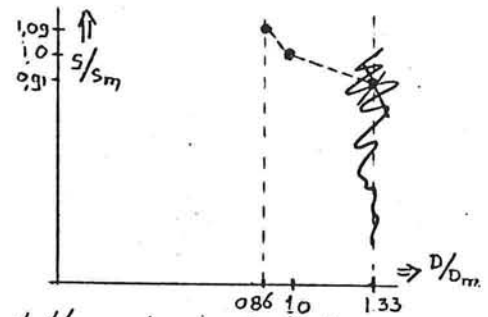
D_{50}	changing variables (% with regard to S_t)					
	S_b	%	B	%	S_t^*	%
$h=1.30$ SI $D=130\mu$ $D=170\mu$	-2.070	100	52.3	100	1.08×10^5	100
	-1.810	87	64.8	124	1.17×10^5	108
	-2.325	112	42.2	81	0.98×10^5	91
$h=0.75$ SI $D=130\mu$ $D=170\mu$	-1.134	100	25.7	100	2.91×10^4	100
	-0.997	88	32.1	125	3.20×10^4	110
	-1.267	112	20.7	81	2.62×10^4	90

The variation of the total transport due to variation of the grain-size (D_{50}) is:

$$\begin{aligned} S_t &: S_{tot} = 1.612 \times 10^6 \text{ m}^3/\text{year} & 100\% \\ D=130\mu &: S_{tot} = 1.754 \times 10^6 \text{ m}^3/\text{year} & 109\% \\ D=170\mu &: S_{tot} = 1.464 \times 10^6 \text{ m}^3/\text{year} & 91\% \end{aligned}$$

Because the grain-size and its distribution can be determined easily, it is clear that the relative error in the sand transport due to variations in grain-size can be kept small. For $0.87 < D/D_m < 1.13$ the following (linear) relation can be given between S_t/S_m and D/D_m :

$$\frac{S_t}{S_m} = (\frac{D}{D_m} - 1) * (-0.69) + 1$$



Because the sand of the beaches in the Bengkulu area has almost the same distribution, the influences of variations in D_{50} is not more than + or - 10%

Calculation of the influence of beach-slope α

This calculation is executed with standard case II; for this case the same deepwater data was taken, only the breaker-index was not estimated correctly.

Standard case II: $+ \alpha = 0.020$ and $\alpha = 0.030$

$$h_{br1} = 1.70 \text{ m}, T_1 = 10 \text{ sec}, g_{br} = -13.5^\circ, \gamma_1 = 0.6 \quad h_{br2} = 0.75 \text{ m}, T_2 = 15 \text{ sec}, g_{br} = 1.7^\circ, \gamma_2 = 0.8.$$

Δ	V	%	S_b	%	B	%	X	%	S_{st}	%
$h=1.70 S_{II}$	-1.44	100	-1815	100	56.5	100	38.0	100	-1.015×10^5	100
$\alpha = 0.020$	-1.23	86	-1537	85	52.1	92	47.5	125	-1.000×10^5	98
$\alpha = 0.030$	-1.63	113	-1036	114	60.6	107	31.7	83	-1.034×10^5	101
$h=0.75 S_{II}$	-0.52	100	-695	100	20.9	100	30.0	100	-1.453×10^5	100
$\alpha = 0.020$	-0.43	83	-570	82	20.3	97	37.5	125	-1.446×10^5	100
$\alpha = 0.030$	-0.61	117	-814	117	21.4	102	25.0	83	-1.455×10^5	100

X is the length between the breakerlines, or the distance between the breakerline and the coast.

Conclusion: The variation of sand transport due to the variation of α is negligible.

With the given relations between S_{st} and T_{st} , resp D_{st} , the influence of small changes (errors) of r and D_{50} can be calculated. These relations are assumed to be valid for all cross-sections. This assumption has to be proved. On the other hand it is known that the grain-size D_{50} and the bottom-roughness r do not vary much along the coast, so a large deviation of the given figures is not expected. The deviation of the calculated sand-transport (due to errors in the determination of D_{50} and r) can be expected to be constant along the coast. The maximum relative error of the sand-transport due to variations of the coastal parameters is valued at 30% (r : 25%, D_{50} : 10%, α : 0%)

Calculation of the influence of wave-parameters

On the foregoing pages the influences of errors in the coastal-parameters (parameters that represent the coast-type) were presented. On the following pages the influences of errors in the wave-parameters (wave-data) are discussed. The parameters which have to be varied are:

H_o - deep water wave height

θ_o - deep water angle of incidence

T - period of the waves

Several problems arise when the influences of the errors of these parameters have to be calculated

- The sand-transport depends on a two-waves system. It is not known which part of the sand-transport is caused by one of these wave systems. When only one wave is breaking (and is activating a longshore current), and the other wave still is not broken, this last wave influences the longshore current too by means of an influence on the bottom-shear-stress. This bottom-shear-stress will increase, so the longshore velocity will become smaller. Turbulence increases, hence suspended load will increase. The total system is very complex.

Examining the calculated sand-transports (Run 1-23, vol A) it becomes clear that the influence of the swell-wave type (in a two-waves situation) is small in comparision with the influence of the monsoon-wave.

- The angle of incidence (at breaking) of the swell waves is very small ($1.5^\circ - 2.5^\circ$). A variation of the deep water angle of incidence will not have much influence on this figure (and therefore also a small influence on the total sand-transport). So the influence of small variations of the breaker-angle of the swell waves, is not taken into account.
- The influences on the total transport of errors in the periods will not be the same for all cross-sections due to refraction. The calculation of these influences are only executed for a one-wave system. If it appears, from this calculation, that the influence of an error in the period is considerable, new refraction patterns have to be calculated. On the other

hand, when the influence of the period on the sand-transport is small, a mean error in all cross-sections can be taken into account

- The influences of errors in the wave-heights are difficult to calculate. Therefore the influences of the wave-heights on the sand transport is only calculated for a one-wave system; the advantage of this method is that the interpretation of the calculations is easy. A disadvantage of this method is that the influence in a two-waves system is not known. But because of the small wave-height of the swell waves, the variation of the monsoon wave-height in a two waves-situation can be assumed to be equal to this variation in a one wave situation. The influence of variations in the height of the swell waves is small in comparision with the influence of variations in monsoon-waves, and therefore neglected.

Calculation of the influence of the period T

For the calculations a one-wave system is used, with the following data: $h_b = 1.32$; $T = 10 \text{ sec}$; $\gamma = 0.8$; $\varphi_0 = 12.4^\circ$ [These are the monsoon-wave data of S_I]. Because the influence of the period on the sand-transport is small, the data h_b and φ_0 are determined until cm, resp tenths of a degree precise. Periods of 8, 10 and 12 seconds are used for the calculations.

T	changing variables (% with regard to S_I)													
	h	%	T	"%"	φ	%	v	%	S_b	%	B	%	S^*_I	%
$h=h_b$	S_I	100	0.8	100	-12.4°	100	-1.608	100	-2192	100	50.5	100	$-1.07 \cdot 10^5$	100
	$T=8 \text{ sec}$	103	0.7	88	-15.8°	127	-1.618	101	-2118	100	50.1	99	$-1.09 \cdot 10^5$	102
	* $T=8 \text{ sec}$	99	0.8	100	-14.9°	120	-1.674	104	-2245	106	48.7	96	$-1.01 \cdot 10^5$	94
	$T=12 \text{ sec}$	108	0.8	100	-10.7°	86	-1.561	97	-2033	96	52.5	104	$-1.15 \cdot 10^5$	108
$h=\frac{1}{2}h_b$	S_I	0.66	100	-	-	-	-0.772	100	-1022	100	17.3	100	$-1.77 \cdot 10^4$	100
	$T=8 \text{ sec}$	0.68	105	-	-	-	-0.778	101	-1017	100	17.0	98	$-1.78 \cdot 10^4$	101
	* $T=8 \text{ sec}$	0.61	92	-	-	-	-0.803	104	-1020	107	16.8	97	$-1.68 \cdot 10^4$	95
	$T=12 \text{ sec}$	0.71	108	-	-	-	-0.751	97	-982	96	17.9	103	$-1.90 \cdot 10^4$	107

* In these cases the breaker index was not changed, which was necessary the breaker criterium had become different ($\frac{h}{\sqrt{g_m T^2}} \approx 0.068 \rightarrow \gamma = 0.7$)

The variations of the total transport:

$$\begin{aligned} S_{\text{tot}} (S_I) &= 1.707 \cdot 10^6 \text{ m}^3/\text{year} & 100\% \\ S_{\text{tot}} (T=8 \text{ sec}) &= 1.733 \cdot 10^6 \text{ m}^3/\text{year} & 102\% \\ * S_{\text{tot}} (T=8 \text{ sec}) &= 1.621 \cdot 10^6 \text{ m}^3/\text{year} & 95\% \\ S_{\text{tot}} (T=12 \text{ sec}) &= 1.822 \cdot 10^6 \text{ m}^3/\text{year} & 107\% \end{aligned}$$

The above figures indicate that the influence of an error in the period T is small. Therefore it is not necessary to determine new refraction-diagrams

$$(T/T_m - 1) \cdot \alpha + 1 = (\frac{S}{S_m}) \quad \text{for } T/T_m \leq 1 \quad \alpha = 0.25 \\ T/T_m \geq 1 \quad \alpha = 0.35$$

Conclusions:

- The influence of the variation of the period ($\pm 20\%$) is small ($\pm 5\%$).
- The influence of the variation of the period is almost the same for all depths.
- When the breakerindex is changed because of a variation of the period, the sand transport does not change much. The differences between the two sand transports, calculated with $T=8 \text{ sec}$ is caused by a different breakerindex γ . The influence of errors in this breaker-index γ is not regarded because no reliable information is available. The influence of these errors are considered as errors in the formula, which are totally unknown. The above conclusions are valid for a one-wave system. For a two-wave system the error caused by variations of the periods become larger. The maximum variation will be about two times the calculated variation, so $2 \cdot 5 = 10\%$

Calculation of the influence of the angle of incidence on deep water (φ_0)

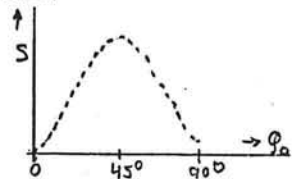
For the calculations a one-wave system is used. The data of S_I (but only with monsoon-waves) and a variable φ_0 ($60^\circ, 70^\circ$ and 80°) are used for the calculations.

changing variables (% with regard to S_2)													
φ_0	h	%	φ_{br}	%	v	%	S_b	%	B	%	S_t	%	
$h=h_{br}$	S_I	1.32	100	-12.4°	100	-1.608	100	-2122	100	50.5	100	$-1.07 \cdot 10^6$	100
	S_I	1.55	117	-12.3°	99	-1.786	111	-2327	110	63.0	125	$-1.72 \cdot 10^5$	160
	S_I	1.00	76	-11.4°	92	-1.259	78	-1687	80	33.4	66	$0.43 \cdot 10^5$	40
$h=\frac{1}{2}h_{br}$	S_2	0.66	100	-	-	-0.772	100	-1027	100	17.3	100	$-1.78 \cdot 10^4$	100
	S_2	0.77	117	-	-	-0.862	112	-1145	111	21.4	124	$-2.87 \cdot 10^4$	161
	S_2	0.50	76	-	-	-0.596	77	-780	76	11.7	68	$-0.63 \cdot 10^4$	39

The variation of the total sand-transport: $S_{tot}(S_2) = 1.707 \cdot 10^6 \text{ m}^3/\text{year}$ 100%
 $S_{tot}(\varphi_0=60^\circ) = 2.734 \cdot 10^6 \text{ m}^3/\text{year}$ 160%
 $S_{tot}(\varphi_0=80^\circ) = 0.685 \cdot 10^6 \text{ m}^3/\text{year}$ 40%

The above figures indicate that a variation in the angle of incidence on deep water has a large influence on the total sand transport. From theoretical considerations follows:

- when $\varphi_0 = 0^\circ$ (the direction of wave propagation is perpendicular to the coast) the sand transport will be zero.
- when $\varphi_0 = 90^\circ$ (the direction of wave propagation is parallel to the coast) the sand transport is also zero, because the waves do not reflect and will travel parallel to the coast.



When there should be no refraction, it is clear that the maximum sand transfer will occur when $\varphi_0 = 45^\circ$. (since $\cos \varphi_0$ has its maximum for $\varphi=45^\circ$). Because of refraction the maximum value S will be lagged to the direction of $\varphi_0=0$. So the variation of the sand-transport depends on the value of φ_0 mean.

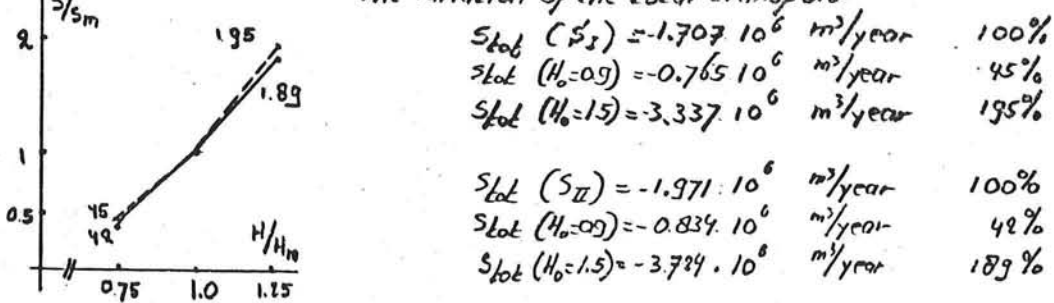
From adjacent figure it becomes clear that for $\varphi_0 \approx 70^\circ$ the slope of the relation between φ_0 and S_t is maximal. So the calculated variance is the maximum variance which can occur.

Calculation of the influence of the deep water wave-height H_0

calculations are executed with a one-wave system and the data of S_2 and S_{II} , with a varying H_0 , viz. 0.90, 1.20, 1.50 m.

H_0	changing variables (% with regard to S_2 or S_{II})												
	h	%	φ_{br}	%	v	%	S_b	%	B	%	S_t	%	
$h=h_{br}$	S_2	1.32	100	-12.4°	100	-1.608	100	-2122	100	50.5	100	$-1.07 \cdot 10^6$	100
	S_2	1.05	80	-11.1°	90	-1.274	79	-1669	79	35.3	70	$-0.47 \cdot 10^5$	44
	S_2	1.60	121	-13.7°	110	-1.945	121	-2536	120	68.2	135	$-2.09 \cdot 10^5$	195
$h=\frac{1}{2}h_{br}$	S_2	0.66	100	-	-	-0.772	100	-1027	100	17.3	100	$-1.78 \cdot 10^4$	100
	S_2	0.52	80	-	-	-0.602	78	-789	77	12.4	72	$-0.78 \cdot 10^4$	44
	S_2	0.80	121	-	-	-0.945	122	-1263	123	23.1	133	$-3.53 \cdot 10^4$	195
$h=h_{br}$	S_{II}	1.70	100	-14.0°	100	-1.479	100	-1847	100	53.3	100	$-3.84 \cdot 10^6$	100
	S_{II}	1.32	78	-12.5°	89	-1.181	80	-1482	80	36.0	68	$-4.16 \cdot 10^5$	42
	S_{II}	2.01	118	-15.3°	109	-1.782	120	-2214	120	71.2	134	$-18.6 \cdot 10^5$	189
$h=\frac{1}{2}h_{br}$	S_{II}	0.85	100	-	-	-0.713	100	-870	100	17.5	100	$-1.52 \cdot 10^4$	100
	S_{II}	0.66	78	-	-	-0.561	79	-665	76	12.2	70	$-0.63 \cdot 10^4$	42
	S_{II}	1.00	118	-	-	-0.869	122	-1078	124	23.0	131	$-2.93 \cdot 10^4$	195

The variation of the total transport.



$$S_{tot}(S_2) = -1.707 \cdot 10^6 \text{ m}^3/\text{year} \quad 100\%$$

$$S_{tot}(H_0=0.9) = -0.765 \cdot 10^6 \text{ m}^3/\text{year} \quad 45\%$$

$$S_{tot}(H_0=1.5) = -3.337 \cdot 10^6 \text{ m}^3/\text{year} \quad 195\%$$

$$S_{tot}(S_{II}) = -1.971 \cdot 10^6 \text{ m}^3/\text{year} \quad 100\%$$

$$S_{tot}(H_0=0.9) = -0.834 \cdot 10^6 \text{ m}^3/\text{year} \quad 42\%$$

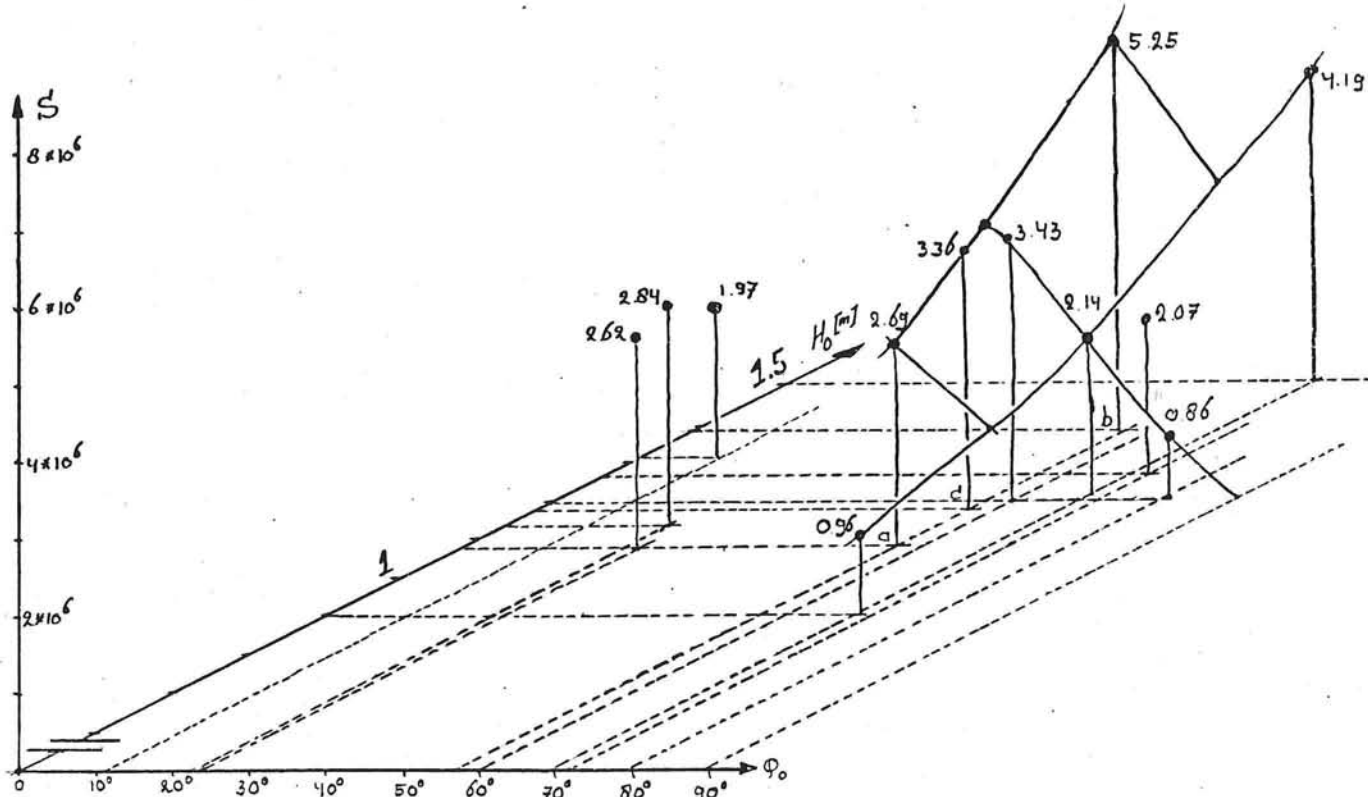
$$S_{tot}(H_0=1.5) = -3.724 \cdot 10^6 \text{ m}^3/\text{year} \quad 189\%$$

Approximated relations between S/S_m and H_0/H_{0m} :

$$\{ \left(\frac{H_0}{H_{0m}} \right) - 1 \}^2 (\alpha) + 1 = \left(\frac{S}{S_m} \right)$$

	S_I	S_{II}
$\frac{H_0}{H_{0m}} \leq 1$	2.90	3.80
$\frac{H_0}{H_{0m}} > 1$	2.32	3.56

It is possible that the relation between S/S_m and H_0/H_{0m} is a function of H_{0m} . Therefore a figure is made for all transport calculations with a one wave system and a period of 10 seconds. The total sand transport (vertical) is plotted as a function of H_0 and ϕ_0 .



The relation between H_0/H_{0m} and S/S_m can be checked with the sand-transport calculations presented in the above figure. For point c it appears that the transport of point a and b can be computed with an error of about 2%. As a first approximation we assume that the relation between H_0/H_{0m} and S/S_m is valid for all values of ϕ_0 and H_0 .

Acceleration of a longshore current

Annex VIII

All theoretical derivations of transport formulae are based upon fully developed currents, so no acceleration of the current would occur. Problems will arise when sand transports have to be calculated near areas where the longshore current velocity changes. Therefore is tried to find a formula for the acceleration of a longshore current. The problem can be approached in two ways:

1. Using the law of Newton $F = ma$

2. By means of a differential equation

- ① At a depth h the accelerating force can be calculated, also the mass which has to be accelerated. $F = \frac{\partial S_{xy}}{\partial z} + \frac{\partial S_{xx}}{\partial y} = F_{\text{breaking}} - F_{\text{set-up}}$ (1) y is parallel to the coast
 $m = \rho \cdot h \cdot 1 \cdot 1$ (2)

Note: F is a force per unit width and unit length.

The maximum velocity which can occur can be calculated by means of

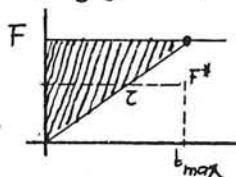
$$F = \tau \quad (3)$$

$$\tau = (0.75 + 0.45 \left(\frac{E U_0}{v} \right)^{1.13}) \frac{\partial g v^2}{\partial z} \quad (4) \quad [\text{Bijker 1967}]$$

when v_{\max} is found (e.g. by means of Regula Falsi) the time in which the current is accelerated (at depth h) can be calculated:

$$v_{\max} = a \cdot t_{\max} \quad (5)$$

The developing current will cause a reacting force τ , which becomes the same as the acting force F when $v = v_{\max}$. During acceleration this reacting force will be developed, so the acting force F will not be used fully for the acceleration. Therefore is assumed that the mean accelerating force is half the acting force.



$$\text{at } t=0 \quad F^* = F - \tau = F \quad (\tau=0) \quad (6)$$

$$\text{at } t=t_{\max} \quad F^* = F - \tau = 0 \quad (\tau=\tau_{\max}) \quad (7)$$

For each t is assumed that $F^* = \frac{1}{2} F$ (8)

So t_{\max} becomes

$$t_{\max} = \frac{v_{\max}/a}{1/2} \quad (a = \frac{1}{2} a) \quad (9)$$

The distance in which the current is accelerated will be

$$s = \frac{1}{2} a^* (t_{\max})^2 + S_0 \quad (S_0 = 0) \quad (10)$$

$$s = \frac{1}{2} a^* \left(\frac{v_{\max}}{a^*} \right)^2 = \frac{1}{2} \frac{v_{\max}^2}{a^*} = \frac{v_{\max}^2}{4a} \quad (11)$$

$$s = \frac{(F/a)^2}{4} \cdot \frac{F}{\tau h} = \frac{1}{4} \frac{\rho h F}{\tau h} \quad (\text{with Bokker}) \quad (12)$$

- ② The differential equation is derived by means of adjacent figure; the derivation is made by means of a balance of momentum, assuming a time-interval of 1 second. The force acting on this piece of water is:

$$F_g = +F \times 1 \times dy \quad (13)$$

The reacting force on the bottom, due to the resistance to the current velocity: $F_{re} = +\tau \times 1 \times dy$ (14)

The amount of momentum coming through the plane y, z (in one second)

$$m_y \cdot v_y = \rho h 1 v \cdot v \quad (15)$$

The amount of momentum leaving through the plane $y+dy, z$ (in one second)

$$m_{y+dy} (v_{y+dy}) = \rho h 1 (v+dv) \cdot (v+dv) \quad (16)$$

The balance of momentum becomes (13, 14, 15, 16)

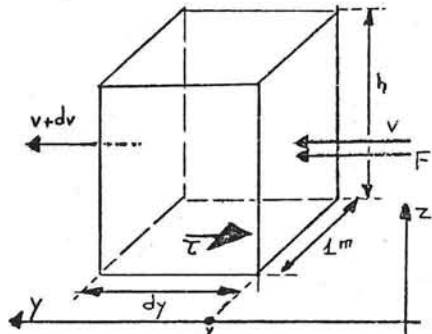
$$F_g + F_{re} = m_{y+dy} \cdot v_{y+dy} - m_y v_y \\ (F + \tau) dy = \rho h \{ (v+dv)^2 - v^2 \} = \rho h \{ 2vdv + (dv)^2 \} \quad (17)$$

When the formula of Bijker (1967) for τ is used this equation cannot be solved analytically. For this solution a computer program is made.

An analytical solution can be found when the simplification of Bokker is used, and assuming $E U_0 \gg v$ in the breakerzone. Then τ becomes

$$\tau = \frac{2 \rho g \xi u_b^2}{\pi C_1} - v \quad (18)$$

When v is positive, τ is negative, so:



$$c = -\frac{2\rho g \xi v_b^2 v}{n d^2}$$

(19)

At depth h : ξ , v_b and d are constant, so:

$$c = -A \cdot v$$

$$(10) \quad A = \frac{2\rho g \xi v_b^2 v}{n d^2}$$

(20)

$$(F-Av) dy = \{2v dv + (dv)^2\} \rho h$$

(21) ... (12)

When this formula (12) is rewritten into:

$$(F-Av) = \{2v \frac{dv}{dy} + \frac{dv}{dy} dv\} \rho h$$

(22)

for $dv \rightarrow 0$ and $dy \rightarrow 0$ the formula becomes:

$$(F-Av) = \{2v \frac{dv}{dy} + \frac{dv}{dy} \cdot 0\} \rho h$$

(23)

$$F-Av = 2v \frac{dv}{dy} \rho h$$

$$(F-Av) dy = 2\rho h v \frac{dv}{dy} = 2B v dv \quad [B = \rho h]$$

(24)

$$\frac{dy}{dy} = \frac{2Bv}{F-Av} \cdot dv$$

$$\int dy = \int \frac{2Bv}{F-Av} dv$$

(25)

$$\int dy = \int -\frac{2B}{A} + \frac{2BF}{A(F-Av)} dv$$

$$y + C = -\frac{2Bv}{A} + \frac{2BF}{A} \cdot \left\{ -\frac{1}{A} \ln(F-Av) \right\}$$

(26)

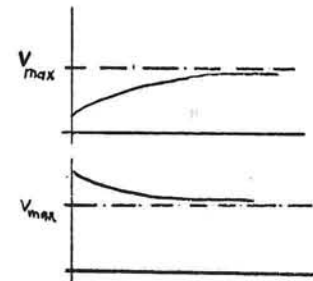
Initial conditions:

$$y=0 \quad v=v_0 \Rightarrow C = -\frac{2Bv_0}{A} - \frac{1}{A} \left\{ \ln(F-Av_0) \right\} \frac{2BF}{A}$$

$$y = -\frac{2Bv}{A} + \frac{2Bv_0}{F} + \frac{2BF}{A^2} \left\{ \ln(F-Av_0) - \ln(F-Av) \right\}$$

$$y = \frac{2B}{A} \frac{(v_0-v)}{v_{max}} \cdot \frac{F}{A} + \frac{2BF}{A^2} \left\{ -\ln \left(\frac{F-Av}{F-Av_0} \right) \right\}$$

$$y = \frac{2BF}{A^2} \left\{ \frac{v_0-v}{v_{max}} - \ln \left(\frac{1 - \frac{v}{v_{max}}}{1 - \frac{v_0}{v_{max}}} \right) \right\}$$



for $y=0 \quad v=0 \Rightarrow$ special case

for $y \rightarrow \infty \quad v \rightarrow v_{max}$

$$\text{when } v \rightarrow v_{max} \text{ then } c \rightarrow F; F = c = A \cdot v_{max} \Rightarrow v_{max} = \frac{F}{A}$$

$$y=0 \quad C = -\frac{2BF}{A^2} \ln(F) = -\frac{2BF}{A^2} \quad (27)$$

$$y \rightarrow \infty \quad (F-Av) \rightarrow 0, \text{ so } \ln(F-Av) \rightarrow -\infty$$

$$\lim_{y \rightarrow \infty} \left(-\frac{2BF}{A^2} \ln(F-Av) \right) = +\infty$$

The initial condition for $y \rightarrow \infty$ is satisfied

$$y = -\frac{2Bv}{A} + \frac{2BF}{A^2} \left\{ \ln F - \ln(F-Av) \right\}$$

(28)

$$y = -\frac{2Bv}{A} + \frac{2B}{A} \cdot \frac{F}{A} \left\{ -\ln \left(1 - \frac{A}{F} \cdot v \right) \right\}$$

$$y = -\frac{2B}{A} \left\{ v + v_{max} \ln \left(1 - \frac{v}{v_{max}} \right) \right\}$$

$$y = -\frac{2B}{A} v_{max} \left\{ \frac{v}{v_{max}} + \ln \left(1 - \frac{v}{v_{max}} \right) \right\}$$

$$y = -\frac{2BF}{A^2} \left\{ \frac{v}{v_{max}} + \ln \left(1 - \frac{v}{v_{max}} \right) \right\} = + \frac{2BF}{A^2} \cdot K$$

(29)

$$y = \frac{2\rho h F}{(\frac{2\rho g \xi v_b^2}{n d^2})^2} \cdot K = \frac{n^2 C^4 h F}{2\rho g^2 \xi^2 v_b^4} \cdot K$$

$$K = f \left(\frac{v}{v_{max}} \right) = - \left\{ \frac{v}{v_{max}} + \ln \left(1 - \frac{v}{v_{max}} \right) \right\}$$

(30)

Note: $Y_0 = \frac{2BF}{A^2} K = 2k \frac{C^4 F}{A^2}$ (29)
When this is compared with (12):
 $2k = \frac{1}{4}$

There is a constant ratio between ξ and Y_0 , viz $Y_0 = \frac{1}{4} \xi$. The formula derived with $F = m \alpha$ is almost the same as the formula derived with the diff eq, only a constant B is missing. Therefore the formula of the diff eq is preferable

v_{max}	K
0.1	0.0054
0.2	0.023
0.3	0.057
0.4	0.11
0.5	0.19
0.6	0.32
0.7	0.50
0.8	0.81
0.9	1.40
0.95	2.05
0.99	3.62

The dimension of y is [m]. K has no dimension, so the dimension of $\frac{n^2 C^4 h F}{2\rho g^2 \xi^2 v_b^4}$ has to be [m] too. This can be checked.

$$\frac{n^2 C^4 h F}{2\rho g^2 \xi^2 v_b^4} = Y_0 \quad (\text{for } y = Y_0, k = 1 \Rightarrow \frac{v}{v_{max}} = 0.84) \quad (31)$$

$$\text{or } Y_0 = \frac{2BF}{A^2}$$

Some calculations. assume: $h_{br} = 1.00 \text{ m}$

$$\begin{aligned} r &= 0.015 \text{ m} \\ \rho_{br} &= 10^0 \text{ kg/m}^3 \\ T &= 10 \text{ sec} \\ A &= 0.8 \\ \alpha &= 0.025 \end{aligned}$$

$$\text{Then, at a depth } h=1 \text{ m}$$

$$v_b^2 = \frac{\pi H}{T \sinh \frac{\pi h}{L}} = \frac{4.08 \cdot 1}{10 \cdot 0.2035} = 1.24 \text{ m/s}$$

$$c_0 = \frac{v_b T / 2\pi}{L} = 1.97 \text{ m}$$

$$c = 18 \log \frac{v_b h}{L} = 52.26 \text{ m/s}$$

$$\xi = c \sqrt{\frac{F}{\rho g L}} = 1.63$$

Assuming that from $y=0$ until $y=0.8$ the breaker depth is 1.00 m, the force caused by differences in set-up will be zero. $F = F_{br} = \frac{5}{16} \frac{\rho g A^* h^2}{V h_{br}} \sin \phi_b \cos \phi_b \cdot \alpha = 3.41 \text{ N/m}^2$

The mass which has to be accelerated: $m = 1.1 \cdot \rho h = 1000 \text{ kg}$

The maximum velocity (acc. to Bijkers) $F = \tau = (0.75 + 0.45 \frac{F_{br}}{V_{max}})^{1/3} \frac{\rho g V_{max}^2}{c^2} \Rightarrow V_{max} = 0.62 \text{ m/s}$

(with the simplification of Bakker) $F = A \cdot V_{max} ; A = \frac{2 \rho g F_{br}}{\pi C^2} = 4.62 \Rightarrow V_{max} = 0.74 \text{ m/s}$

Examining the ratio between τ and V for the Bijkers formula, it appears that the ratio is almost constant. So for an approximation can be assumed that $\tau = A^* \cdot V$, in which $A^* = \frac{C_{max}}{V} = \frac{F}{V}$. With the given data A^* becomes $3.41/0.62 = 5.50 \text{ (kg/m}^2\text{s)}$

	$V=0.05 \text{ m/s}$	0.1 m/s	0.2 m/s	0.3 m/s	0.4 m/s	0.5 m/s	0.55 m/s	0.6 m/s
τ calculated with Bijkers (1)	0.27	0.51	0.99	1.50	2.04	2.63	2.94	3.26
τ calculated with $\tau = A^* V$ (2)	0.28	0.56	1.10	1.65	2.20	2.75	3.03	3.30
percentage in regard to (1)	99%	93%	90%	91%	93%	96%	97%	99%

Because the velocities calculated by means of the simplification of Bakker are too large, it is clear that the length over which they are accelerated is also too large. So a better approximation can be made with the adopted Bijkers formula:

$$Y_* = \frac{2 \rho h F}{(A^*)^2} = 22.5, \text{ so } Y = 225.5 \text{ K.}$$

The numerical computations

In the derivation of eq (29) an approximation ($\tau = -A^* v$) is made. Therefore a numerical approach for solving the differential equation is made too. The calculations for this approach are made with the help of a computer-program [this program is added to this report]. In this program the Bijkers-equation is used for calculating τ :

$$\tau = (0.75 + 0.45 \frac{F_{br}}{V})^{1/3} \frac{\rho g V^2}{c^2} \quad [\text{Bijkers 1967}]$$

The step in the program has a finite length. In the derivation of eq (29) this length decreased to the limit zero. ($dy \rightarrow 0$). So when the step-length in the program becomes smaller, the results have to approach the results calculated with eq. 29. Because of the approximation $\tau = -A^* v$ (in eq. 29) the results will not be exactly the same.

The following input-data are used: $h_{br} = 0.90 \text{ m}$ $F_{br} = 3.50$ $T = 7 \text{ sec}$
 $A = 0.8$ $r = 0.015 \text{ m}$ $\alpha = 0.025$
 $\rho = 1000 \text{ kg/m}^3$ $g = 9.8 \text{ m/s}^2$ Step-length 1m and 0.5m

For 8 depths the length Y_1 (eq 31) is calculated:

depth $h \text{ [m]}$	chety-factor $c \text{ [m}^{1/3}/\text{s]}$	orb. veloc. $v \text{ [m/s]}$	ξ	max veloc $v \text{ [m/s]}$	acc. Force $F \text{ [N/m}^2]$	$A^* \text{ [kg/m}^2]$	$Y_1 \text{ [m]}$
0.056	29.8	0.30	1.41	0.012	0.048	3.50	0.4
0.17	38.4	0.51	1.58	0.059	0.218	3.69	5.4
0.28	42.4	0.66	1.64	0.117	0.469	4.01	16.4
0.39	45.0	0.78	1.67	0.180	0.778	4.39	32.8
0.51	47.0	0.88	1.70	0.247	1.134	4.59	54.4
0.62	48.5	0.97	1.72	0.317	1.532	4.83	81.4
0.73	49.8	1.05	1.73	0.388	1.968	5.07	111.8
0.84	50.0	1.12	1.75	0.458	2.439	5.33	144.2

$$y = Y_1 \cdot K$$

By means of the program the velocities are calculated for eight depths for different values of y . The results of both methods can be compared in two ways:

- for a ray $y = \dots$ compare both velocities (v)
- for a ratio $y/V_{max} = \dots$ compare both calculated lengths (y)

The ratio V/V_{max} in a ray $y=10, 20, 50, 100$ and $200m$ in %

ray $y=10$			ray $y=20$			ray $y=50$			ray $y=100$			ray $y=200$		
depth	diff eq	num eq	diff eq	num eq	diff eq	num eq	diff eq	num eq	diff eq	num eq	diff eq	num eq	diff eq	num eq
	step=1	step=0.5		step=1		step=1		step=1	step=0.5	step=1	step=0.5	step=1		step=0.5
0.056	100	100	100	100	100	100	100	100	100	100	100	100	100	100
0.17	94	95	94	99	100	99	100	100	100	100	100	100	100	100
0.28	74	75	74	88	88	88	98	98	98	100	100	100	100	100
0.39	59	60	60	74	75	75	91	92	92	98	99	99	99	100
0.51	49	50	50	63	64	64	83	84	84	94	95	95	99	100
0.62	42	43	42	55	56	56	74	76	76	88	89	89	97	98
7.3	36	37	37	48	49	49	68	69	69	82	84	83	94	95
8.4	33	33	33	44	44	44	62	63	63	77	78	78	90	91

The length y for certain ratios of V/V_{max} (in %)

V/V_{max}	y_{diff}	y_{num}		y_{num}/y_{diff}	
		st=1	st=0.5	st=1	st=0.5
63	52	50	50	95	95
78	106	100	100	94	94
86	159	150	150	94	94
91	216	200	200	93	93
94	270	250	250	93	93
96	326	300	300	92	92
97	370	350	340	94	92
98	423	400	400	95	95

depth 0.84m

V/V_{max}	y_{diff}	y_{num}		y_{num}/y_{diff}	
		st=1	st=0.5	st=1	st=0.5
50	10	10	10	95	95
64	21	20	20	96	96
84	54	50	50	92	92
95	111	100	100	90	90
98	160	145	145	91	91
99	197	175	175	89	89
99.5	234	195	195	83	83

depth 0.51m

Conclusions:

- The numerical computations give no better result than the (differential) equation (79)
- The calculation of sand-transport is not very reliable; errors of more than 25% are usual. So the computation with eq (79) is accurate enough
- Only when differences in breakerdepth occur, and thus differences in set-up, the computer-program will minimize calculations
- The step-length is not very important for the accuracy, only for small depths a too large step-length will cause instability of the program. The maximum step-length can be estimated: $(F-\tau)dy = \{2vdv + (dv)^2\}ph$ (32)
- dv has to be small: $(F-\tau)dy < (2vdv + (dv)^2)ph$

when is assumed that $\tau = Av$, so $F = A V_{max}$, and for a certain v , dv cannot be larger than $(V_{max}-v)$ so eq.(32) becomes:

$$(AV_{max} - Av)dy < \{2v(V_{max}-v) + (V_{max}-v)^2\}ph$$

$$dy < \frac{\{2vV_{max} - 2v^2 + V_{max}^2 + v^2 - 2vV_{max}\}}{A(V_{max}-v)} ph$$

$$dy < \frac{(V_{max}-v)(V_{max}+v)}{(V_{max}-v)} ph$$

$$dy < \frac{(V_{max}-v)ph}{A}$$

so when $v \rightarrow V_{max}$

$$dy < \frac{2V_{max}ph}{A}$$

$$dy < \frac{2phF}{A^2} = Y_1$$

$$\text{so: } dy < Y_1$$

$$V_{max} = F/A$$

Calculation of the sand-transport near the Bengkulu-harbour.

The velocities of the longshore current west of the Bengkulu-harbour are calculated by means of the computer program added to this report. The input data for this program are determined in vol.D. The breakerdepth at 250 m west of the western harbourmole is 0.80 m and near this harbourmole it will be about 0.90 m. Because of this difference in breakerdepth, set-up differences will occur. Determination of this difference in breakerdepth is very important, because large differences in $\Delta h_{br/dy}$ along the coast cause problems with the numerical computation, and are also not realistic.

A problem in these computations is that the velocity in a ray may give a shear-stress in the same direction as the accelerating force F .

Because the direction of the coastline changes, g_{br} changes also along the coast. The following input data are used.

$$\begin{array}{lll} \text{Ray } y=0: h_{br} = 0.80 \text{ m} & \text{Ray } y=280: h_{br} = 0.90 \text{ m} & \text{for both rays: } r = 0.015 \text{ m} \\ g_{br} = 6^\circ & g_{br} = 3.5^\circ & \rho = 1000 \text{ kg/m}^3 \\ \gamma = 0.8 & \gamma = 0.8 & g = 9.8 \text{ m/s}^2 \\ & & d = 0.025 \end{array}$$

Between the rays $y=0$ and $y=280$ the breakerdepth and breakerangle are changed slowly. With the calculated velocities in the last ray the sand transport can be calculated.

depth [m]	calculated $V [m^6]$	μ	τ_r/τ_c	$S_b [m^2/yr]$	$B+1$	$St [m^3/year]$	V_{max}	$(\tau_r/\tau_c)_{max}$	$S_{b_{min}}$	$B+1_{min}$	St_{max}
0.056	0.01	0.32	0.0896	3.3	2.5	37	0.01	0.0896	3.3	2.5	37
0.17	0.06	0.39	0.328	54	4.6	632	0.06	0.328	54	4.6	632
0.28	0.12	0.41	0.600	131	7.1	4185	0.12	0.600	131	7.1	4185
0.39	0.18	0.43	0.881	209	10.3	9687	0.18	0.881	209	10.3	9687
0.51	0.24	0.44	1.177	287	13.2	17048	0.24	1.177	287	13.2	17048
0.62	0.31	0.45	1.488	377	15.4	31912	0.31	1.488	377	15.4	31912
0.73	0.38	0.46	1.794	465	22.3	46663	0.38	1.794	465	22.3	46663
0.84	0.36	0.46	2.050	438	25.8	50852	0.46	2.050	561	26.0	65637
Total						$16 \times 10^5 \text{ m}^3/\text{year}$			Total		
									$1.8 \times 10^5 \text{ m}^3/\text{year}$		

$$D_{50} = 150 \times 10^{-5}$$

$$\mu = \left\{ 18 \log \frac{12h_f}{18 \log \frac{12h_f}{\rho g_0}} \right\}^{1.5}$$

$$\tau_r/\tau_c = \left\{ 1 + \frac{1}{2} \left(\frac{\tau_r}{\tau_c} \right)^2 \right\}^{1/2}$$

$$S_b = 5D_{50} \frac{V}{C} \sqrt{g} \exp \left\{ \frac{-0.27 \Delta D c^2}{\mu v^2 \left\{ \tau_r/\tau_c \right\}^{1/2}} \right\}$$

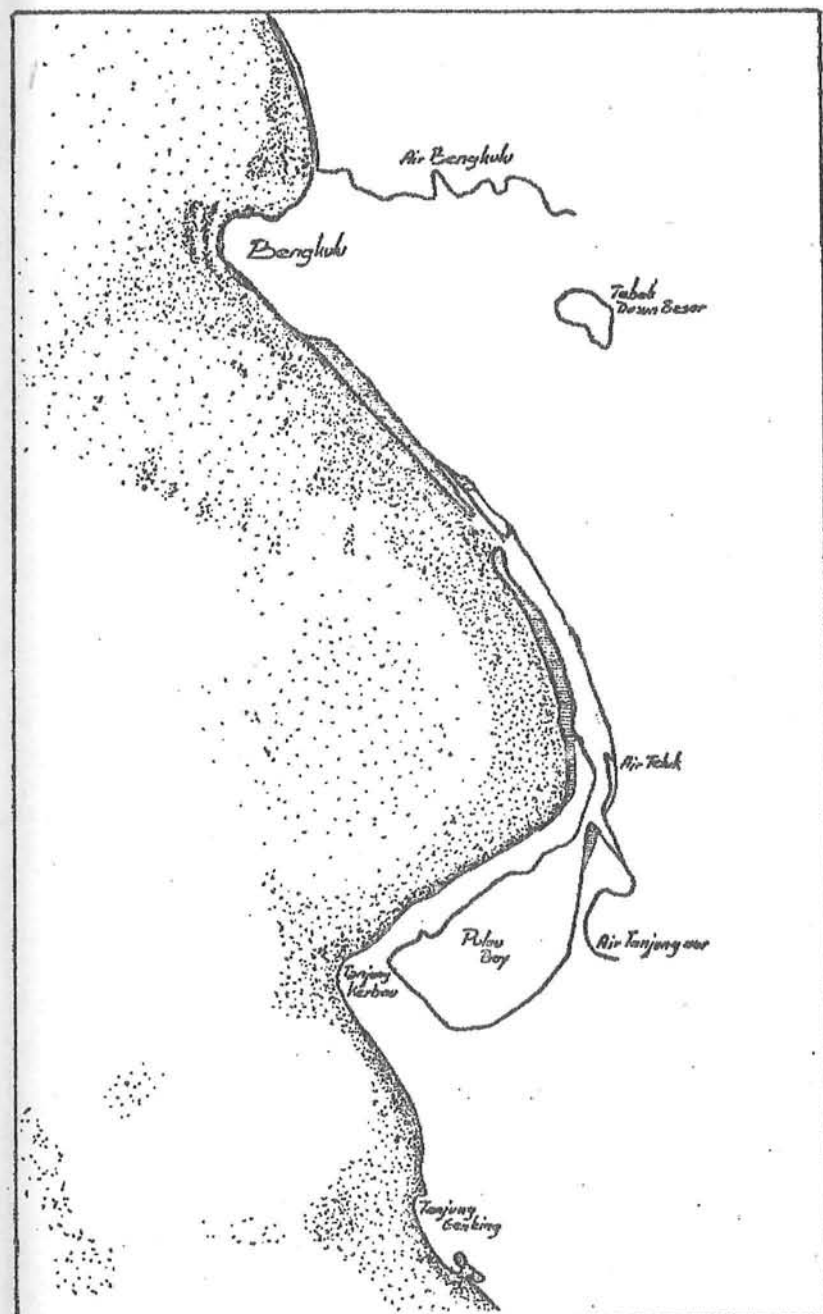
$$St = S_b \times (B+1) \times \frac{h}{8d}$$

So transport along the harbour-mole is $\frac{1}{2} \times 1.6 \times 10^5 = 80000 \text{ m}^3/\text{year}$ (waves come from NW-directions for only half a year) The max. transport at the beach west of the harbourmole is $90000 \text{ m}^3/\text{year}$. The accuracy of this computation is not known. With the determined accuracy, mentioned in vol A, a certain variance can be given:

$$\begin{aligned} \text{coastal parameters: } & \text{ca. } 30\% \\ \text{wave parameters: } & \text{ca. } 50\% \end{aligned} \quad \left. \begin{aligned} \text{Total variance } S_e^2 + S_i^2 = 60\% \end{aligned} \right\}$$

So the sand-transport near the Bengkulu harbour is estimated to be a value between

$$35000 \text{ m}^3/\text{year} \text{ and } 125000 \text{ m}^3/\text{year}.$$



BENGKULU HARBOUR PROJECT

FINAL REPORT

VOL C

Refraction analysis

Feb '78

Dik Ludikhuize & Henk Jan Verhagen

Contents

Part one Refraction analysis

- Introduction
- The graphical method
- The numerical method
- The lens effect
- Interpretation of the refraction diagrams
- Wave periods

Part two Refraction of 7 second waves

Part three Refraction of 10 second waves

Part four Refraction of 15 second waves

part one

Refraction analysis

Introduction

In the preliminary report some refraction diagrams were presented. These are diagrams of 7, 10 and 15 seconds. Although refraction is important on the Bengkulu coast, it is difficult to describe its effect accurately, because of the irregular shape of the coastline. Analytical computations are only possible for a straight coast with parallel depth contours, so other methods have to be applied to achieve a result.

The graphical method

The refraction diagrams presented in the preliminary report were made with the graphical method, as described in the Shore Protection Manual (US Army 1973, vol I, pp 268-275). The advantage of this method is that it allows to get an idea of the refraction pattern with very simple means, and also that problems with singularities are solved by interpolating on a visual way. Small shoals and channels do not influence the refraction pattern, which is very realistic. Further the process is controlled with every step, because it is easy to see when the process goes wrong. A disadvantage is that its accuracy is small on a small scale map, and that it takes a lot of work when many rays are needed.

The numerical method

At the fluid mechanics group of this department a computer program for ray refraction calculation was developed by K. Popp and extended by N. Booij (Popp & Booij, 1977). With this program it is possible to carry out many refraction calculations for a certain area without time consuming procedures. When a detailed depth-matrix is made, the computer can draw charts with depth contours, and draw on these charts the required wave rays. Also the imported wave data along a ray are printed out (direction, celerity, wave length).

With this program refraction was analysed for the Bengkulu area. Two depth matrices were made for these calculations. A 40 x 23 matrix with a mesh-size of 2619 km was made from data of the British hydrographic charts 2780 and 2781. A 33 x 38 matrix with mesh-sizes of 654.8 km was made from the Dutch hydrographic chart "Vaarwaters naar Benkoelen"

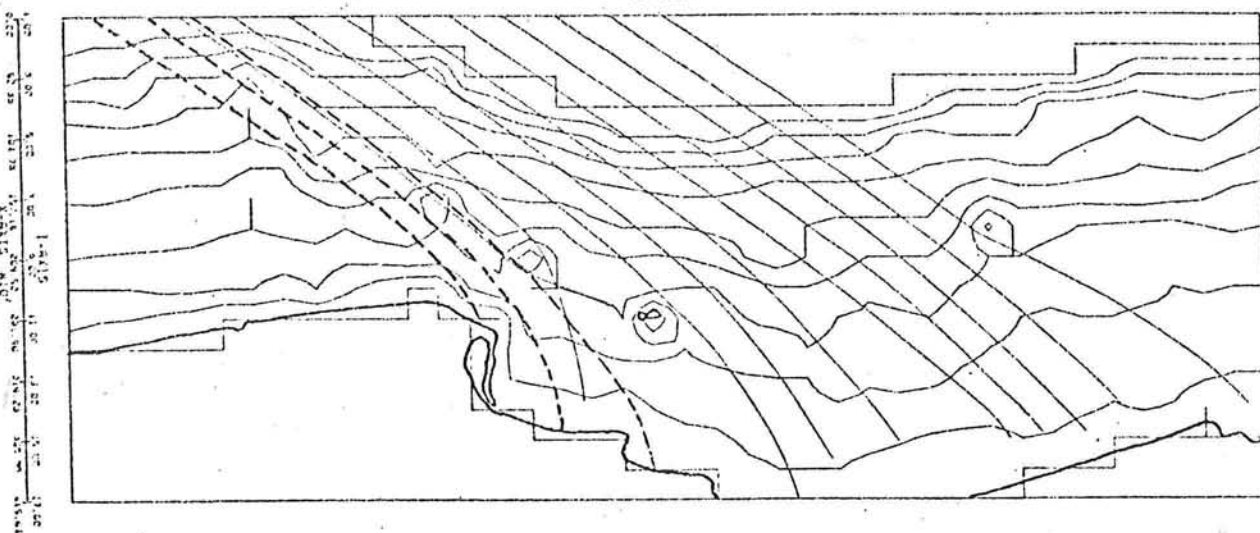
(1918-1919). More recent sounding data are not available at this moment. The small scale refraction calculation (on a chart with scale 1:500 000) serves as a boundary calculation for the large scale calculation (1:50 000). As could be expected this is only important for the 15 second waves, because the 7 and 10 second waves are not refracted beyond the 50 m depth contour.

This small scale matrix is also used for a check of the computer program. On the same scale as in the preliminary report four directions of 10 second waves were calculated. The results are presented in fig. 1 and fig. 2 [#]. As can be seen the differences are small, so the computer program is reliable in cases when no channels or reefs have to be passed.

Because of reproduction the charts presented in this report are scaled down.

[#] The upper and the lower horizontal lines of the frame of these figures are parallel, although because of an optical effect it seems not to be so. The effect is very clear in the lower figure of fig. 1.

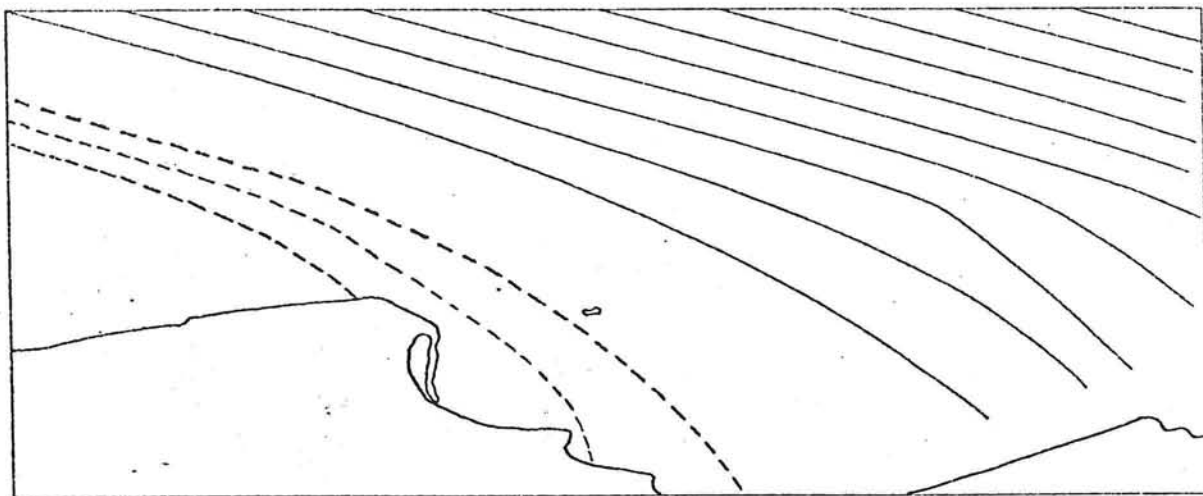
4.02 32.32 48.72 52.08 203.52 21.32 58.21 325.52 31.31 35.32 31.32 31.32 31.32 31.32 31.32 31.32 31.32 31.32 31.32 31.32 31.32



$w=0.63$

$W=0.00$

$T=10.00$



$w=0.63$

$W=0.00$

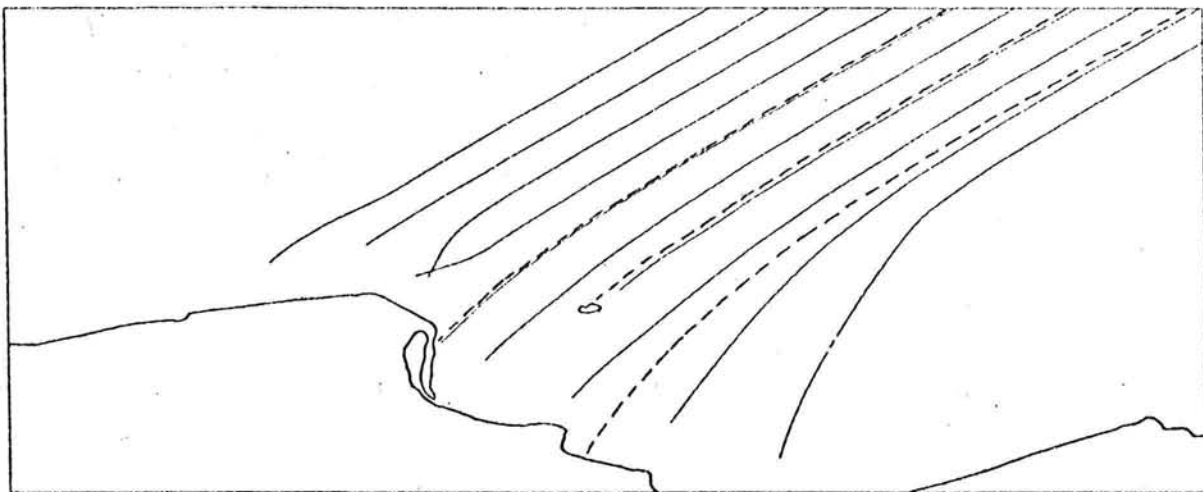
$T=10.00$

— computer calculation
- - - graphical method

Comparision of the graphical and the numerical method to determine wave rays.

Periods of 10 seconds, waves from 170° and 150° (cf. fig. 3-12 in the preliminary report)

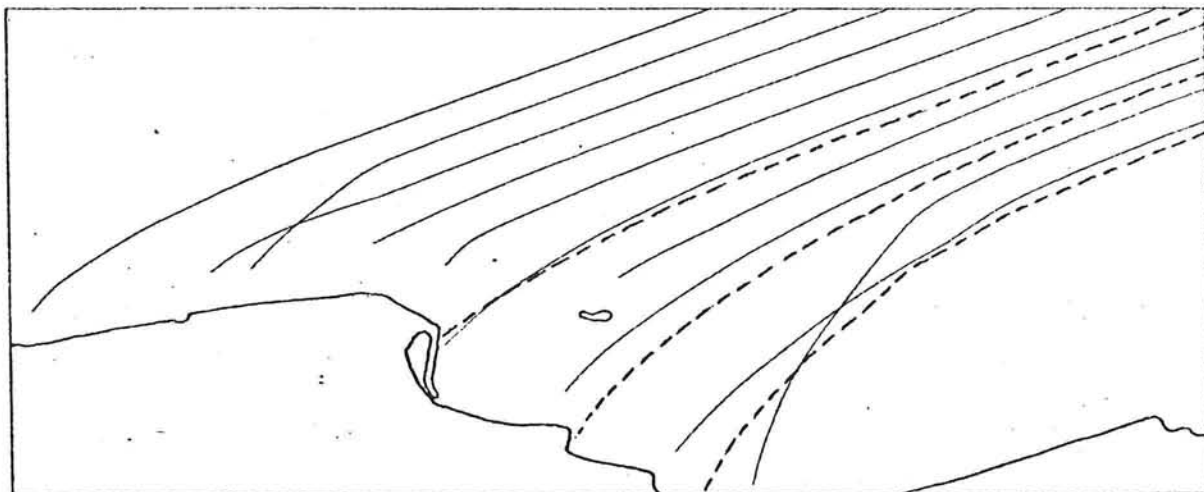
fig. 1.



$w = 0.63$

$N = 0.00$

$T = 10.00$



$w = 0.63$

$N = 0.00$

$T = 10.00$

— computer calculation
- - - graphical method

Comparision of the graphical method and the numerical method to determine wave rays.

Periods of 10 seconds, waves of 285° and 295° (cf. fig. 3-12 in the preliminary report)

fig.2.

The lens effect

In areas with channels and reefs the program is inaccurate in so far that the single drawn wave rays are not representative for a wave situation. The main problem is that the program calculates one ray at a time, applying Snell's law, but is not taking into account that the energy between two rays has to be constant. So when two rays cross each other all the energy is forced into one single point. This is physically impossible.

The wave energy in cross-section A (see fig. 3) is $\frac{1}{8} \rho g H_A^2 b$. In cross-

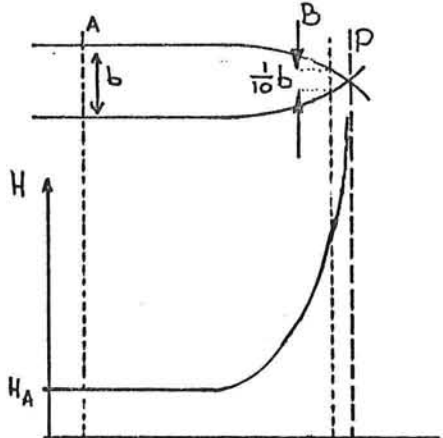


fig. 3.

section B this energy has to be the same, hence:

$$\frac{1}{8} \rho g H_A^2 b = \frac{1}{8} \rho g H_B^2 \frac{1}{10} b$$

$$\text{Hence: } H_A^2 = \frac{1}{10} H_B^2$$

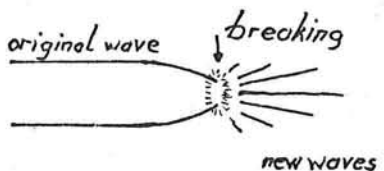
$$H_B = \sqrt{10} H_A$$

In P the wave height becomes infinite, due to the fact that the distance between the wave rays becomes zero.

Of course such a wave will break, as a result of its steepness. After breaking the waves will continue, probably with a shorter period and in several directions but a major part of the energy will continue in the original direction.

These shorter waves have a total different refraction pattern, but will be no longer important for sand transport calculations, because of the small heights of these

fig. 4.



waves (energy is small in comparison with the original 10 second waves). The above mentioned effect occurs specially in the neighbourhood of almost circular reefs. It is comparable with the focussing of light by a lens, therefore it is called the lens effect. Because of this lens effect behind reefs waves might be very steep and high.

The effect is very clear at the Lebar reef. As can be seen on the refraction diagrams wave rays are always crossing each other on this reef. (Because of the special form of this reef crossing mostly occurs on the shallowest point of it). Hence the Lebar reef will nearly always be marked by breaking waves, without regard of their original direction.

This is confirmed by the British admiralty pilot (Admiralty, Malacca Strait Pilot, 1971): "Lebar reef, with a depth of 19 feet (5m8) over it, lies about 3½ miles west-south-westward of Tanjung Kerbau. This reef is nearly always marked by breakers." (p.374). Because this reef has a depth of about 6 meters over it, breaking as a result of shallow water is only possible for waves of 4 meters and more. Fortunately these waves seldom occur in the Bengkulu area.

Another type of ray crossings is sketched in adjacent figure. This

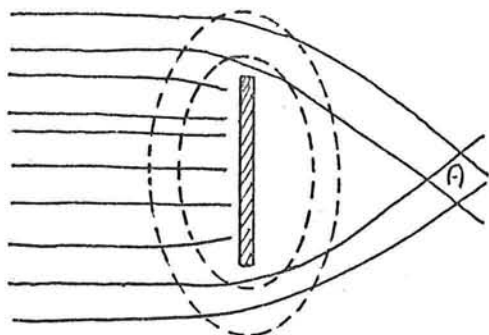


fig. 5.

situation is physically possible. In the area A behind the barrier waves come from two directions (so called "cross-swell"). The maximum wave height in such an area is two times the normal wave height, but $\bar{\eta}$ is only $\sqrt{2}$ - times the normal $\bar{\eta}$ ($\bar{\eta}$ is the time-average of the difference between the momentaneous water level and the still water, without regard of its sign).

When the incoming waves are monochromatic in A, a regular pattern appears, but when the incoming waves have a wide spectrum, this wave pattern becomes very complicated. This type of ray crossings is also very difficult for normal navigation.

In the Bengkulu area it is possible that two or three wave systems from different directions occur at the same time, e.g. swell from SW and monsoon waves from NW. These wave-systems already give a pattern of cross-swell, and when this pattern is refracted the surface of the sea will be very irregular. Loading and unloading of ships is nearly impossible, even with rather low waves.

Hence roadstead and harbour entrances should never be planned in such areas. Although on a superficial view the presence of reefs before a roadstead or an harbour entrance seems to provide calm water, this is not necessaraly true.

As can be seen on the refraction diagrams this occurs in the area in front of the Bengkulu harbour, in particular when SW swell as well as NW monsoon waves occur at the same time, viz. in December-February. In this case the Pata Sambilan is one of the lenses which deteriorates the situation. Therefore one may expect that loading and unloading on the existing Bengkulu roadstead will be difficult in the period from

December until January, in spite of rather low waves. This conclusion is confirmed by local observation of several visitors.

Interpretation of the refraction diagrams

The computer program does not take any care of breaking and wave rays do cross each other frequently. After such a crossing the wave ray might be only theoretical (in case of ground swell wave rays will not pass the crossing, in case of cross swell however they will). For these reasons the computer drawn refraction diagrams have to be interpreted with care; they do not necessarily represent the real refraction, even not in case of monochromatic waves. Therefore it is not allowed to estimate the refraction coefficient (K_r) at the coast by simple measurement of the distance between two adjacent waverays. At first it has to be determined if these wave rays do reach the coast. The same problem plays also a rôle with the determination of the angle of incidence (ϕ_{br}) of the waves at the breakerline.

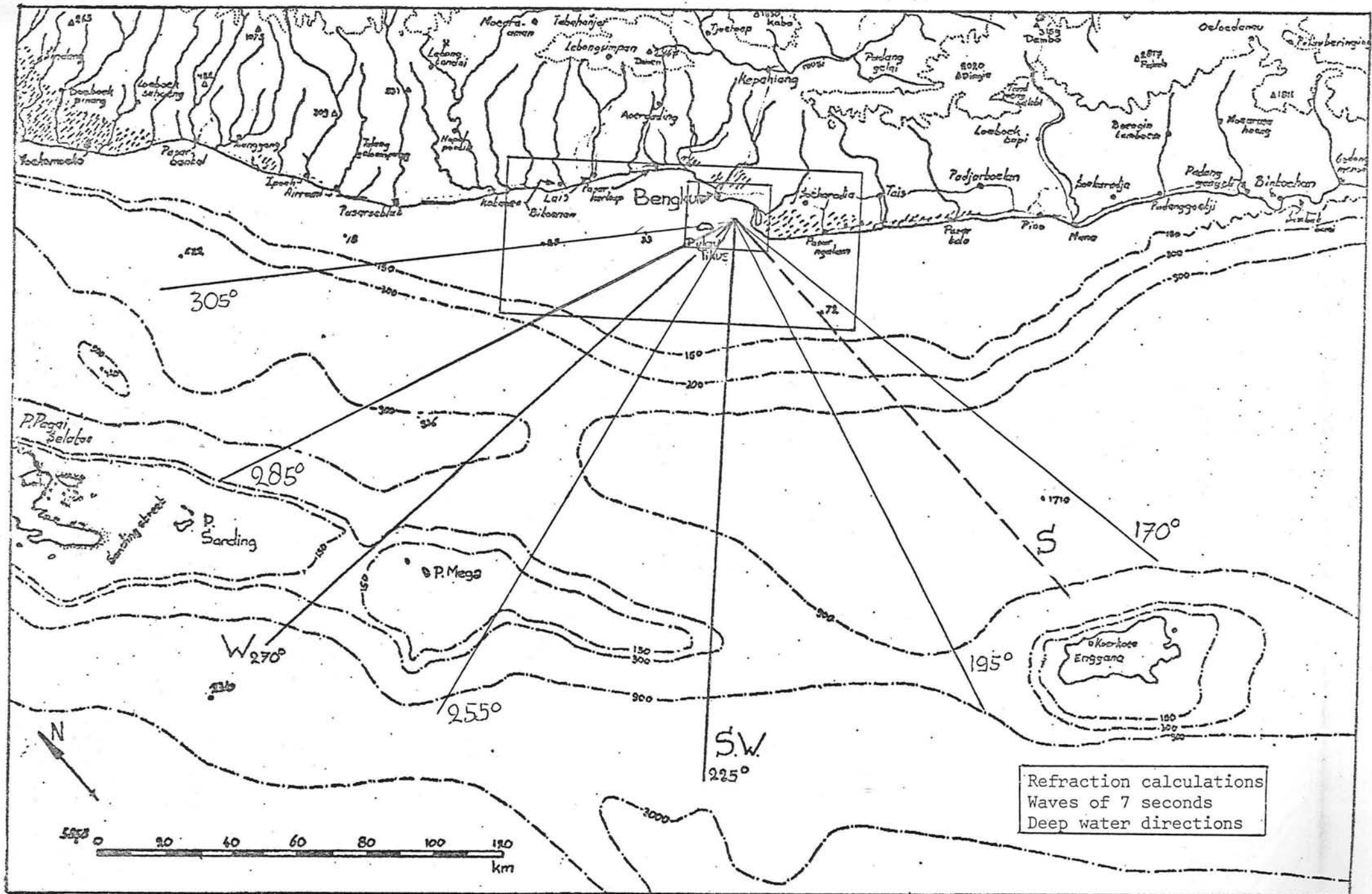
Wave periods

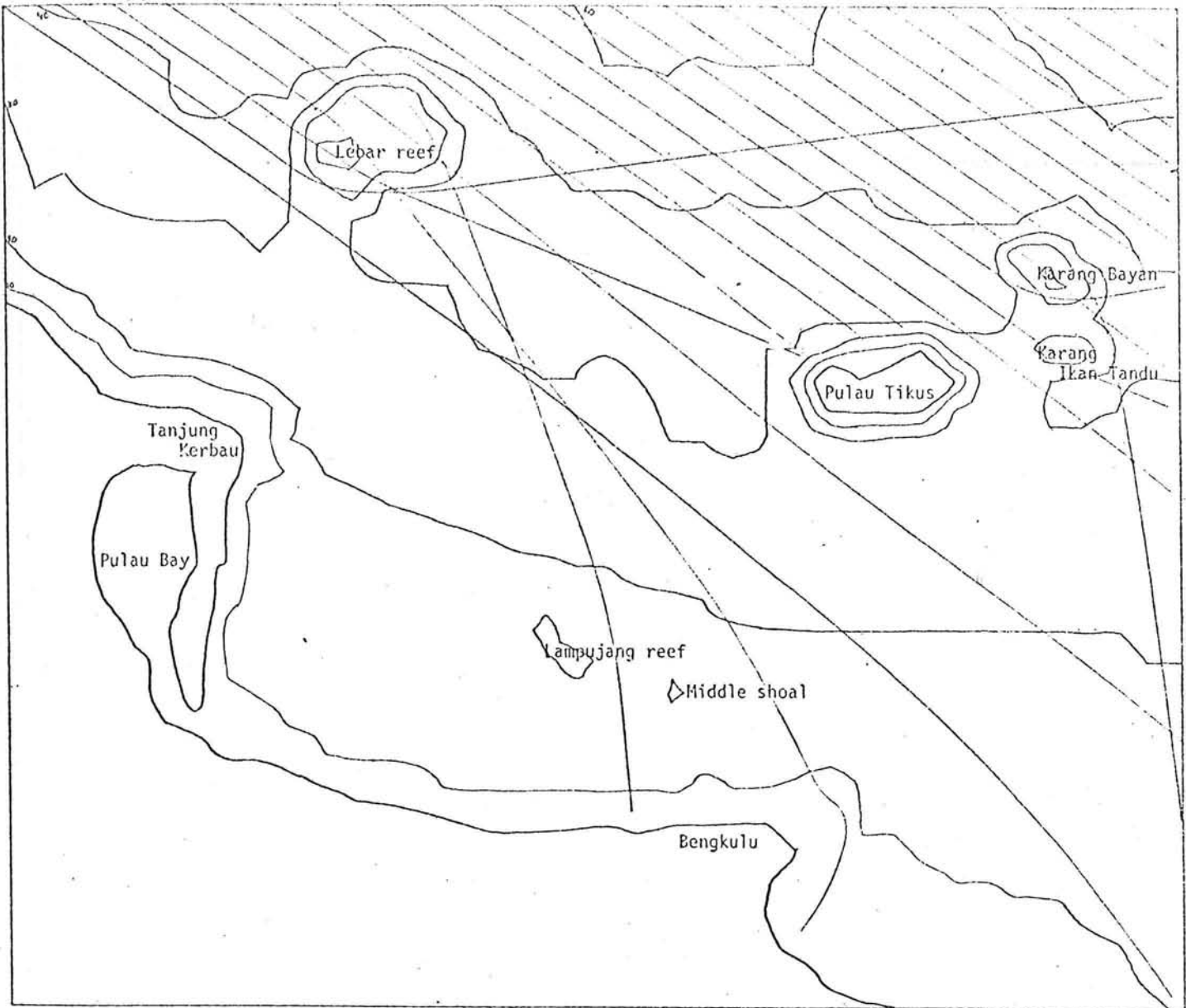
As indicated refraction calculations were carried out for waves with periods of 7, 10 and 15 seconds. This is done because these periods represent the three groups of wave types in the Bengkulu area. Of course waves are not monochromatic in reality, especially not the monsoon and the diurnal waves (10 and 7 seconds) and a spectral approach should have been made.

But because refraction calculations with spectral components is very complicated, and on the other hand not sufficient reliable wave data are available to determine a spectrum, it is not appropriate to make a spectral approach.

Interpreting the refraction diagrams one should keep in mind that periods will vary somewhat in reality, which may have a large influence, in particular when the radius of curvature of the wave rays is small.

part two





$\mu = 0.90$

$W = 0.00$

$T = 7.00$

$A = 55.$

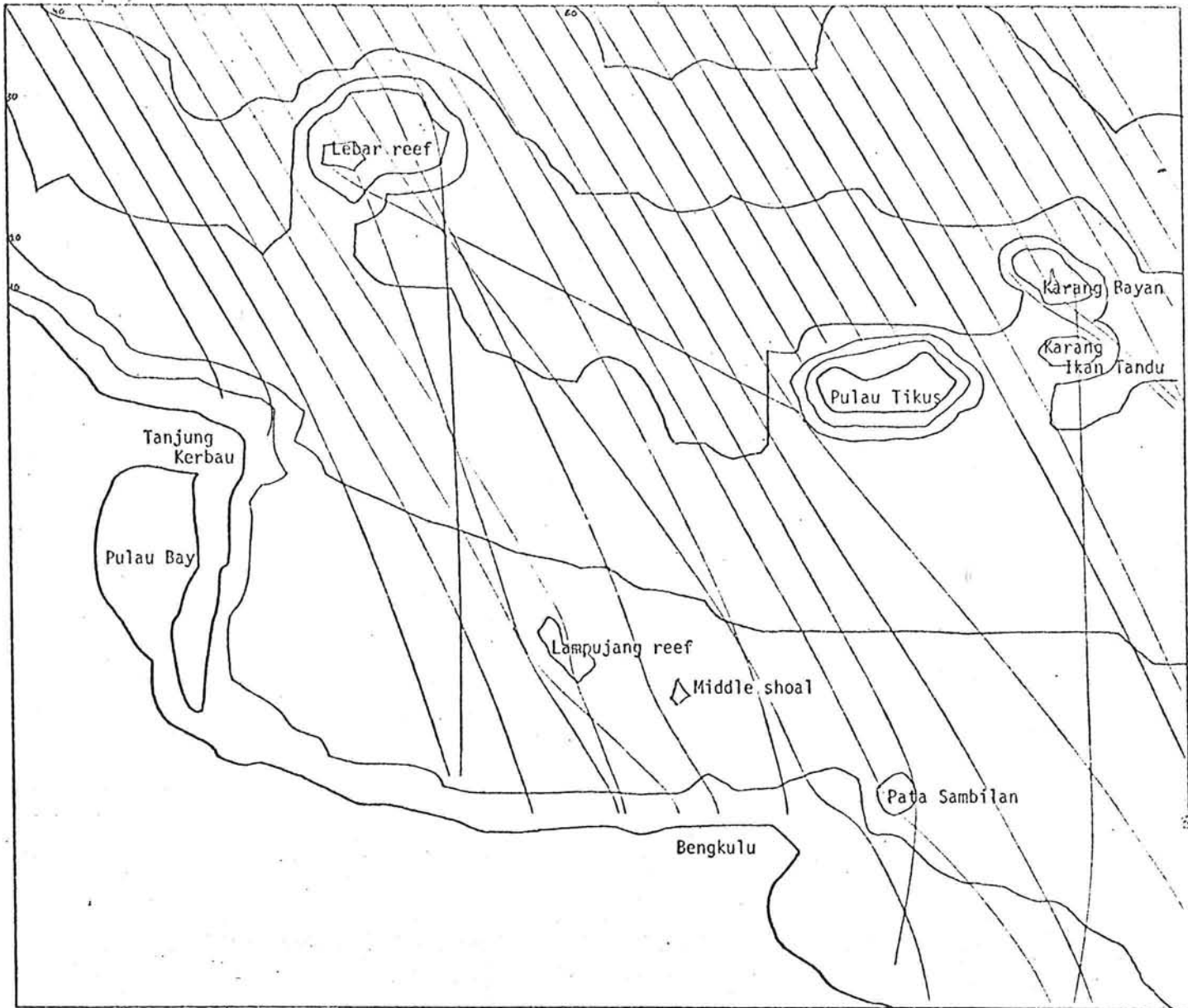
Refraction diagram

Wave period 7 seconds

Direction of the incoming waves 170°



DELFT UNIVERSITY OF TECHNOLOGY
Dept. of civil engineering
Coastal engineering group
-- BENGKULU HARBOUR PROJECT --



$w=0.90$

$W=0.00$

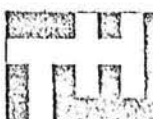
$T=7.00$

$A=30.$

Refraction diagram

Wave period 7 seconds

Direction of the incoming wave 195°



DELFT UNIVERSITY OF TECHNOLOGY
Dept. of civil engineering
Coastal engineering group
-- BENGKULU HARBOUR PROJECT --



$v=0.90$

$W=0.00$

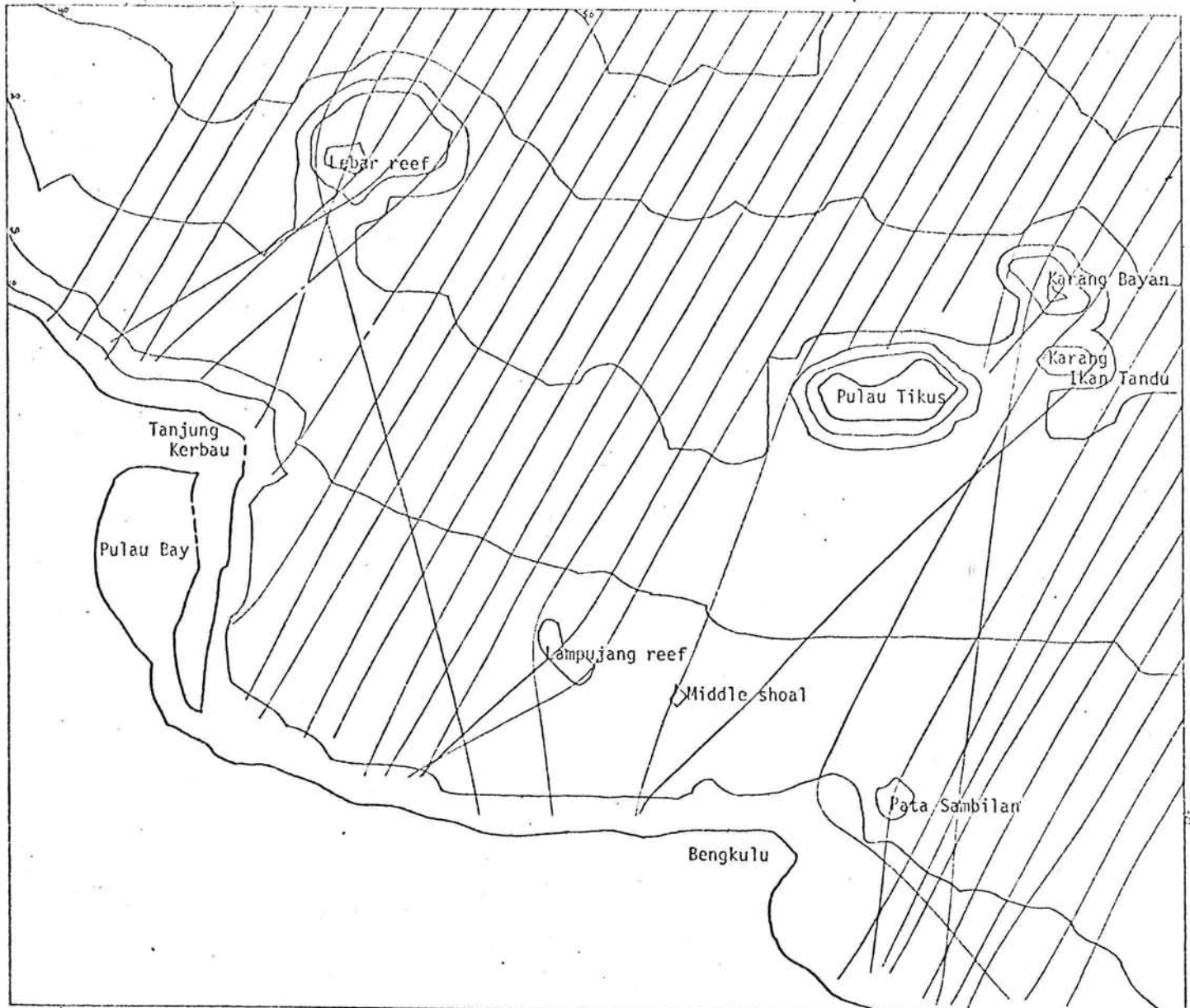
$T=7.00$

$\theta=0.$

Refraction diagram

Wave period 7 seconds

Direction of the incoming wave 225°



$v=0.90$

$W=0.00$

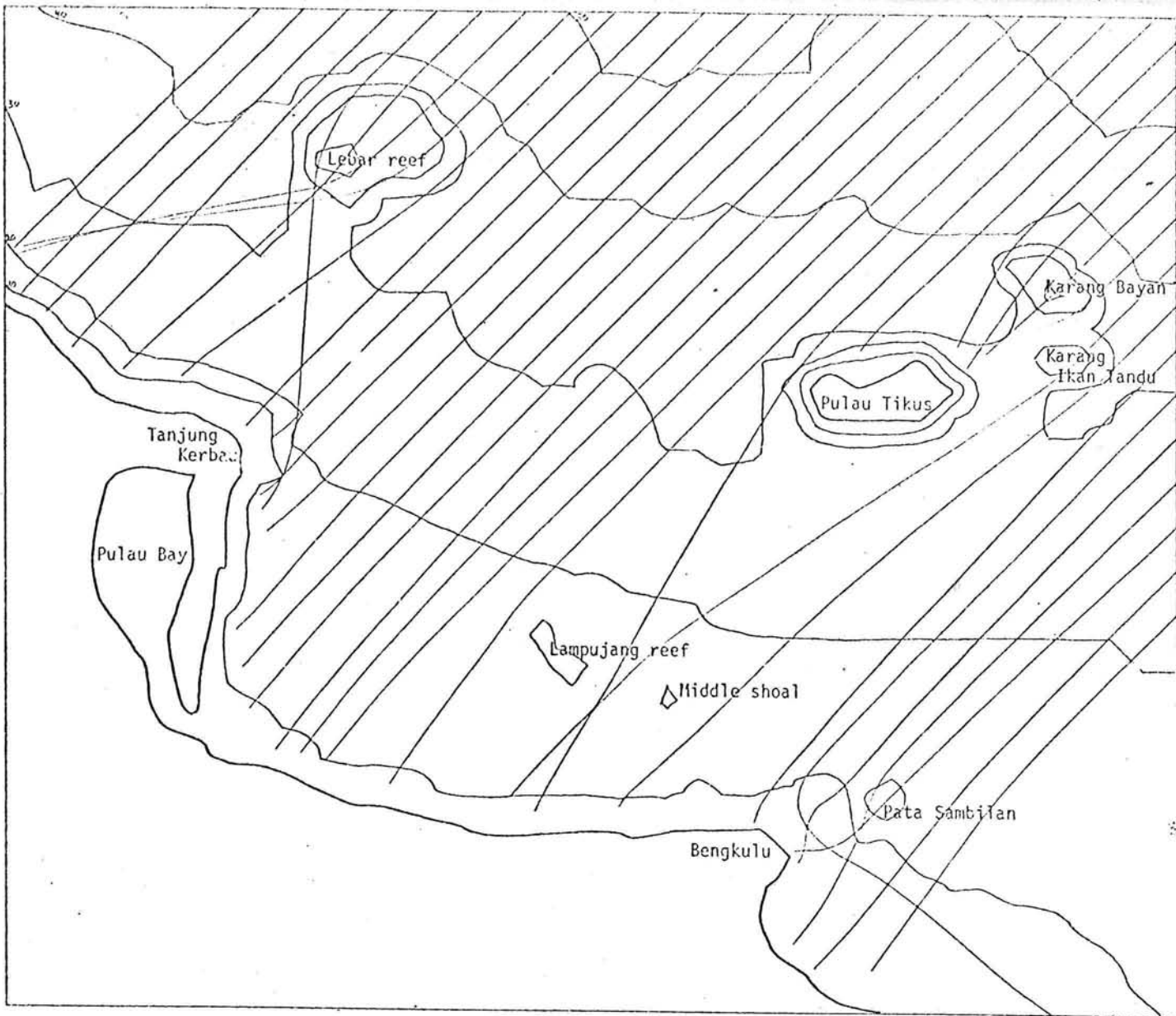
$T=7.00$

$\alpha=330.$

Refraction diagram

Wave period 7 seconds

Direction of the incoming wave 255°



$w=0.90$

$W=0.00$

$T=7.00$

$R=315.$

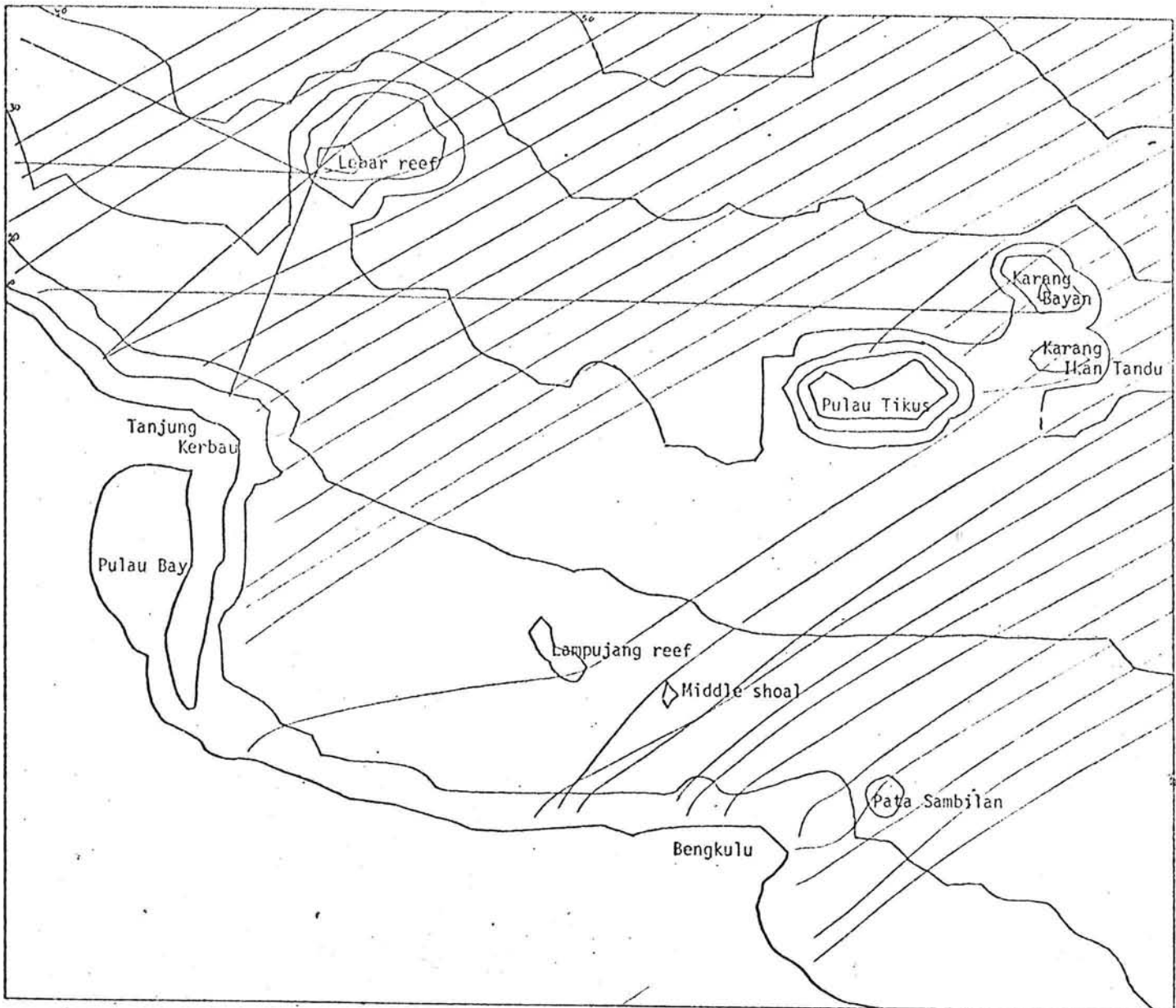
Refraction diagram

Wave period 7 seconds

Direction of the incoming wave 270°



DELTU
Delft University of Technology
Dept. of civil engineering
Coastal engineering group
-- BENGKULU HARBOUR PROJECT --



$\nu = 0.90$

$W = 0.00$

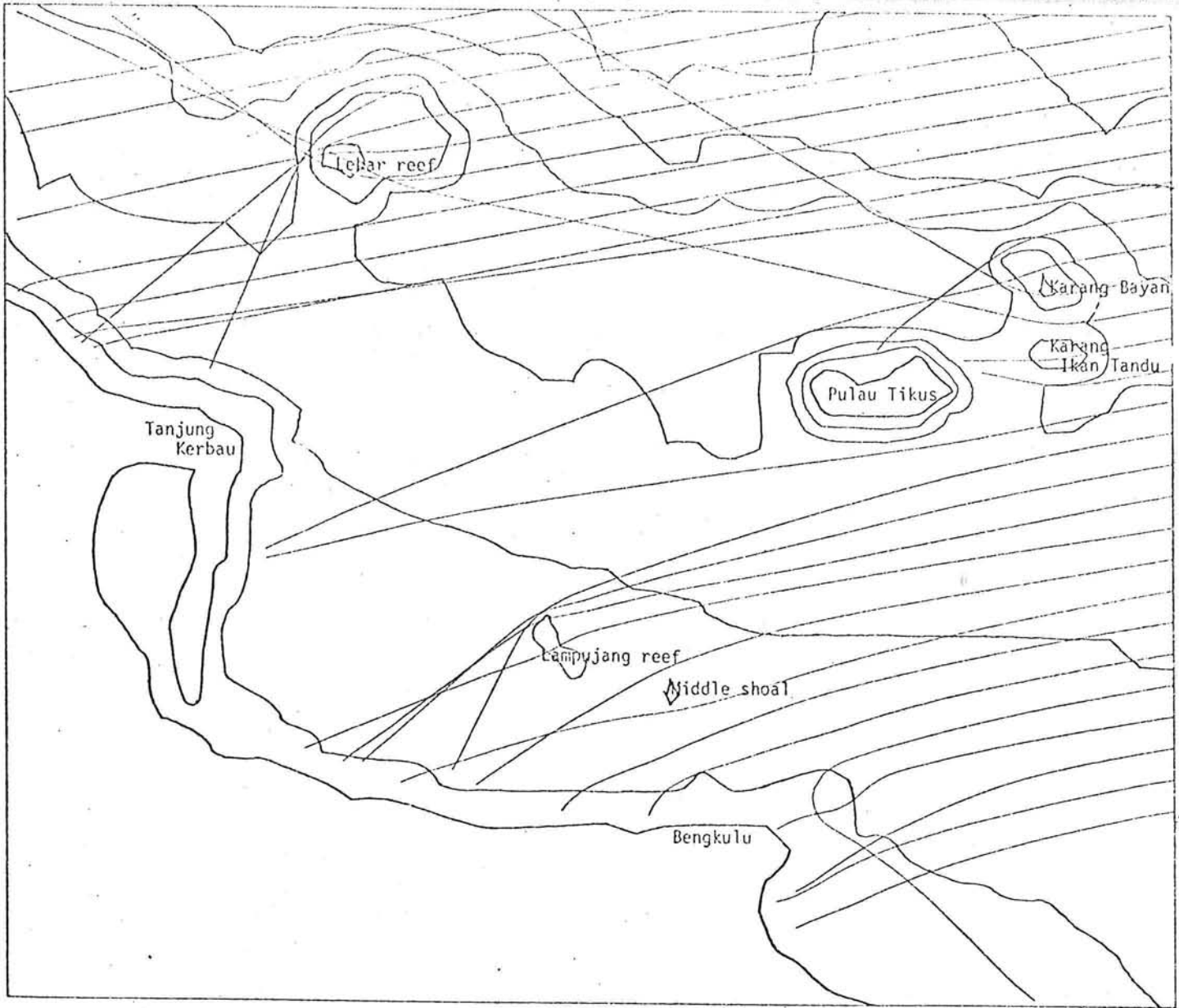
$T = 7.00$

$R = 300.$

Refraction diagram

Wave period 7 seconds

Direction of the incoming wave 285°



$w=0.90$

$W=0.00$

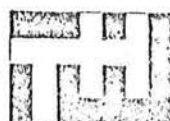
$T=7.00$

$\lambda=280.$

Refraction diagram

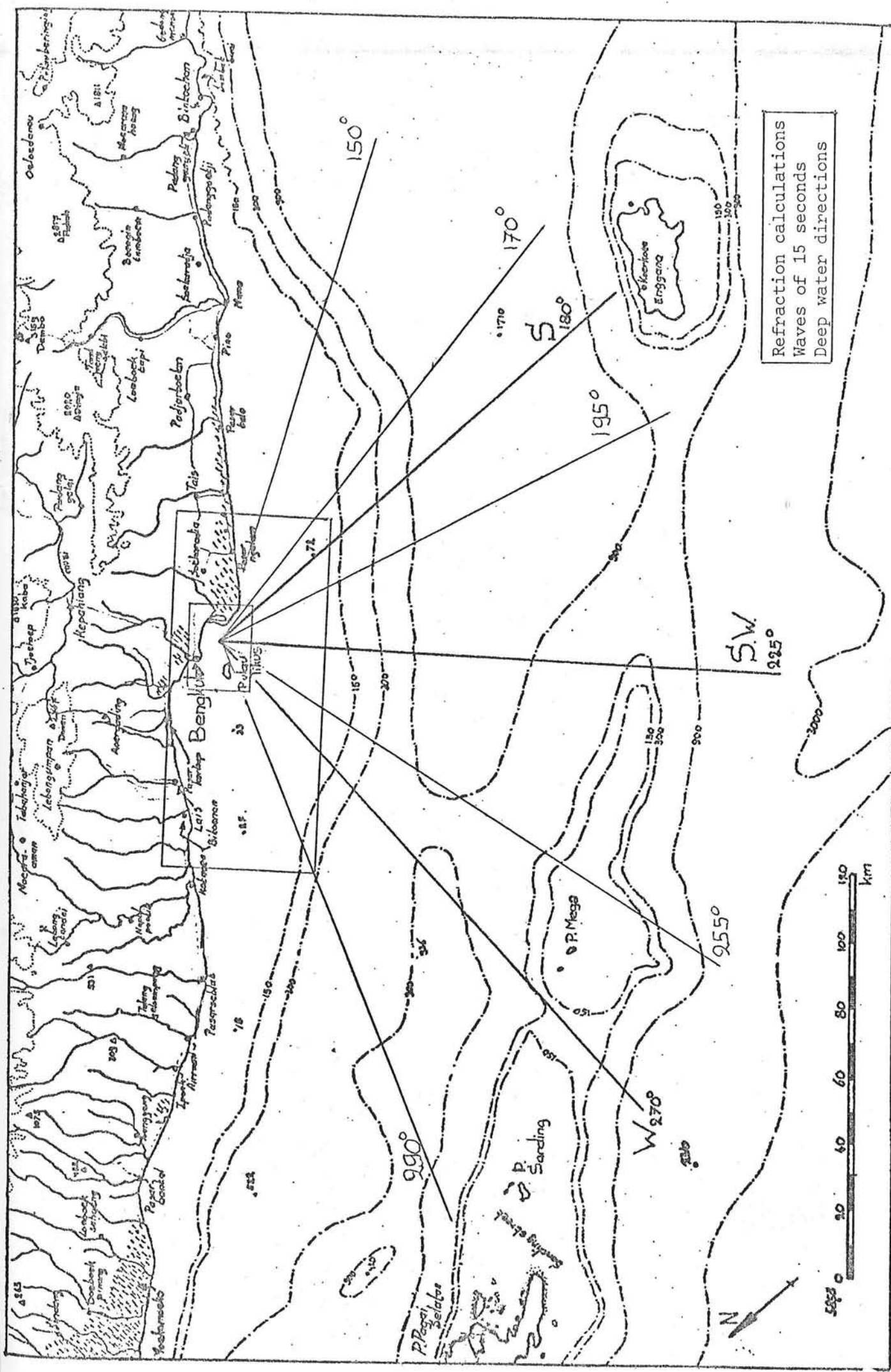
Wave period 7 seconds

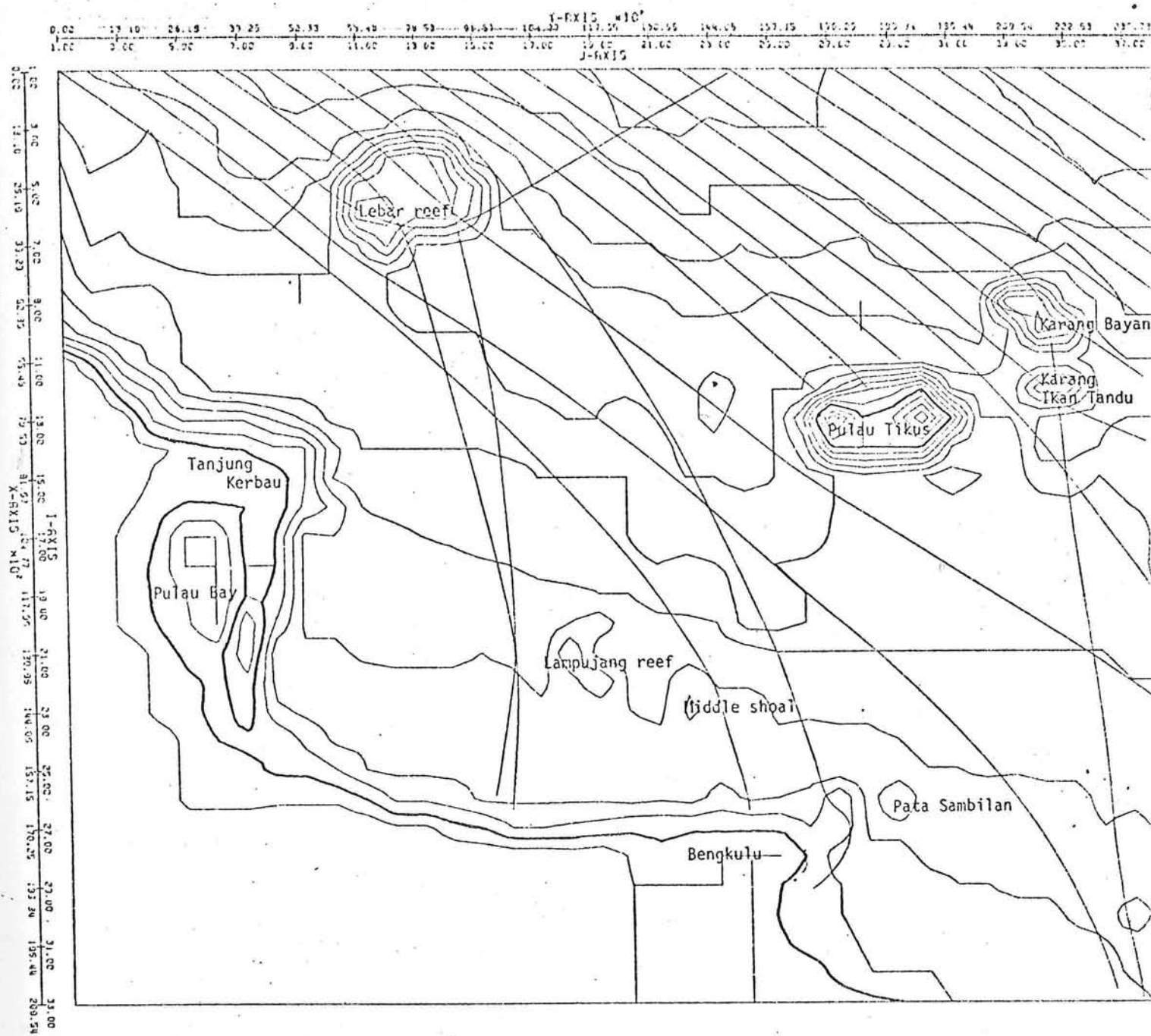
Direction of the incoming wave 305°



DELFT UNIVERSITY OF TECHNOLOGY
Dept of civil engineering
Coastal engineering group
-- BENGKULU HARBOUR PROJECT --

part three





w = 0.63

W = 0.00

T = 10.00

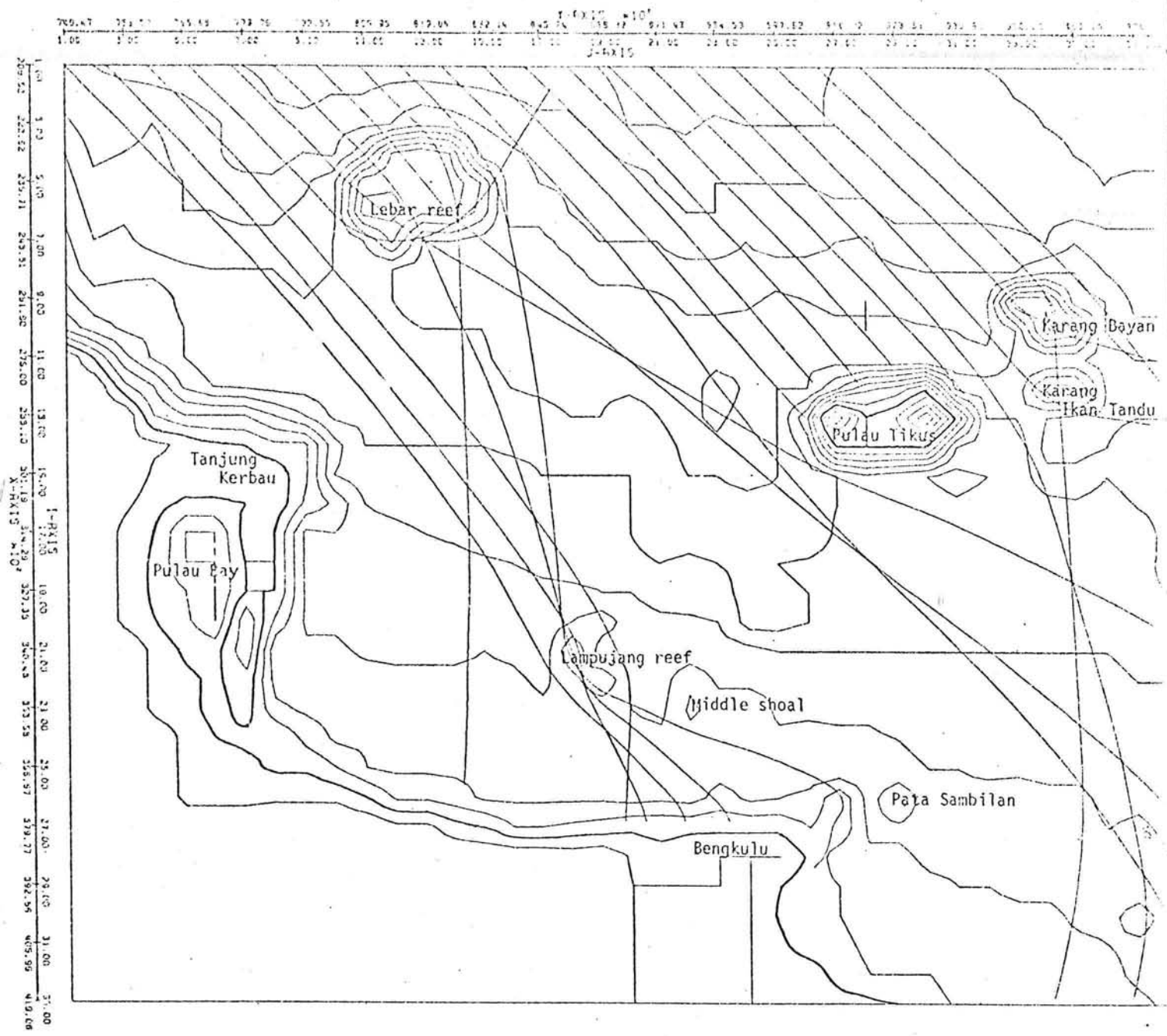
S = 0.30

A = 2.52

Refraction diagram

Wave period 10 seconds

Direction of the incoming waves 170°



$w = 0.63$

$W = 0.00$

$T = 10.00$

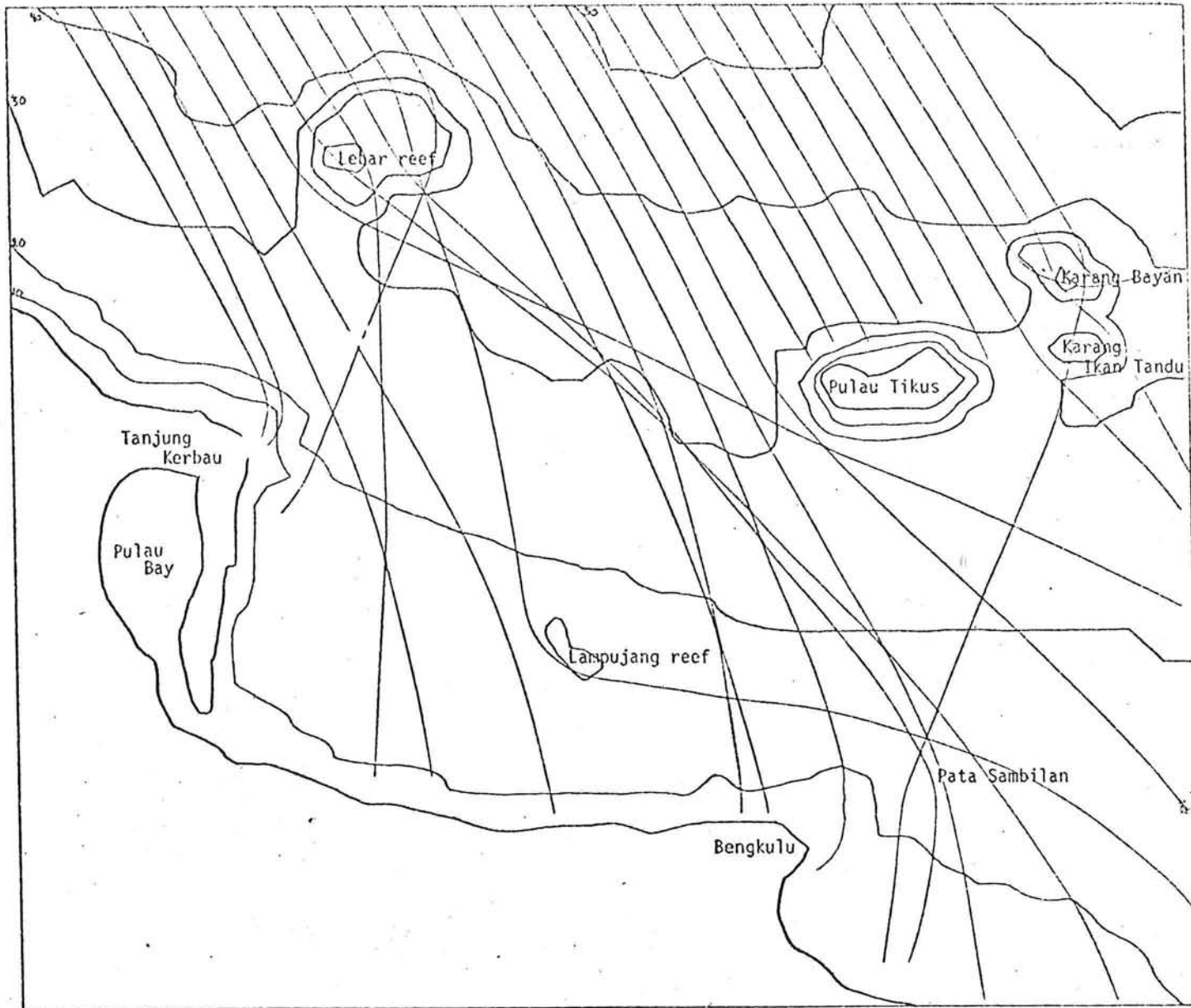
$S = 0.30$

$R = 2.52$

Refraction diagram

Wave period 10 seconds

Direction of the incoming waves 180°



$w = 0.63$

$W = 0.00$

$T = 10.00$

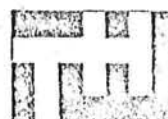
$S = 0.30$

$A = 2.52$

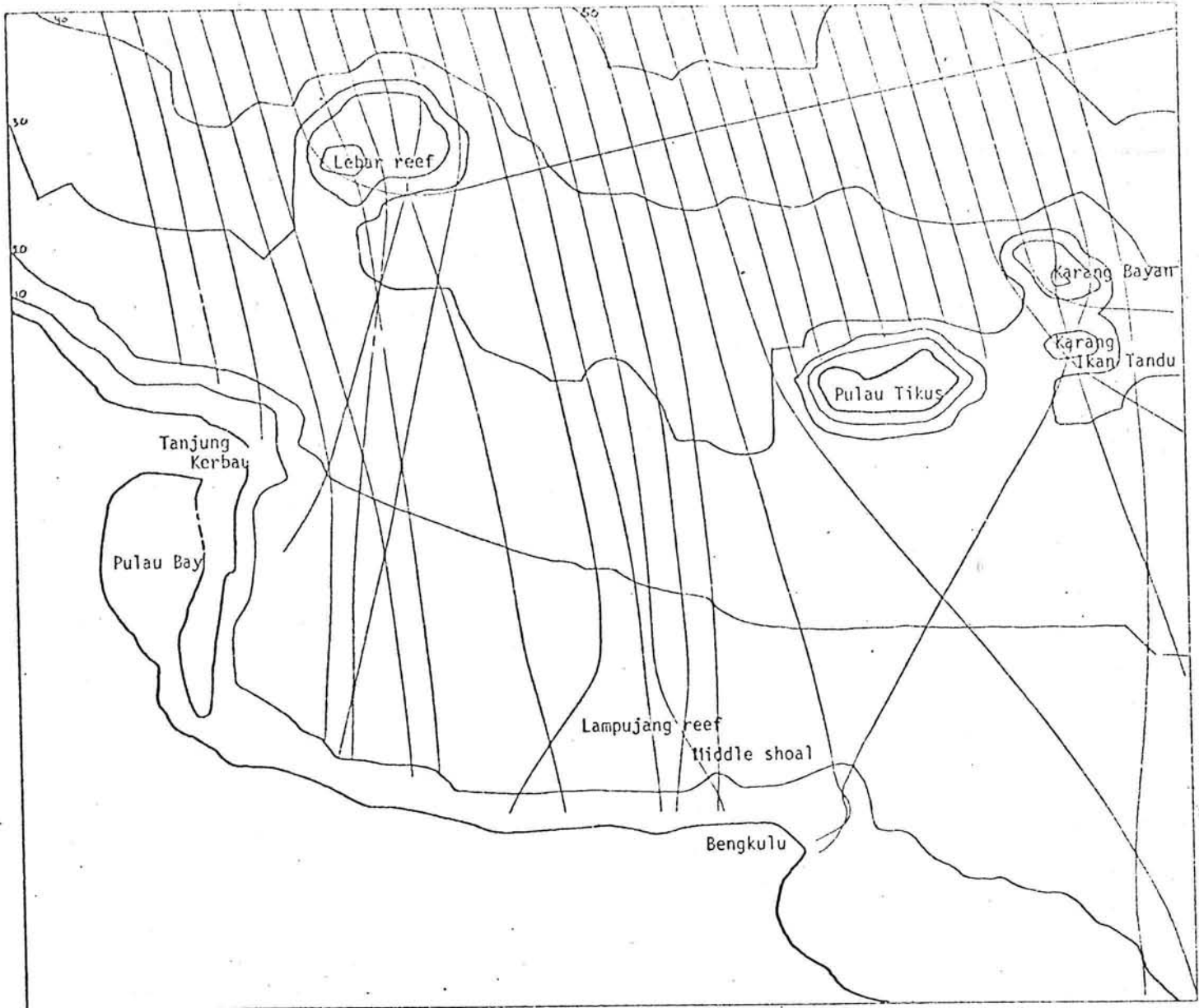
Refraction diagram

Wave period 10 seconds

Direction of the incoming waves 195°



DELTU UNIVERSITY OF TECHNOLOGY
Dept of civil engineering
Coastal engineering group
-- BENGKULU HARBOUR PROJECT --



$w=0.63$

$W=0.00$

$T=10.00$

$S=0.30$

$R=2.52$

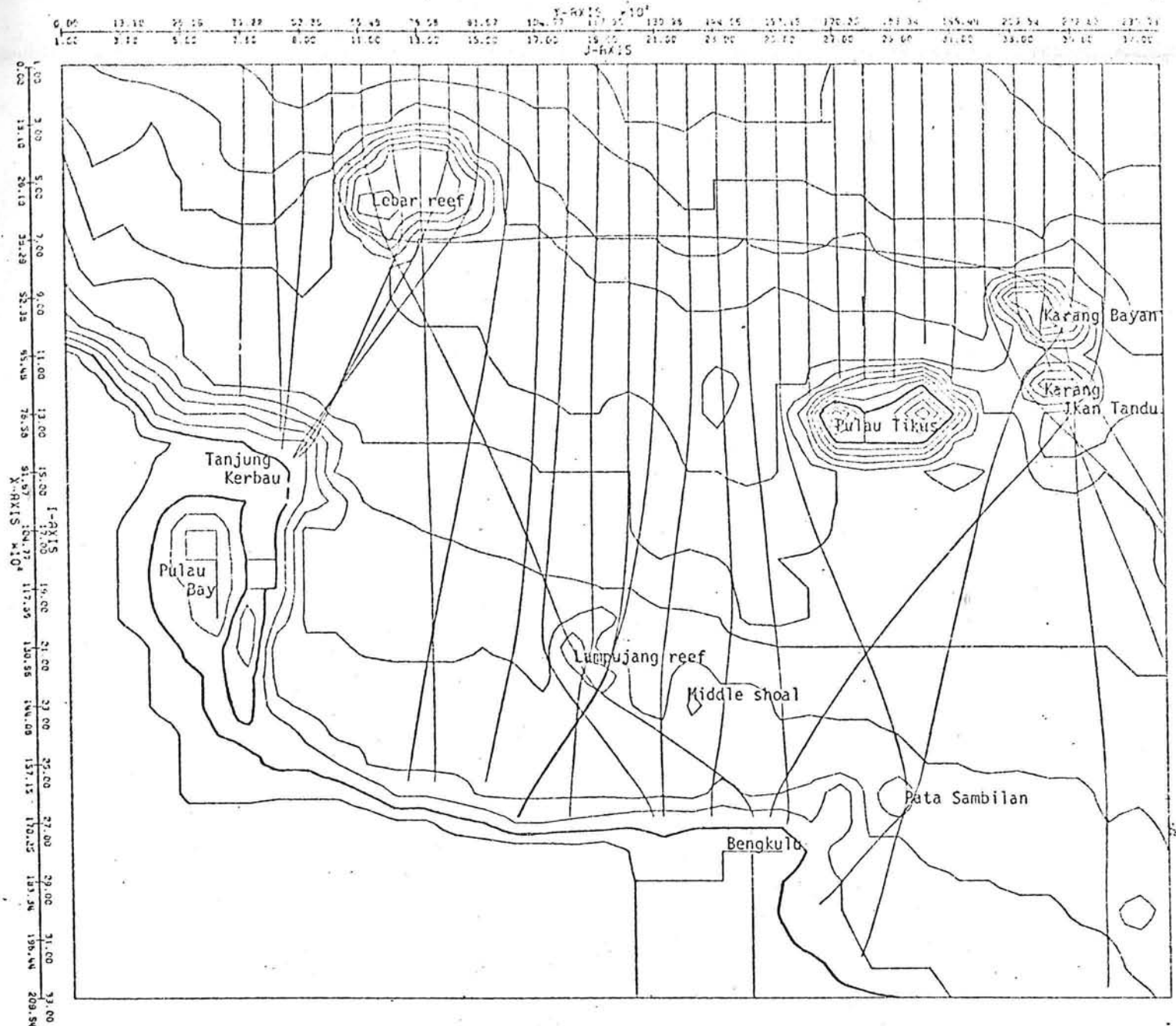
Refraction diagram

Wave period 10 seconds

Direction of the incoming waves 210°



DELTU
Delft University of Technology
Dept. of civil engineering
Coastal engineering group
-- BENGKULU HARBOUR PROJECT --



$$w = 0.63$$

$W=0.00$

T = 10.00

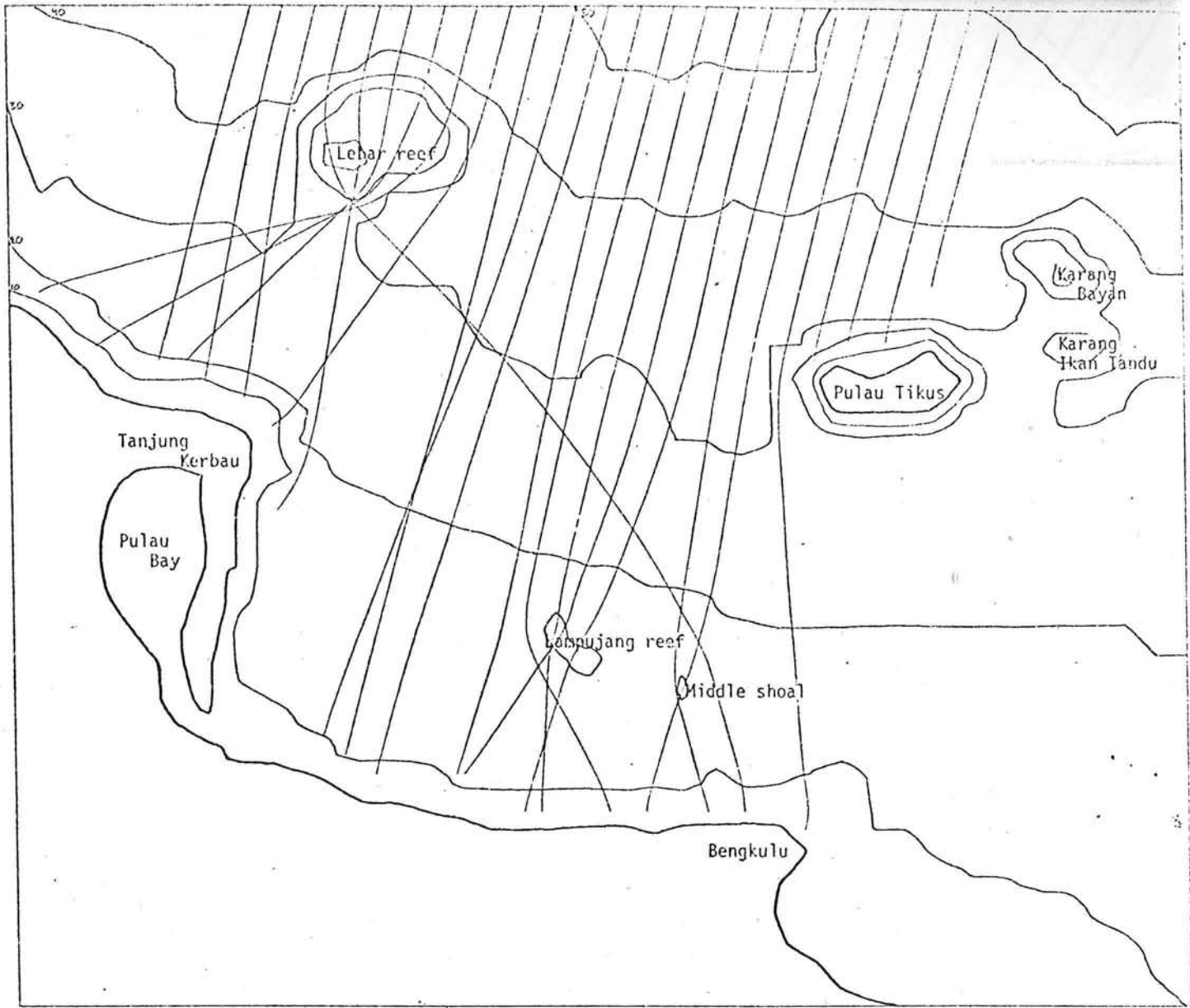
S=0.30

$$A=2.52$$

Refraction diagram

Wave period 10 seconds

Direction of the incoming waves 225°



$$w = 0.63$$

$W=0.00$

T = 10.00

S = 0.30

$$A=2.52$$

Refraction diagram

Wave period 10 seconds

Direction of the incoming waves 240°



$w = 0.63$

$W = 0.00$

$T = 10.00$

$S = 0.30$

$A = 2.52$

Refraction diagram

Wave period 10 seconds

Direction of the incoming waves 255°



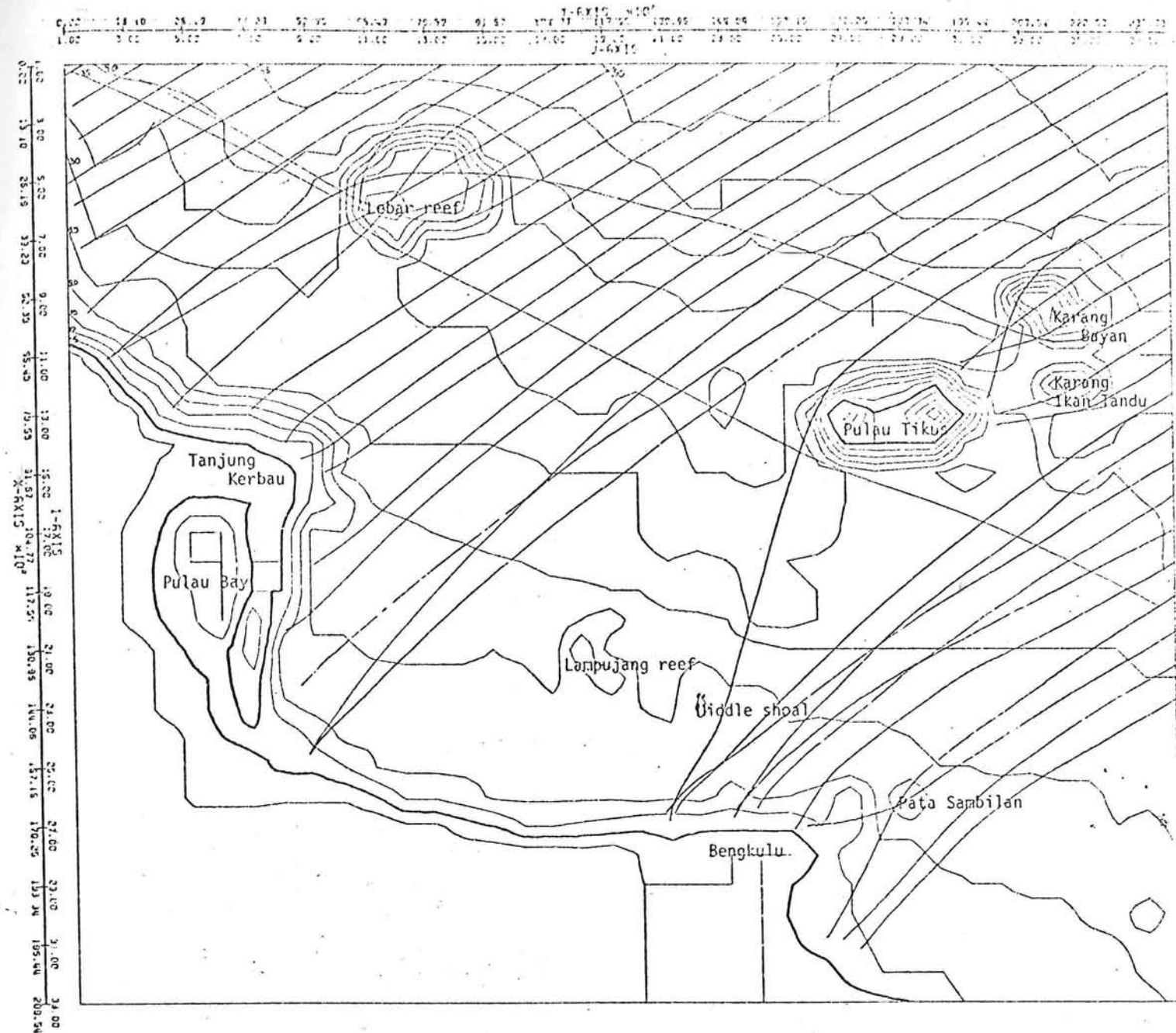
DELFT UNIVERSITY OF TECHNOLOGY
Dept of civil engineering
Coastal engineering group
-- BENGKULU HARBOUR PROJECT --



Refraction diagram

Wave period 10 seconds

Direction of the incoming waves 270°



$\alpha = 0.63$

$W = 0.00$

$T = 10.00$

$S = 0.30$

$A = 2.52$

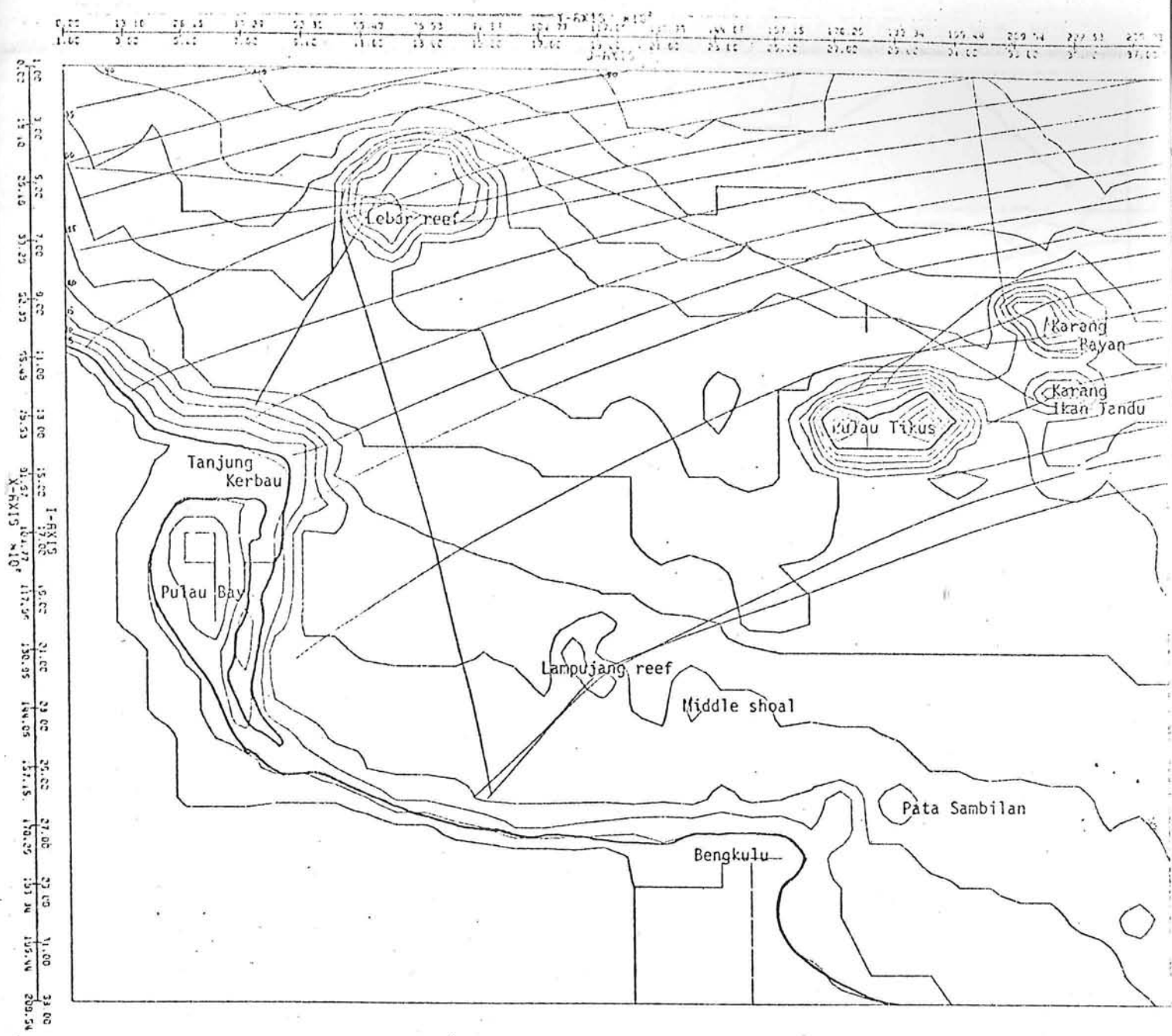
Refraction diagram

Wave period 10 seconds

Direction of the incoming waves 285°



DELFT UNIVERSITY OF TECHNOLOGY
Dept of civil engineering
Coastal engineering group
-- BENGKULU HARBOUR PROJECT --



$w = 0.63$

$W = 0.00$

$T = 10.00$

$S = 0.30$

$R = 2.52$

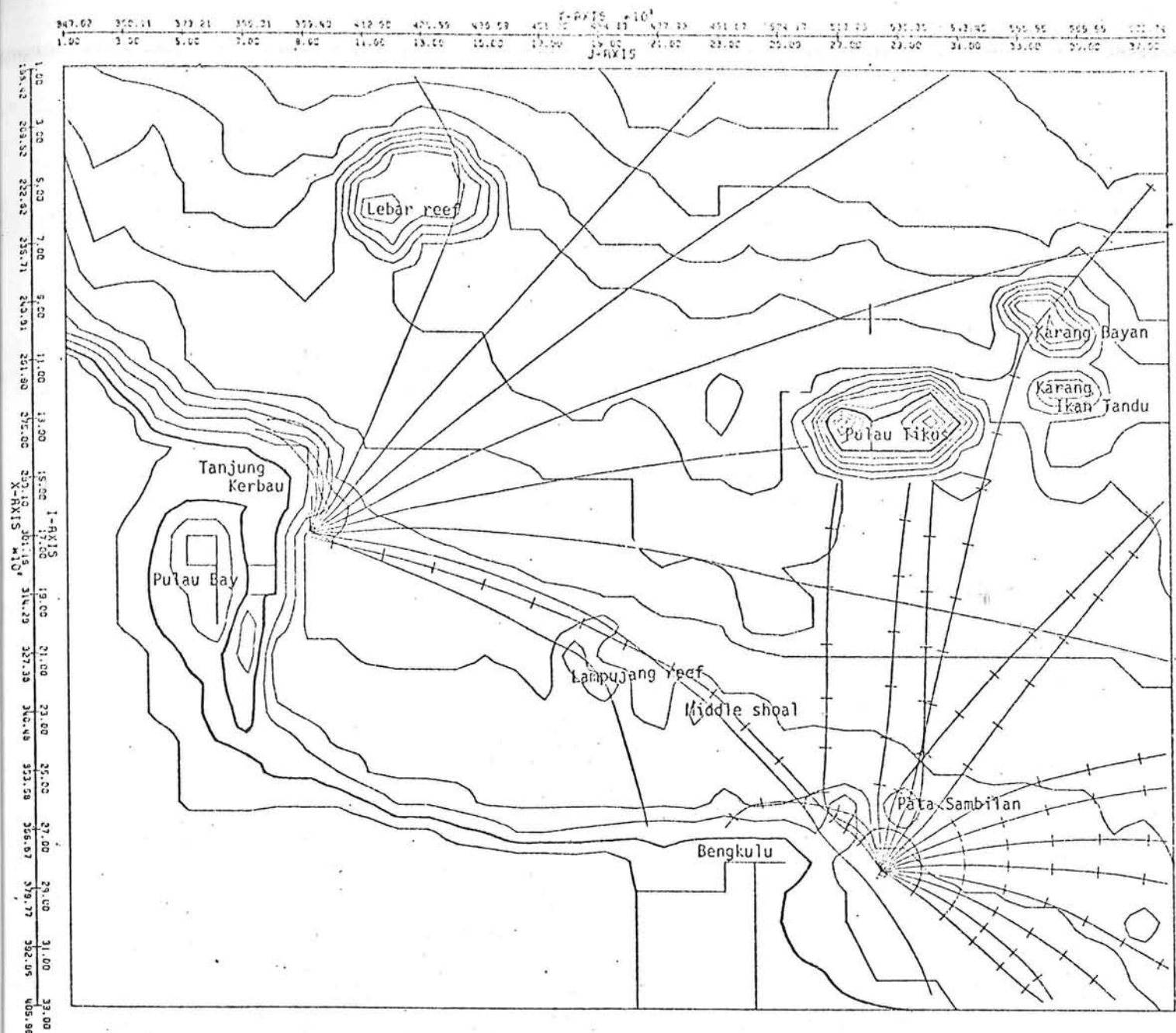
Refraction diagram

Wave period 10 seconds

Direction of the incoming waves 305°



DELFTE UNIVERSITY OF TECHNOLOGY
Dept. of civil engineering
Coastal engineering group
-- BENGKULU HARBOR PROJECT --



w = 0.63

$\bar{W} = 0.00$

T = 10.00

$$A=60^\circ$$

$w = 0.63$

$W = 0,00$

T=10,00

$\theta = 60^\circ$

Refraction diagram

Wave period 10 seconds

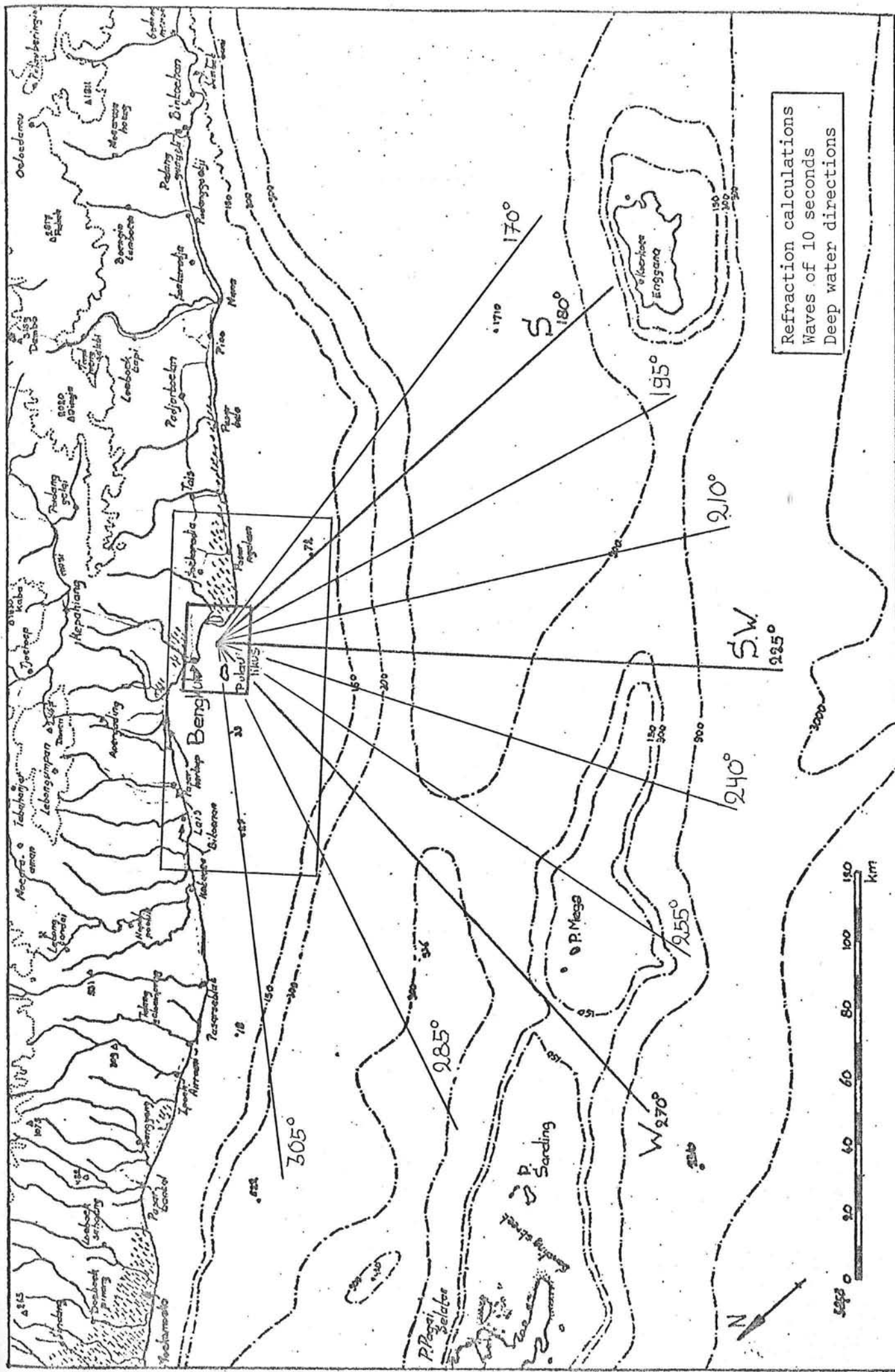
— waves refracted to Pulau Bay

— waves refracted to Bengkulu harbour

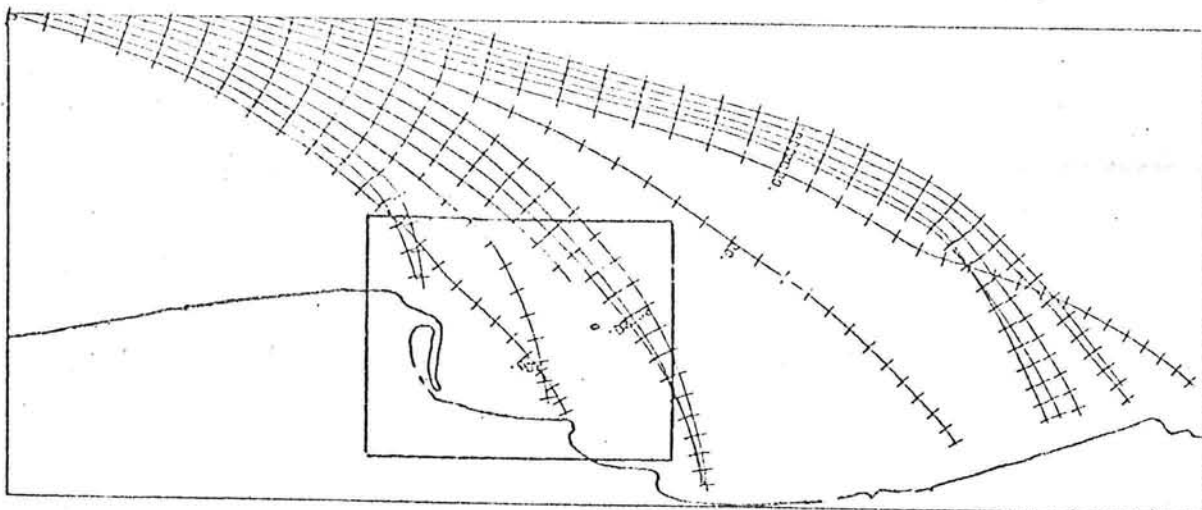


DELFT UNIVERSITY OF TECHNOLOGY
Dept of civil engineering
Coastal engineering group
-- BENGKULU HARBOUR PROJECT --

part four



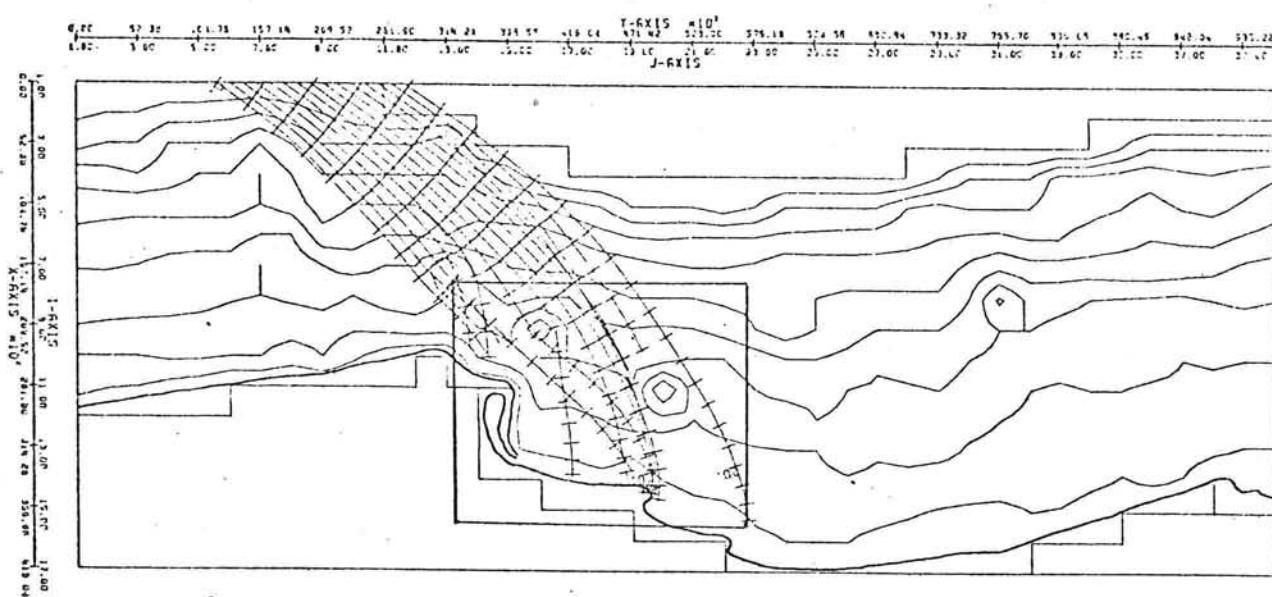
Refraction calculations
 Waves of 10 seconds
 Deep water directions



$w = 0.42$

$W = 0.00$

$T = 150$



$w = 0.42$

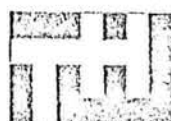
$W = 0.00$

$T = 150$

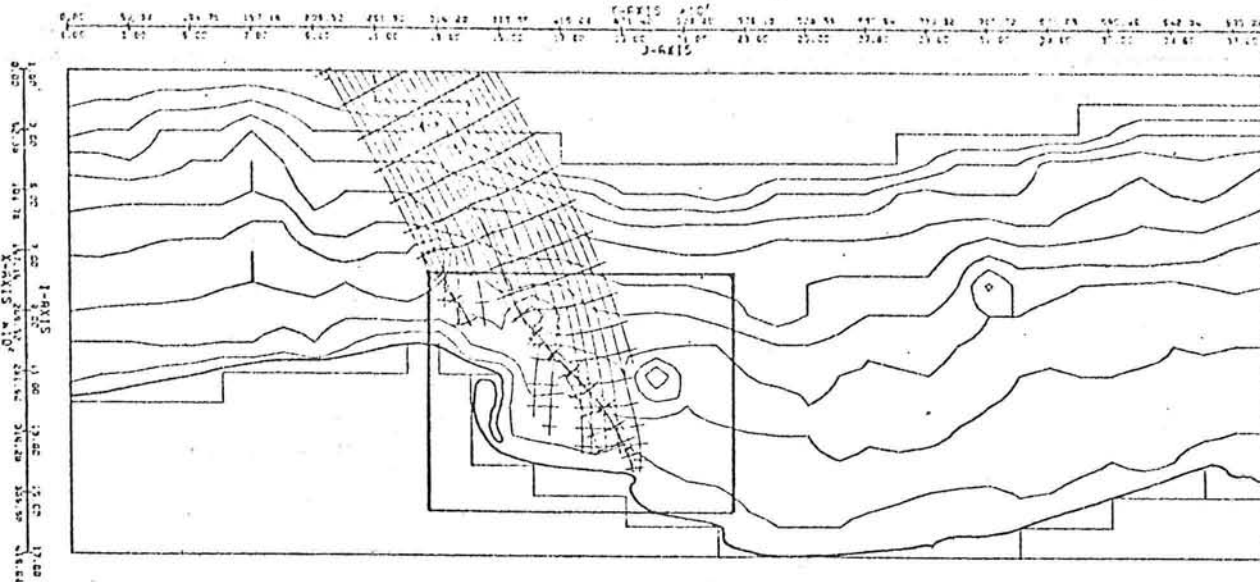
Refraction diagram (boundary calculation)

Wave period 150 seconds

Direction of the incoming waves 150° and 170°



DELFT UNIVERSITY OF TECHNOLOGY
Dept of civil engineering
Coastal engineering group
-- BENGKULU HARBOUR PROJECT --

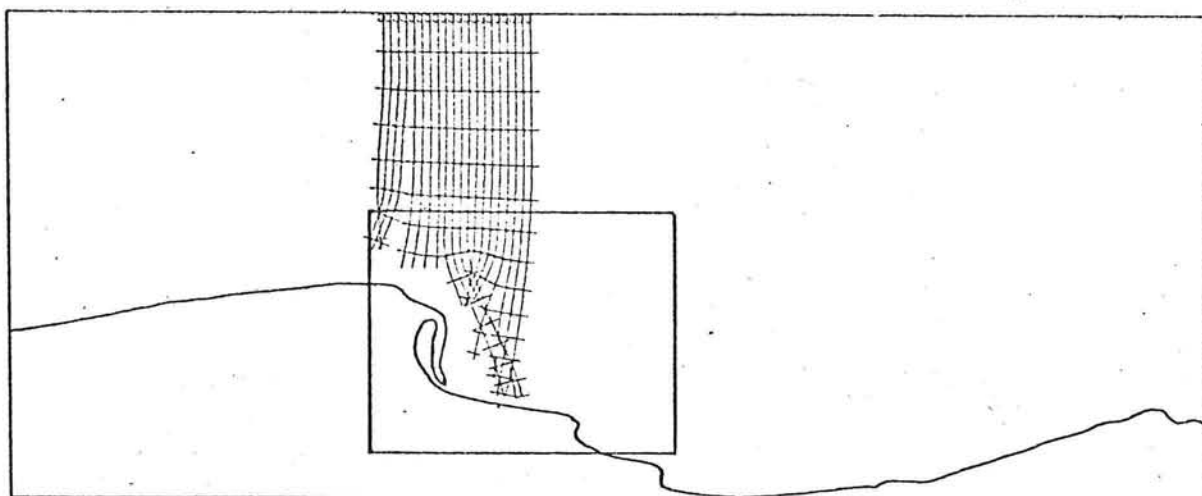


$w=0.42$

$W=0.00$

$T=15.00$

$A=30.$



$w=0.42$

$W=0.00$

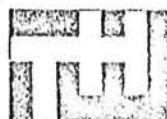
$T=15.00$

$A=0.$

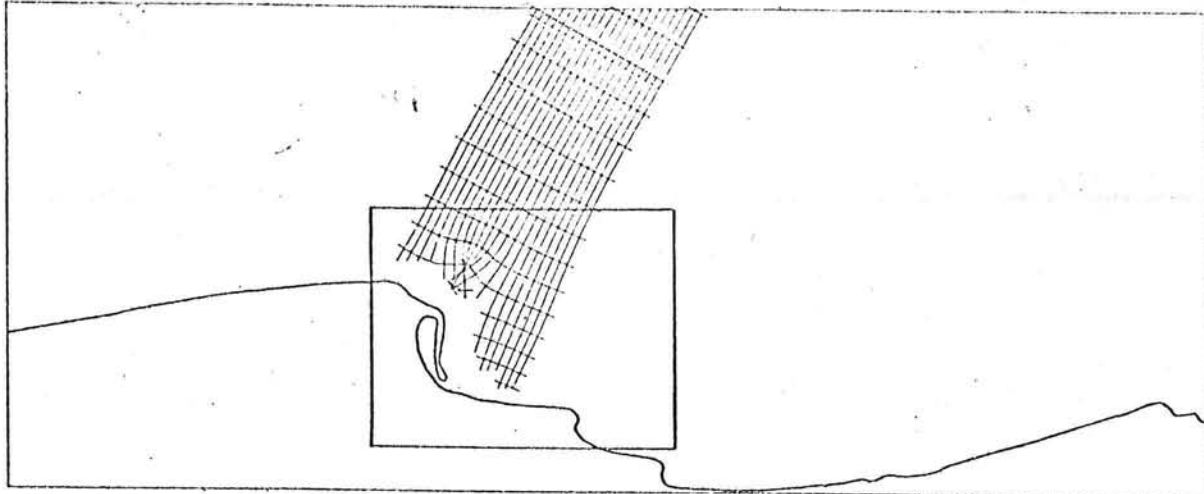
Refraction diagram (boundary calculation)

Wave period 15 seconds

Direction of the incoming waves 195° and 225°



DELFT UNIVERSITY OF TECHNOLOGY
Dept of civil engineering
Coastal engineering group
-- BENKULU HARBOUR PROJECT --

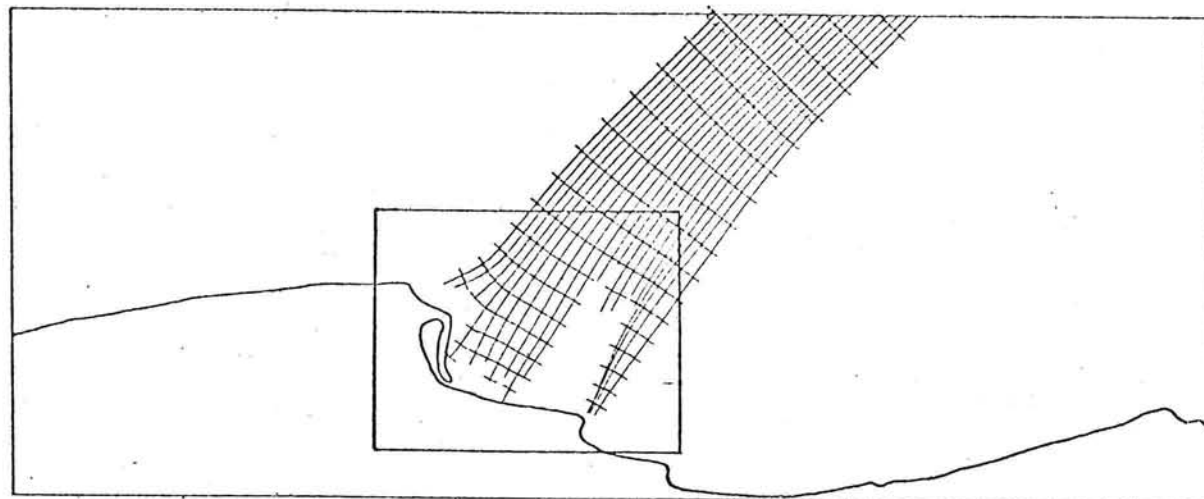


$w=0.42$

$W=0.00$

$T=15.00$

$\alpha \approx 330^\circ$



$w=0.42$

$W=0.00$

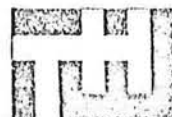
$T=15.00$

$\alpha = 315^\circ$

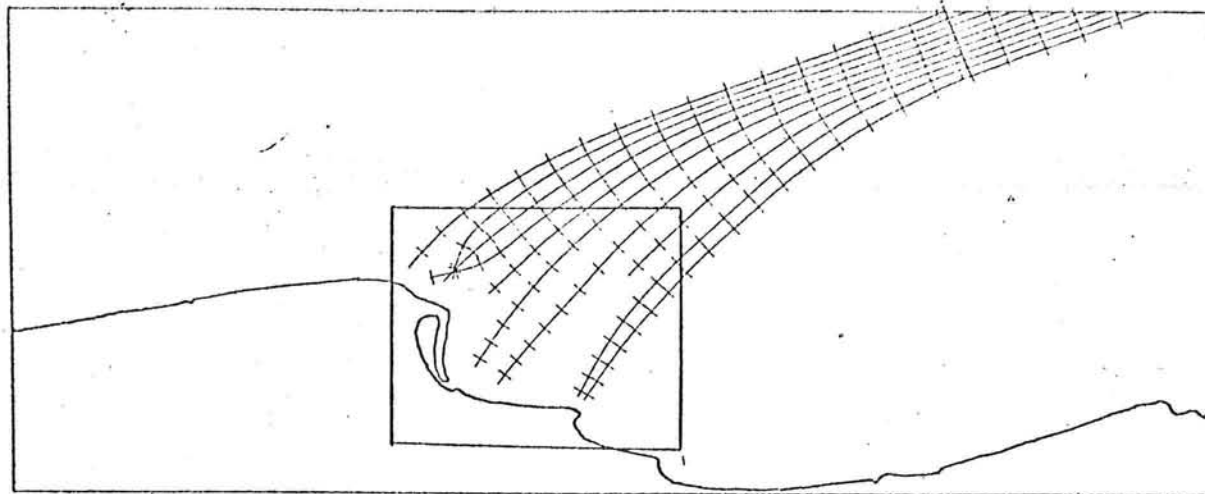
Refraction diagram (boundary calculation)

Wave period 15 seconds

Direction of the incoming waves 255° and 270°



DELF
T
U
NIVERSITY OF TECHNOLOGY
Dept of civil engineering
Coastal engineering group
-- BENKULU HARBOUR PROJECT --



w=0.42

W=0.00

T=15.0

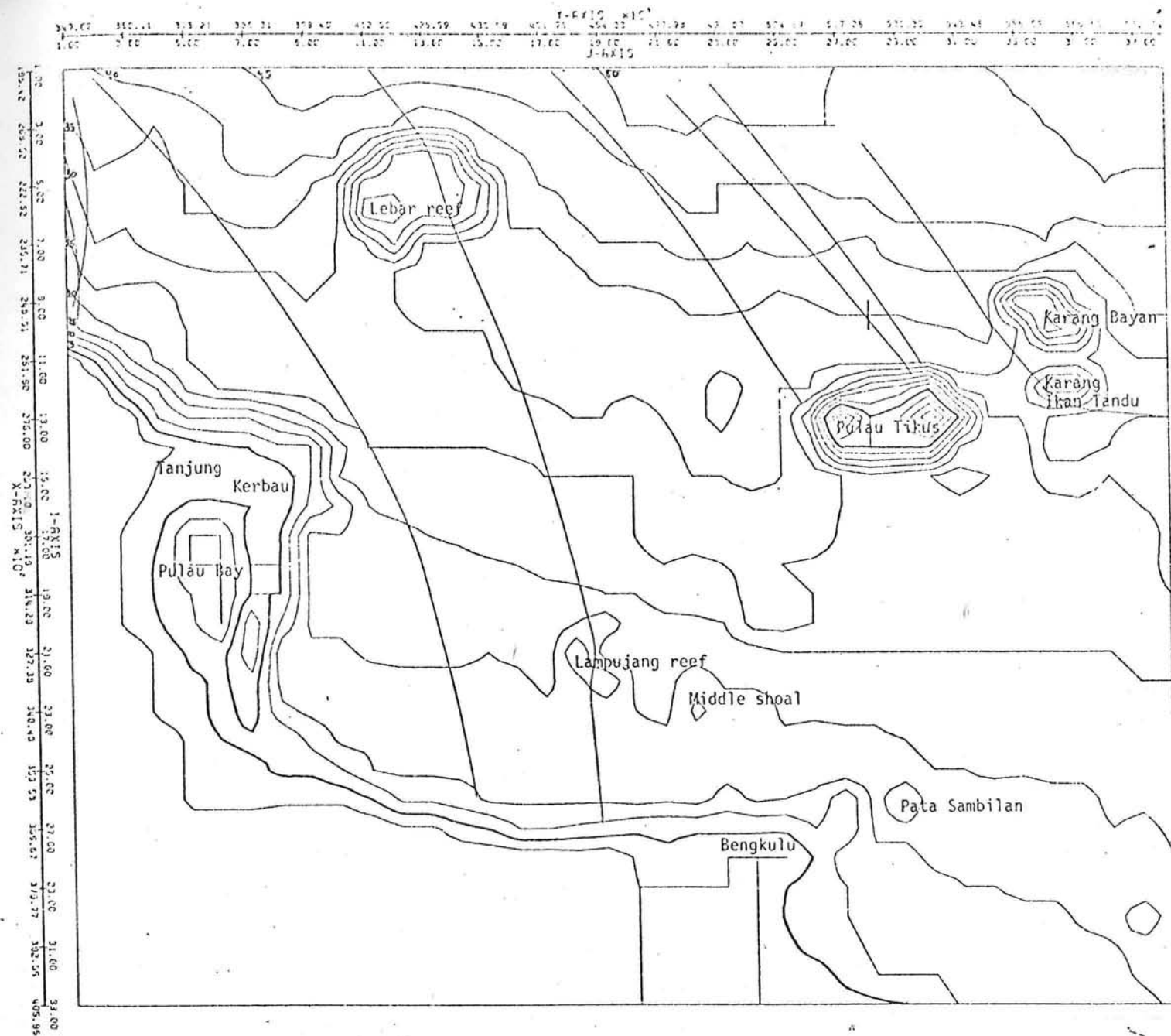
Refraction diagram (boundary calculation)

Wave period 15 seconds

Direction of the incoming wave 290°



DELTU
DELT
Delft University of Technology
Dept. of civil engineering
Coastal engineering group
-- BENGKULU HARBOUR PROJECT --



w = 0.42

W = 0.00

T = 15.00

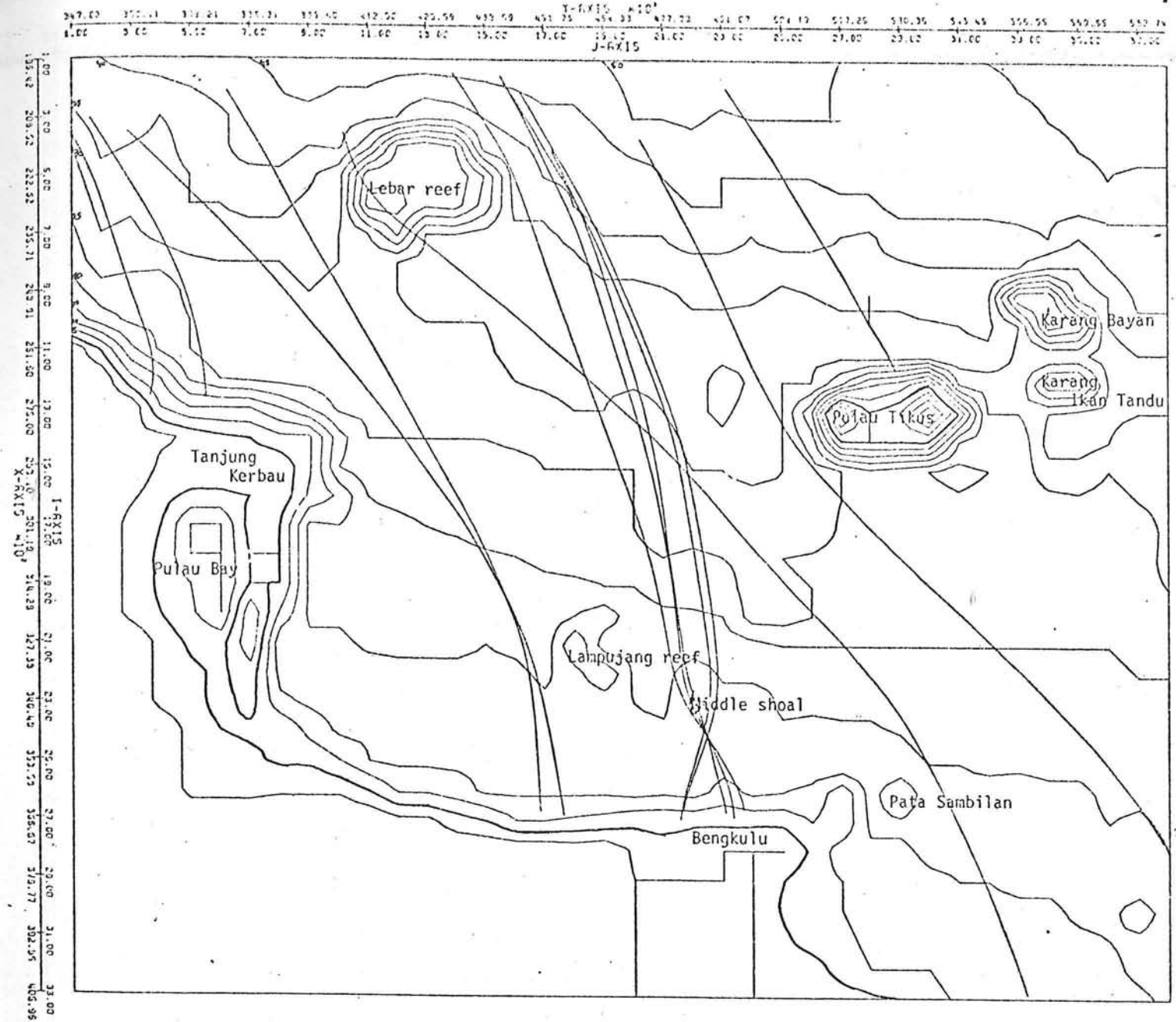
Refraction diagram

Wave period 15 seconds

Direction of the incoming wave 150°



DELTU UNIVERSITY OF TECHNOLOGY
Dept of civil engineering
Coastal engineering group
-- BENGKULU HARBOUR PROJECT --



$w = 0.42$

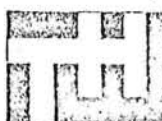
$W = 0.00$

$T = 15.00$

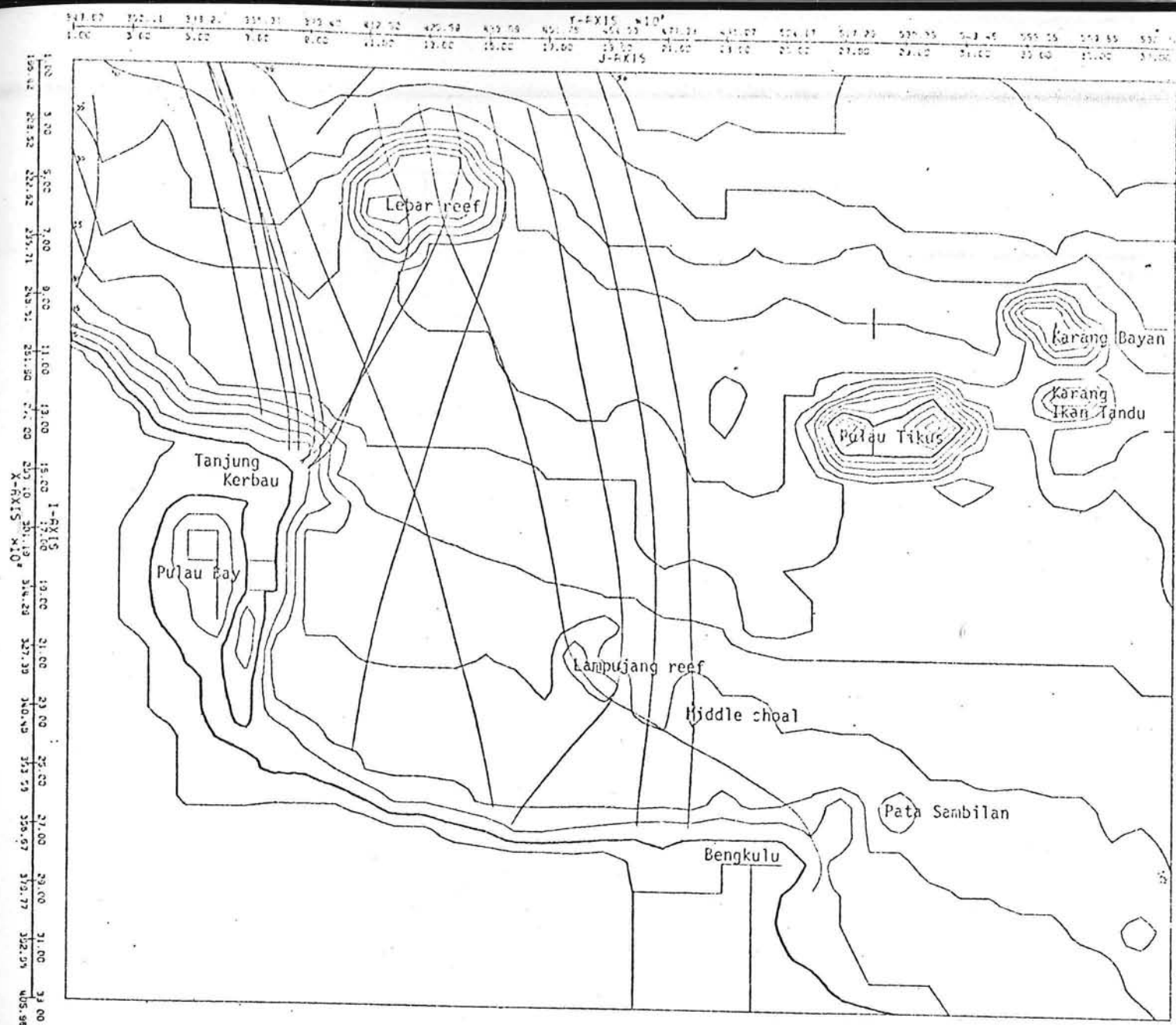
Refraction diagram

Wave period 15 seconds

Direction of the incoming wave 170°



DELFT UNIVERSITY OF TECHNOLOGY
Dept of civil engineering
Coastal engineering group
-- BENGKULU HARBOUR PROJECT --



w = 0.42

W = 0.00

T = 15.00

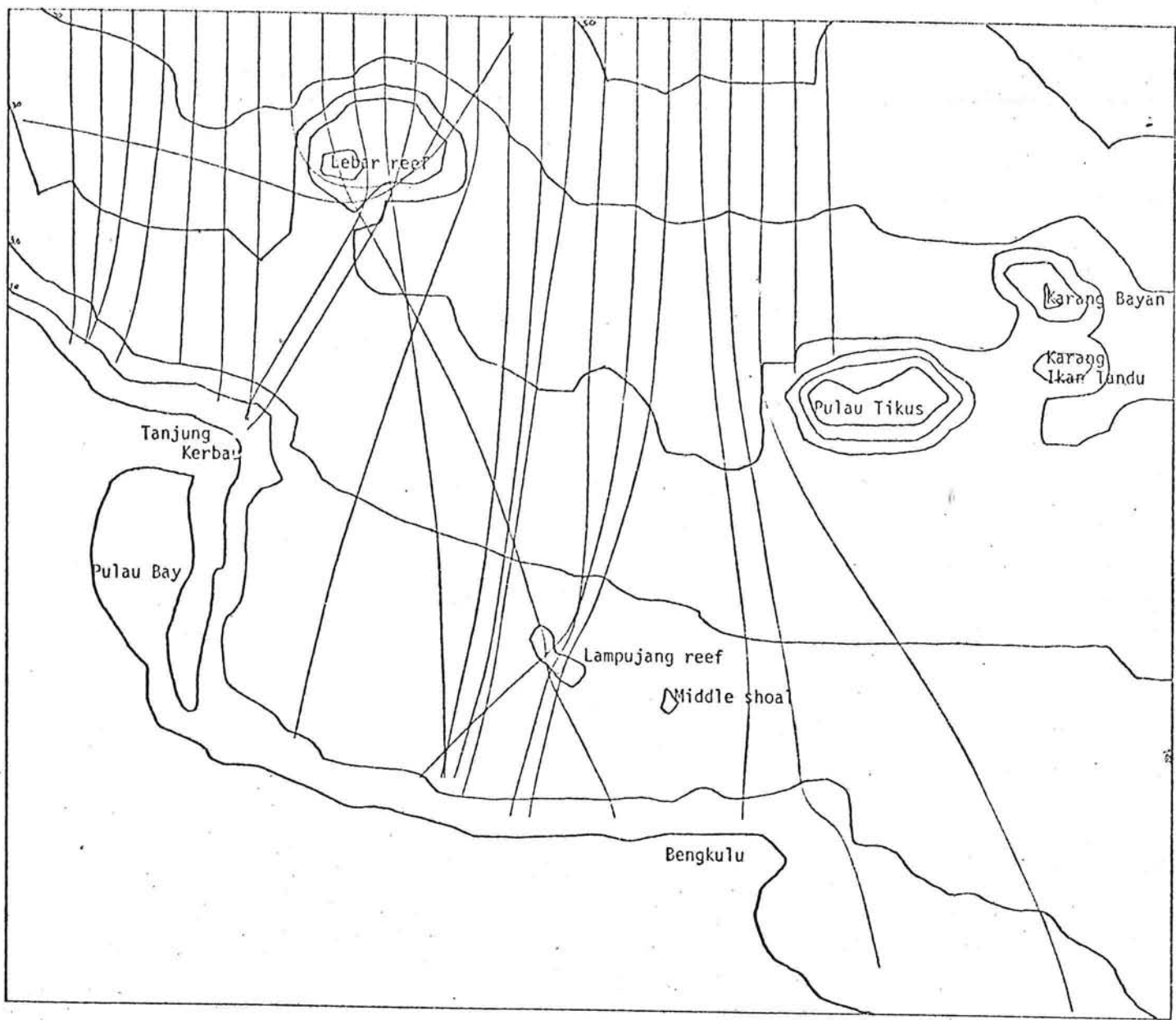
Refraction diagram

Wave period 15 seconds

Direction of the incoming wave 195°



Delft University of Technology
 Dept. of civil engineering
 Coastal engineering group
 -- BENGKULU HARBOUR PROJECT --



$w=0.42$

$w=0.00$

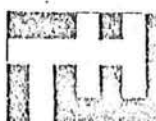
$T=15.00$

$A=0.$

Refraction diagram

Wave period 15 seconds

Direction of the incoming waves 225°





$w = 0.42$

$W = 0.00$

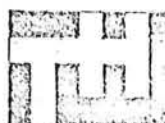
$T = 15.00$

$\theta = 333.$

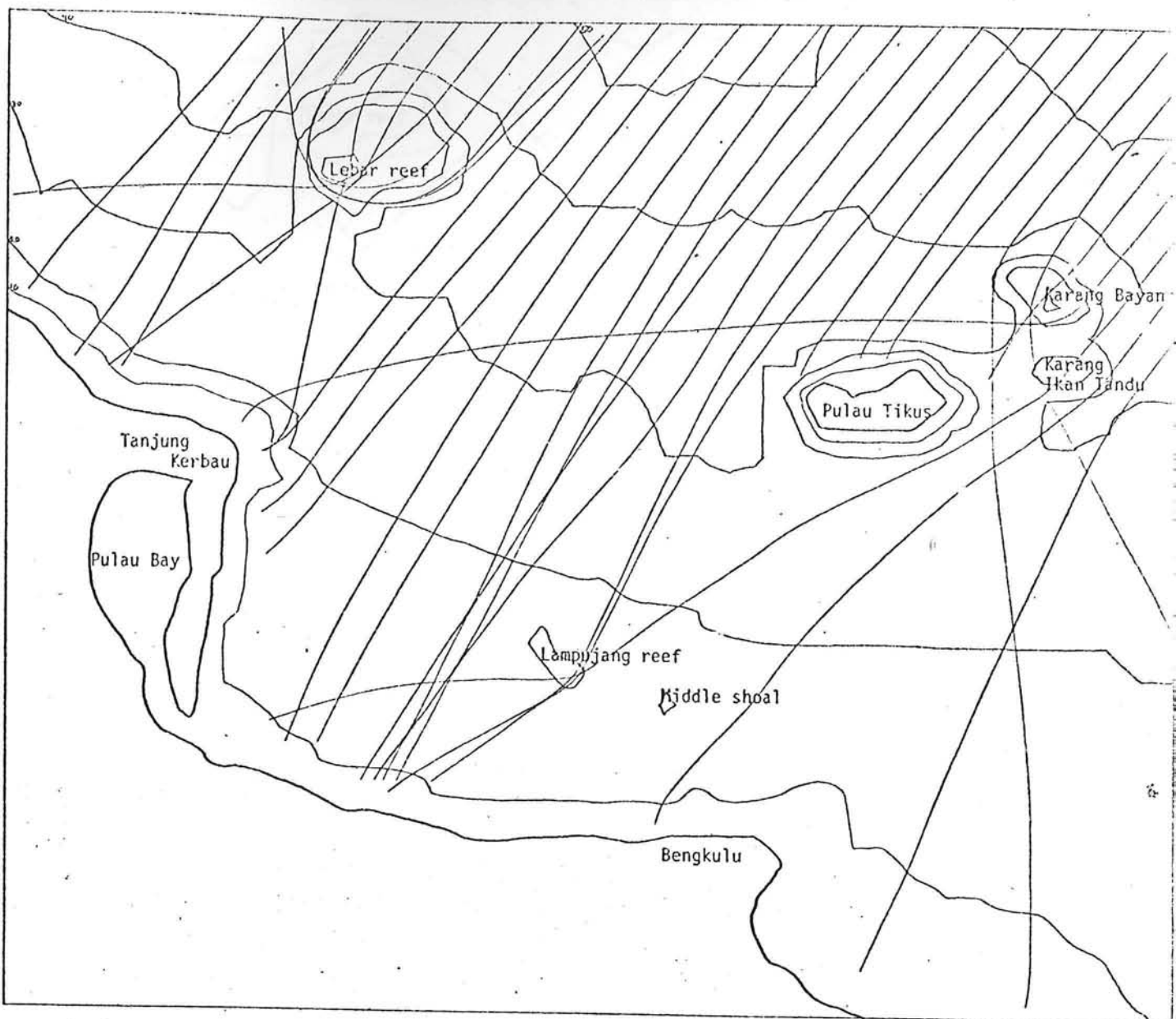
Refraction diagram

Wave period 15 seconds

Direction of the incoming wave 255°



DELFT UNIVERSITY OF TECHNOLOGY
Dept. of civil engineering
Coastal engineering group
-- BENGKULU HARBOUR PROJECT --



$w=0.42$

$W=0.00$

$T=15.00$

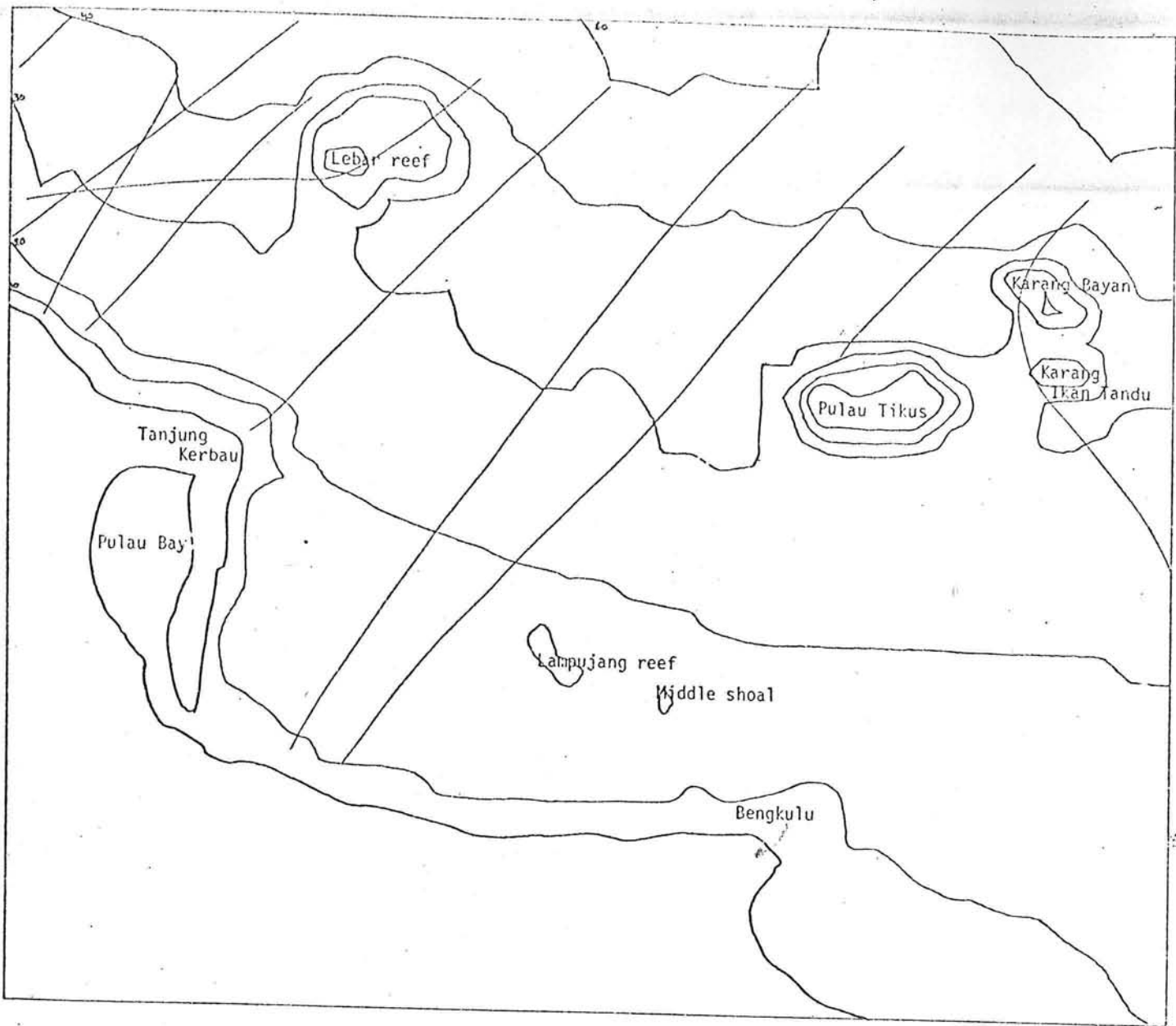
Refraction diagram

Wave period 15 seconds

Direction of the incoming wave 270°



Delft University of Technology
Dept. of civil engineering
Coastal engineering group
-- BENGKULU HARBOUR PROJECT --



$w = 0.42$

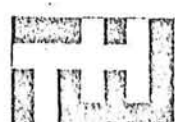
$W = 0.00$

$T = 15.00$

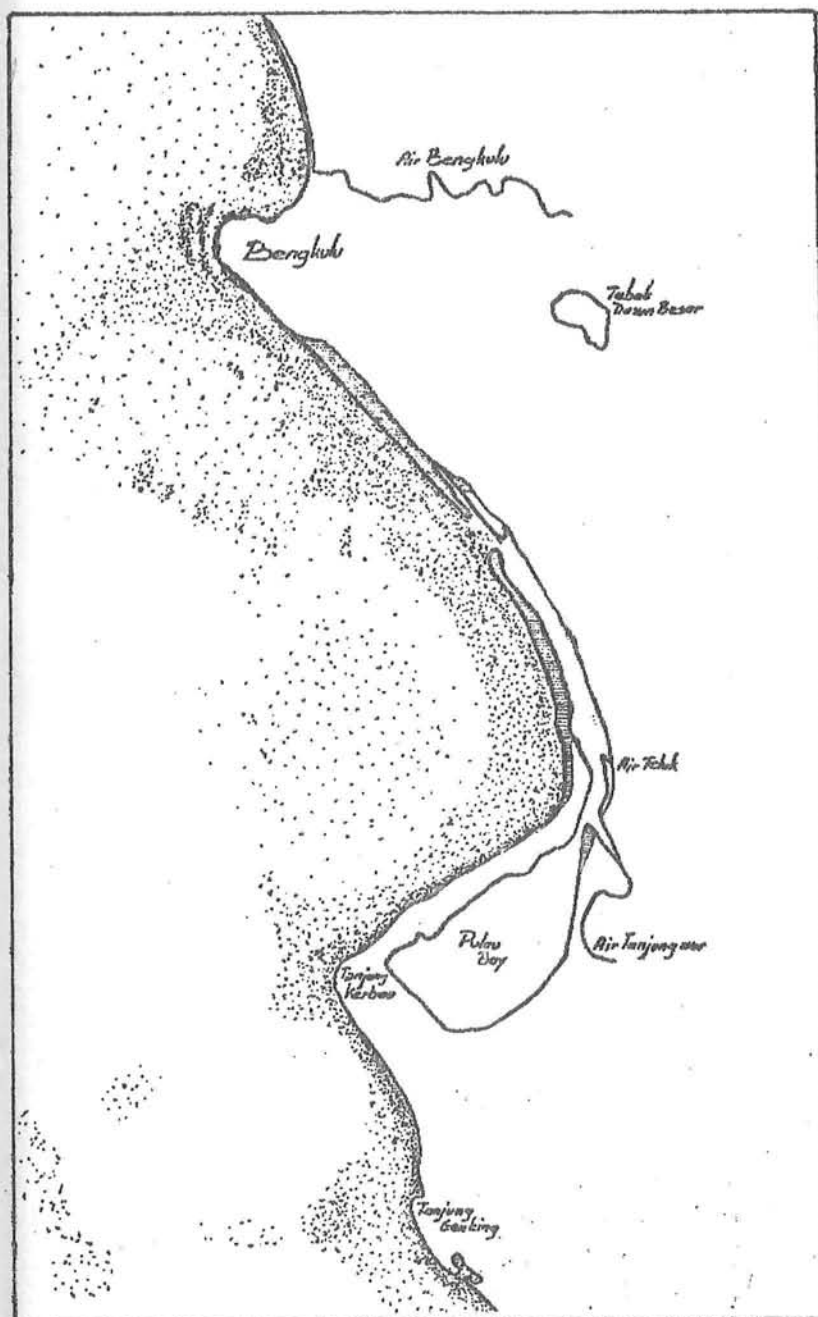
Refraction diagram

Wave period 15 seconds

Direction of the incoming wave 295°



DELTU
Dept. of civil engineering
Coastal engineering group
-- BENGKULU HARBOUR PROJECT --



BENGKULU HARBOUR PROJECT

FINAL REPORT VOL D
Upgrading the existing
harbour facilities at
Bengkulu
Feb '78

Contents

1. Introduction	3
2. Transport quantities	8
3. Port facilities	10
4. Loading and unloading on the roadstead	11
5. Morphological considerations	12
6. Calculation of wave height near the Bengkulu harbour	14
7. Determination of the armour stone weight	19
8. Improvement of the existing harbour	21
9. A new jetty east of the harbour	23
10. Conclusion	26
Annex: Investigation of data from the archives of the Dutch colonial government from the Arsip Nasional at Jacarta (1913-1923)	27

1. Introduction

The existing harbour of Bengkulu has silted up totally. To improve sea-transport a new harbour will be built in the Pulau Bay, some 15 km south of Bengkulu. This new harbour will not be able to handle ships before 1983. So for a period of at least 5 years the Bengkulu area lacks any harbour facilities. This will not only give problems to the short term developments in the area, but it will also have influences on longer terms. As already indicated in vol A, chapter 5, most transport will go by road and rail to Palembang in the next five years, when there is no reasonable harbour. After these years it will be very difficult for a new Pulau Bay harbour to regain its place in the total transport flow. When land transport has been established, every company will have its connections in Palembang and although sea transport will be cheaper, there is a big chance that many goods will be sent via Palembang. Only gouvernemental instructions with penalties can change this. Perhaps it is easy to change these customs, but it is better to prevent that all goods are transported via Palembang.

An other aspect is that for the construction of the Pulau Bay harbour a temporary work harbour is necessary. An upgraded harbour at Bengkulu can serve as such a work harbour.

Morphological conditions

The total sand-transport which was calculated for the area in front of the Bengkulu harbour was about 0.5 million m^3 /year. This figure is probably too high, because:

- sand transport decreases south of Bengkulu harbour (south of cross-section VII, see fig. 2)
- morphological considerations of the Bengkulu harbour area (see chapter 5)
- the 'beach-slope' isn't a normal slope.

These items are discussed in detail in the chapters 5 to 7 of this report.

Maintenance by continuous dredging will be an expensive operation too, in particular because one cannot dredge only once a year (because of the coral-reefs it is not possible to dredge to an overdepth, the deposits have to be removed several times a year).

So one should try to design a construction which will not influence longshore current very much. The only way to do so is finding a construction in which the entrance channel does not cross the breakerzone. This means that several port facilities (wharfs) have to be constructed off-shore,

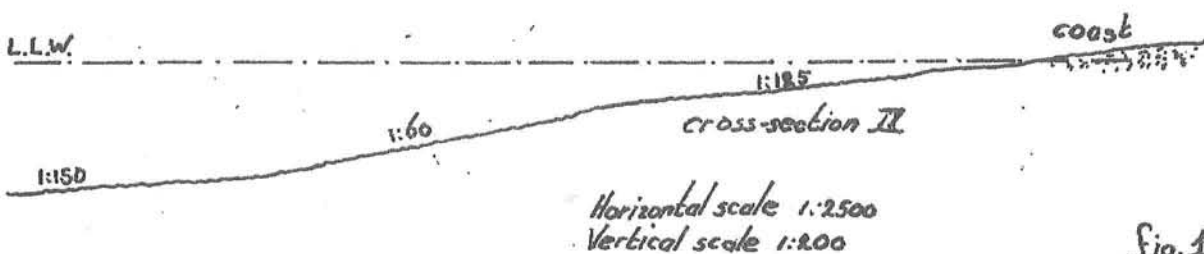
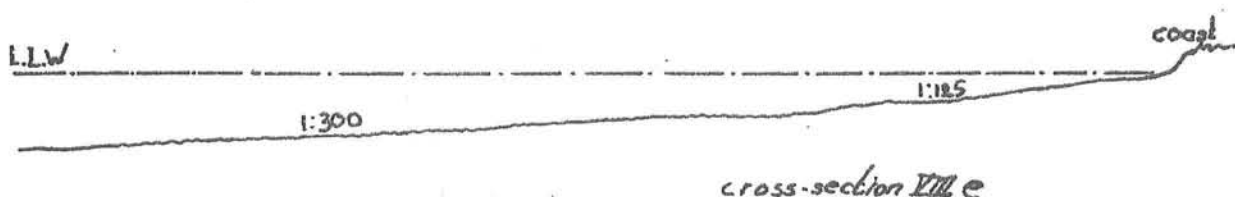
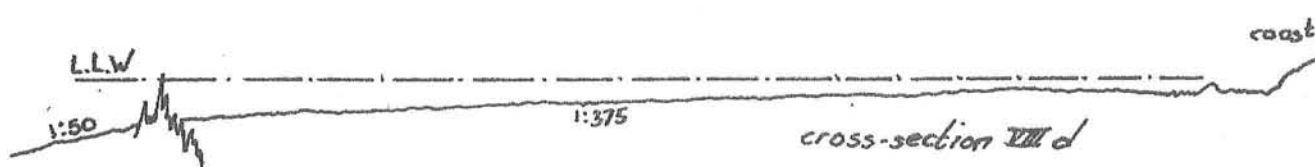
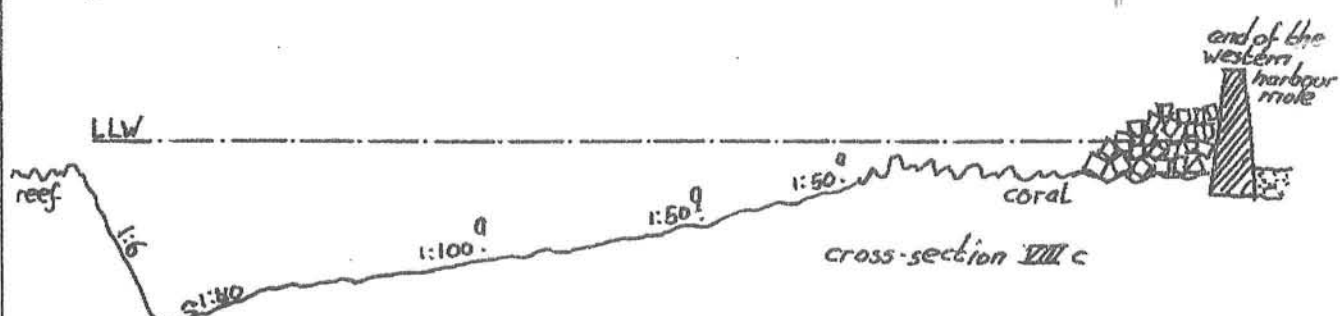
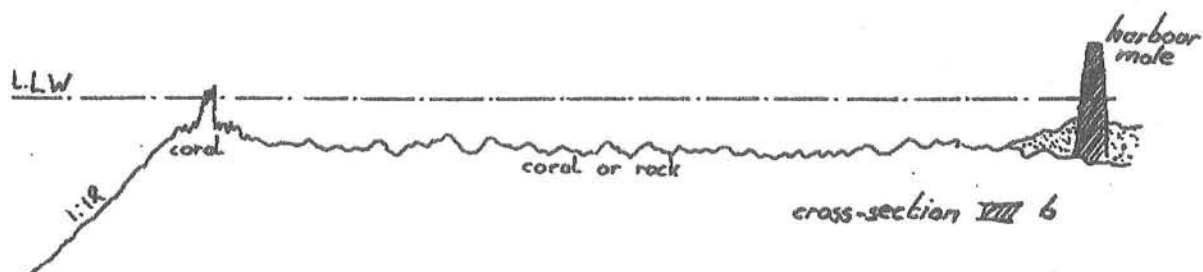
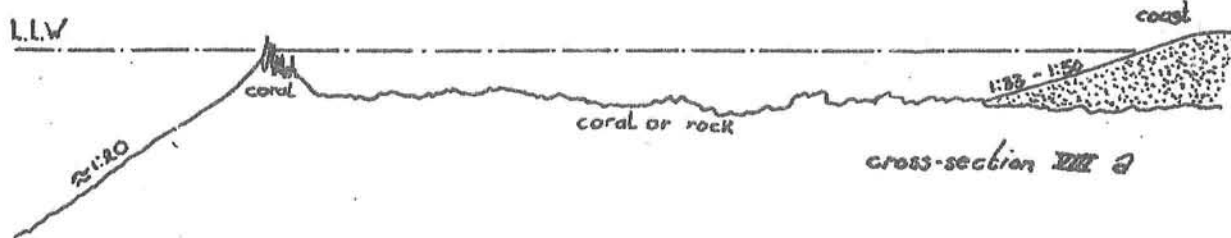
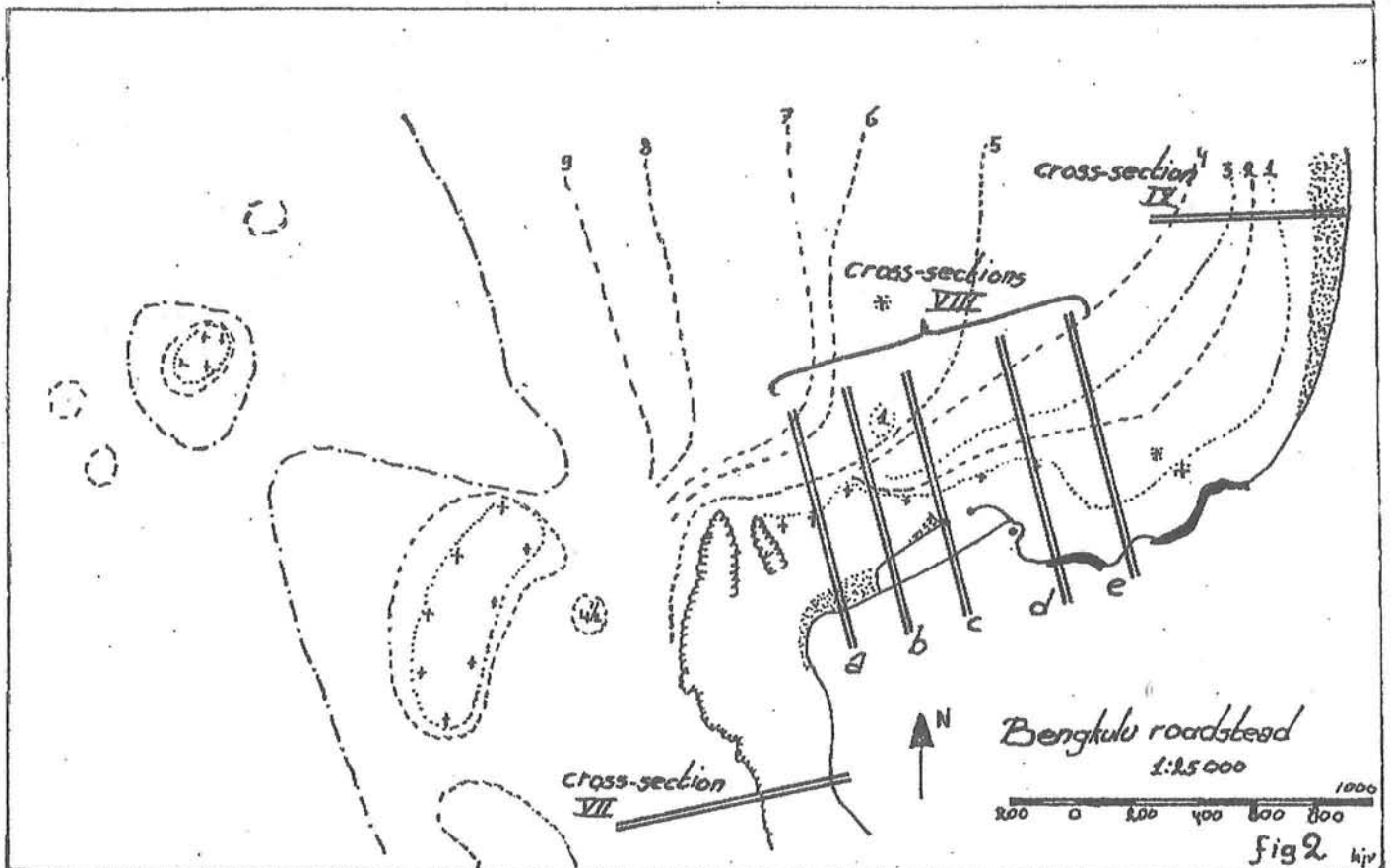


Fig. 1



and connected to the shore-based storage area by means of a bridge. The best and cheapest way is to construct the facilities as a pier or jetty. Consequently the off-shore construction may not be situated too far off the coast, and has to be constructed in shallow water. The minimal distance is the extend of the breakerzone. Near Bengkulu the breakerzone has a width of approx. 100 m. Waves should be able to pass through the gap between the coastline and the construction, to propulse the longshore current (and the longshore transport) as long as possible.

Shipping requirements

The construction should be allow save bearthing of at least barges, small coasters and wooden sailing-ships. Bearthing accomodation for bigger coasters is to appreciate, but not strictly necessary. The small coasters and wooden ships in Indonesia have a draught of about 2.5 m, a length of 15 m and a width of 3.5 to 4.5 m.

So the entrance channel needs a depth of about 2.5 m below l.l.w. (the tidal difference is about 0.8 m). At the bearthing places also a depth of 2.5 m is necessary (For these ships a min. keel-clearance of 0.15 m is sufficient to leave the harbour, if the bottom consists of sand. Eventual rock or coral reefs have to be removed).

The entrance channel requires a width of about 20 m (5 times 4 m) and a good marking by means of some buoys. The channel has to be as straight as possible. The width of the basin depends on the way of mooring but is

estimated at 50 m in view of the bearthing manouvers of the vessel. The wave height at the bearthing places should be very small, about 30 cm in normal conditions.

The distance from the bearthing places to the roadstead should not be longer than half an hour sailing by barges (approx. 5 km).

Financial requirements

The costs have to be low because of the temporary character of the construction. The economic lifetime is estimated to be 10 years. After these 10 years the Pulau Bay harbour is into full service. It is possible that for local use the Bengkulu facilities will be still important, but this should not be taken into account, when judging the necessity of certain investments. The financial aspect is not worked out in detail in this report. The decision to invest a certain amount of money is a political decision. In this report is searched for the cheapest possibility. It is to the Indonesian government to decide whether this investment should be made or not.

Necessity of transshipment on the roadstead

Because of the large sand transport and the limited budget it is not possible to construct shore connected bearthing facilities for "large ships", i.e. ships with a draught of 3 m and more. So goods from these ships have to be transshipped on the roadstead into barges, which bring these goods to the facilities on the coast.

The Bengkulu roadstead is an open roadstead, offering little shelter. This causes some difficulties for transshipment, especially in the afternoon during the December-February monsoon period. The only way to solve this problem is to construct a breakwater to protect the transshipment area. This offshore breakwater has to be built in a waterdepth of 8 to 10 m, to ensure suitable circumstances for cargo-handling. Such a breakwater should have a length of at least 200 m. A stone breakwater, with a slope of 1:3 and a crest height of 0.5 above SWL contains 30 000 m³ of quarry stone, and will cost approx. 600 millions Rp. Probably this will be too expensive, specially when this breakwater is used only for 10 years.

An other possibility is a breakwater composed of caissons. This is only an acceptable solution when caissons constructed in a cheap way are available. As far as we know this is not so. A variation of this caisson type breakwater is a breakwater formed by old ships. If one or two ships are available it is possible to run them aground, and form a breakwater. In this report this solution will not be regarded, because it depends on the availability of old ships.

The consequences of not building an offshore breakwater in deep water are

that ships can only be loaded during a part of the day in the December January monsoon. At some days transshipment will be totally impossible and one has to wait for better weather. Although no cost-benefit analysis is made, we assume the construction of this offshore breakwater as economically unattractive.

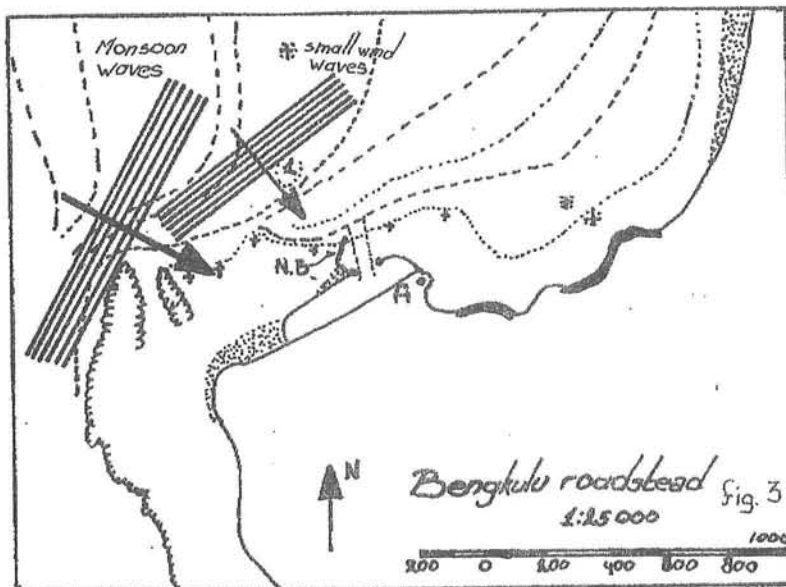
Two alternatives

Two alternatives will be discussed, viz.:

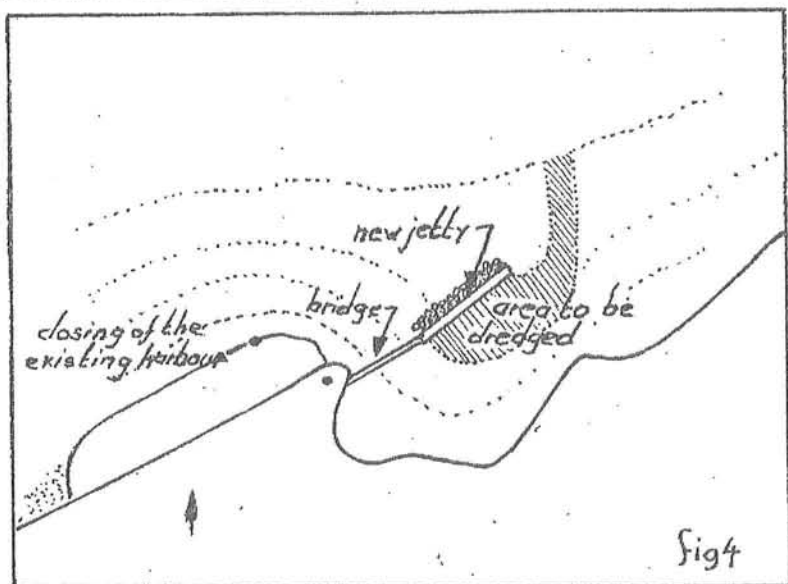
1. an improvement of the existing harbour, and
2. a new-constructed, wave protected jetty.

In both cases the existing facilities can be used, which is important for a quick development.

1. The existing harbour can be improved by dredging it to a depth of 2.5 m (below l.l.w.) and the dredging of an approach channel. The (damaged)



quay wall opposite to the harbour entrance (near A) is protected from waves by the new extension of the breakwater (NB). Because of the morphological situation near the harbour it might be possible to maintain a channel during a large part of the year without great costs.



2. The other alternative is the construction of a new jetty east of the existing harbour. Nowadays the area east of the existing harbour is eroding. If a jetty is designed in the right way most sand will pass behind the jetty when this sand is not already trapped near the old harbour.

It is very easy to connect this new jetty by means of a bridge (ca. 50 - 80 m) with the old harbour facilities. The silted-up area in the old harbour basin can be used as a new marshalling and storage yard. The jetty itself can be built very simple, as a staging or as a wooden cofferdam, or something like that, protected by armourstone on the seaward side.

Both alternatives are regarded in detail in the next chapters.

2. Transport quantities

For the determination of the length of the harbour-pier it is important to know the amount of ships which call at Bengkulu, their size and the amount of cargo which is loaded and unloaded. In a report of Dwidelta (1975b) some figures are given. The sea-transport can be split into three parts, viz.:

- transport with local vessels (20 - 200 tons)
- transport with domestic shipping companies (200 - 1000 tons)
- transport with international shipping companies (until 7000 tons)

For each of these ways of transport the following tables are given:

year	amount of ships	total volume of ships	unloaded (tons)	loaded (tons)	passenger embark	passenger deboard	volume per ship (m³)	unloaded per ship (m³)	loaded per ship (m³)	passenger embark per ship	passenger deboard per ship
1968	233	37318	3123	2980	3654	833	160	13.4	9.8	15.7	3.6
1969	538	38764	4681	6268	3058	5899	184	16.1	11.7	11.7	5.7
1970	1125	57808	10123	5217	997	2336	136	23.8	12.3	2.3	5.6
1971	254	144820	6938	3364	590	707	152	23.6	11.4	1.8	2.4

Table 1

Sea transport with local ships

year	amount of ships	total volume of ships	unloaded (tons)	loaded (tons)	passenger embark	passenger deboard	volume per ship (m³)	unloaded per ship (m³)	loaded per ship (m³)	passenger embark per ship	passenger deboard per ship
1968	13	814216*	371	101	1557	2785	62632*	285	7.8	120	214
1969	73	471103	309	422	529	1156	64153	4.2	7.3	7.3	15.8
1970	56	359403	1775	263	2062	2641	6416	31.7	4.7	36.8	47.2
1971	14	142709	1192	-	176	609	10194	85.1	-	12.6	43.5

Table 2

Sea transport with domestic ships

*) It is obvious that this figure has to be devided by ten.

year	amount of ships	total volume of ships	unloaded (tons)	loaded (tons)	passenger embark	passenger deboard	volume per ship (m³)	unloaded per ship (m³)	loaded per ship (m³)	passenger embark per ship	passenger deboard per ship
1968	-	-	-	-	-	-	-	-	-	-	-
1969	1	610	867	-	-	-	6120	867	-	-	-
1970	7	21724	-	2676	-	-	3103	-	525	-	-
1971	12	90637	-	6388	-	-	2470	-	532	-	-
until now 1972	1	3755	-	1357	-	-	3756	-	-	-	-

Table 3

Sea transport with international ships

year	amount of ships	local %	domestic %	internat. %	unloaded (tons)	local %	domestic %	internat. %	loaded (tons)	local %	domestic %	internat. %
1968	246	95	5	0	3494	89	11	0	9381	96	4	0
1969	612	88	12	0.2	9860	88	3	9	6690	94	6	0
1970	488	87	11	1	11898	85	15	0	9156	57	3	40
1971	320	99	4	4	8130	85	15	0	9753	34	0	65

year	passenger embark	local %	domestic %	internat. %	passenger deboard	local %	domestic %	internat. %	total transport (tons)	local %	domestic %	internat. %
1968	5211	70	30	0	3618	23	77	0	5875	92	8	0
1969	3587	85	15	0	7055	81	16	0	16550	90	9	6
1970	3059	33	67	0	5037	48	52	0	21054	73	10	17
1971	696	75	25	0	1316	59	46	0	17883	58	67	36

Table 4

Summary of the total transport

Table 4 is calculated by means of table 1, 2 and 3.

The incoming commodities are:

cement, corrugated iron sheets, rice, salt, salted fish, merchandise, sugar and construction materials

The outgoing commodities are:

rubber, coffee, rotan and resin

The export of rotan and resin is decreasing; in 1974 they were not mentioned as outgoing commodities.

Conclusions:

- 85 % of the incoming commodities are transported by local vessels; the amount of goods per vessel is valued at 25 tons (unloaded in the harbour).
- 15 % of the incoming commodities are transported by domestic shipping companies; the volume of these ships is somewhat increasing, so the amount of goods per vessel is valued at 100 tons (unloaded on the roadstead).
- the international shipping companies do not transport goods to Bengkulu.
- the amount of exported goods transported with domestic shipping companies is about 5 %. The amount of goods per vessel is valued at 10 tons.
- in 1968 about 95 % of the exported goods were transported by local vessels. In 1971 this figure was about 35 %. The rapid decrease in importance of this transport certainly did not stop in 1971 (the last year of which we have figures). So it is not clear which part of the outgoing goods are transported by local vessels, we assume it is 25 %. The amount of goods per vessel is valued at 15 tons.
- the international shipping companies will transport about (100-5-25) = 70 % of the outgoing goods. The goods transported with these ships are mostly rubber and coffee (in the last years ('74 and '75) coffee was no more mentioned as an outgoing commodity). The mean amount of goods per ship is valued at 750 tons, the maximum at 1500 tons.

3. Port facilities

The existing harbour of Bengkulu has a basin of 500 by 100 m. The length of the quay is 500 m, 180 m has a concrete apron behind the quay-wall. The remaining 320 m can not be used because of its bad condition. The total harbour area has a surface of 36250 m² (Dwidelta 1974) in which the following parts are located:

- 8 sheds with a total area of 2070 m² and a total storage capacity of 4000 tons (2 ton/m²)
- 5000 m² storage yard with a heaping capacity of 0.5 ton/m², thus a total open storage of 2500 tons.
- 625 m² of accomodation for the attendance of max. 200 passengers.
- an area of 180 x 40 = 7200 m² with no special use.
- an apron around the quay of about 320 x 7 = 2240 m².

The area near the harbour is about 500 x 40 = 20 000 m²; of which about 3000 m² (20000 - 2070 - 5000 - 625 - 2700 - 2240) is used for roads and other facilities. The remaining part, namely 36250 - 20000 = 16000 m² is situated at a distance of more than 50 m from the quay. This area can be used as secondary port area for supporting facilities.

The total storage capacity of the harbour nowadays is

4000 tons in sheds

2500 tons on the surrounding aprons

6000 tons total

The maximum amount of goods transported through Bengkulu harbour in 1985 is valued at 18 000 tons. So the storage capacity will be enough until 1985. If, according to the situation measures are taken in time (e.g. the creation of more covered storage room, etc.).

4. Loading and unloading on the roadstead

The self propelled barges used for loading and unloading of ships on the roadstead have an average load-capacity of 10 tons. The amount of barges is 12 according to Dwidelta, with an average condition on 60 % (so about 7 barges can be used). During his visit in July 1977 Bijker estimated a much worse condition of the barges.

The distance between the roadstead and the harbour is about 1000 m. The estimated speed is 10 km/hour (a motor-capacity of ca. 40 HP). So the time to sail from ship to harbour is about 8 to 10 minutes.

According to Dwidelta an average capacity of 25 tons per barge per hour was obtained during high tide and good weather. So the return time is $\frac{60}{25/10} = \frac{60}{2.5} = 24$ minutes.

In this case ships were loaded only, so the barge sailed back empty.

Hence loading and unloading costs $24 - (2 \times 8) = 8$ minutes. It is not to expect that this is possible in normal situations. To load a 10 tons barge in 4 minutes is only possible with special goods, which are very easy to handle.

A loading time of 6 to 8 minutes is expected in normal cases, so the turn-around time of one barge is $7+9+7+9 = 32$ minutes

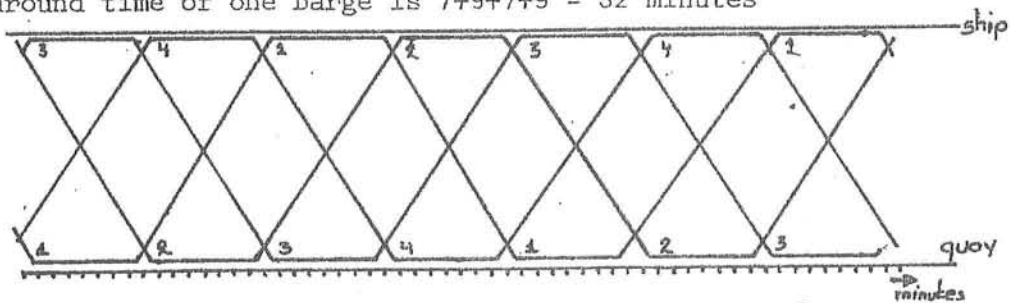


fig. 5

So one crane can serve four barges (see fig. 5). The loading (cq. unloading) capacity is $4 \times 10 = 40$ tons per 32 minutes, which is about 80 tons per hour. Increasing the number of barges is not usefull when only one crane is used. It is economically not attractive to use more cranes.

The average amount of hours on which can be worked each day is valued at 6 hours (from 6 am. until noon). So the average capacity per day is 500 tons. The mean amount of goods to be loaded in international ships was valued at 750 tons, so these ships can be loaded in two days. The maximum amount of goods was 1500 tons. Such an amount of goods can be loaded in 3 or 4 days.

5. Morphological considerations

The net sand transport near the Bengkulu harbour is very small (in comparison with the calculated sand transport south of Bengkulu). The transported amount of sand is about $30\ 000 - 100\ 000 \text{ m}^3/\text{year}$. The transport capacity is much larger, about $500\ 000 \text{ m}^3/\text{year}$; the reason why this capacity is not utilized will be explained in this chapter.

During the June-August monsoon period sand is transported in northern direction (in a). Because the coast line turns east near Bengkulu, sand will settle near b. During the December-February period sand is transported in southern direction from b to a (and further on). The accretion area b will erode, but also the coast between b and a (observed by ir. Burger of Nedeco).

In this Dec-Feb period and during local storm periods, which generate

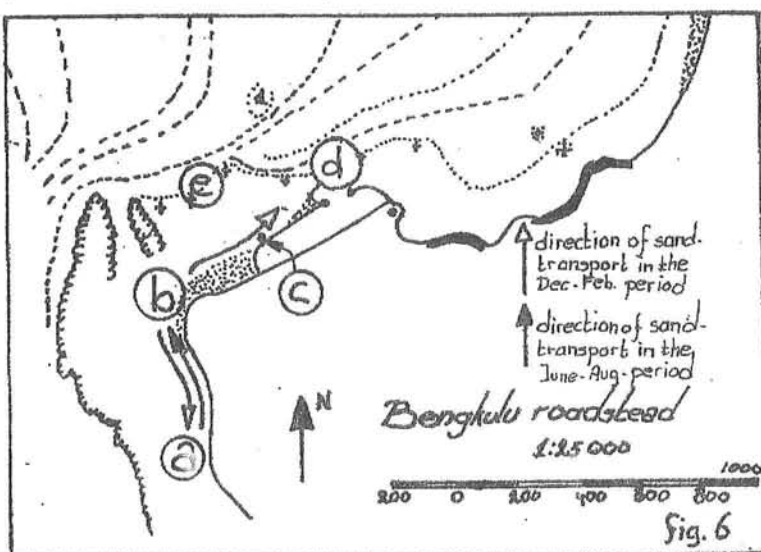
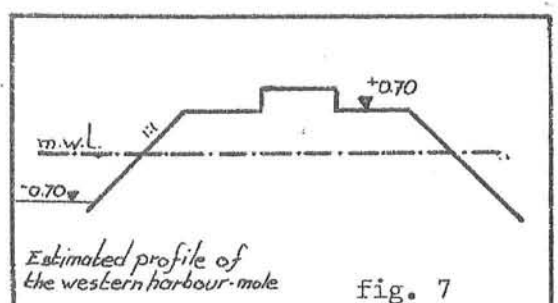


Fig. 6

wind waves from north-western directions, sand is also transported in eastern direction (from b to c and further on). This transport will start in b, so the area near b will erode.

Before the extention of the western mole had been built, the beach between b and c has never grown so far forward that the beach was extended (in eastern direction) in front of the western harbour mole. This means that the transport capacity in front of this harbour mole (between c and d) is large enough to transport the amount of sand which passes c. The waterdepth in front of this mole is more than -0.70 m below m.w.l. (l.l.w.l. is -0.65 m below m.w.l.), because there is no indication for a beach.

As a result of this depth only a part of (all) waves will break in front of this mole. (The other part breaks on the mole or is reflected back to the sea). Therefore only a part of the radiation stress (parallel to the direction on the mole) is used as a propulsing force for the longshore current. This indicates that in c the longshore current is not fully developed. The same conclusion can be drawn in another way. The longshore current will be accelerated between b and a (and further on), because



Estimated profile of the western harbour-mole

fig. 7

the current starts in b (thus the current velocity is almost zero). So there can be expected that the longshore current is not fully developed in c, because of the short distance between b and c (ca. 250 m).

A part of the amount of sand which is transported along the western harbour mole will settle in the harbour. The sand enters the harbour in several ways:

- it can be washed over the western harbour mole during severe storms. Behind this harbour mole the wave activity is small, so the sand will settle.
- because of the breaking of the waves on the harbour moles, set-up will occur. So there will be set-up differences near the harbour entrance; in the harbour entrance set-up will be about zero because waves will seldom break at a depth of 1.5 - 2.0 m.

Because of these set-up differences currents will occur in several directions, as indicated in fig. 8.

Probably the inward transport is larger than the outward transport.
(This tranport is observed by ir. Burger/Nedeco)

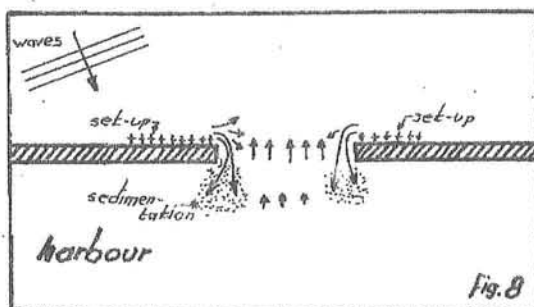


Fig. 8

6. Calculation of wave-heights near the Bengkulu harbour

The incoming waves near the Bengkulu harbour will break on the reefs in front of this harbour. Nevertheless some of the waves (or wave energy) will reach the coast. By means of the following methods the wave-height behind the reef are estimated.

a. Fuchs' equation (Shore protection manual, vol II) $H_t/H_i = \sqrt{1 - \frac{h+z_c}{h}}$

b. Experiments of Saville, presented in figures

c. Experiments of Hall and Hall, also presented in figures

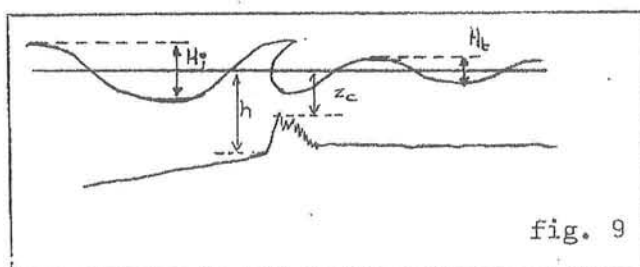
d. Rules of thumb, $z_c/H_i = 0$; $H_t/H_i = \frac{1}{2}$; $z_c/H_i < -\frac{1}{2}$; $H_t/H_i > \frac{3}{4}$

H_i is the incident wave height

H_t is the transmitted wave height

z_c is the elevation of the crest above the water level

h is the water depth in front of the reef



The waterdepth in front of the reef is valued at 1 m below l.l.w.l. Two reefs can be distinguished, one in front of the harbour (A), which is submerged by l.l.w.l., and another west of the harbour which dries at l.l.w.l.

Assume that: z_c for reef A is -0.10 - -0.30 m (at l.l.w.l.)

z_c for reef B is $+0.10$ - $+0.30$ m (at l.l.w.l.)

A At l.w.l. $H = 1.25$ m $z_c = -0.35$ - -0.55 m

a. $H_t/H_i = 0.53 - 0.66$;

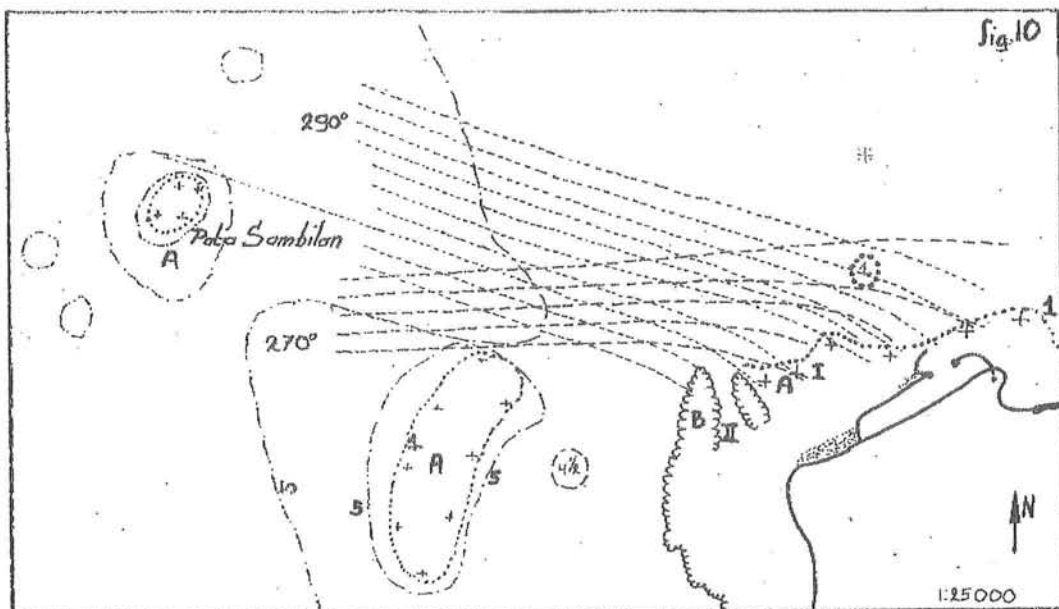
b. $H_t/H_i > 0.5$ (Saville only gives figures for $\frac{h+z_c}{h} = 1.133, 1.013$ and 0.899)

c. $H_t/H_i = 0.65 - 0.8$

d. $\frac{1}{2} < H_t/H_i < \frac{3}{4}$

reef	water level	$-z_c$	h	H_t/H_i				average
				a	b	c	d	
A	l.w.l	0.35 - 0.55	1.25	0.53-0.66	> 0.5	0.65-0.8	$\frac{1}{2} - \frac{3}{4}$	0.65
B	l.w.l	0.15 - 0.35	1.25	0.35-0.53	> 0.5	0.6 - 0.7	$\frac{1}{2} - \frac{3}{4}$	0.55
A	m.w.l	0.80 - 1.00	1.70	0.69-0.77	> 0.5	0.75-0.9	$\frac{1}{2} - 1$	0.75
B	m.w.l	0.60 - 0.80	1.70	0.59-0.69	> 0.5	0.65-0.85	$\frac{1}{2} - \frac{3}{4}$	0.70
A	h.w.l	1.20 - 1.40	2.10	0.76-0.82	> 0.5	0.95-1.0	$\frac{3}{4}$	0.88
B	h.w.l	1.00 - 1.20	2.10	0.69-0.76	> 0.5	0.9 - 0.95	$\frac{1}{2} - 1$	0.83

The relation between H_t/H_i and the water level is almost linear. Because of the inaccuracy of the whole calculation it is acceptable to calculate the wave-heights only by m.w.l.



Refraction analysis near Bengkulu harbour

fig. 10

direction	reef	$K_r(5m)$	$K_D(5m)$	$K_{br}(5m)$	$H_s(5m)$
270°	I	$\sqrt{1/1.9}$	-	-	1.0
270°	II	$\sqrt{1/1.3}$	1	-	1.2
280°	I	$\sqrt{1/2.1}$?	?	?
280°	II	$\sqrt{1/1}$	1	-	1.3
290°	I	$\sqrt{1/1.6}$	-	-	1.1
290°	II	$\sqrt{1/1.75}$?	?	?

$K_{sh}(5m) = 0.981$, K_r = refraction coeff. K_D = diffraction coeff. K_{br} = breaking coeff.

It is almost impossible to calculate the significant wave height (at 5 m) for section I and II, respectively for 280° and 290°, because the waves will break first at Pata Sambilan, so a part of their energy is lost, and secondly just behind this reef (because of the "lens-effect").

Diffraction around Pata Sambilan will cause difficulties; the wave height behind the reef is also influenced by this phenomenon.

Because these wave-heights can not be calculated, an estimation is made. For reef I, $H_s = 1$ m (at a depth of 5 m), the direction is 30°-35° (with regard to reefline I; angle between coastline and reefline is about 10°) For reef II $H_s = 1.2$ m, the direction (only north of the reef) is 30°-35° (with regard to reefline I).

With the following assumptions the wave heights just behind the reefs are calculated.

- parallel depth contours until the reefs
- breaking on the reef will not influence the direction of wave propagation
- because of the shape of reef II, the wave will break twice

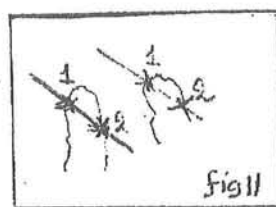


fig. 11

-the depth just behind the reefs is the same as the depth just in front of the reefs (at m.w.l. 1.70 m)

The wave height (H_s) just in front of the reefs:

	H_s (5m)	$\phi(5m)$	$K_r(5-1.7m)$	H_s (1.7m)	$\phi(1.7m)$
reef I	1.0	$30^\circ - 35^\circ$	0.95-0.94	1.15	$17.5^\circ - 20.5^\circ$
reef II	1.2	$30^\circ - 35^\circ$	0.95-0.94	1.40	$17.5^\circ - 20.5^\circ$

$$T = 7 \text{ sec}, K_{sh} = 1.22$$

The depth in front of the reef is 1.70 m. the max. wave-height which can occur at this depth is about 1.35 m (slope $\alpha = 0.05$, so γ (breakerindex) is 0.8). So specially at reef II the depth limits the wave-height in front of the reef. When is assumed that the wave-height is Rayleigh-distributed the wave-height behind the reef can be calculated in the following way

reef I $H_s = 1.15$		H_m	$P\{H_m\}$	K_{br}	H_m^*	$(H_m^*)^2 P\{H_m\}$
H_d	$P\{H>H_d\}$	1.35	0.06	0.75	1.01	6.2×10^{-2}
H_{max}	0.064	1.25	0.07	0.75	0.94	6.2×10^{-2}
1.15	0.135	1.05	0.12	0.75	0.79	7.4×10^{-2}
0.95	0.255	0.85	0.17	0.75	0.64	6.9×10^{-2}
0.75	0.427	0.65	0.21	0.85	0.55	6.4×10^{-2}
0.55	0.633	0.45	0.20	1.00	0.45	4.1×10^{-2}
0.35	0.831	0.25	0.14	1.00	0.25	8.8×10^{-3}
0.15	0.967	0.05	0.03	1.00	0.05	7.5×10^{-3}
0.00	1.000					$\sum (H_m^*)^2 P\{H_m\} = 0.381$

The waterdepth above this reef is about 0.90 m; so waves less than about 0.50 m ($\gamma = 0.6$; $H_{max} = 0.6 \times 0.9 = 0.55$ m) will not break.

The H_{rms} behind the reef is about $\sqrt{0.381/1} = 0.6$ m. The H_{rms} behind the reef can also be calculated in the following way: $H_{rms} = H_s \times K_{br} / \sqrt{2} = 1.15 \times 0.75 / \sqrt{2} = 0.6$ m. The same result is obtained because the percentage of waves larger than H_{max} is small.

An identical calculation is made for reef II on page 17. There the water-depth above the reef is about 0.7 m. So the max. waveheight is 0.35 m (at 1.7 m depth, at 0.7 m it is 0.42 m).

The H_{rms} after breaking one time is $0.415 = 0.65$ m, after the second breaking the H_{rms} becomes $\sqrt{0.230} = 0.5$ m. The H_{rms} calculated in the other way becomes $1.4 \times 0.7 / \sqrt{2} = 0.7$, resp. $1.4 \times 0.7 \times 0.7 / \sqrt{2} = 0.5$ m.

The wave heights just behind the reef are now determined, so the wave heights in front of the coast can now be calculated. The depth between the reef and the coast is not known exactly. An old chart of the harbour of Bengkulu

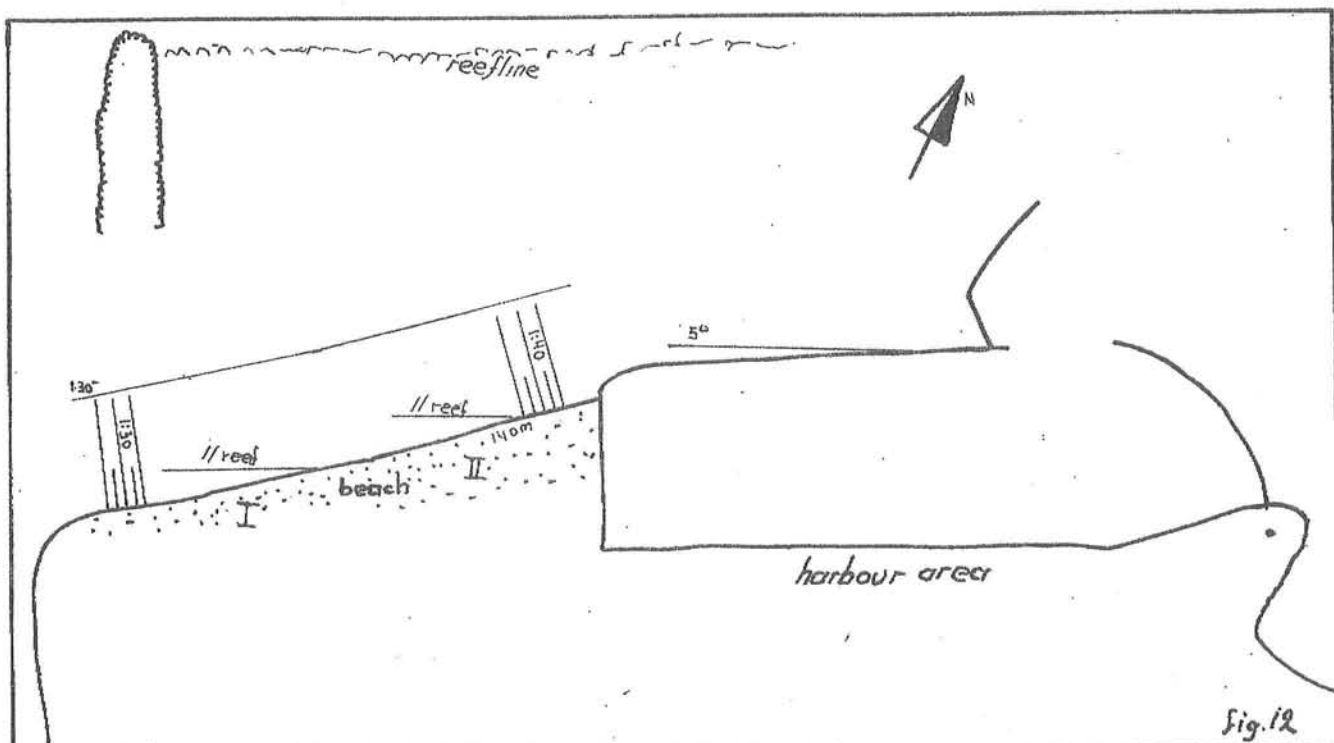
reef II $H_s = 1.4$ m

H_d	$P\{H > H_d\}$	H_m	$P\{H_m\}$	$K_{br}^{(1)}$	H_m^*	$(H_m^*)^2 P\{H_m\}$	$K_{br}^{(2)}$	H_m^{**}	$(H_m^{**})^2 P\{H_m\}$
1.35	0.156	1.25	0.10	0.7	0.88	0.077	0.7	0.62	0.038
1.15	0.259	1.05	0.14	0.7	0.74	0.076	0.7	0.52	0.038
0.95	0.398	0.85	0.14	0.7	0.60	0.050	0.7	0.42	0.025
0.75	0.563	0.65	0.20	0.7	0.46	0.041	0.85	0.39	0.031
0.55	0.734	0.45	0.15	0.85	0.38	0.022	1.0	0.37	0.021
0.35	0.882	0.25	0.10	1.0	0.25	0.006	1.0	0.25	0.006
0.15	0.977	0.05	0.02	1.0	0.05	0.000	1.0	0.05	0.000
0.00	1.000					$(H_m^*)^2 P\{H_m\} = 0.415$		$(H_m^{**})^2 P\{H_m\} = 0.230$	

indicated that the depth in front of the harbour was more than 1.3 m (at m.w.l.). Assuming that the breakerindex was 0.8, the max. wave-height in front of the coast (beach) is about 1.0 m.

The maximum wave-height behind the reefs was valued at 1.15 (at 1.3 m) or 0.77 (at 1.3 m). So nearly all waves which travel from the reef to the coast will break on the beach.

The breakerdepths and breakerangles can now be calculated, assuming parallel depth contours between the reef and the coast.



A different direction of the coastline of beach I and II is chosen because this was "indicated" on some pictures of prof. Bijker. The reason for this phenomenon is probably that the amount of sand transported around the corner (at b, see fig. 10) will limit the transport capacity. When the transport capacity is too large the beach will erode until an equilibrium is attained. So the direction of the coastline will change.

Because it is not known where the 1.30^- depth contour is situated, the breakerangle can be calculated at two ways:

-assume the 1.30^- depth contour lies parallel to the 1.70^- depth contour directly behind the reef, angle at 1.70^- : $18^\circ - 20^\circ$, angle at 1.30^- : $16^\circ - 17.5^\circ$ (with regard to the reefline). This means that at beach I the angle of incidence at 1.30^- is $7^\circ - 8.5^\circ$, and at beach II $2^\circ - 3.5^\circ$.

-assume the 1.30^- depth contour lies directly in front of the beach (this means a depth of 1.70^- between the reef and the beach); angle of incidence at beach I (at 1.70^-): $9^\circ - 11^\circ$. The angle at 1.30^- will be $8^\circ - 9.5^\circ$.

For beach II the angle of incidence at 1.30^- m will be $3.5^\circ - 5^\circ$.

Both assumptions are extremes. So a mean value will be a good guess:

$$\begin{array}{ll} \text{beach I} & \phi_{130^-} = 8^\circ \\ \text{beach II} & \phi_{130^-} = 4^\circ \end{array}$$

At the west side of the beach the rms wave height is 0.5 m (at 1.70^-) and at the east side of beach II the rms wave height is 0.6 m (at 1.70^-). Between the west side of beach I and the east side of beach II the rms wave height will rise from 0.5 m until 0.6 m.

The breakerheights, -depths and -angles can now be calculated:

$$\text{Beach I (west side)} h_{br} = 0.80 \quad \phi_{br} = 6^\circ \quad \gamma = 0.8 \quad H_{br} = 0.64 \text{ m}$$

$$\text{Beach II (east side)} h_{br} = 0.90 \quad \phi_{br} = 3.5^\circ \quad \gamma = 0.8 \quad H_{br} = 0.72 \text{ m}$$

(H_{br} is breakerheight, h_{br} is breakerdepth)

By means of the calculation method described in Annex VIII of vol B the long-shore current velocities are calculated along beach I and beach II. The amount of sand transported along the western harbour mole is about $80\,000 \text{ m}^3/\text{yr.}$

7. Determination of the armour stone weight

Only in the period from October until March the heights of the waves from northern directions can be large near the Bengkulu harbour. In the other periods (waves from southern directions) only diffracted waves (around the reefs west of Bengkulu) will reach the harbour. The wave-height of these waves will be very small.

For the determination of a significant wave-height, which appears only once per π years, the months between October and March are important.

The refraction coefficients of these waves (from northern directions) are:

period $T = 7 \text{ sec}$ $K_r = 1/\sqrt{1.6} - 1/\sqrt{2.4}$

period $T = 10 \text{ sec}$ K_r is small (lens effect due to Pata Sam-bilan, see vol C)

The distribution of the significant wave heights during a period of months or years is not known. But it has to be expected that the wave-heights will be limited by depth. The harbour moles or breakwater do not have to extend until a waterdepth of more than 2 - 2.5 m beneath s.w.l., because of the small draught of the ships that will enter Bengkulu harbour.

A solution with a breakwater on deeper water to facilitate the trans-shipment of goods on the roadstead is not chosen because of the high costs, as already indicated. In such a case the distribution of the significant wave height should be very important.

The waterdepth at the end of the harbour-mole or breakwater will be about 2.5 m below s.w.l. With high tide and under storm conditions the maximum wave will be about

$$\gamma \times (h + \text{amplitude of the tide}) =$$

$$\gamma \times (2.5 + 0.50) = \gamma \times 3.$$

for waves with a period of 7 sec the breaker index γ will vary between 0.6 and 0.8. So the largest wave-height will be about $0.8 \times 3 = 2.4 \text{ m}$ at the end of the harbour mole.

The root-mean-square wave-height which had been used for sand transport calculations was: $H_o \text{ rms} = 1.00 \text{ m}$ (deep water). The significant wave height (at 3 m) to match will be about 1.20 m

This last figure shows that storms with wave-heights of 2.4 m will appear "several" times per year.

During the last 2 of 3 years one harbour mole of the Bengkulu harbour was extended. This extension is made by concrete blocks. The precise dimensions of these blocks are not known, but it can be valued at $0.6 \times 0.6 \times 0.6 (\text{m}^3)$. Assuming that the mass density of the concrete is about 2400 kg/m^3 the weight of these blocks is about 500 kg. Using the Hudson formula the damage (under storm conditions) of this harbour mole can be calculated.

$$K_D = \frac{\rho_a H^3}{\Delta^3 \cot \theta W} \quad \text{in which}$$

K_D = damage coefficient; because the waves are breaking this value is about 87 % of the value with non-breaking waves

ρ_a = mass density of the armour blocks (2400 kg/m^3)

H = wave height (m)

Δ = relative density of the armour unit; $\Delta = \frac{\rho_a - \rho_w}{\rho_w} = 1.35$

$\cot \theta$ = slope of the breakwater

W = weight of the armour unit (kg)

In a waterdepth of 3 m H is about 2.4 m, $\cot \theta = 1.5 - 2$; then K_D is (with a stone weight of 500 kg) 18 - 13.5.

The K_D for non-breaking waves will be 20.7 - 15.5.

This means that the damage is more than 5 % (Paape & Walther 1962). Thus more than 5 % of the armour-units are de-placed. This damage is large, it is therefore more economical to use larger armour-units at the end of the harbourmole. Assuming a damage of about 2 % is acceptable. The damage-coefficient becomes $K_D^A = 0.87 \times 8 = 7$. So, W is about 1000 - 1300 kg; thus the height of the cubes is 0.75 - 0.82 m. So cubes with the dimensions $0.8 \times 0.8 \times 0.8$ are sufficient (ca. 1200 kg).

These blocks have to extend from the depth at which the damage of smaller blocks becomes larger than 2 %, until the end of the harbour mole. Using $W = 500 \text{ kg}$ and $K_D^A = 7$ the wave height H becomes 1.75 - 1.90 (m).

So the smaller blocks can be used until a depth of $1.75/0.8 = 2.2 \text{ m}$. (breaking index $\gamma = 0.8$) This means 2.2 m at H.W.L., so about 1.5 m below L.L.W.

In the above calculation wind set-up is not taken into account. Because of the large depths in front of the Bengkulu coast the wind set-up will be very small. The wind comes from NNW or SSE, i.e. parallel to the coast, so in general there will be no wind-set-up. Only near Bengkulu the NNW wind is perpendicular to the coast, but has only a short fetch.

Assume: wind speed $W = 32 \text{ mph}$

fetch $F = 10 \text{ miles}$

meand depth $D = 33 \text{ ft (10 m)}$

constant $C = 1.2 \times 10^{-3}$

ws = wind set-up, $\theta = 0^\circ$

$$ws = \frac{C W^2 F}{D} \cos \theta = 0.37 \text{ ft} = 0.11 \text{ m}$$

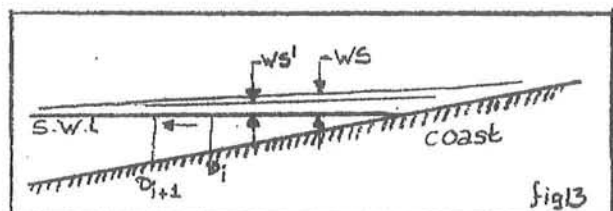
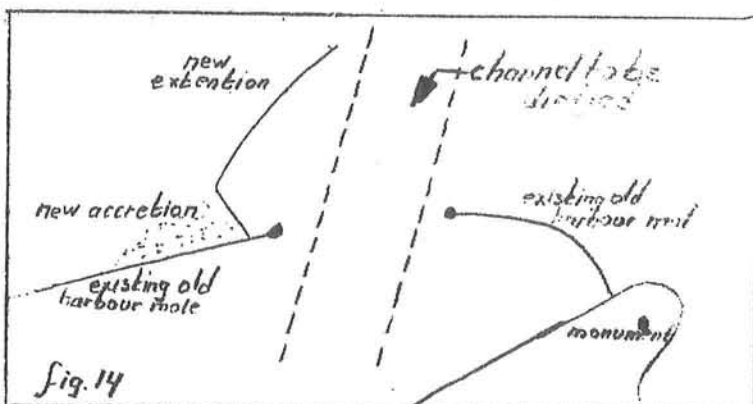


fig13

Because of set-up differences between D_i and D_{i+1} (set-up in D_{i+1} will be smaller) a current will start perpendicular to the coast. This current will decrease the wind set-up up to ws' , which is not known. This ws' depends on the ratio between the fetch and the distance perpendicular to the coast. For a flat (underwater) slope ws' will be almost the same as ws , for a steep slope ws will be almost zero.

8. Improvement of the existing harbour

As indicated in the former chapters the amount of sand transported along the harbour is not as large as expected from the preliminary calculations. So a possibility to dredge an entrance-channel and keep this channel open



by maintenance-dredging exists. An advantage of this alternative is that the new extention of the harbour mole can be used optimal. The best technique to keep the channel open is to prevent sand passing the channel. This can only

be achieved by dredging away the same quantity as is transported by the longshore current. In annex VIII of vol B an amount of 35 000 to 125 000 m³/yr was calculated; this is a large quantity to dredge when no succion dredges are available. But when this channel is not deep (2.5 m below l.l.wl) and the shape of the western breakwater is correct it is not necessary to remove all the sand. We expect that 10 - 20 % will pass the entrance without sedimentation. The lay-out of the new extention is well fitted for this purpose. Note: As already indicated in chapter 7 we expect large damage at the end of the new extention, because the relative small weight of the blocks. So it is advisable to protect the head of the new extention with cubes of 0.8 x 0.8 x 0.8 m³.

In the nowadays situation it is very important that the new accretion near the new harbour-mole is removed as quick as possible. Removing the accretion west of the existing harbour should be advisable too; however a problem is that this area is already let out for housing. The sand dredged from the harbour, the entrance channel and the accretion area may be dumped east of the monument. Sand dumped in this location will not return to the harbour. It will decrease, or even prevent, the erosion east of the monument.

As initial dredging the harbour basin should be dredged out. We advise dredging the harbour basin to a depth of 2.50 m below l.l.w. Dredging should be carried out in the area indicated on the map. This area was the dredged area in the colonial period, an one may expect that here no reefs are present up to a depth of 2.5 m.

A very important advantage of this solution is that the existing port facilities can be used optimal. Although the space available on the aprons between the front of the quay and the sheds is somewhat small for a modern

harbour, one should advise to use it, and not to build new aprons in the old harbour area. The costs of such aprons are high, and because this harbour will only be used intensively until the Pulau Bay harbour is put into service, building new aprons is not justified from an economical point of view.

In a harbour several areas can be distinguished. In Bengkulu four areas are to distinguish:

1. Roadstead
2. Boatharbour (lighter basin)
3. Primary port area
4. Secondary port area

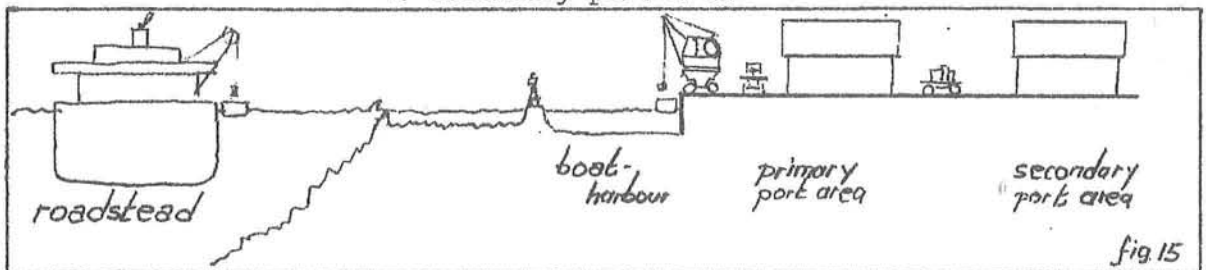


fig.15

The flow of goods is indicated in fig. 16.

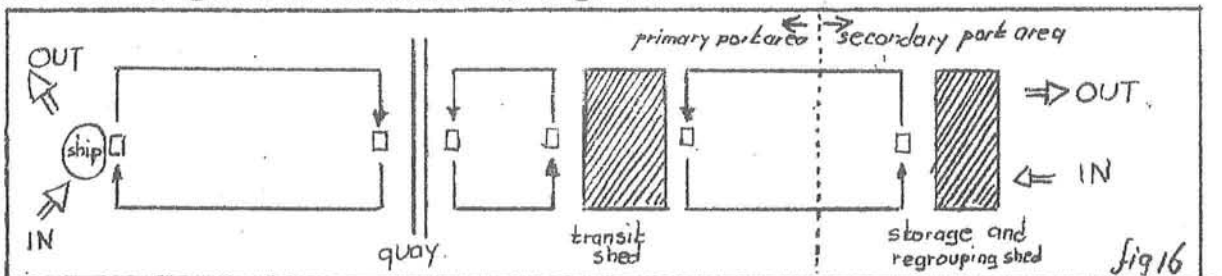


fig.16

Incoming goods are brought in with barges alongside the quay. There they are unloaded and brought to the transit shed. From the transit shed they can be transported directly to the consignee or via the warehouses in the secondary port area, in which the goods are stripped and packed in order to the bill of lading.

On the Bengkulu port area there is not enough space to develop the secondary port area, with small industries. This is no problem, because the objective is that such small industries are settled near the new Pulau Bay harbour. In Bengkulu the unpaved storage area east of the sheds can be used as such a secondary port area. For the next few years the total area is large enough when no secondary port activities are developed. Only the covered area (sheds) is too small. Because the construction of new sheds is not advisable for such a short period a more temporary solution has to be found, for example an installation for packing palletized goods in shrinkage plastic. When the new Pulau Bay harbour is ready this installation can be moved to the new harbour.

On the quay a mobile crane with a capacity of ca. 10 tons should be available for loading and unloading of the barges. It is advisable to keep a second (5 tons) general-purpose-crane in reserve.

9. A new jetty east of the harbour

shipping requirements

At the jetty a depth of 2.5 m below l.l.w. is necessary to allow bearding of coasters and wooden ships, this is about 3 m below the mean water level. The access channel requires a minimal depth of 2.5 m below mean water level. In such a situation the larger ships can enter the harbour only with flood tide, which does not seem to be a large problem. The height of the platform has to be about 1.5 m above m.w.l., the minimum width is 5 m to allow access with a crane. The minimum length of the jetty is estimated to be 100 m. This stage or cofferdam has to be protected by a rubble-mound, made by concrete cubes or armour stone.

Morphological requirements

This alternative is only interesting when nearly all the sediment is transported behind the construction. As already indicated in the former chapter, most waves break on the reef (near the 1 m line). On this reef only a small sand transport is expected, because of the absence of sand. The remaining waves break at the coast and cause a longshore transport (t_1 , see fig. 17).

This sand is transported along the harbour moles to the monument-cape (Note: the new extension is not considered) Without any human construction this sand should settle east of the monument. Because of the activity of small wind waves no spit is formed, but a very shallow "platform" with a small slope. The new accretion is spread over the platform and will reach its edge (at the reef, near the 1 m line). On this reef a large transport capacity exists and the sand will be transported to the north.

To guarantee the stability of this system, it should not be disturbed.

So from a morphological point of view there are two requirements

1. The direction of the construction (ϕ) must have such a direction that all the eventual transport along the construction is directed south (to prevent siltation of the access channel)
2. The gap between the coast and the construction (d) must have such a dimension that all the sediment can be transported by wave activity through this gap.

The direction of the construction

In fig. 17 refraction of 7 second waves from the west is indicated. It is clear that near the construction the influence of the 1 m shoal becomes important, so nearly no western waves will reach the construction. But waves with a direction a little more from the

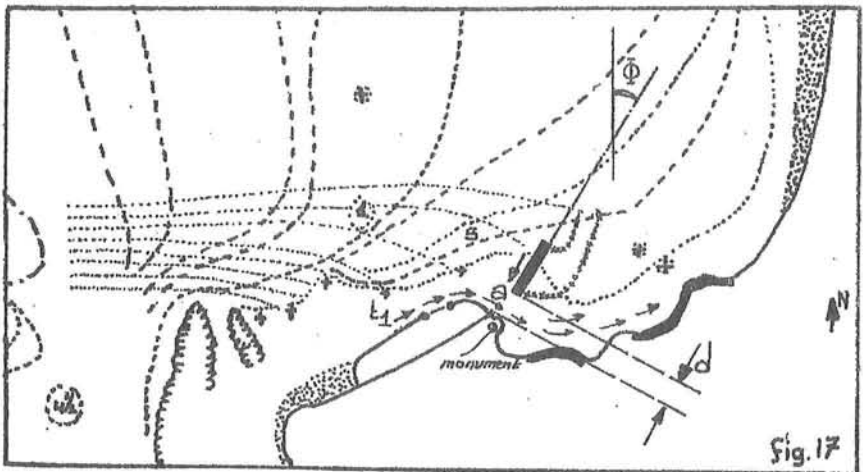


Fig. 17

slope, the width of the second breakerzone is 40 m. So the distance from the coast has to be at least 40 m. But as can be seen the angle of incidence near the monument is large ($80^\circ - 90^\circ$). Due to this fact sand transport is small (which is the reason for the shallow "platform").

So the transport capacity through the gap might be too small to cause enough transport.

Behind the construction a small basin has to be dredged with a depth of about 2.5 m. Because of the small distance from this basin to the above expected settlement area, it is to fear that the settled sediment will flow into the dredged basin. Two solutions are possible to prevent this:

1. The construction of a wall around the basin (which is very expensive).
2. To enlarge the distance d to ca 150 m (and consequently to use of a bridge of 150 m).

But even if one of these improvements is made, transport capacity under the bridge remains small and a shoal outside the bridge (near a, fig. 17) might be formed. The consequences of such a shoal are that waves will break on it and cause a transport. This transport will have a northern direction near a, and a southern direction near the construction. So the shoal will grow fast. After a short time (a few months) the shoal will have reached the northern end of the construction. Then the sand, until now transported by a long-shore current caused by small waves

north will reach the construction. They arrive at the construction from 310° . So ϕ has to be 40° or less. the width of the gap. The waves which do not break on the reef have a breakerdepth of ca. 80 cm.

Expecting a 1:50 beach-

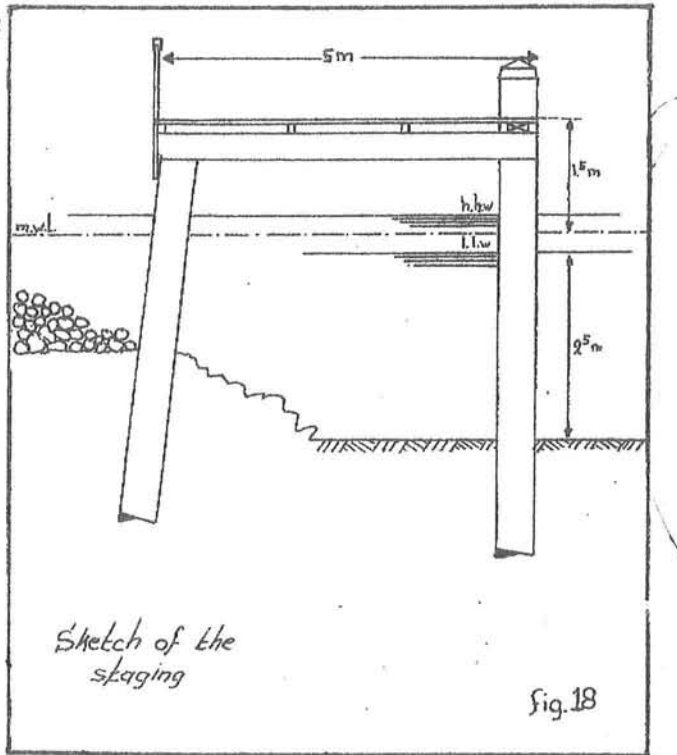


Fig. 18

(which did not break on the reef), will come into the area of large longshore transport capacity. And within a short period the acces channel will be silted up.

So from these morphological requirements one may conclude that this solution might be possible when detailed data of waves and sediment transport are available. But they are not.

constructive requirements

The requirements to the staging itself are simple, for an example see fig. 18. The protecting breakwater should be constructed as a rubble mound.

The piles of the staging have to be driven into the bottom, which probably contains a lot of coral. So pile driving will be expensive.

Instead of a staging a coffer-dam is also possible, but this solution is more expensive.

For the initial dredging one has to expect that on several sites coral reefs are present , which have to be removed.

10. Conclusions

Summarizing one can conclude that the first alternative (improving the existing harbour with maintenance dredging) is favorable, because:

- * The existing extention of the western mole can be used optimal.
- * No difficulties will occur with the construction of a jetty in coral.
- * The costs of the solution are less.
- * The costs are spread about many years, no large investment is necessary.

Annex

Investigation of data from the archives of the Dutch colonial government from the Arsip Nasional at Jacarta (1913-1923)

This annex is written in Dutch because of the numerous quotations from the old files.

Plans to construct a Pulau Bay harbour are already very old. Private investors planned a harbour with regard to the exploitation of coal, or to the production of fertilizer.

The government did not allow such private investment in harbour construction.

Three important reports are made about the Pulau Bay, viz. a note of the resident (Westenenk), a report of a governmental civil engineer (ir. Van Oppen) and a report of a harbour consultant (ir. Van Lidth de Jeude).

In these reports many details about development of the area are given. Also much information about the fysical situation of the Pulau Bay is presented in these reports.

The report of ir. Van Oppen is reprinted at the end of this annex.

Onderzoek naar de archiefstukken uit het Arsip Nasional te Jacarta betreffende de haven van Bengkulu over de periode 1913 - 1923.

Om dat ook in het begin van deze eeuw de havenfaciliteiten van Bengkulu niet zo best waren, zijn er toen al plannen geweest voor het aanleggen van een haven in de Pukiu Baai.

Een en ander is aan het rollen gebracht door de heer Van der Vossen, concessionaris van de mijn-concessie "Boekit Soenoer" (een gebied ca 40 km ten oosten van de Pulau Baai). Om in dit gebied steenkool te kunnen exploiteren had hij goede verbindingen nodig, en hij heeft zich dan ook op 25 juni 1914 met een request tot de Gouverneur Generaal gewend om hem een concessie te verlenen voor de aanleg van een spoorlijn naar de Pulaubaai en het bruikbaar maken van de Pulau Baai voor grote zeeschepen. De resident van Benkoelen, L. Knappert steunde deze concessie-aanvraag in zijn schrijven aan de Gouverneur Generaal van 11 juli 1914. Ook van de kant van de Spoor- en Tramwegdiensten van de Gouvernementbedrijven en van de dienst Burgerlijke en Openbare Werken waren er geen bezwaren, zodat een voorstel gemaakt is om deze concessie te verlenen.

Echter, na nader beraad, maakte de Commandant van de Zeemacht op 17 okt. 1914 toch bezwaar. Dit gebeurde omdat geconstateerd was dat de concessioneerissen het plan hadden hun concessie over te doen aan een amerikaans consortium. En omdat de vlootvoogd liever geen havens in buitenlands bezit zag, heeft de Gouverneur Generaal op 21 november 1914 besloten om wel de concessie voor de spoorlijn, maar niet die voor de haven te verlenen. Van der Vossen liet het daar niet bij zitten en diende op 23 april 1915 opnieuw een request in, waarin hij stelde dat het winnen van steenkool alleen dan zinvol is, als deze steenkool ook afgevoerd kan worden.

Om goed op dit request te kunnen reageren is toen aan de Algemeen Adviseur van het Havenwezen advies gevraagd inzake de mogelijkheden en kosten van een haven in de Pulau Baai.

Op 26 jan. 1916 heeft de Algemeen Adviseur, Wauter Cool, een voorlopig verslag gedaan van zijn bevindingen. Zijn conclusie was dat de enige realistische oplossing zou zijn een doorbaggeren van de zandspit, en dat een uitdiepen van de bestaande toegang onmogelijk zou zijn.

Verder moeten "om het zeewaartsche gedeelte van het te graven toegangs-kanaal tegen verzanding te beschutten alzoo twee dammen aangelegd worden, welke tevens als zeebrekers dienst moeten doen teneinde het binnenvaren van het kanaal te vergemakkelijken. Verder zal het wenselijk zijn te beletten, dat bij vloed zinkstoffen van de Selabar afkomstig in de baai worden gede-

poneerd. Dit kan gebeuren door het leggen van een sfsluitdam in verbinding met het havenemplacement".

Cool heeft in dit verslag ook een raming gemaakt van de kosten. Volgens hem was het nodig een kanaal te baggeren met een diepte van 12 m beneden L.L.W. met een breedte van 50 - 150 m. Bij taluds van 1:2 betekend dit 650.000 m³ grondverzet. Verder zou er nog 240.000 m³ in de voorhaven en 1.100.000 m³ in de baai zelf gebaggerd moeten worden. In totaal dus ca 2 miljoen m³, hetgeen hij begrootte op f. 900.000.=.

De havendammen, bestaande uit caissons met een steenbestorting een opgemetselde borstwering tot 250⁺ boven de middenstand zouden tot de -9 m lijn moeten lopen. De kosten worden geraamd op f. 1.500.000,=. Het havenemplacement zou ca f. 1.900.000,= gaan kosten. De totale ontwikkelingskosten voor een haven in de Pulau Baai zouden daarmee op f. 4.500.000,= komen. Cool voegt hieraan toe: "Dit cijfer is van zoodanige bescheidenheid voor een oceaanhaven aan de open kust dat ik aan flinke tegenvallers niet twijfel".

Enige tijd later (in januari 1913) brengt Cool een definitief verslag uit. Hierin worden de cijfers uit bovengenoemde voorlopige verslag ongewijzigd overgenomen. Een tekening met situering van de havendammen, de loswallen e.d. is bij dit verslag bijgevoegd. fig. 1 is een deel van deze tekening. Opmerking: het nul-niveau op deze tekening ligt op ca. 1.10 m boven de middenstand.

In het vervolg van het verslag gaat Cool in op de rentabiliteit van de haven, en concludeert dat een dergelijke grote haven alleen rendabel is als de kosten gedragen worden door de exploitant van de kolencoconcessie. Daar echter het mijnwezen t.a.v. de exploitatie van deze kolen een vrij sceptische houding aanneemt, adviseert Cool de haven aan te leggen door het gouvernement op kosten van de kolencoconcessionaris.

Na alle adviezen ingewonnen te hebben besluit de gouverneur-generaal "aan den adressant te kennen te geven dat, wat betreft het verlenen van een havenconcessie by het besluit van 21 November 1914, No: 16 wordt volhard en dat hem geenerlei uitzicht kan worden geopend op havenaanleg door het Gouvernement" besluit nr. 12, dd 5 juli 1916 .

Intussen heeft men bij Benkoelen de westelijke havendam van het prauhaventje voltooid. Nu blijkt echter dat ten oosten van deze dam de situatie verslechterd. Besloten wordt daarom (Besluit nr. 28 dd 3 juli 1917) om ook een oostelijke havendam aan te leggen, en tevens een kleine wijziging aan

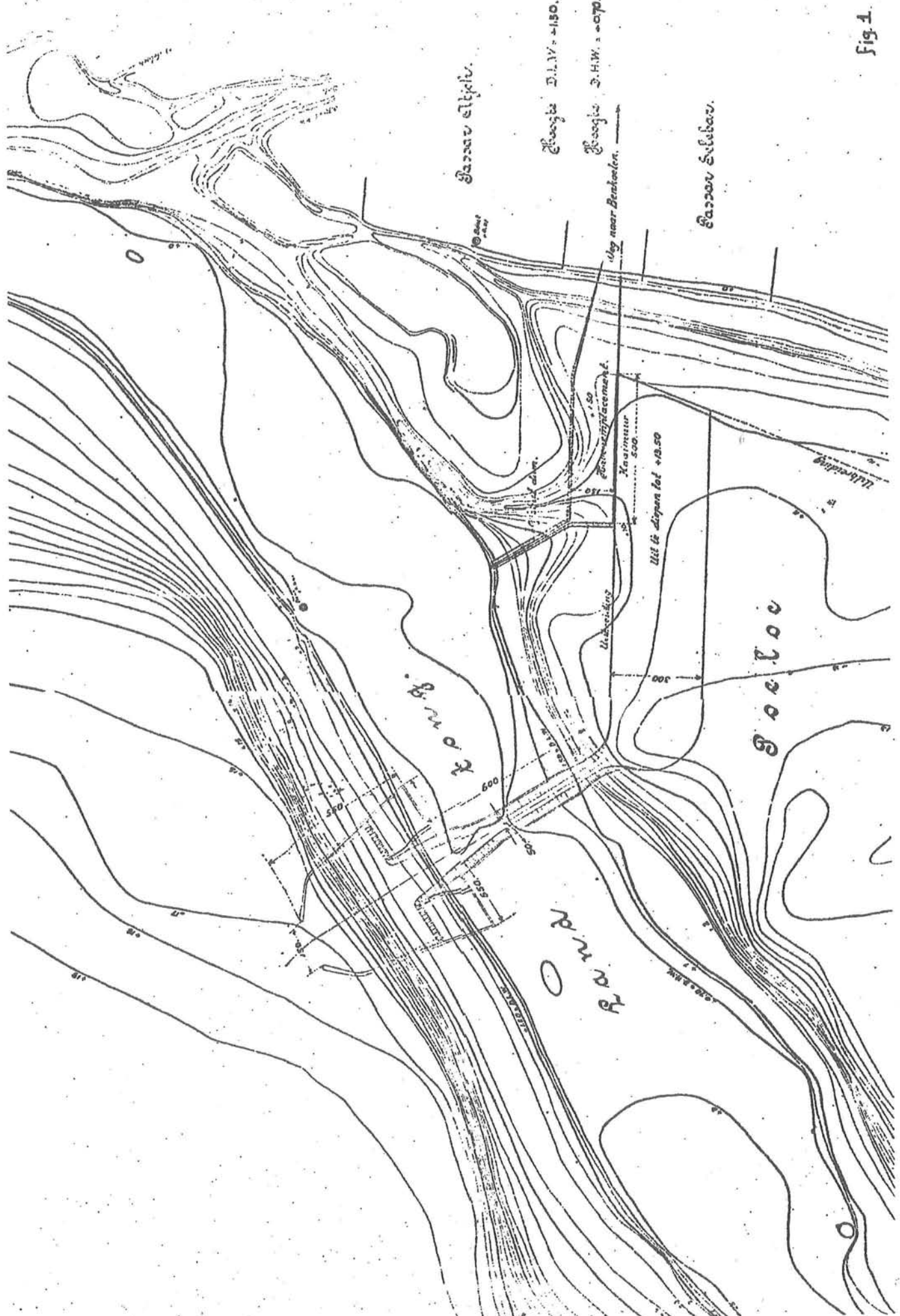


Fig. 4.

te brengen in de richting van de kademuur.

De nota Westenenk

De Resident van Benkoelen in die tijd, Westenenk, was een sterke voorstander van een haven in de Pulau Baai. Om nogmaals de aandachte te vestigen op een mogelijke haven in de baai schrijft hij in 1919 een vrij uitvoerige nota over de mogelijkheden van de Pulau Baai. Eerst geeft hij een aantal historische details, zoals bijv. de brief die Jan Pietsz. Coen op 10 dec. 1616 aan de bewindhebbers stuurt: *De schip "Enckhuysen" van hier vertreckende, op syn eerste gedestineerde plaetse wel (is) aangecompen, namentlyck in Celebar, leggende op 3³/₄ graden Zuyder breete, daar een seer goede reede is... Daar is op dese westcuste omtrent de gemelde quartieren wel goede anckergrondt, maar gants geen verschut, soo dat alle den pepper van Indapoura mootlyck met prauwen in Ticco, Priaman off Celebar moet worden gebracht, ende soude het de lieden, na ons voor desen door Chinesen bericht is, veel gelegener wesen haren peper in Celebar, dan in Ticco te brengen". Verder schreef Coen dat het schip bij Celebar bleef liggen, en dat "de oppercoopman Everard Deyns met de boot na Lamma Juta voer, waar hy met Radja Itam van Indrapoera een overeenkomst aanging dat deze Coninck aan het schip in Celebar leveren soude 2000 bhaeren peper tegen 15 realen de bhaer ende dat 2 maanden naer den dagh"*

Celebar is een oude schrijfwijze voor Sillebar, een nu verlaten passar aan de Pulau Baai. De Pulau Baai wordt in 1658 nog meer opgehemeld, en wel door Wouter Schouten, die haar met moeite binnenzeilde:

"Vonden in het inseylen van deze bogt van Sillebar, welckers omkreits met seer hooge bergen sagen beset soo quaden anckergront, dat peryckel liepen met ons schip tegens een klippige droogte, daar op de zee geweldigh sloegh, geworpen te worden. Doch onse anckers noch ter rechter tyt en plaetse vallende, wierden van sulkcks beschut. Quamen aldus behouden (Gode zy lof en danck voor syne genade) tot in deze vermaerde bogt van Sillebar te arriveren, vonden ons niet heel verre van het Vleck der Sumatranen".

Opgemerkt moet worden dat in dit citaat sprake is van klippen. Momenteel zijn er langs de spit geen klippen. In een anderrapport vermoedt Cool dat in de kern van de spit koraalriffen aanwezig zijn. Aangehaald verhaal van Schouten zou deze gedachte kunnen bevestigen. Anderzijds zijn bij de boringen, die door Dwidelta zijn verricht, geen duidelijke riffen geconstateerd. Hierbij moet wel worden aangetekend dat de gebezigde boringen met SPT-waarnemingen dergelijke riffen niet altijd aangeven.

In zijn nota wijst Westenenk er verder op dat de spit aan de mond van de

Air Tanjangaur vroeger niet zo lang geweest is. Aan deze observatie verbindt Westenenk geen conclusies, doch men kan hieruit concluderen dat er in de 17^e eeuw langs deze monding een noordwaarts transport was en de baai dus nog vrijwel geheel open geweest moet zijn.

Ook uit de lokatie van twee geschutsbatterijen is op te maken dat de in-vaart van de baai ongeveer daar lag waar Cool zijn doorgraving gepland had. In de 18^e eeuw schijnt Sillebar een aanzienlijke inlandse vloot bezeten te hebben, die in de Pulau Baai gestationeerd was.

Benkulu diende in die tijd als tussenstation voor de smokkelhandel tussen Brits-Indiëen Java. Het bedrijfskapitaal hiervoor waren Engelse gouvernementsgelden, die door corrupte Britse ambtenaren beschikbaar gesteld worden. Een goed idee over de omvang hiervan geeft het bericht dat in 1804 een Frans fregat in de Pulubaai de inlandse handelsvloot vernietigde, waarbij een partij opium ter waarde van 24.000 dollar buitgemaakt werd. Deze partij behoorde aan de commisioner Mr. Ewer te Benkoelen, en was bestemd voor de smokkel naar Java.

Aan de zuidkant, bij het voormalige Pondok Kapoer bevond zich een soort kade van opgestapelde koraalbanken. Westenenk kon hier nog resten van terugvinden. De inlandse bevolking wist ook nog te vertellen dat daar Engelse gebouwen en huizen gestaan hebben.

Na de Engelse periode wordt de Pulau-Baai steeds minder gebruikt. Westenenk merkte op dat gedurende 250 jaar de Pulau Baai de grootste schepen een veilig verblijf gewaarborgd had, toen de ingang vrij plotseling zodanig was vernauwd en verzand, dat vaartuigen van enige meters diepgang op de drempel stootten (1866). "Een Arabisch zoutschip, dat er in zinkende staat aan de grond kwam, zou volgens de overlevering de oorzaak geweest zijn dat de verzanding van de baai-ingang een versneld tempo aannam".

Westenenk vervolgt met een overzicht van de ontwikkelingen in de periode vanaf 1900 zoals het verzoek van Van der Vossen.

Hij stelt vervolgens voor om een klein geultje door de spit te graven, en dan te hopen dat het getij deze geul verder uitschuurt.

In het slot van zijn nota betoogt Westenenk dat het verzorgingsgebied van Benkoelen niet alleen de kuststrook omvat, maar ook een deel ten oosten van het Barisan-gebergte, en dat het daarom zeer wenselijk is de haven in de Pulaubaai verder te ontwikkelen.

In deze tijd wordt door Sand en Upton een concessie-aanvraag ingediend om kool, kalk en andere stoffen te winnen voor de fabricage van kunstmest. Onderdelen van deze aanvraag zijn tevens de bouw van een waterkrachtcentrale, een spoorlijn en een haven in de Pulaubaai. Zoals te verwachten steunt

Westenenk deze aanvraag volledig.

Door ir. F.J. van Oppen van de alg. dienst der burgerlijke en openbare werken in Zuid-Sumatra is deze concessie-aanvraag van commentaar voorzien. Hierin is ook een passage opgenomen over de Pulaubaai, die zeer lezenswaardig is, en daarom in zijn geheel als bijlage bij dit rapport is gevoegd.

Op 31 oktober 1919 wordt wederom door de Algemeen Adviseur van het Havenwezen advies uitgebracht inzake de Pulaubaai, welk advies vrijwel identiek is aan dat wat in 1916 is uitgebracht i.v.m. de aanvraag van Van der Vossen. Wel is nu toegevoegd, dat in het licht van de nota van Westenenk (1917), de slechte toestand van de prauwhaven van Benkoelen en de beide verzoekschriften, een diepgaand onderzoek gewenst is.

In augustus 1920 wordt besloten de concessie aan Sand en Upton te verlenen, m.u.v. de bouw van de haven. Deze zal door het gouvernement op kosten van Sand en Upton uitgevoerd worden. Eveneens in 1920, kort voor het nemen van bovengenoemd besluit zijn in Benkoelen een aantal belanghebbenden bijeen gekomen om zich te beklagen bij het gouvernement over de verwaarlozing van de infrastructuur van de residentie Benkoelen. De resident (Westenenk) stelt zich volledig achter deze klachten, en vindt ook dat het tijd wordt gelden uit te trekken voor een verbetering van de situatie.

Het gouvernement wil hier wel enigszins gehoor aan geven en verzoekt ir. Van Lidt de Jeude een onderzoek te doen "*met betrekking tot het havenvraagstuk voor Benkoelen, dus in het byzonder ten aanzien van de vraag of aaneene haveninrichting ter plaatse van de tegenwoordige reede Benkoelen, dan wel in de Pulaubaai de voorkeur moet worden gegeven*".

In een brief van 19 februari 1921 aanvaardde Van Lidt de Jeude deze opdracht, waarbij hij opmerkt dat het honorarium, afgezien van de reis- en verblijfkosten, nog niet te bepalen is maar een bedrag van F 2500.== niet zal overschrijden.

Op 31 mei 1921 presenteert Van Lidt de Jeude zijn rapport (37 bladzijden, 9 kaarten en 6 foto's), samen met een declaratie van f 6463,=.

De directeur van de dienst de Burgerlijke en Openbare Werken is niet erg onder de indruk van de kwaliteit van het rapport. De Gouvernements-Secretaris is dat wel voor wat de hoogte van de declaratie betreft, en blokkeert de uitbetaling. Er ontstaat nu een uitgebreide correspondentie over het al dan niet uitbetalen van dit honorarium. (we tellen 29 stukken betreffende deze zaak). Uiteindelijk wordt op advies van de directeur B.O.W. een bedrag van f 4463,= uitgekeerd. In zijn argumentatie stelt de directeur B.O.W. onder meer: "*Het is zoals vanzelf spreekt, uiterst moeilijk het aequivalent*

van geestelijken arbeid in klinkenden munt te betalen. Behalve de gewone factoren: tijd en mechanische arbeid, schrijf- en teekenloon welke een honararium zouden moeten bepalen treedt evenals bij de kunst een onmogelijk te waarderen genialiteitsfactor op".

De inhoud van het rapport Van Lith de Jeude

Van Lith de Jeude begint met een onderzoek naar de hoeveelheid goederen die jaarlijks ingevoerd en uitgevoerd worden. De invoer (in de periode 1911-1920) varieert van 14.000 - 20.000 ton/jaar, de uitvoer van 1700 - 8000 ton (opmerking: in 1974 werd via de haven 8000 ton uitgevoerd en 9000 ton ingevoerd, wat ca 20% van de totale in- en uitvoer van Bengkulu was). Het achterland van deze haven wordt nadelig beïnvloed door het Barisan-gebergte, en transport langs de kust per vrachtwagen is erg kostbaar. Voor de dagelijkse levensbehoeften stelt van Lith de Jeude een hoeveelheid van 50 kg per inwoner per jaar. Al met al komt hij tot de volgende cijfers:

40.000 ton voor
5.000 ton voor mijnbouw
12.000 ton voor de bevolking
<u>3.000 ton voor diversen</u>
totaal 60.000 ton in- én uitvoer

Dit bij een normale, koloniale ontwikkeling. In deze cijfers is een ontwikkeling van nieuwe kolenvelden niet betrokken. Van Lith de Jeude verwacht wel dat deze steenkool-exploitatie in belangrijke mate zal groeien.

In het volgende hoofdstuk wordt de havensituatie in 1920 beschreven. Benkoelen wordt aangedaan door schepen van de K.P.M., de N.I.T. en enkele schepen van de S.M.N. en de Rott. Lloyd. De diepgang van deze schepen varieert van 16' - 30'. Deze schepen gaan voor anker bij Pata, Sambilan en worden geladen en gelost met prauwen met een laadvermogen van 7 - 27 ton. Er zijn 24 prauwen beschikbaar met een totaal laadvermogen van 315 ton.

De prauwen worden gelost aan de 70 m lange kade van de prauw-haven.

"Het bezwaar, dat ondervonden wordt is de als regel zware deining aan de westkust van Sumatra, zich voortplantende uit den Indischen Oceaan, welke indien gepaard gaande met eenigszins krachtigen zeewind, het lichterbedrijf ten zeerste belemmt. Beschadiging van prauwen en lading komt daardoor niet zelden voor, evenals de moeilijkheid voor passagiers om te landen of aan boord te komen. Niet zelden, eenige malen per maand, zoeken de stoombooten beschutting van het eiland Poeloe Tikoes, waarbij het lossen en laden gestaakt wordt, of varen onverrichterzake door.

Uit een staatje, in 1915 door den agent der K.P.M. verstrekt, blijkt, dat

gedurende het tijdvak 1914 t/m 17 Aug. 1915 bij het lossen van niet minder dan 25 stoomscheepen, meer of minder lading verloren ging; een groote hoeveelheid van het SS van Noort op 28/6 '14. Voorts blijkt, dat vanaf 24 Dec 1914 tot 17 Aug. 1915 niet minder dan 16 stoomscheepen -niet begrepen in de 25 stoomscheepen vorenvermeld- lading, voor Benkoelen bestemd, mede doornamen"^{x)}
"De deining zet zich voort in de prauwenhaven waardoor het oostelijk deel daarvan meestentijds onbruikbaar is, terwijl daardoor een hinderlijke verdieping van de havenkom optreedt"

In hoofdstuk III wordt ingegaan op de Pulaubaai. Van Lith de Jeude ziet een haven in de Pulaubaai, gezien de hoge kosten en de slechte bereikbaarheid niet zo zitten. Hij stelt dat een haven in de Pulaubaai alleen dan overwogen kan worden, als een zeehaven bij Bengkoelen rond 2,5 miljoen guldens meer zou vergen. Daarom gaat hij niet verder op de Pulaubaai in.

In hoofdstuk IV wordt de rede van Benkoelen besproken.

Van Lith de Jeude noemt twee voordelen, te weten "de aanwezigheid van koraalriffen, met name Pata Sambilan, nagenoeg ter hoogte van L.L.W., waar door de energie der golfbeweging deels wordt uitgeput, onder vorming van een zware branding alvorens de eigenlijke kustlijn te bereiken. Bij laagwater is de golfverheffing, door de branding ontstaan, zichtbaar zich voortplantende langs den buitenrand van het rif in noordelijke richting. Bij zwaar weer is het duidelijk merkbaar, dat de waterbeweging tusschen de kust en genoemd rif minder is dan noord- en westwaarts van deze plaats.

Ten tweede de aanwezigheid van een vasten fundeeringsbodem, deels gevormd door de vorenbedoelde riffen, deels door een vasten napalbodem met redelijke waterdiepte."

Vervolgens worden er wat opmerkingen gemaakt over wind, golven en stromingen. Er wordt geconstateerd dat er te weinig meetgegevens zijn.

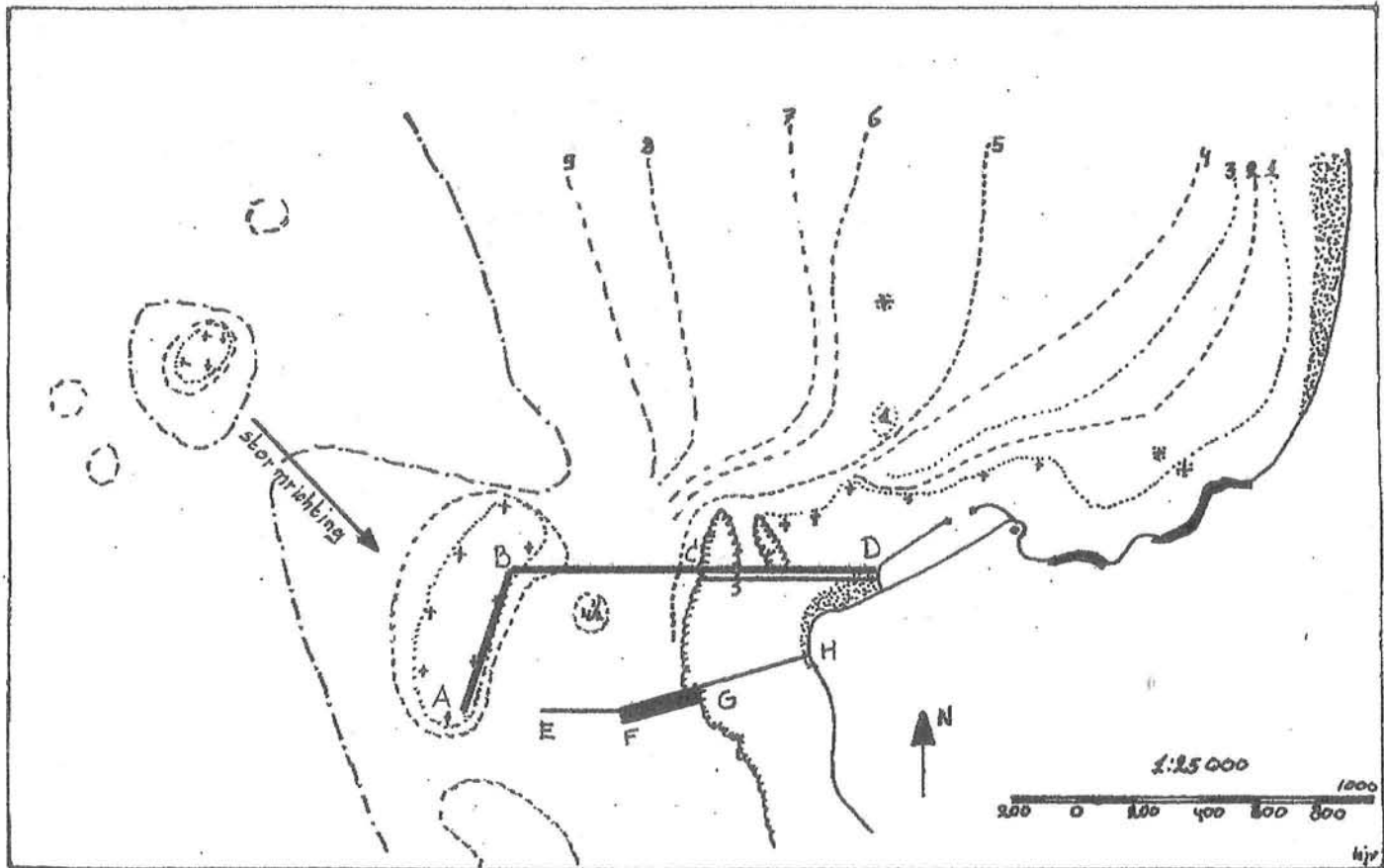
In hoofdstuk V wordt een ontwerp besproken voor de bouw van een haven op de rede van Benkoelen. Zie hiervoor ook fig. 2.

"De uit te voeren werken bestaan uit:

- a. een golfbreker A-B op den oostelijken rand van het koraalrif Pata Sambila ter lengte van ongeveer 625 m.
- b. Een afsluitdan B-C aansluitende met het oeverrif nabij C, ter lengte van ongeveer 500 m.

x) Een ander voorbeeld, aangehaald in de reeds genoemde "klachten van belanghebbenden" (15 juli 1920) is een partij dakpannen voor een ziekenhuis in het Barisan gebergte. Deze partij kwam met 30% breuk aan.

Verder moet opgemerkt worden dat tot op heden (1978) in het geheel niets verbeterd is.



- c. Een prauwenkanaal met noordwaarts daarvan gelegen beschermingsdam C-D, op den noordelijken rand van het oeverrif, ter lengte van ongeveer 600 m., aansluitende met den westelijken dam der prauwenhaven gepaard gaande met dichting van de bestaande mond en vorming van een nieuwe uitmonding naar genoemd kanaal nabij D.
- d. Een havenhoofd E-G ter lengte van ongeveer 550 m tot vorming van den havenmond AE, tevens dienstdoende als kolenkade voor het gedeelte F-G ter lengte van 200 m. met aansluitend gedeelte GH over het oeverrif
- e. Baggerwerk in de gevormde havenkom A-B-C'D. F-E tot een diepte van mindstens 27" - L.L.W."

Vervolgens wordt een korte beschrijving van de genoemde werken gegeven.

In hoofdstuk VI worden de kosten van dit projekt bekenen:

a) Golfbreker A-B	f. 875.000
b) Afsluitdam B-C	f. 550.000
c) Prauwenkanaal met dam C-D	f. 125.000
d) Kolenkade met kademuur F-G.	f. 1100.000
havenhoofd E-F	f. 450.000
e) Baggerwerk	f. 500.000
	sluitpost f. 50.000
	Totaal f. 3.650.000

Tot slot wordt het rapport samengevat in een tiental conclusies die hier integraal worden overgenomen.

1. De tegenwoordige scheepvaart- en handelsbewegingen van Benkoelen rechtvaardigen geenszins beteekenende uitgaven voor verbetering der haven.
2. Meerdere beteekenis als uitvoerhaven is te verwachten, door den aanleg van een spoorwegverbinding met het achterland, waardoor het afzetgebied zich aanmerkelyk zal uitbreiden.
3. De in de naaste toekomst te verwachten toename van uit- en invoer, door de ontwikkeling van het achterland, wettigt niet de kosten, verbonden aan den aanleg van een zeehaven.
4. Indien wordt overgegaan tot de ontginnung van de Boekit Soenoer kolenvelden op behoorlyken schaal, dient: zulks noodwendig gepaard te gaan met den aanleg van een zeehaven (met aansluitenden spoorweg).
5. Een vergelyking met de haven van Palembang leidt niet tot de gevolgtrekking, dat een ontwikkeling van Benkoelen en omgeving geen reden tot bestaan zou hebben.
6. De bestaande haveninrichting brengt bezwaren met zich welke by aanmerkelyke toename van het verkeer overwegend wordt.
7. Niettegenstaande de Poelau-baai als beschutte ligplaats in het oog vallende voordeelen biedt, is het hoofdzakelyk wegens economische redenen uitgesloten, dat deze voor inrichting als zeehaven in aanmerking komt.
8. De aanleg van een zeehaven te Benkoelen, met instandhouding van de prauwenhaven, voldoende aan de in de naaste toekomst te stellen eischen en vatbaar voor latere uitbreiding, is blykens het aangegeven schetsontwerp alleszins uitvoerbaar.
9. Alvorens tot uitvoering over te gaan, is het noodzakelyk de gebruikelijke waarnemingen betreffende de natuurverschynselen en nadere onderzoeken ter plaatse te verrichten.
10. Volgens een globale raming van kosten worden met de aanlegkosten van een zeehaven redelyke grenzen van rentabiliteit niet overschreden, waarby de verdeeling der daaruit voortvloeiende lasten in nader overleg met belanghebbenden, zooveelnoodig tevoren, moeten geregeld worden.

Bijlage

Advies van de algemene dienst der burgelijke en openbare werken
in Zuid-Sumatra

door ir. F.J. van Oppen. (4 september 1919)

Pulaubaai

Evenals bij de haven van Banjoewangi is ook hier sprake van een haffvorming, zoals men die bij zovele rivieren vindt.

Deze haffvorming ontstaat door de geleidelijke verplaatsing van zand langs de kusten in de richting van de zeestroming en wordt dus veroorzaakt door de zee, die dat zand weliswaar weer op de kusten werpt maar toch geleidelijk in de richting van de zeestroom verplaatst.

Zodra met dit zand een rivier of een inham met stilstaand water ontmoet wordt, ontstaat er stroomverlamming en dus neerslag van het zand aan de monding van de rivier op de bodem en wel zo lang tot deze mond is aangeslibd.

De door de werking destijds reeds ondiepe monding geeft aan de golfwerking van de zee alle gelegenheid om die monding dicht te slaan vooral in de droge tijd, wanneer er weinig binnenwater is. Slechts de grotere rivieren houden haar monding ten alle tijde open, terwijl de zwakkere rivieren alleen in de bandjirtijd daartoe in staat zijn.

Wegens de aldus door de zee belemmerde uitwatering zoekt de rivier een zijdelingse uitwatering langs de kust, die haar niet door de zee wordt belet en dus in de richting van de zeestroom.

Terwijl de zee zand blijft aanvoeren in een bepaalde richting en er ruggen van maakt, die de rivier met al haar vermogen zijwaarts naar zee tracht terug te dringen, komt er eindelijk een evenwichtstoestand, waarbij de rivier en het door de zee opgeworpen zand als landtong als het ware vreedzaam naast elkaar voortschrijden.

Op deze wijze moet mijns inziens in het algemeen de langs de kusten voorkomende haffvorming worden verklaard.

Wel kan zich ook het geval voordoen, dat de oude kust bestaat uit slappe grond zoals moeras grond en dat dan de opgedrongen rivier deze grond aantast en binnen de oude kustlijn blijft, maar in de meeste gevallen is de oude kust beter tegen de rivier bestand dan het losse zand van de landtong.

Bij een baai als de Poelaubaai slaat vanzelf het zand neer op de plaats waar de golven gebroken worden door het stille water, te eerder waar er riffen zijn, die daartoe meehelpen.

Bij de Poelaubaai vindt men een dubbele haffvorming. De ene gewone haffvorming is die van de Selebar, terwijl daarnaast met de Poelaubaai als

begin een tweede monding bestaat, waarnaast de landtong, die bij het rif van Buffelpunt begint.

Van de Selebar bevond zich de oude monding vermoedelijk benoorden de batterij I, die van ongeveer 1756 dateert volgens het merk op de kanonnen, terwijl het oude Pasar Selebar toen ook nog aan de linkeroever was gelegen volgens de tekening, de baai was toen nog vrijwel open.

. Daarop volgde de landtong vorming tot de monding zich verplaatste naar Moeara Selebar en verder op tot waar batterij II de latere monding aangeeft.

Door doorbraken in deze zich vormende landtong vindt men in dat gedeelte nog verschillende doorgangen en kreken, welke echter vrij ondiep zijn. Op deze landtong vormden zich de nieuwe Pasar Selebar en Pasar Atjeh.

Terwijl de monding van de Selebar of Tandjongauer zo goed mogelijk wordt opengehouden door deze rivier zelf, wellicht ook met behulp van bij eb uitstromend vloedwater, wordt de tweede monding van de Poelaubaai bijna uitsluitend door het laatst genoemde vloedwater met de baai als reservoir open gehouden.

De buitenste landtong, die de Poelaubaai van de zee afsluit, is ongeveer op dezelfde wijze gevormd door de zee en het heeft lange tijd geduurd voor zij deze vorm had, waarvan de oorspronkelijk grote diepte op die plaats ook als hoofdoorzaak moet worden aangenomen.

Hieromtrent heeft het archief van de Resident van Benkoelen mij enige gegevens verstrekt.

Ik maak hierbij de opmerking, dat het Arabische zoutschip, waarvan sprake is als schuld van de verzanding, juist daar moet gestrand zijn ten gevolge van de nog niet zichtbare verzanding en daarom niet als een gewichtige factor voor de verzanding moet worden beschouwd, die toch wel geregeld zou zijn voortgegaan.

Het eerste duidelijk gegeven omtrent het begin van de landtongvorming vindt men uit het jaar 1793, waaruit blijkt, dat toen reeds een beduidende landtong bestond aan de Noordzijde van Buffelpunt.

Volgens de oude berichten uit de tijd van Coen was aldaar een goede ligplaats en een veilige rede, terwijl aldaar uit de Engelse tijd ook overblijfselen van steigers (landingsplaatsen voor sloepen) en vestiging worden gevonden, die er op wijzen, dat reeds toen een dergelijk begin van zandaanwas bestond als door de bovenbedoelde tekening wordt aangegeven voor 1793.

In die tijd was de baai overigens nog geheel open doch was deze toestand blijkbaar voor de eisen, die men toen stelde voor zeilschepen al zeer gunstig.

Bij mijn bezoek viel het mij op, hoe de golfvorming zich bij Buffel-

punt als het ware cirkelvorming omboog en zich niet onmiddelijk daarnaast op het strand stortte.

Indien zich dit verschijnsel ook bij de punt van de oude landtong (1793 en te voren) heeft voorgedaan, dan geeft dit ook enige verklaring voor de veiligheid van de rede achter de landtong.

Er is geen bepaalde reden om aan te nemen, dat in de tijd van Coen deze landtongvorming nog in het geheel niet bestond.

Zoals ik boven vermeldde wordt de geul van de monding van de Poelaubaai opengehouden door aflopend vloedwater. Indien eenmaal een haveningang zal zijn gemaakt, dient de baai aan de Noordzijde te worden afgesloten door een dam bij Pasar Atjeh ten einde zowel bij bandjur in de Selebar het bandjurwater dat uit de doorbraken komt tegen te houden als om het vloedwater te benutten voor de opdiepte houding van de haveningang.

De diepte van de Poelaubaai bedraagt op het diepste gedeelte 14 M. beneden middelbare eb over 0.37 km^2 wijl de dieptelijn van 10 m een oppervlak van 3.42 km^2 insluit.

In een brief aan de Resident van Benkoelen van de heer Upton wordt gesproken over de natuurlijke neiging der rivieren om zuidwaarts te stromen.

Dit is blijkbaar een verkeerde mening, daar dit moet zijn volgens de richting van de terreinhelling dus dwars op de kust in ongeveer zuid westelijke richting. Deze natuurlijke neiging wordt bedwongen door de zee, die de rivier in noordelijke richting opdringt.

Ook beweert de heer Upton, dat het maken van de brug in de grote Postweg over de Tandjong Auer deze rivier belet heeft om zuidwaarts te gaan en aldus bezuiden de Poelaubaai in zee uitmondde, in welk geval de Selebar haar slib niet in deze baai had kunnen brengen.

Ik meen, dat deze rivier reeds lang haar bedding had bepaald voordat de brug zal zijn gebouwd en dus deze brug niet zoveel schuld heeft.

Verder spreekt de heer Upton van een opbouwing van de kust in N.W.-Z.O. richting terwijl de zeestroming in hoofdzaak noordwaarts is.

Dat de richting van de zeestroom noordwaarts is blijkt niet alleen uit de vorming van de landtong bij de Poelaubaai en de loop van de Selebar monding doch bijv. ook uit die van de Benkoelenrivier.

Echter zijn er ook enkele rivieren verder langs de kust, die in zuid-oostelijke richting een hals vormen, doch moet dit vermoedelijk worden verklaard uit andere plaatselijke omstandigheden of hindernissen.

Aannemende dat de haven binnen de landtong op diepte wordt gehouden door het in- en uitgaande water of anders op gemakkelijke wijze op diepte kan worden gehouden rest thans nog de haveningang zelf te bespreken.

Ten einde niet al te veel werk te hebben aan opruiming van koraal zou

men een plaats moeten uitzoeken met weinig koraal, waardoor wellicht vroeger de baai werd binnengevaren vooral omdat men dan gemakkelijker kan baggeren. Vermoedelijk zal dit baggerwerk wegens golfslag en deining niet zonder bezwaar gaan.

Uit dit oogpunt zou dus een punt benoorden de kustlijn 1793 in aanmerking kunnen komen.

Deze doorgraving zou echter wel een lengte van 1000 m. (afstand tussen de dieptelijnen van 10 m) hebben; bij een breedte van 50 m en een gemiddelde diepte van 10 m geeft dit reeds een grondverzet van ongeveer een half miljoen M3.

De voornaamste bescherming van de haveningang tegen de zee zal wel zijn een havenhoofd aan de zuidzijde, dat zich desnoods verder in noordwestelijke richting om buigt. Met het oog op de soliditeit van dit hoofd zou het wellicht de voorkeur kunnen verdienen om dit hoofd te beginnen op het rif van Buffelpunt en de haveningang even benoorden daarvan te maken, doch vermoedelijk zit in de landtong aldaar veel koraal hetgeen de kosten sterk zou verhogen.

Op den duur zal het uit het zuiden aangevoerde zand zich buiten dat hoofd neerzetten en dus de diepte van de zee aan de kust doen verminderen doch dit kan geruime tijd duren. Ook aan de monding kan dan aanzanding plaats hebben, welke slechts met moeite en met grote kosten kan worden verwijderd.

Alvorens een beslissing te nemen om de Poelaubaai te maken, dient dus een grondig onderzoek te geschieden naar het voorkomen van koraal op enkele plaatsen, die voor de haveningang in aanmerking komen, terwijl ook nadere waarnemingen omtrent de zandverplaatsing langs de kust evenals bij de haven van Banjowangi dienen te geschieden.

Een opname van dieptelijnen is vroeger reeds door de ingenieur van Haeften verricht, een calque van deze opname zal wel bij afdeling H berusten.

Met deze gegevens zou dan ten slotte een ontwerp voor de haven kunnen worden opgemaakt en een begroting van kosten, doch dan dient nog het maken van deze kosten gerechtvaardigd te worden door te verwachten in een uitvoer in vergelijking met de bestaande prauwenhaven, die men dan zou willen verlaten.

Dit dient met cijfers te worden aangetoond.

Om als oceaanhaven te dienen zou de Poelaubaai de concurrentie van de Emmahaven moeten breken. De toestand moet dus al zeer gunstig worden en succes te geven, daar anders de grote vrachtschepen de voorkeur zouden kunnen geven aan de Emmahaven als enige aanleghaven.

Zelfs is het de vraag of de Paketvaart met het oog op de grote kosten van de haven, waaraan zij zou moeten medebetalen, er niet de voorkeur aan zal geven om buiten te lossen en te laden ook met het oog op tijdverlies.